**PLEASE TYPE**

**THE UNIVERSITY OF NEW SOUTH WALES**
**Thesis/Dissertation Sheet**

Surname or Family name: Vizesi

First name: Frank Other name/s:

Abbreviation for degree as given in the University calendar: Ph.D.

School: Graduate School of Biomedical Engineering Faculty: Engineering

Title: The Creation and Repair of Osteochondral Defects and the Effect on the Opposing Surfaces


**Abstract 350 words maximum: (PLEASE TYPE)**

The repair of articular cartilage defects is a topic that has received significant focus from both basic science and clinical perspectives. The current gold standard treatment for significantly damaged or degenerated articular cartilage in the knee is a total joint replacement, although there are several drawbacks including reduced range of motion and increased instability. Whilst the total knee replacement will continue to be a valuable treatment, there is a need to find alternatives and part of the solution is having an appropriate animal model to effectively evaluate said alternative treatments.

The first part of this dissertation describes the characterization of an ovine osteochondral defect model which ultimately could be used to validate the efficacy of a variety of osteochondral implants. The effect of this femoral defect on the tibial surface, including the meniscus, was also studied and a metallic resurfacing device (HemiCAP) evaluated for its efficacy in protecting the knee from further degenerative changes. Additionally, pressure footprint and contact stresses were measured with flexible pressure sensors at flexion angles and loads determined from the sheep gait cycle. This study found that the HemiCAP device increased peak pressure when compared to all other conditions tested, especially at a point corresponding to heel strike. Since loading is known to modulate bone remodelling, micro computed tomography was used to measure changes in the subchondral and cancellous bone on the tibia opposing the surgical site. Biologically, there were no significant differences detected in the knees treated with the HemiCAP device when compared with those that had untreated osteochondral defects, which suggests that the HemiCAP device is not effective in protecting against tibial degeneration, but at least it does no more harm than not treating the defect in the first place.




**FOR OFFICE USE ONLY** Date of completion of requirements for Award:

# The Creation and Repair of Osteochondral Defects and the Effect on the Opposing Surfaces

Submitted to the Graduate School of Biomedical Engineering,
University of New South Wales

for the degree of

PhD (Biomedical Engineering)

in the year 2008.

Frank Vizesi

I hereby declare that this submission is my own work and the best of my knowledge it contains no material previously published or written by another person, or substantial proportions of material which have been accepted for the award of any other degree or diploma at UNSW or any other educational institution, except where due acknowledgment is made in the thesis. Any contribution made to the research by others, with whom I have worked at UNSW or elsewhere, is explicitly acknowledged in the thesis.

I also declare that the intellectual content of this thesis is the product of my own work, except to the extent that assistance from others in the project's design and conception or in style, presentation and linguistic expression is acknowledged.

Frank Vizesi

## Acknowledgments

For his mentorship and supervision throughout this project I would like to give my deepest thanks to Bill Walsh. Without his guidance and encouragement I certainly would not have embarked upon this learning experience, nor would I have garnered the valuable experiences that I have. May our friendship continue on long after this PhD.

To my colleagues at the Surgical & Orthopaedic Research Laboratories, I thank you for inspiring me with ideas and providing a supporting environment for potential PhD graduates to excel. Especially I would like to acknowledge JR and Greg for their help with the animal surgery, Rema and Yan for histology, Alex Turner for helping me learn the art of the MTS and last but not least Gina, who has been like family.

For help with the mechanical indentation testing I would like to thank Richard Appleyard and Alex Leung.

For her intelligent guidance on polymer synthesis and significant assistance in organising my thoughts on other aspects of this thesis I'd like to thank Martina Stenzel. I'm disappointed that the body of work we did together couldn't fit into this dissertation, but I certainly learned a great deal along the way.

Finally, to my friends and family who watched my sense of humour disappear at times throughout this process, I thank you for your patience and most of all for the encouragement I needed to finish the job.

*"An ounce of action is worth a ton of theory"* Friedrich Engels

# Contents

# List of Figures

# 1. Abstract

The repair of articular cartilage defects is a topic that has received significant focus from both basic science and clinical perspectives. The current gold standard treatment for significantly damaged or degenerated articular cartilage in the knee is a total joint replacement, although there are several drawbacks including reduced range of motion and increased instability. Another serious concern with total knee arthroplasty is that a significant quantity of bone must also be resected to achieve fixation of the implant. Additionally, total knee replacements are not recommended for younger patients who would be expected to live longer than the implant is able to function appropriately. Whilst the total knee replacement will continue to be a valuable treatment, there is a need to find alternatives and part of the solution is having an appropriate animal model to effectively evaluate said alternative treatments.

The first part of this dissertation (Chapter 3) describes the characterization of an ovine osteochondral defect model which ultimately could be used to validate the efficacy of a variety of osteochondral implants. This model consisted of a single defect 6mm deep and 6mm in diameter in the weight bearing region of the medial femoral condyle of 18 month old crossbred merino sheep where the longest time point was 52 weeks. The defects were created bilaterally using either a high speed drill or a manual punch. It is shown in the histology that creating the defect with a punch causes less damage to the surrounding cartilage. This leads to the recommendation that osteochondral defects should be created with a punch rather than a drill, since preserving the health of the rest of the joint is of vital importance clinically.

Where Chapter 3 is concerned with the creation and healing of a femoral osteochondral defect, Chapter 4 reports the degeneration of the tibia and meniscus that

oppose the defect. Macroscopic and histological grading were used to reach the conclusion that an untreated femoral osteochondral defect causes a significant level of damage to the tibial articular cartilage after 26 weeks, although by 52 weeks there was a small, but statistically significant reduction in damage. Histology also highlighted changes in the subchondral bone plate, which was the impetus for a closer evaluation of the bony changes to the tibia in the subsequent study where a defect was treated with a metallic resurfacing device.

The efficacy of the HemiCAP™ resurfacing device (Arthrosurface, Franklin, MA) was evaluated as a major part of this dissertation. The HemiCAP device is a smooth metallic resurfacing device which replaces part of one condyle and articulates directly with the other condyle. This device had previously been tested in a goat model where it was implanted into a pristine knee with good results. The experiment described in Chapter 5 involved testing the HemiCAP device in a more challenging and aggressive model in which an osteochondral defect was created and left untreated for five weeks to illicit some degeneration in the joint. The HemiCAP device was then implanted and the animals were sacrificed after a further 6 or 26 weeks. The same histological techniques as in Chapter 4 were used to conclude that the health of the tibial cartilage became progressively worse from 5 weeks after the initial defect, to another 6 weeks either with or without the HemiCAP device, although there was some improvement by 26 weeks afterwards. There were no significant differences detected in the knees treated with the HemiCAP device when compared with those that had untreated osteochondral defects, which suggests that the HemiCAP device is not effective in protecting against tibial degeneration, but at least it does no more harm than not treating the defect in the first place. Additionally, micro computed tomography was

used to measure changes in the subchondral and cancellous bone on the tibia opposing the surgical site. The method devised is described in detail in Chapter 6.

One of the main focuses of the HemiCAP device is to restore a smooth surface to the condyle such that the mechanics of the joint are also restored during articulation. Hence, Chapter 7 reports the pressure footprint of the sheep knee in the normal state, as well as with various defects and with the HemiCAP resurfacing device. Pressure footprint and contact stresses were measured with flexible pressure sensors (Tekscan, Boston, MA) at flexion angles and loads determined from the sheep gait cycle. This study found that the HemiCAP device increased peak pressure when compared to all other conditions tested, especially at a point corresponding to heel strike.

The conclusions and recommendations for future work are addressed in Chapter 8.

# 2. Structure and function of articular cartilage

Cartilage is a smooth, white and durable connective tissue comprised primarily of water and collagen and sparsely populated with only a single type of cell, the chondrocyte. Cartilage is an aneural and avascular tissue that receives its nutrient supply by diffusion through the interstitial water as the tissue is repetitively loaded and unloaded (Lu et al. 2001). Cartilage is found throughout the body in many locations, such as lining the ends of long bones, the intervertebral disc, the external ear and the larynx. There are three major subcategories of cartilaginous tissue: hyaline, elastic and fibrocartilage.

Elastic cartilage is more flexible than hyaline cartilage and more yellow in colour. It is found in areas such as the epiglottis and the external ear. Fibrocartilage differs from hyaline cartilage with increased tensile strength from the addition of type I collagen in the composition (Mow & Ratcliffe 1997). The two most frequently studied fibrocartilaginous structures are the annulus fibrosis of the intervertebral disc and the meniscus. Hyaline cartilage is smooth and white and its extracellular matrix is composed primarily of type II collagen. Hyaline cartilage is found in areas of endochondral ossification, although the greatest abundance of hyaline cartilage is found lining the ends of long bones within articular joints. This type of hyaline cartilage is referred to as articular cartilage and this is the type of cartilage that forms the focus of this thesis.

Articular cartilage is a load bearing, shock absorbing material that is essential for uninhibited transmission and distribution of load across a joint. Articular cartilage

also has a very low coefficient of friction, which assists in smooth and efficient articulation of a joint. It is a durable tissue which, once mature, can withstand large repetitive and static loading in some cases for the lifetime of the body.

Before delving into the structure and function of articular cartilage, it is worthwhile to review the anatomy of a diarthrodial (or synovial) joint. This is a joint in which two bones meet and articulate against each other (Figure 1). Diarthrodial joints exist in the knee, hip and shoulder to name just a few. In all diarthrodial joints, the bones are lined on the articulating surfaces with articular cartilage. These articular cartilage surfaces then either articulate against each other directly, or against a fibrocartilaginous structure called the meniscus that is located in between. The joint is protected by a synovial capsule (and internal synovial membrane) which also serves the purpose of secreting and retaining the synovial fluid within the joint (Mow & Ratcliffe 1997). Synovial fluid acts as a lubricant and also as a mechanism for nutrient diffusion into the cartilage tissues.

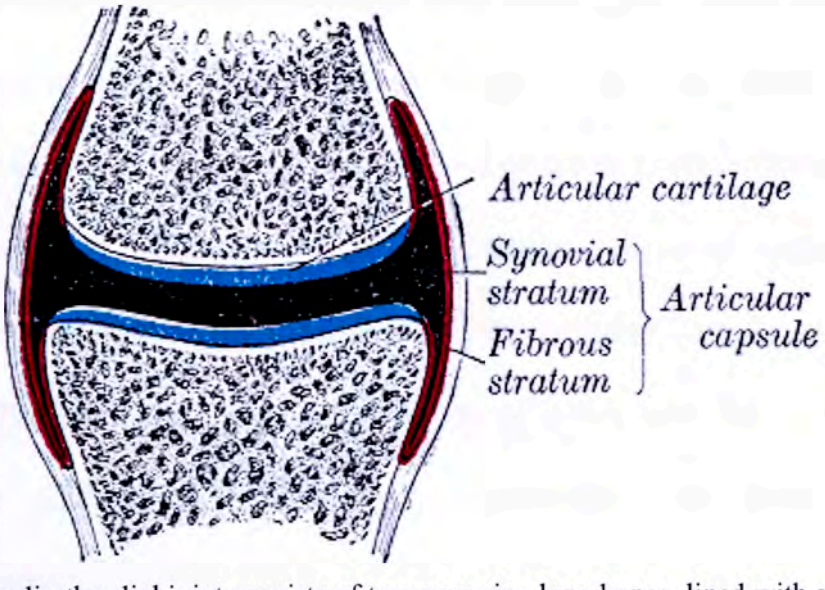


**Figure 1** A simple diarthrodial joint consists of two opposing long bones, lined with articular cartilage, awash in synovial fluid and encased with a synovial capsule (Gray 1918). A more complex diarthrodial joint such as the knee contains a meniscus in between the two cartilage layers to assist in load distribution

Articular cartilage can be considered a biphasic, or even multiphasic material. The two major phases in the cartilage composition are the fluid phase and the charged solid phase and the mechanical behaviour of the tissue is inextricably linked to the relationship between the two. The third phase that is often referred to is the ion phase, which has been proven to be significant in the mechanical behaviour by neutralizing the fixed charge of the solid phase (Mow & Wang 1999). The mechanical behaviour of articular cartilage will be discussed in more detail in Section 2.1.

Thus, the main components of articular cartilage are water, and the charged solid phase or the extracellular matrix. Typically, water accounts for 65 to 85% of the weight of the cartilage, depending on the depth from the surface. The remainder of the tissue is comprised of collagen, proteoglycans and a range of minor constituents (Hall & Newman 1991;Mankin et al. 2000;Mow & Wang 1999). Chondrocytes make up only a small fraction of the volume of articular cartilage.

### *2.0.1 Water*

The amount of water in articular cartilage varies from approximately 65% by weight in the deep zone to approximately 85% by weight in the superficial zone. Water is responsible for delivery of nutrients and removal of waste products from the cartilage. Most of the water is located within the interstitial spaces of the loose collagen network and is responsible for most of the load bearing capacity of the tissue in compression. The interstitial fluid is made up of water with the inclusion of ions (primarily Na+, Ca2+ and Cl-) which provide balance to the fixed charge of the extracellular matrix.

## 2.0.2 Collagen

The second most abundant component of articular cartilage is collagen. There are at least 18 different types of collagen, however, the vast majority of collagen in hyaline cartilage is type II collagen, with smaller quantities of types V, VI, IX and XI (Mow & Ratcliffe 1997;Poole et al. 2001). Collagens are long protein chains in a triple helix that connect end to end to form collagen fibrils (Figure 2) which are subsequently arranged in a loose network known as the extracellular matrix (ECM). The collagen fibrils of the ECM provide strength to the cartilage in tension and shear.

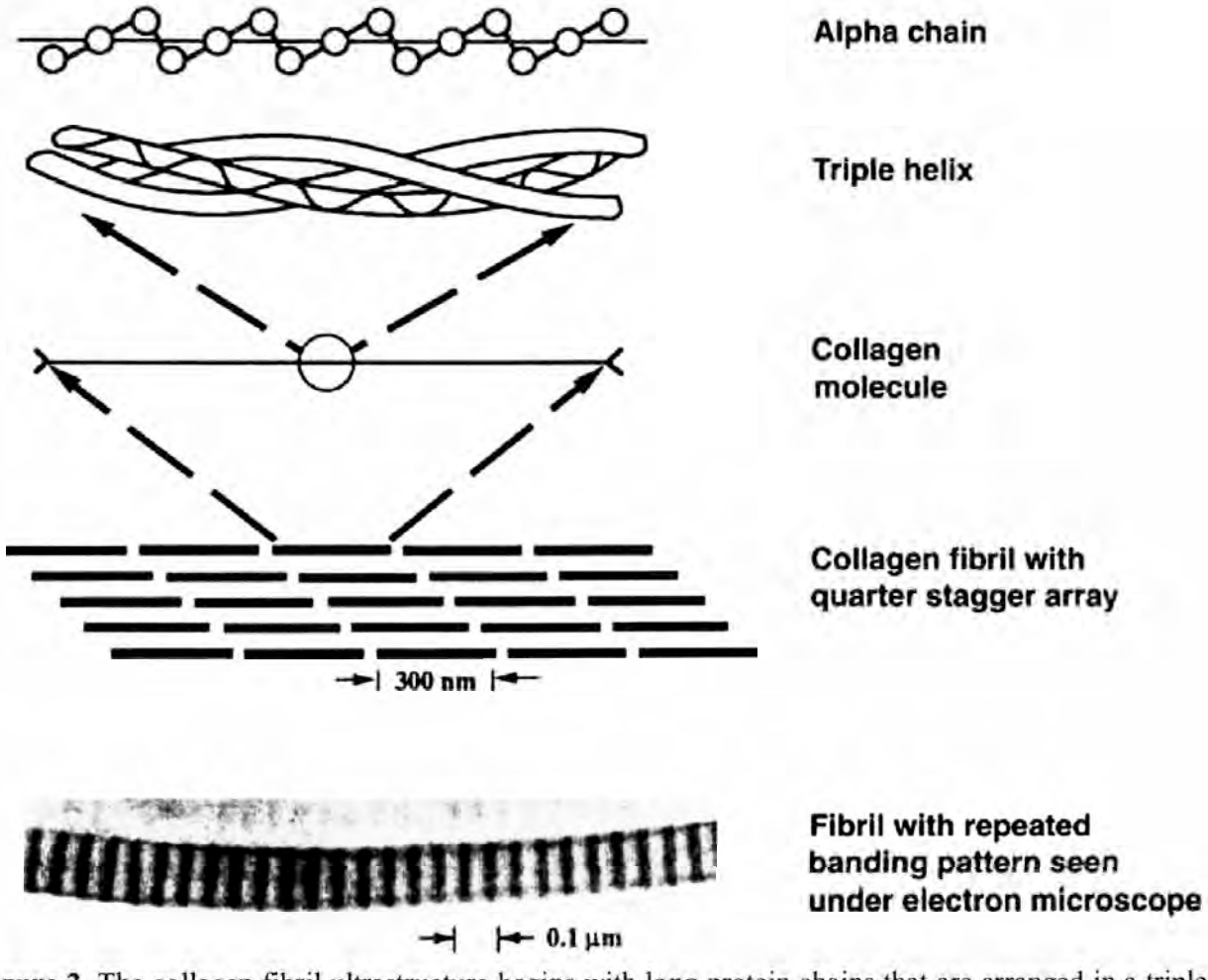


**Figure 2.** The collagen fibril ultrastructure begins with long protein chains that are arranged in a triple helix structure. These collagen molecules are then arranged in a quarter stagger array that gives a banded appearance to the fibril (Mow & Wang 1999) .

## 2.0.3 Proteoglycans

Proteoglycans also comprise a substantial volume of articular cartilage, approximately 4 to 7% of the wet weight. Proteoglycans are complex macromolecules consisting of a protein backbone with covalently bound glycosaminoglycans (GAGs). They are

negatively charged molecules that contribute swelling (osmotic) pressure to the tissue. The most common proteoglycan in articular cartilage is aggrecan, which is composed of a protein core with up to 100 chondroitin sulphate and 50 keratan sulphate molecules attached. This structure is then bound to a hyaluronan chain via the link protein (Figure 3) and many aggrecan molecules attach to a single hyaluronan chain (Figure 4). The chemical structure of chondroitin sulphate (CS), keratan suphate (KS) and hyaluronan (HA) are depicted in Figure 5.

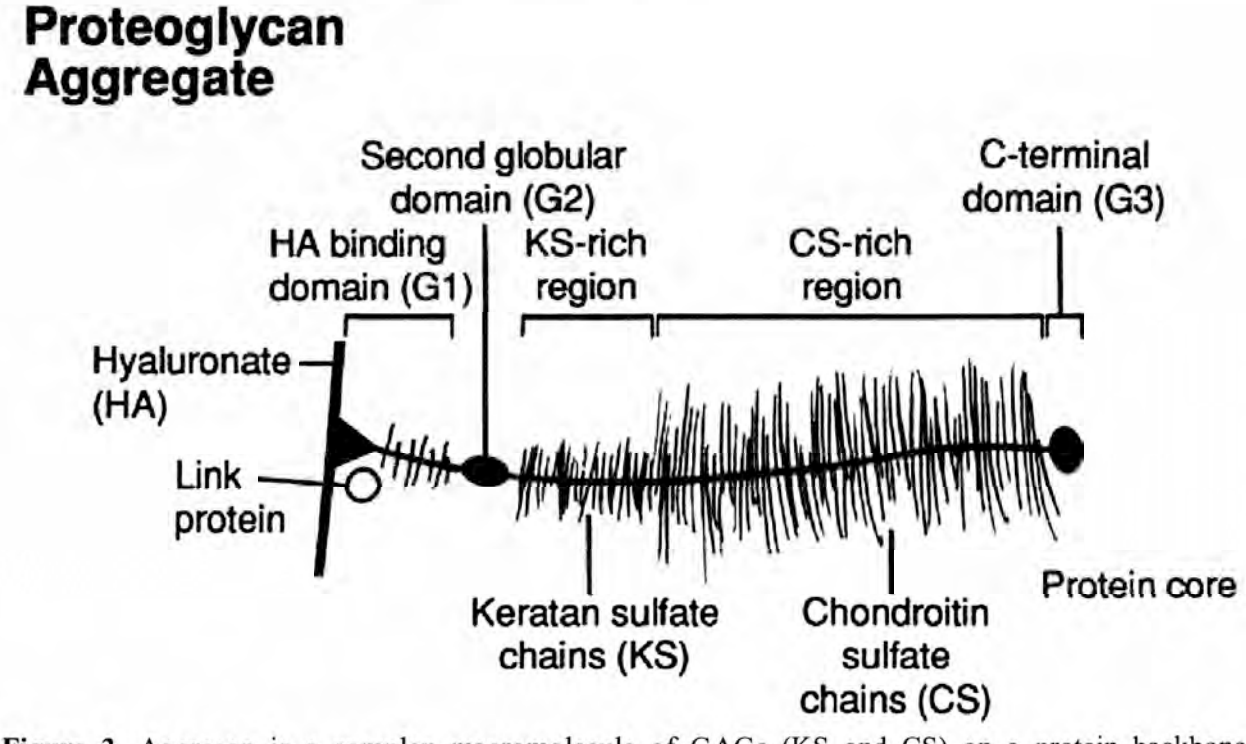


**Figure 3.** Aggrecan is a complex macromolecule of GAGs (KS and CS) on a protein backbone (Mankin, Mow, Buckwalter, Iannotti, & Ratcliffe 2000).

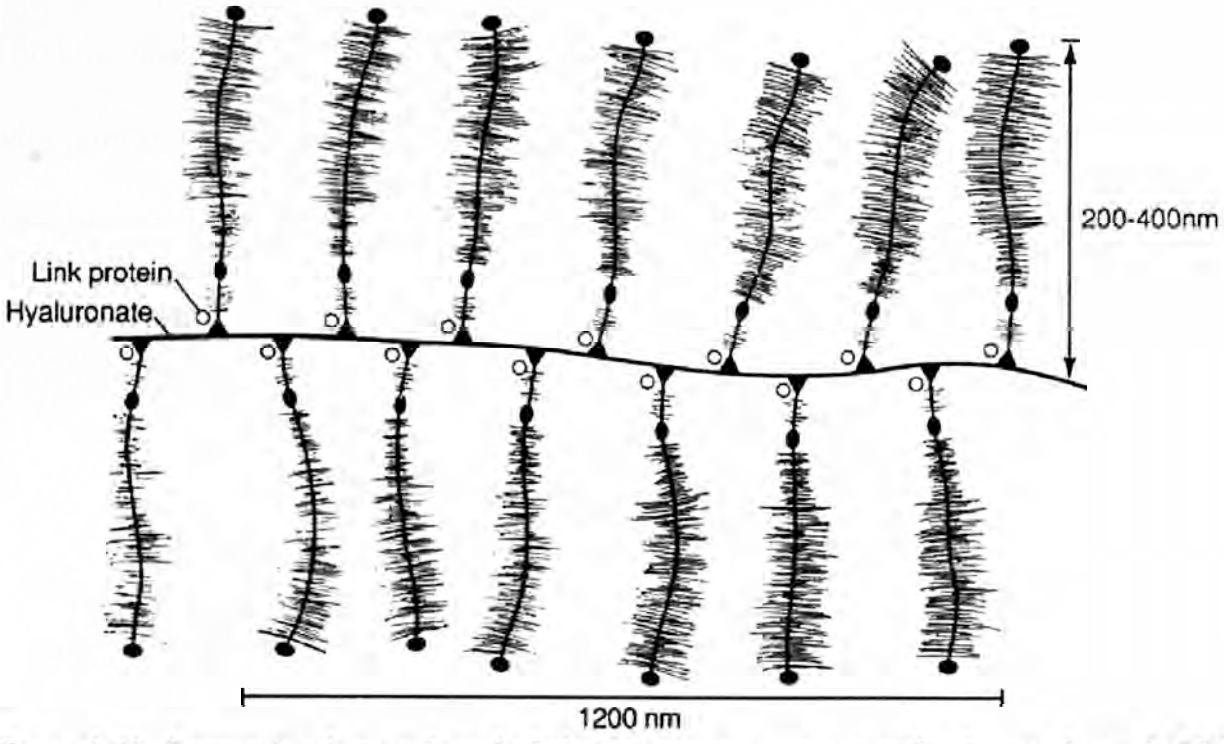


**Figure 4.** Hyaluronan is a long, unbranched chain that many aggrecan molecules attach to, via Link protein (Buckwalter, Kuettner, & Thonar 1985).

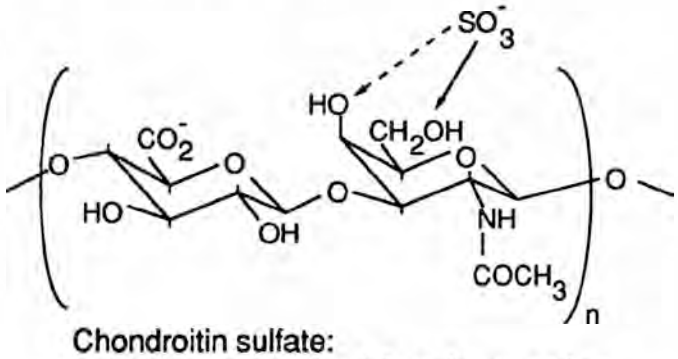


Chondroitin sulfate:
1,4-glucuronic acid - 1,3- galactosamine

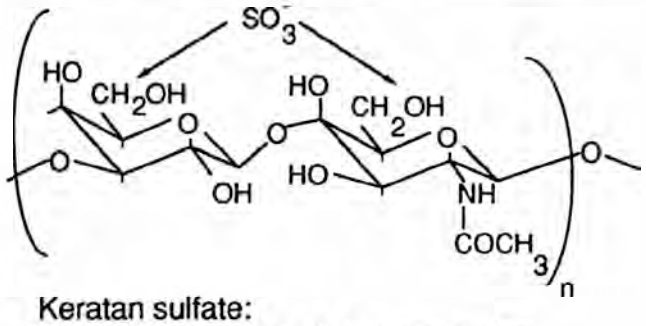


Keratan sulfate:
1,3-galactosamine - 1,4-glucosamine

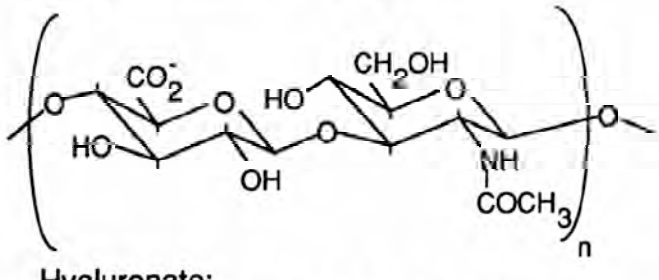


Hyaluronate:
1,4-glucuronic acid - 1,3-glucosamine

**Figure 5.** Chemical composition of the common GAGs (Wight & Heinegard 1991).

The long chains of proteoglycans and collagen fibrils are arranged in a loose network with pore size around the 2.5 to 6.5nm range (Nigg & Herzog 1998) which essentially traps water molecules with both mechanical and osmotic forces (Figure 5).

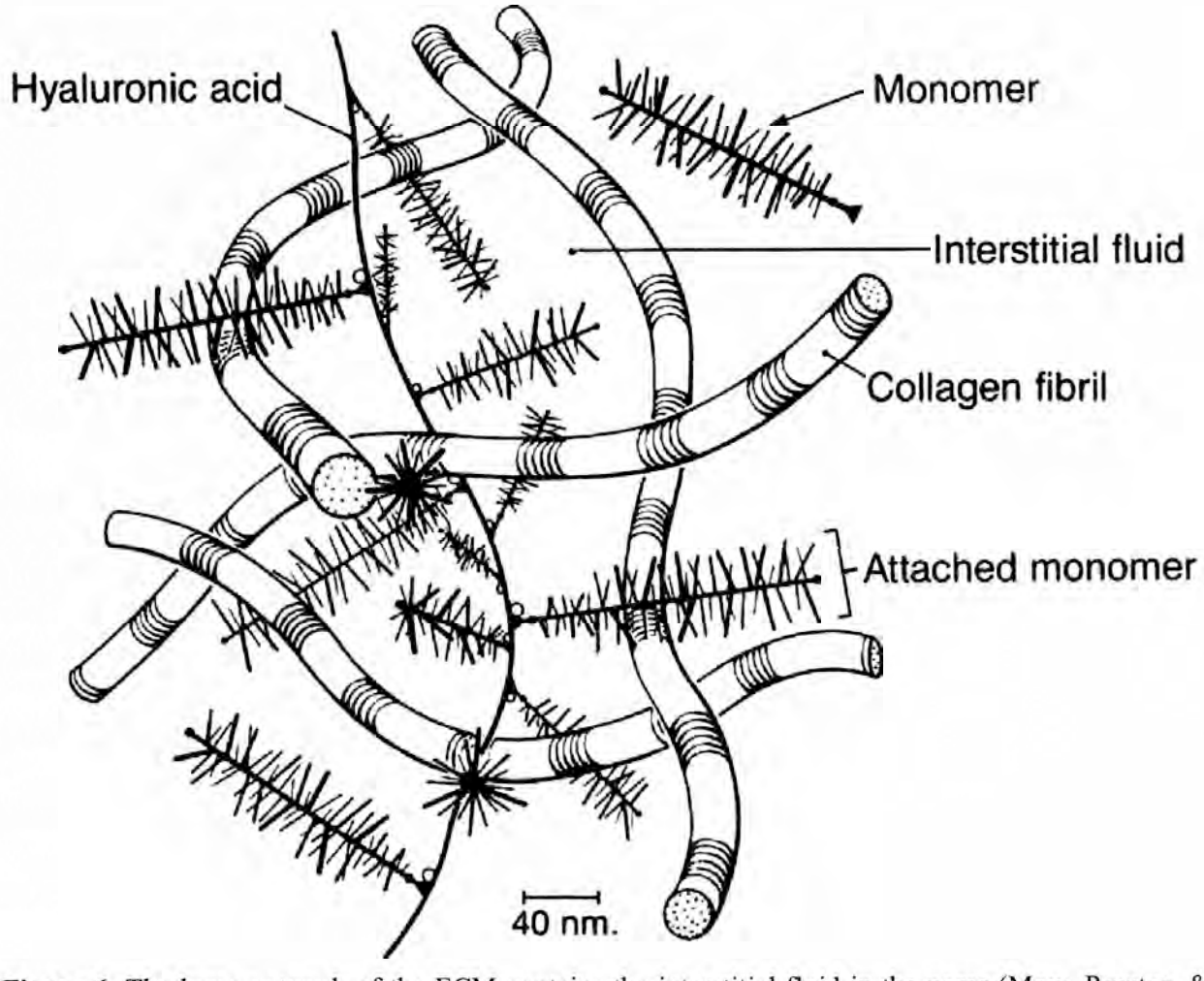


**Figure 6.** The loose network of the ECM contains the interstitial fluid in the pores (Mow, Proctor, & Kelly 1989)

### *2.0.4 Depth related variations*

The structure and composition of articular cartilage varies with the depth from the surface and has been subclassified into four zones: superficial, transitional, deep and calcified cartilage (Figure 7).

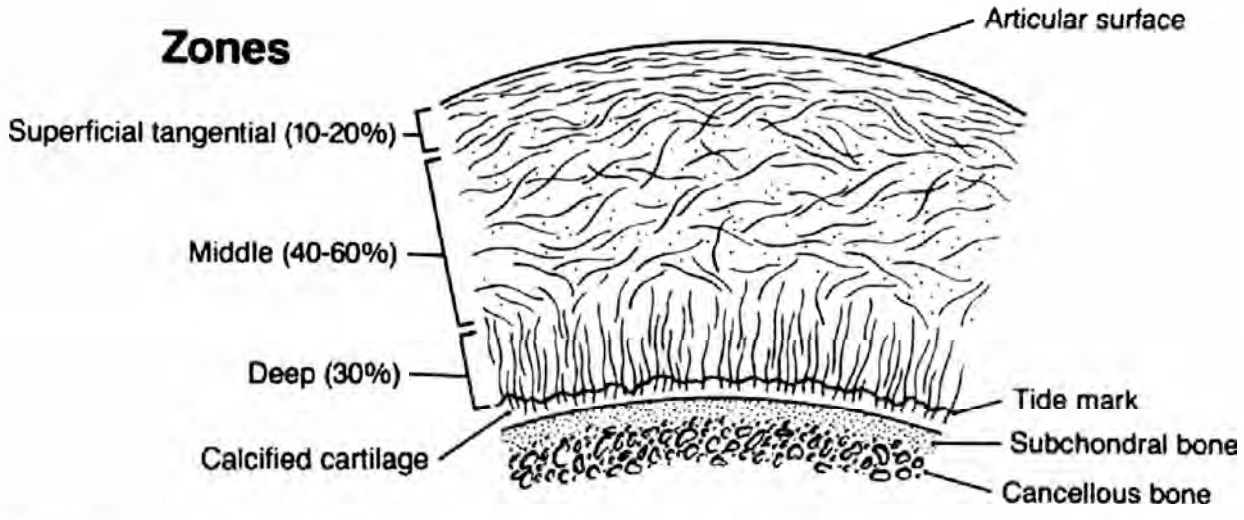


**Figure 7.** The articular cartilage structure varies with depth and can be classified into four distinct layers; superficial, middle (transitional), deep and calcified cartilage (Mow, Proctor, & Kelly 1989)

The superficial zone comprises approximately 10-20% of the thickness of the entire layer of cartilage and contains the highest level of water, with approximately 80% of the wet weight. Chondrocytes are elongated and aligned parallel to the surface, and in this zone they also produce lubricin, a joint lubricating molecule. Collagen fibrils are thin and aligned parallel to the surface. The superficial zone also has the highest tensile properties and the lowest concentration of proteoglycans (Mankin, Mow, Buckwalter, Iannotti, & Ratcliffe 2000;Mow & Ratcliffe 1997;Poole, Kojima, Yasuda, Mwale, Kobayashi, & Laverty 2001).

The transitional, or middle, zone comprises between 40 and 60% of the cartilage thickness (Mow & Ratcliffe 1997). It has less organised collagen fibrils that are larger in diameter and oriented in a transitional phase between the tangential fibrils of the superficial zone and the perpendicular fibrils of the deep zone. The chondrocytes are more spherical in shape and more metabolically active. The transitional zone is also rich is aggrecan (Nigg & Herzog 1998;Poole, Kojima, Yasuda, Mwale, Kobayashi, & Laverty 2001).

The deep zone contains the lowest amount of water (approximately 65%), but has the highest concentration of proteoglycans (Nigg & Herzog 1998). The collagen fibrils are large and oriented perpendicular to the cartilage surface, and the round chondrocytes are arranged in a classic columnar structure, although the concentration of collagen and cells is at their lowest. Aggrecan concentration is maximal in the deep zone (Poole, Kojima, Yasuda, Mwale, Kobayashi, & Laverty 2001).

The calcified cartilage is a thin layer bounded superficially by the tidemark and deep by the subchondral bone through which the deep zone collagen fibrils extend, anchoring the cartilage to the subchondral bone (Mow & Ratcliffe 1997;Nigg & Herzog 1998). The cells in the calicified cartilage zone are capable of synthesising type X collagen and calcifying the extracellular matrix (Poole, Kojima, Yasuda, Mwale, Kobayashi, & Laverty 2001).

## 2.1 Biomechanical behaviour of articular cartilage

Articular cartilage is able to withstand large repetitive and static forces for many decades and often for the lifetime of the body. This durability is due to the multiphasic nature of the tissue and the ability to absorb the majority of the compressive stress in the fluid phase. As described earlier, cartilage biomechanics can be described as multiphasic, where the three phases are the charged solid phase, the fluid phase and the ion phase which make up 20%, 80% and less than 1% of the tissue respectively. It may be surprising then that almost 95% of the compressive load is taken up by the fluid phase (including the ions) and only 5% by the solid phase (Mow & Wang 1999). The explanation for this lies in the relationship between the charged solid phase and the fluid phase.

As previously described, the solid phase, also known as the extracellular matrix (ECM), is a loose collagen network with associated proteoglycans. The interstitial fluid is able to flow through the pores in the ECM, however, this flow is resisted by extremely low permeability, of the order of $k=10^{-15}$ to $10^{-16}m^4/Ns$. Permeability is inversely related to drag by the equation $K=(\varphi^f)^2/k$, where $\varphi^f$ is the porosity of the tissue (0.6 to 0.85 for cartilage). Hence, the flow of interstitial fluid through the ECM requires a very large drag force of the order of $10^{14}$ to $10^{15}$ $Ns/m^4$ to be overcome (Mankin, Mow, Buckwalter, Iannotti, & Ratcliffe 2000). Thus, interstitial fluid flow through the ECM is the primary mechanism by which cartilage can withstand very large compressive forces. Importantly, as the tissue is compressed, the flow of fluid becomes more difficult because the pore size will be reduced and hence so will the permeability (Broom & Oloyede 1998).

The ability of the ECM to trap water molecules and withstand compressive loading is improved with the addition of the proteoglycans which introduce a fixed charge density to the ECM. This charge comes from the $SO_3^-$, $COO^-$ end groups fixed to the proteoglycan aggregate molecules (chondroitin sulphate, keratan sulphate and hyaluronan) (Broom & Oloyede 1998;Sah 2001;Sun et al. 2004). These charges are neutralised by the ions within the interstitial fluid and create an osmotic swelling pressure which contributes approximately 0.25MPa of resistance (Mankin, Mow, Buckwalter, Iannotti, & Ratcliffe 2000).

Articular cartilage is a viscoelastic material with properties that are dependent on strain rate and flow of interstitial fluid. The typical stress relaxation response can be described as an initial period of fluid efflux, followed by compaction of the ECM,

then redistribution of the fluid within the tissue before reaching equilibrium (Figure 8).

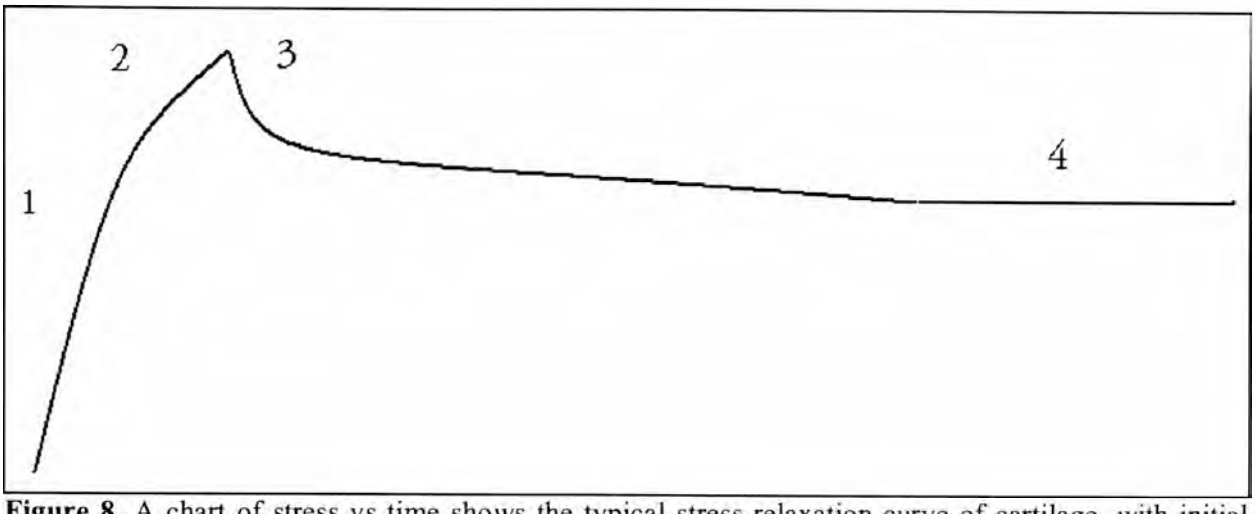


**Figure 8.** A chart of stress vs time shows the typical stress relaxation curve of cartilage, with initial fluid efflux (1) followed by ECM compaction (2), fluid redistribution (3) and equilibrium (4)

One of the most impressive properties of articular cartilage is the near negligible coefficient of friction, which helps maintain a smooth articulating joint. The coefficient of friction of the collagen matrix is determined experimentally as approximately 0.15, however, the coefficient of friction of articular cartilage is a mere fraction of this. The difference is accounted for by Amonton's Law which indicates that because only 5% of the compressive load is taken by the collagen matrix, then the coefficient of friction can be calculated as 0.05*0.15, which is 0.0075 (Mow & Wang 1999).

Some other important mechanical properties of articular cartilage and their average values in human cartilage are:

| | |
|---|---|
| Compressive modulus | |
| 0.79MPa | (Lu, Zhu, Valenzuela, Currier, & Yaszemski 2001) |
| 0.7MPa | (Mankin, Mow, Buckwalter, Iannotti, & Ratcliffe 2000) |
| 0.2 to 5MPa | (Mow & Wang 1999) |
| Shear modulus | |
| 0.68MPa | (Lu, Zhu, Valenzuela, Currier, & Yaszemski 2001) |
| Tensile modulus | |
| 0.32 to 10MPa | (Lu, Zhu, Valenzuela, Currier, & Yaszemski 2001) |

The compressive modulus, or compressive aggregate modulus ($H_A$), is found experimentally in a confined compression test using the following equation:

$$H_A = \frac{E(1-\nu)}{(1+\nu)(1-2\nu)}$$

Where E is the elastic modulus derived from the experiment and ν is the Poisson's ratio, which is typically 0.1 to 0.4 for human cartilage (Mankin et al. 2000).

## 2.2 Damage to cartilage and the healing response

Cartilage is a remarkably durable tissue, due to the factors described in the previous sections on the interplay between the collagen matrix, the proteoglycans and the interstitial fluid. Nonetheless, articular cartilage is still susceptible to damage, and as Hunter is quoted to have said in 1743 "it is universally allowed that ulcerated cartilage is a troublesome thing and that, once damaged, it is not repaired" (Hunter 1743). In fact, the quest to treat cartilage defects is estimated to cost more than US$65 billion per year (Lu et al. 2001). This excessive cost is thought to arise because even minor cartilage lesions can progress to joint degeneration and/or osteoarthritis (Custers et al. 2007;Guilak, Butler, & Goldstein 2001;Hunziker 2002;Jackson et al. 2001;Kirker-Head et al. 2006;Sah 2001).

The poor reparative capacity of cartilage is attributed to the lack of a blood supply and the lack of undifferentiated cells (Mankin et al. 2000). Chondrocytes are a highly differentiated cell which exhibits only a short lived proliferation in response to articular cartilage damage and this response is aborted after approximately 2 weeks. The ability of chondrocytes to repair cartilage defects is hampered by their low mitotic activity, low mobility through the matrix and their general scarcity throughout the tissue.

Cartilage may be damaged from various scenarios. These include acute damage (such as impact or blunt trauma) and chronic damage (such as interfacial wear, fatigue, disuse and ageing) (Nigg and Herzog 1998). Damage to articular cartilage in the knee is also frequently associated with damage to the ligaments in and around the knee (Hunziker 2002), or with chronic malalignment, osteonecrosis or infection. Disuse of

a joint leads to less synthesis of collagen, lower proteoglycan concentration and therefore results in easier fluid exudation and weakened mechanical properties. Ageing leads to reduced cartilage thickness, reduced proteoglycan concentration and decreased concentration of water which has the same effect of reducing the ability of cartilage to dampen and distribute load through the joint. Ageing and degeneration of cartilage also have a profound effect of reducing the mechanical properties of articular cartilage (Armstrong & Mow 1982;Hunziker 2002).

The normal healing response to damage in a vascular tissue is a three phase process. The first phase is necrosis of tissue surrounding the damaged region, the extent of which depends on the type of trauma and the blood supply. The second phase is inflammation where blood brings a fibrin clot and a variety of cells to the site of damage. The third phase is the repair phase, which begins with new vasculature that leads the repair of the tissue by fibrous scar, which may or may not be remodelled depending on the type of tissue (Mankin 1982). In the case of articular cartilage, which is avascular, the second and third phase of repair cannot eventuate because each of these phases are dependent on the local blood supply and angiogenesis to increase the vasculature. Although, when the damage to the cartilage penetrates through the tidemark and into the subchondral bone, then the vasculature of the bone becomes part of the mix.

Articular cartilage damage has been grouped into three different categories; blunt trauma (microdamage), partial thickness (chondral fracture) and full thickness (osteochondral fracture) (Frenkel & Di Cesare 1999;Mankin 1982). Blunt trauma can cause damage in the deep layers of the cartilage and also the subchondral bone,

without being evident from the cartilage surface. This type of damage can occur from a single high impact load or be accumulative from repetitive loading. Human articular cartilage can withstand up to 25MPa of blunt trauma before chondrocyte death and damage to the ECM become obvious (Buckwalter 2002). Repeated overloading of rabbit joints in vivo has been linked with chondrocyte clustering, fibrillations of the matrix, thickening of the subchondral bone and blood vessels from the subchondral bone penetrating the tidemark (Dekel & Weissman 1978). Trauma is also thought to be the underlying aetiology behind osteochondritis dissecans, a disease involving an osteochondral separation, particularly in the juvenile knee (Schindler 2007).

Partial thickness lesions generally do not elicit a healing response and do not necessarily progress to higher orders of damage such as osteoarthritis (Mankin 1982; Buckwalter 2002). The reason that there is no strong spontaneous healing response is that the damage extends from the articular cartilage surface, but does not penetrate into the subchondral bone so there is no bleeding and the triphasic healing response is truncated at the first phase.

Full thickness lesions (osteochondral defects, or osteochondral fractures) are cartilage defects that extends from the surface of the cartilage all the way into the subchondral bone, or even the cancellous bone beneath. In this instance there is a supply of blood from the vasculature in the subchondral bone and cancellous bone; both of which have a high concentration of blood vessels. The generally accepted pathway of repair in a full thickness lesion begins with the fibrin clot from the bone vasculature and it has been shown in a goat model that the clot is established within the osteochondral defect in 2 days (Jackson et al. 2001). Subsequent vascular invasion brings fibroblastic cells,

undifferentiated cells such as mesenchymal stem cells and growth factors (TGF-b, BMP, PDGF, IGF-I and IGF-II) (Buckwalter 2002) and fibrous repair tissue begins to bridge the defect by 1 week (Jackson, Lalor, Aberman, & Simon 2001).

Radioactive markers have proved that these undifferentiated cells originate from the bone, not the adjacent cartilage (Shapiro, Koide, & Glimcher 1993). After a period of weeks, the cells differentiate into chondrocytes which begin to synthesise a hyaline-like repair tissue, although the mechanical properties and structural organisation are always inferior to normal hyaline cartilage. This repair tissue progressively increases in quantity and at some stages may even resemble hyaline cartilage. Although the repair tissue may resemble hyaline cartilage, it is not true hyaline cartilage and is more of a mixture of fibrocartilage and hyaline cartilage. The repair tissue has reduced stiffness and increased permeability when compared to normal articular cartilage and it tends to revert to fibrocartilage after a period of time (Armstrong & Mow 1982;Buckwalter 2002;Frenkel & Di Cesare 1999;Furukawa et al. 1980).

While this repair tissue can initially alleviate symptoms such as pain and loss of joint function, the tissue begins to degrade in less than one year (Mankin 1982; Shapiro et al. 1993; Jackson et al. 2001; Buckwalter 2002). In fact, researchers have found that the repair tissue from spontaneous healing of an osteochondral defect in the rabbit begins to degrade after only 12 to 20 weeks (Shapiro et al. 1993). The repair cartilage is more prone to degradation due to it's increased permeability to water which leads to damage of the extracellular matrix from an increased share of the compressive force through the tissue.

The bone compartment of an osteochondral defect will sometimes repair and remodel to resemble the normal cancellous and subchondral bone compartments. However, several studies have shown that the subchondral and cancellous bone do not reconstitute fully, nor does the tidemark re-establish in the scenario of an empty osteochondral defect (Jackson, Lalor, Aberman, & Simon 2001;Sellers et al. 2000;Vizesi et al. 2007b). The study by Sellers, et al. showed that the tidemark was not re-established in an empty osteochondral defect or a defect treated with a collagen sponge, although it was re-established when treated with BMP-2 in a collagen sponge. It is likely that the osseous region of an empty osteochondral defect does not heal fully due to changes in the load path through the joint and subsequent remodelling as dictated by Wolff's Law. Another possibility is that the synovial fluid under pressure in the joint causes damage to the bone as the joint is repetitively loaded and unloaded. Either way, without rapid healing of the osseous compartment of an osteochondral defect, there is no foundation on which to repair the chondral compartment. Hence the deposition and remodelling of bone is a vital component in the overall healing of a full thickness cartilage defect.

## 2.3 Treatments for articular cartilage defects

There are many techniques available to the surgeon for the treatment of articular cartilage defects. These treatments can be classified as repair, regeneration, relief or replacement. Reparative techniques, such as microfracture, stimulate the cells to initiate a reparative response, although the repair is normally fibrocartilage. Regeneration, or restoration, is concerned with attempts to regenerate the articular cartilage layer with normal hyaline tissue, using methods such as osteochondral grafting or tissue engineering. This frequently involves regeneration of the osseous compartment as well. The term relief is normally used referring to correction of malalignment of the joint and I will use replacement to refer to the extensive surgical methods of total or partial joint replacement. There is also a fifth category of surgical treatments that are generally considered to be passive, in that they can alleviate pain and other symptoms, but are generally considered to have little biological value in the long term.

Joint lavage is a simple procedure of rinsing the joint under arthroscopy, which has been reported to relieve pain in many patients (Livesley et al. 1991). This lavage procedure may have the effect of washing away pain mediating molecules (Hunziker 2002) or free particulates in the joint, or may even be simply a placebo effect. Debridement is the surgical removal of tissue flaps or damaged regions of cartilage. This process has little scientific basis, since no repair tissue is formed and the existing tissue surrounding the debrided area progressively degenerates (Kim, Moran, & Salter 1991;Mitchell & Shepard 1987). Although, the procedure can alleviate pain and the feeling of the joint surfaces "catching" each other and/or "locking".

Another therapeutic treatment is the intraarticular administration of sodium hyaluronan, which is ubiquitously distributed throughout the extracellular matrix of healthy articular cartilage. Blinded, randomized clinical trials of these regular injections have shown contradictory results, with some researchers finding the sodium hyaluronan injections to provide superior results to placebo (Altman & Moskowitz 1998;Huskisson & Donnelly 1999) and others finding no difference (Altman et al. 2004;Petrella & Petrella 2006).

### *2.3.1 Reparative techniques*

Abrasion chondroplasty, Pridie drilling and microfracture are three techniques that penetrate the subchondral bone to access the undifferentiated cells and initiate a spontaneous healing response (Insall 1967;Insall 1974;Kim, Moran, & Salter 1991;Steadman et al. 1999). All three techniques result in a fibrocartilage repair that degrades rapidly although the results are improved in younger populations (Furukawa, Eyre, Koide, & Gilmcher 1980;Hunziker 2002). Abrasion chondroplasty is a procedure in which the surgeon uses a burr to scrape away the top layer of the subchondral bone to initiate bleeding, clot formation and fibrocartilaginous repair tissue. Pridie drilling was championed by a surgeon of the same name, and reported by Insall in 1967 and involves drilling into the subchondral bone with drills 2-3mm in diameter. Again, the purpose of this penetration of the bone is to initiate bleeding and spontaneous healing. Microfracture is a modification to the Pridie drilling technique, which differs only in that smaller holes are drilled, with the intention of being less disruptive to the structural integrity of the bone.

These techniques are often considered to be more conservative treatment strategies for articular cartilage because they have the potential to relieve symptoms for a period of a few years and are not likely to cause any more damage to the joint. Although, these techniques are occasionally used in conjunction with other techniques, such as autologous cell transplantation (Dorotka et al. 2005), gene therapy with growth factors (Morisset et al. 2007) and high tibial osteotomy (Miller et al. 2007). The conclusions drawn from these studies must be cautious due to the relative contributions of each component of the treatment being unknown.

### 2.3.2 Relief techniques

The reparative techniques available to the surgeon are limited because they are generally only indicated for patients less than 45 years of age, with an isolated lesion and no osteoarthritis or joint malalignment (O'Driscoll 1998). For patients who have joint malalignment, an osteotomy may be performed. This relief technique is used to correct varus/valgus or to shift the contact area of the joint from a degenerated region of cartilage to a healthier region. This can help alleviate pain for some time, although animal studies have shown osteotomies to be associated with a slow progression to osteoarthritis (Panula, Helminen, & Kiviranta 1997).

### 2.3.3 Regenerative techniques

Surgical interventions to regenerate articular cartilage and subchondral bone are at the forefront of current scientific research. These techniques have the ultimate aim of the treated articular cartilage defect being indistinguishable from normal hyaline cartilage in macroscopic and microscopic appearance, biochemical composition and mechanical properties. The realisation of this goal is still a long way off, however, results with several of the techniques are promising.

Autologous tissue transplantation with periosteum, perichondrium or osteochondral plugs into the defect have been popular regenerative strategies for at least two decades. Periosteal or perichondrial tissue continues to be highly osteogenic or chondrogenic throughout the life of the body (Hunziker 2002) which makes it an attractive choice as a graft for osteochondral defects. Although these tissues are a fantastic supply of cells to participate in synthesis of new matrix, 67% of the cells found in the repair tissue actually originate from the bone below (Zarnett & Salter 1989). Complete restoration of the articular cartilage does not normally occur and the repair tissue is not stable over the long term. This has been reported in rabbits (Carranza-Bencano et al. 1999) and humans (Homminga et al. 1990). Although, when combined with continuous passive motion, periosteal grafts with the cambial layer facing up into the joint produced excellent results in rabbits (O'Driscoll, Keeley, & Salter 1986).

### 2.3.3.1 Osteochondral transplantation

Osteochondral transplantation is also known as mosaicplasty or the OATS technique (Osteochondral Autograft Transfer System, trademark of Arthrex, Naples, FL). In this technique, a cylinder of healthy osteochondral tissue is harvested from a non-weight bearing region of the knee and transplanted into a hole created in the cartilage lesion (Figure). Good short term results have been reported in humans (Laprell & Peterson 2001;Miniaci & Martineau 2007), rabbits (Kuroki et al. 2007) and sheep (Burks et al. 2006;Tibesku et al. 2004), however, the real proof of the efficacy of osteochondral grafting will not be known until long term data from human patients is published. One paper reported good-to-excellent results in 92% of femoral condyles restored with mosaicplasty over a period of 10 years, although this was reduced in other areas

of the knee (Szerb et al. 2005). This is a promising result although data from blinded, multicentre clinical trials is required for confirmation.

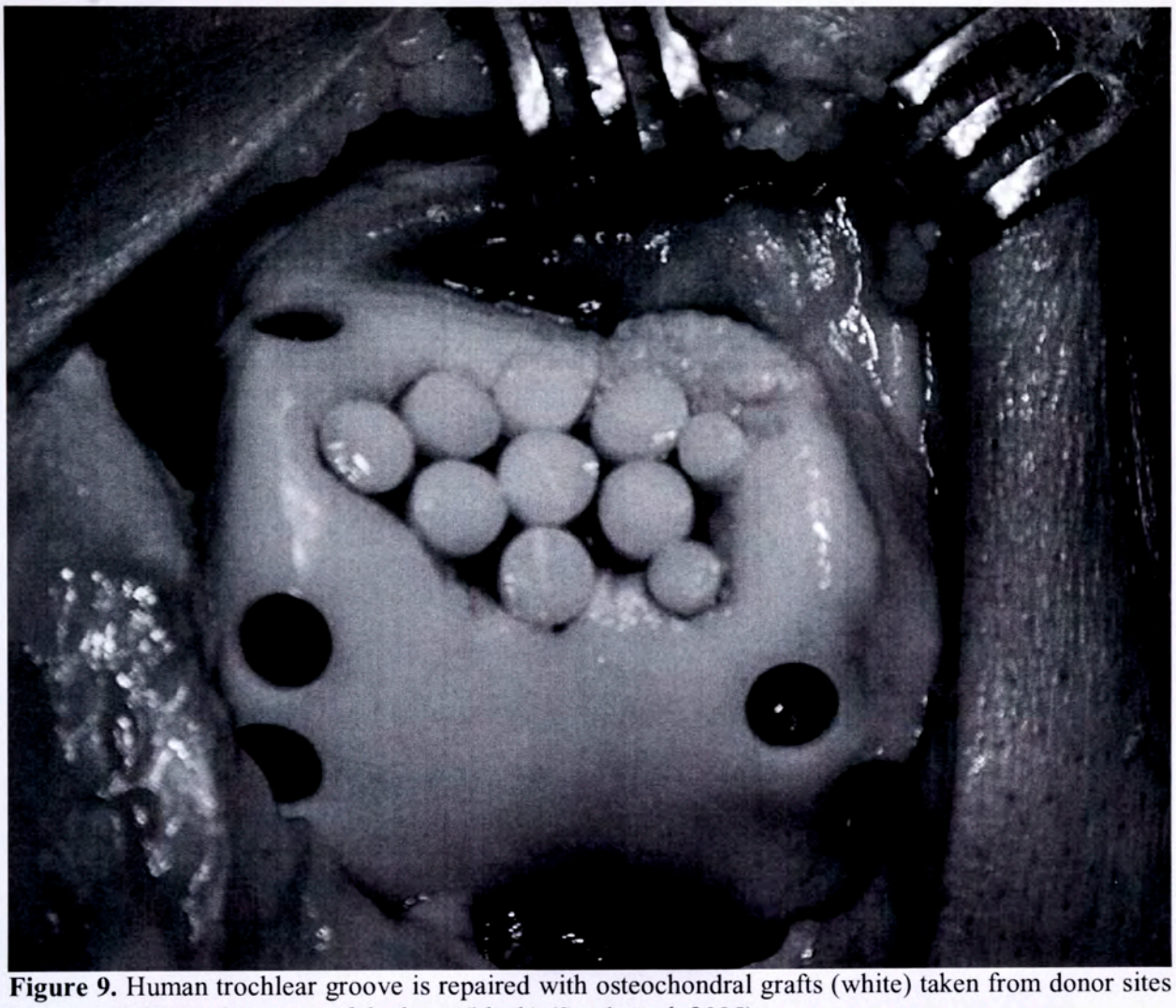

**Figure 9.** Human trochlear groove is repaired with osteochondral grafts (white) taken from donor sites in non-weight bearing areas of the knee (black) (Szerb et al. 2005).

Osteochondral grafting has disadvantages stemming from the graft harvest sites. Donor site morbidity is a concern and it also limits the number of grafting procedures that a patient can have in a lifetime because the donor sites are empty osteochondral defects and would therefore not be expected to heal. Another cause for concern is that the grafts are taken from non-weight bearing areas and are transplanted into load bearing areas for which the cartilage is not adapted (Hunziker 2002). Mosaicplasty also results in a smaller area of contact (Figure 9), which translates to higher stress in the cartilage and could possibly lead to early degradation of the matrix in the graft. Another possible damage mechanism is the blunt trauma to the graft in the form of hammering it into the defect to achieve a press-fit for stable fixation (Hunziker

1999a;Hunziker 1999b). A lack of integration with the adjacent cartilage is also common, even though the osseous region is well integrated (Tibesku et al. 2004; Burks et al. 2006) (Figure 10). Nonetheless, osteochondral grafting is an attractive technique for treatment of focal cartilage lesions in young patients (Willers, Wood, & Zheng 2003) with a high percentage of hyaline cartilage remaining in the graft after several months (Harman et al. 2006).

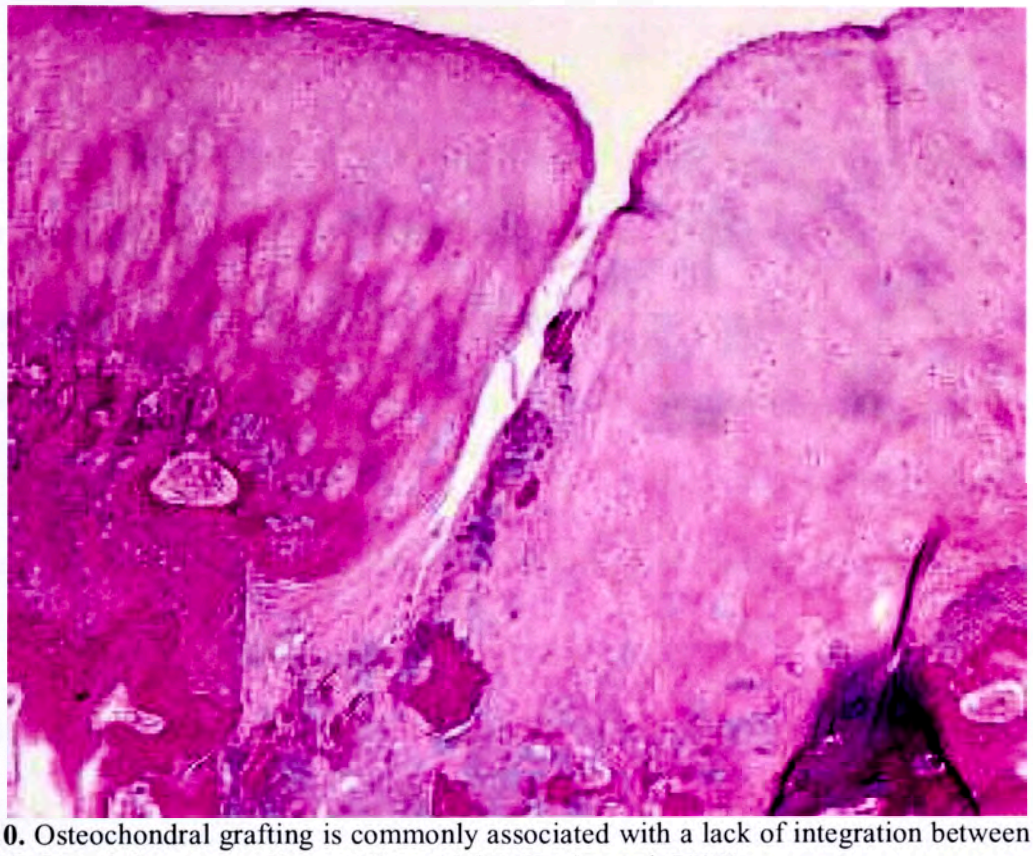

**Figure 10.** Osteochondral grafting is commonly associated with a lack of integration between the graft cartilage (left) and the surrounding cartilage (right) (Burks et al. 2006).

### 2.3.3.2 Autologous Chondrocyte Implantation

Autologous chondrocyte implantation (ACI) is a controversial treatment that makes use of autologous chondrocytes that are expanded in culture using the Carticel™ technique (Genzyme, Cambridge, MA). Essentially, the ACI technique involves two separate surgeries; first to harvest healthy cartilage to extract the chondrocytes from, and secondly to re-implant them into the prepared defect. In between these surgeries, the graft tissue is sent away to the Carticel™ laboratory where the chondrocytes are expanded in culture for several weeks until approximately $12x10^6$ cells are obtained.

The second surgery involves trimming away the damaged cartilage to create a well defined defect. Normally the subchondral bone is not penetrated. A piece of periosteum is then harvested from the tibia and sutured over the top of the defect, creating an enclosed environment. The autologous cells are then injected under the periosteal flap into the defect. Whilst this technique is pioneering the way for cellular based therapies, the overly positive published results from a single group of surgeons has not been met with widespread acceptance (Willers et al. 2003).

ACI was first reported clinically in 1994 (Brittberg et al. 1994), and it remains to be a popular technique although it has several drawbacks and associated disadvantages. The drawbacks associated with ACI include the inconvenience and cost associated with two surgeries and the long wait during the cell culturing process. Also the ability of the periosteal flap to contain the cells is questionable. Complications such as periosteal flap calcification and degradation of the adjacent cartilage from suturing are also of concern (Willers et al. 2003). Nonetheless, several papers have reported that ACI outperforms grafts treated with periosteum alone (Brittberg et al. 1996;Grande et al. 1989).

The rehabilitation program for patients treated with ACI is also restrictive. Patients treated with ACI for defects in the trochlea groove were required to undergo continuous passive motion 6-8hrs per day for up to 6 weeks, before being allowed full weight bearing (but not walking) at the eighth postoperative week. Intensive physiotherapy including electrical muscle stimulation as part of a strengthening program was conducted and the patient was allowed gentle exercise (walking, swimming etc) after 5 to 6 months. Jogging was allowed after 8 to 12 months, and

restrictions on the joint were removed after 12 to 18 months (Mandelbaum et al. 2007). Such an intensive and restrictive rehabilitation prevents the patient from being able to work or participate in normal daily activities for much longer than the other popular cartilage treatment techniques.

The ACI technique is expensive and it is still too early for the results from cost-benefit analysis to determine if the procedure is worthwhile over techniques such as mosaicplasty and microfracture (Clar et al. 2005). Healthcare systems around the world have raised concern over reimbursement for this technique and the Australian healthcare system has suspended reimbursement due to scepticism of the benefit to the patient against the cost to the healthcare system. This scepticism is not unfounded since the results from various clinical and preclinical trials are contradictory. For example, when ACI is compared to microfracture, some authors suggest that ACI gives better results (Dorotka, Windberger, Macfelda, Bindreiter, Toma, & Nehrer 2005), whilst others report no difference (Knutsen et al. 2004). The same scenario is presented with comparison between ACI and mosaicplasty, with one study reporting better success with ACI (Bentley et al. 2003) and another reporting better success with mosaicplasty (Horas et al. 2003). The paper by Bentley, et al. measured success by functional clinical scores and arthroscopy; however, the paper by Horas, et al. also included histology of biopsies. These biopsies showed the ACI regenerated cartilage to be mostly fibrocartilaginous with only occasional regions of hyaline-like tissue, whereas the osteochondral grafts remained as hyaline tissue.

The technology behind ACI has more recently been modified with the addition of a matrix constructed from either collagen I/III or hyaluronic acid. Rather than injecting

12 million cells into the defect underneath a periosteal flap, the MACI technique (matrix-induced autologous chondrocyte implantation) seeds the cells onto a three dimensional matrix. This matrix is then secured within the defect using fibrin glue, avoiding the potential complications of the periosteal flap and also being more technically simple to perform. The MACI technique is reported to have similar results to ACI, possibly with accelerated hyaline cartilage formation (Zheng et al. 2007). Although at least one of these authors has a potential conflict of interest through association with Genzyme. To compound this, other authors have found that ACI results in a higher percentage of hyaline tissue compared to MACI (Bartlett et al. 2005). Therefore, long term, randomised clinical trials are needed to determine the efficacy of the MACI technique.

### 2.3.3.3 Other biological solutions

**Allografts**

Osteochondral and chondral allografts or allogenic chondrocytes are also available to the surgeon, however, as with all allogenic tissue, there are complications relating to sterilisation, immunological response and the shortage of supply. Nonetheless, results with allogenic chondrocytes and osteochondral plugs have shown significant quantities of hyaline tissue after more than a year in rabbit models (Rahfoth et al. 1998;Schreiber et al. 1999;Wakitani et al. 1989).

**Demineralised bone matrix**

Demineralised bone matrix (DBM) is produced by solubilising the mineral from allogenic bone using hydrochloric acid (Walsh & Christiansen 1995). The resulting material is soft and rich in growth factors such as BMPs (bone morphogenetic

protein). Bone retains it osteoinductivity after demineralization with HCl, which means that even when implanted ectopically, new bone will form inside the material. This new bone forms through an endochondral pathway, which has sparked interest for DBM to be used for cartilage regeneration since the endochondral pathway might be expected to truncate at the level of hyaline cartilage when exposed to the specific environment of the articulating surface.

DBM has had mixed success when used to treat osteochondral defects. Gao, et al. reported that defects treated with DBM from a cortical bone source exhibited reconstituted subchondral bone and tidemark, and a smooth cartilage layer expressing collagen type II at 12 weeks in a rabbit model. The results from DBM from a cancellous bone source were much less impressive, which is probably due to a lower concentration of growth factors and other cytokines (Gao et al. 2004). Others have reported repair tissue with extremely variable quality, although never calcifying towards the joint surface (Dahlberg & Kreicbergs 1991). Perhaps then, this is indicative of the ability of the synovial environment to truncate the endochondral pathway at the hyaline cartilage stage.

**Mesenchymal stem cells**

A major drawback from using autologous chondrocytes is that the cells must be harvested from an area of healthy cartilage, potentially causing degeneration in the surrounding areas, or possibly being unavailable for a host of reasons. Autologously derived mesenchymal stem cells (MSCs) are an attractive solution because they can be derived from adult sources such as the synovium, bone marrow, periosteum or adipose tissue (Sakaguchi et al. 2005). MSCs are pluripotent cells, meaning that they

are undifferentiated cells that can differentiate into specific cell phenotypes, such as chondrocytes. They have been utilised by many researchers for the purpose of articular cartilage regeneration with excellent results in terms of both cartilage and subchondral bone regeneration (Awad et al. 2004;Guo et al. 2004;Sakaguchi, Sekiya, Yagishita, & Muneta 2005;Uematsu et al. 2005;Wakitani et al. 1994;Yoneno et al. 2005). The aim of MSC treatment is to replicate the good results of the MACI and ACI techniques with lower cost and a more plentiful supply of cells.

**Growth factors**

Cytokines are proteins that can direct cell proliferation and differentiation in either a positive or negative direction. Growth factors are essentially cytokines that direct the differentiation of cells in a positive direction. Due to this characteristic, growth factors, and in particular the transforming growth factor-beta (TGF-β) superfamily including bone morphogenetic proteins 2 and 7 (BMP-2 and BMP-7), are drawing significant attention in the field of osteochondral regeneration. TGF-β has been reported to induce formation and differentiation in both bone and cartilage in osteochondral defects (Willers et al. 2003). Yoneno, et al. reported that MSCs treated with TGF-β differentiate into osteoblasts in culture, but when dexamethasone is included they will differentiate into chondrocytes. The chondrogenic potential of both BMPs and TGF-β have been confirmed in vitro (Fisher et al. 2004;Hunziker 2001;Johnstone et al. 1998;Mackay et al. 1998;Yoneno, Ohno, Tanimoto, Honda, Tanaka, Doi, Kawata, Tanaka, Kapila, & Tanne 2005). Also, the ability of these proteins to increase chondrocyte proliferation has been confirmed (Fisher et al. 2004), however, these experiments are much more difficult to validate in vivo where many other signalling molecules and cells are unable to be controlled. An in vivo study by

Sellers, et al. showed improved osteochondral healing with BMP-2, including the re-establishment of the tidemark, which was not seen in groups without the growth factor.

Similar to the cellular therapies, administration of growth factors must occur through a vehicle, such as a controlled-release matrix (Elisseeff et al. 2001). This study encapsulated PLGA microspheres, loaded with TGF-β into a PEO hydrogel and noted significant improvement in proteoglycan production in vitro compared with the same construct minus the growth factors. A major area of interest with growth factors and cytokines is the dose and dose-rate dependence on the biological response. In other words, it is not yet known when a growth factor should be administered, and what quantity should be administered at that time. Caterson, et al. showed no differences in cell cultures that received a single dose of TGF-β compared to a continuous dose, although they make no mention of how they came up with the dose administered (Caterson et al. 2001).

#### 2.3.3.4 Biomaterial matrices

Many different permutations and combinations of biomaterials have been suggested to overcome the scarcity of suitable autograft or allograft material and to avoid the complications with autograft transplantations, such as donor site morbidity. These materials can be fast degrading, slow degrading or non-degradable, and may be derived either synthetically or naturally. Although, if a non-degrading material is used the technique is referred to as a cartilage replacement technique, rather than regeneration. Degradable biomaterial matrices are frequently used in combination with cells and growth factors in the rapidly emerging field of tissue engineering.

Two popular naturally derived materials are hyaluronic acid and collagen, both of which are found naturally in both bone and cartilage. Both materials have been used with and without cells with good success in articular cartilage defects, although the addition of cells is almost always reported to be beneficial (Bartlett, Skinner, Gooding, Carrington, Flanagan, Briggs, & Bentley 2005;Frenkel et al. 2005;Grigolo et al. 2001;Marcacci et al. 2002;Zheng, Willers, Kirilak, Yates, Xu, Wood, & Shimmin 2007). Other naturally derived materials under consideration for cartilage defect repair are chitosan (Frenkel, Bradica, Brekke, Goldman, Ieska, Issack, Bong, Tian, Gokhale, Coutts, & Kronengold 2005;Hoffman 2002), agarose (Rahfoth et al. 1998; Awad et al. 2004) and alginate (Awad, Wickham, Leddy, Gimble, & Guilak 2004;Cohen et al. 2003;Lee et al. 2007). These naturally derived polymers are frequently used in combinations with each other and with synthetic polymers. They are all biodegradable and have long histories of biocompatibility that makes them attractive as temporary support for cell synthesis of cartilage matrix, or to act as a vehicle for growth factors. None of the natural derived materials have sufficient mechanical properties or chemical stability to successfully repair a cartilage defect alone (Frenkel and Di Cesare 2004).

Synthetic materials are also under consideration for the purpose of articular cartilage regeneration, and also for cartilage replacement. The most popular are the polyesters, such as polylactic acid (PLA, PLLA, PDLA), polyglycolic acid (PGA) and combinations of the two (PLGA) (Aamer et al. 2004;Ara, Watanabe, & Imai 2002;Chen et al. 2004;Cohen, Meirisch, Wilson, & Diduch 2003;Elisseeff, McIntosh, Fu, Blunk, & Langer 2001;Park et al. 2005;Uematsu, Hattori, Ishimoto, Yamauchi, Habata, Takakura, Ohgushi, Fukuchi, & Sato 2005). Sometimes the materials are

biphasic with one region with mechanical properties similar to articular cartilage and another with properties similar to cancellous bone. Sherwood, et al varied the composition of PGA and PLLA and the porosity in their construct to create a gradient from the cartilage surface to the bone compartment, which contained 25% βTCP by weight (Sherwood et al. 2002). These constructs showed positive staining for Safranin-O after 4 weeks in culture, indicating synthesis of proteoglycans by the chondrocytes. However, the neo-tissue did not resemble hyaline cartilage.

Chen et al, provided another example of a hybrid material utilising the popular degradable polyester PLGA, but with collagen microspheres interspersed in the pores. The addition of collagen to the material resulted in more homogenous cell morphology compared to PLGA alone (Chen, Sato, Ushida, Ochiai, & Tateishi 2004). Park, et al. showed that chondrocytes will interact more positively with PLGA matrices that have been treated with NaOH to etch the surface. PLGA treated with 1N NaOH for 10mins was reported to have significant increases in cell number and quantity of proteoglycans synthesised in vitro compared to untreated PLGA (Park et al. 2005). Other synthetic matrices that are being investigated for cartilage regeneration include polyethylene glycol (PEG) hydrogels (Bryant et al. 2004) and polyethylene oxide (PEO) hydrogels (Bryant & Anseth 2001).

### *2.3.4 Replacement*

The definition of cartilage replacement for the purposes of this thesis is that of a non-biological substitute for a damaged osteochondral or chondral region. Perhaps the most recognisable treatment falling under this definition is the total joint replacement, which was first mastered in the hip before meeting success in the knee and now more recently the shoulder. Total joint replacements are also available for the elbow,

temporomandibular joint, intervertebral disc and even the metacarpo-phalangeal joints. It is also possible now for the knee to be treated with a unicompartmental knee replacement, which typically replaces the medial condyle of the femur and tibia but leaves the lateral side intact. Another possibility is joint resurfacing, in which only one condyle, or part thereof, is replaced. Joint resurfacing in the distal femur has recently become a reality with the HemiCAP™ device (Arthrosurface), which is detailed more thoroughly in Chapter 5.

With the exception of joint resurfacing, all of these total joint replacements are indicated for end-stage treatment of severely degenerate joints, such as in the case of advanced osteoarthritis. They require significant resection of bone stock to anchor the non-degradable metallic, ceramic or polymeric components which make revisions challenging and expensive. Hence, these treatments are not ideally suited to a young patient who might be expected to be revised on more than one occasion. Most other treatments discussed so far have been indicated for focal, full-thickness cartilage lesions, with the aim of offsetting, or preventing the necessity of a joint replacement. However, there is also a small market for non-degradable biomaterials for cartilage replacement in focal lesions, such as physically crosslinked polyvinyl alcohol hydrogel plugs (Falez & Sciarretta 2005). The aim of these implants is to prevent further degeneration of the joint by replacing a small damaged region with a soft, but strong material with similar mechanical properties to the native tissue. This approach might offset a unicompartmental or total joint replacement by several years, and would be much cheaper and have fewer complications than a comparative biological therapy.

## 2.4 Animal models of articular cartilage defects

Whilst valuable information can be gained from in vitro studies and to some extent computer modelling, animal models are essential to evaluate the effectiveness of new treatments for osteochondral defects. Care must be taken to select an appropriate model because the results of the study will, in part, be reliant on what animal model is used. Several factors are important to control: species, age and gender of the animal, as well as the size and location of the defect and the duration of the study.

It is well known that the metabolic activity of chondrocytes and osteblasts and their reactivity to cytokines is reduced in mature tissues when compared to young or developing tissues (ASTM 2005;Mankin, Mow, Buckwalter, Iannotti, & Ratcliffe 2000;Mankin, Mow, & Buckwalter 2000). Hence, it is important to control the animal model for the age of the animal, and normally it would be preferential to select an adult model. A skeletally mature model is evidenced radiographically by fused epiphyseal growth plates.

Relative size and weight of a species can be markedly different between genders. Males generally have increased volume of cartilage irrespective of body size or physical activity, and this difference becomes more pronounced with age (Ding et al. 2003). This in itself is a good reason to gender match animals in an osteochondral defect study, although perhaps more significant are the known influence of gender-related hormones, including steroids such as testosterone and estrogen, on bone and cartilage maintenance. In particular, hormonal variations in menopausal or lactating females are known to influence bone resorption rates. Hence, male animals would often be considered a more favourable model.

The location of the defect will often depend on the desired application of the technology being tested, although it should be known that the healing response in weight bearing and non-weight bearing cartilage is different. The knee is the most commonly selected joint in animal models, partly because localised osteochondral defects are most commonly found in the femur clinically (ASTM 2005), and partly because it is easier to operate on than the hip. The location should be selected with knowledge of the gait of the animal, with associated ground reaction and joint forces, which can be determined using video gait analysis techniques (Taylor et al. 2006). Popular regions for defects include the weight bearing medial femoral condyle (Brittberg, Lindahl, Nilsson, Ohlsson, Isaksson, & Peterson 1994;Burks, Greis, Arnoczky, & Scher 2006;Grigolo, Roseti, Fiorini, Fini, Giavaresi, Aldini, Giardino, & Facchini 2001;Horas, Pelinkovic, Herr, Ainger, & Schnettler 2003;Jackson, Lalor, Aberman, & Simon 2001;Pearce et al. 2001) and the trochlea groove (Mandelbaum, Browne, Fu, Micheli, Moseley, Erggelet, & Anderson 2007;O'Driscoll, Keeley, & Salter 1986;Uematsu, Hattori, Ishimoto, Yamauchi, Habata, Takakura, Ohgushi, Fukuchi, & Sato 2005). Less commonly, the defect is made in the patella (ASTM 2005).

Choice of defect size is normally recommended to be greater than or equal to the critical size defect, i.e. a defect that will not heal itself without treatment. The critical size depends on many factors, including the species, age and location. The approximate critical size defect in the medial femoral condyle of the rabbit, sheep/goat and horse are 3, 6-7 and 9mm in diameter respectively (Jackson et al. 2001; ASTM 2005). Care must be taken to create the defect perpendicular to the surface without damaging the adjacent tissue. Another factor of primary importance is

the method that the defect is created. Evans, et al. showed manual punches provided greater chondrocyte viability in harvesting osteochondral grafts compared to powered trephines, whilst Chapter 2 of this thesis highlights superior healing in an osteochondral defect created with a punch compared with a drill (Vizesi et al. 2007).

The different animal models for research can be grouped into large and small animal groups. The small animals include mice, rats and rabbits. Of these, only the rabbit is of a sufficient size to be any use for osteochondral defect studies. The large animals commonly used for osteochondral defect studies include the horse, sheep and goat. The dog (Klompmaker et al. 1992;Ushio et al. 2004) is intermediate between the rabbit and the large animal models. The specifics of each animal model with respect to osteochondral defect studies are shown in Table 1 (ASTM 2005).

**Table 1.** Animal models for osteochondral defect studies (ASTM 2005)

| Species | Age of Adult Eqivalancy | Weight at Adult Equivalancy | Defect Sites Commonly Used | Cartilage Thickness at Femoral Condyle (mm) | Critical Size Defect (Diameter in mm) |
|---|---|---|---|---|---|
| Rabbit[A] (Lupus or Lupine) | 9 months | 3–4 kg | FC, TG, TP, P | 0.25–0.75 | 3 |
| Dog[B] (Canine) | >1–2 years | 15–30 kg | FC, TG, P | 1.3 | — |
| Pig[B] (Porcine) | 10 months–1 year | 20–40 kg | FC, TG | — | — |
| Goat[B] (Caprine) | 2–3 years | 40–70 kg | FC, TG, TP, P | 1.5–2 | — |
| Sheep[B] (Ovine) | 2–3 years | 35–80 kg | FC, TG | 1.7 | 7 |
| Horse[B] (Equine) | 2–4 years | 400–500 kg | FC, TG, RC | 2–3 | 9 |

[A] small animal.
[B] large animal; FC, femoral condyle; TG, trochlear groove; TP, tibial plateau; P, Patella; RC, radial carpal.

### 2.4.1 Small animals

The New Zealand white rabbit is a popular model for osteochondral defects, primarily due to being more economical and convenient than the large animal models. Rabbits are much easier to handle and have much less demanding housing requirements than the sheep, for example. Due to the low cost and generally good availability, rabbits are often the first choice for an animal model and they are indeed worthwhile for early

screening of devices and to assess biocompatibility (ASTM 2005). However, rabbit joints are very small in comparison to the human equivalent, limiting the size of the defect that can be created and also requiring modification to the standard set of instrumentation. Articular cartilage in the rabbit is approximately only 0.3mm thick, which is much thinner than the typical 3-5mm in the human. The relatively thin cartilage layer also makes implantation of a biphasic device near impossible to achieve with accuracy.

Hence, the rabbit model is not suitable for studies in implant fixation or for other geometric, or pressure sensitive factors (ASTM 2005). For these, a large animal model must be selected. Nonetheless, the New Zealand white rabbit has been used with success in countless osteochondral defect studies, (Brittberg, Nilsson, Lindahl, Ohlsson, & Peterson 1996;Carranza-Bencano, Perez-Tinao, Ballesteros-Vazquez, Armas-Padron, Hevia-Alonso, & Crespo 1999;Cohen, Meirisch, Wilson, & Diduch 2003;Custers, Dhert, van Rijen, Verbout, Creemers, & Saris 2007;Frenkel, Bradica, Brekke, Goldman, Ieska, Issack, Bong, Tian, Gokhale, Coutts, & Kronengold 2005;Furukawa, Eyre, Koide, & Gilmcher 1980;Grande, Pitman, Peterson, Menche, & Klein 1989;Grigolo, Roseti, Fiorini, Fini, Giavaresi, Aldini, Giardino, & Facchini 2001;Kim, Moran, & Salter 1991;Kuroki, Nakagawa, Mori, Kobayashi, Okamoto, Yasura, Nishitani, & Nakamura 2007;O'Driscoll, Keeley, & Salter 1986;Rahfoth, Weisser, Sternkopf, Aiger, von der Mark, & Brauer 1998;Uematsu, Hattori, Ishimoto, Yamauchi, Habata, Takakura, Ohgushi, Fukuchi, & Sato 2005;Wakitani, Kimura, Hirooka, Ochi, Yoneda, Yasui, Owaki, & Ono 1989). One criticism of the rabbit model is the far superior healing capability when compared to the human.

### 2.4.2 Large animals

Animals with larger joints, more closely resembling the human equivalent, are preferential for testing the efficacy of an implant or technique to treat an osteochondral defect. Larger joints with thicker cartilage will often allow the same devices and instrumentation to be used and the placement of defects can be controlled more accurately. In addition, it is easier to control the depth of an implant such that the surface is continuous with the adjacent cartilage. Large animals include the pig (Chang et al. 1999;Harman, Weeden, Lichota, & Brindley 2006;Hunziker 2001;Hunziker, Driesand, & Morris 2001), sheep (Pearce et al. 2001; Guo et al. 2004; Oakley et al. 2004; Tibesku et al. 2004; Dorotka et al. 2005; Burks et al. 2006; Vizesi et al. 2007), goat (Jackson, Lalor, Aberman, & Simon 2001;Kangarlu & Gahunia 2006;Kirker-Head, Van Sickle, Ek, & McCool 2006) and horse (Gratz et al. 2006;Morisset, Frisbie, Robbins, Nixon, & McIlwraith 2007).

#### 2.4.2.1 Sheep comparative anatomy

The sheep knee is anatomically similar to the human, although not nearly as large in either overall size or articular cartilage volume. The average cartilage thickness in the sheep medial femoral condyle (MFC) is 1.1 to 1.7mm and 1.3 to 1.5mm in the medial tibial condyle (MTC) (Appleyard et al. 2003;Armstrong, Read, & Price 1995) with a high degree of variation over the topography of the condyles. This is compared to the human MFC and MTC which have respective average thicknesses of 2.2 to 2.5mm (Frisbie et al. 2006) and 1.8 to 3.5mm (Mow and Ratcliffe 1997). The average body weight of sheep, as measured from 24 randomly selected animals in our laboratory is 63kg, which is compared to the classic $50^{th}$ percentile male, weighing 73kg. Considering the relative similarities in average body weight, the difference in cartilage thickness may be related to the bipedal nature of the human gait compared

with the quadruped. As reported by Taylor et al, typical knee joint forces in the gait cycle of sheep is approximately 2.12 times body weight, whereas in the human it is approximately 2.8 to 3.8 times body weight. Considering the similarities in the sheep and human knee, and the significant body of work published, the sheep model was considered an ideal model for osteochondral defect creation and repair in this dissertation.

# 3.0 Biological response to surgical creation of osteochondral defects and the difference between punching and drilling

## *3.1 Abstract*

Cartilage has an extremely poor capacity to heal, which has lead to intensive research into biomaterials and tissue engineering for the purpose of regenerating cartilage in vivo. Many of these techniques have shown great promise *in vitro,* however, the results have not carried across to the *in vivo* scenario. Furthermore, clinical studies with long term follow-ups have shown that even healthy cartilage autografts do not integrate with the adjacent cartilage (Burks, Greis, Arnoczky, & Scher 2006;Schneider et al. 2003). This in itself is evidence to the poor regenerative capacity of articular cartilage and also suggests that the surgical preparation may be an important factor in the overall clinical healing response.

It is hypothesised in this study that the surgical creation of defects in cartilage causes significant damage to the adjacent and opposing tissues, leading to further degradation of the cartilage and poor outcome for the repair in general. Another potential outcome of the creation of osteochondral defects in weight bearing areas is the progression to an osteoarthritic joint. This study compares the healing response of osteochondral defects created with either a punch or a drill to determine which instrumentation is preferable in the surgical creation of full thickness cartilage defects. Additionally, this study also characterises the state of the tibia and meniscus directly opposing the femoral defects at both 26 and 52 weeks. This knowledge will help characterise and refine the ovine model for cartilage regeneration and may have an influence on surgical technique and instrumentation for clinical cartilage repair.

## 3.2 Introduction

Cartilage is a strong and durable tissue that experiences repetitive dynamic loading with magnitudes exceeding several times body weight under certain conditions. Nonetheless, articular cartilage is still prone to degradation from conditions such as osteoarthritis or damage from traumatic injuries. As famously said in 1743 "ulcerated cartilage is a troublesome thing and that, once destroyed, it is not repaired" (Hunter 1743). The poor reparative capacity of cartilage is often attributed to the lack of blood, nerves and undifferentiated cells to initiate and propagate the healing response.

Promising methods of treatment for focal cartilage defects include regeneration or replacement of hyaline cartilage with biomaterials. These materials may be fast degrading, slow degrading or stable and may be tissue engineered with the addition of cells and signalling molecules. Either way, there is normally a necessity to penetrate the subchondral bone underlying the cartilage defect to provide anchorage for the implant. This is also the case in autologous osteochondral grafting procedures, where grafts of healthy tissue are press-fit into surgically created defects in the region of the damaged cartilage. It should be noted, however, that some treatments such as autologous chondrocyte implantation, do not require penetration of the subchondral bone. However, it is then necessary to introduce some other method of anchorage such as fibrin glue (Marcacci et al. 2005;Nehrer et al. 2005;Peretti et al. 2001), polymeric pegs, suturing to the adjacent cartilage (Breinan et al. 1997;Marcacci, Berruto, Brocchetta, Delcogliano, Ghinelli, Gobbi, Kon, Pederzini, Rosa, Sacchetti, Stefani, & Zanasi 2005;Nehrer, Domayer, Dorotka, Schatz, Bindreiter, & Kotz 2005;Yasunaga, Kimura, & Kikuchi 2001), or a combination. The inclusion of these

factors into the defect may be detrimental to the repair or to the opposing articular surface.

One of the main disadvantages of creating osteochondral defects (defects that penetrate the underlying subchondral bone) is that there is inevitably an influx of blood borne growth factors and signalling molecules (Hunziker 1999a;Hunziker 1999b;Mankin 1982;Shapiro, Koide, & Glimcher 1993;van den Berg et al. 2001). While these factors are desirable for the healing of bone, they are thought to be less desirable for the healing of cartilage due their propensity to encourage the growth of fibrous repair tissue rather than hyaline cartilage (Coutts et al. 2001). The presence of such growth factors may also influence or interfere with the technique (ie. growth factor) being examined. Fibrous repair tissues are mechanically inferior to hyaline cartilage and quickly degenerate in areas of high load bearing. Thus some researchers have highlighted a necessity to include some form of blood barrier in the implant, essentially recreating the tidemark (Frenkel, Bradica, Brekke, Goldman, Ieska, Issack, Bong, Tian, Gokhale, Coutts, & Kronengold 2005).

There has been an abundance of research into repair of cartilage defects, however, the animal models and surgical methods used to evaluate these techniques are not well reported nor have they been adequately validated. Recent *in vivo* studies with sheep (Tibesku et al. 2004; Dorotka et al. 2005) and rabbits (Cohen et al. 2003) have supplied more information on the instrumentation and surgical technique, allowing for more thorough analysis and comparison of their work. Drilling and punching are the only methods currently available to create osteochondral defects in cartilage or to prepare a damaged region for an implant. Mechanically, these represent two

dramatically different methods. Chrondrocyte viability in osteochondral grafts has been reported to be superior with a manual punch compared to serrated power trephines (Evans, Miniaci, & Hurtig 2004). Drills remove material due to rotational movement of the cutting face and result in complex loading and heat generation. Drill geometry is also an important factor in heat generation where temperatures can exceed 47degC at a distance of 0.5mm from the drill hole (Chacon et al. 2006). Punches operate by applying concentrated compressive loads, with minor rotation or bending to remove the material.

Most studies into cartilage repair or regeneration do not clearly identify the method chosen to create the defect and I hypothesise that the biological reaction of bone and cartilage to these two methods are very different. The method of surgical defect creation may have a profound influence on the results of these studies, as well as the healing and repair of the defect irrespective of the quality of the graft or biomaterial implanted subsequent to the creation of the defect.

In any surgery, it is important to observe the primary surgical site as well as any secondary sites that may be affected. This is certainly the case in the knee where the cartilage defect on the femur articulates with menisci as well as the proximal tibia. The in vivo reactions of the bearing surfaces are relevant from the point of view of controlling or minimizing further arthritic changes in the treated joint. There is evidence that damage to the meniscus and the tibia can be caused by metallic implants (Kirker-Head et al. 2006; Custers et al. 2007) and even by sutures in the femoral cartilage (Yasunaga et al. 2001). Hence, it is worthwhile to analyse the articulating

surfaces opposing the empty osteochondral defect on the femur to determine the extent of the flow-on damage from the original surgery.

This study is thus separated into two parts. Part 1 (Chapter 3) involves the healing response of 6mm empty defects in the distal medial femoral condyle. It is the aim of Part 1 of this study to evaluate whether it is more appropriate to create osteochondral defects with a punch or a drill. This study has a focus on the histological appearance of the repair tissue, the adjacent cartilage and subchondral bone associated with empty cartilage defects created with either a punch or a drill. Part 2 (Chapter 4) involves the potential degeneration, damage or other changes to the counter bearing surface opposing the empty defects; in this case the tibial plateau and the menisci.

## *3.3 Methods*

### 3.3.1 Animals

Adult crossbred wethers of age 18 months were used in this study. The sheep were allowed continuous access to water and were fed a diet of chaff and hay once per day. All animals were transported to the holding cells in Level 4 Samuels Building, UNSW and allowed to acclimatise for at least 3 days before surgery. The sheep were fasted overnight before surgery and remained at Samuels Building for at least 1 week postoperatively before being transported to deep cover pens at the Biological Resource Centre, Little Bay. Animal ethics were obtained from the Animal Care and Ethics Committee (ACEC), University of New South Wales.

### 3.3.2 Surgery

The surgical site was shaved and cleaned with an iodine scrub solution and 70% isopropyl alcohol. Sheep were anaesthetised with an injection of Zoletil and controlled inhalation of isofluorane. An endotracheal tube was inserted and the animal ventilated with anaesthesia maintained using isofluorane (2-3%) and 100% oxygen. Prophylactically, an antibiotic (Keflin, 1000mg) and an anti-inflammatory/analgesic (Carprofen, 4mL) were given intravenously. Crystalloid fluids (Hartmann's solution) were given intravenously at 4-10 mL/kg/h prior to and during surgery. A long acting antibiotic (Benacillin, 5mL) was injected intramuscularly prior to surgery. During surgery, a dedicated anaesthetist continually monitored the animal for respiration, heart rate, jaw tone, membrane colour and other vital signs (including oxygen saturation).

A single osteochondral defect was created in each of the left and right medial distal femoral condyles, for a total of 2 defects per animal. These defects were located in the weight bearing region of the femoral condyle (Figure 11). The medial condyle was chosen as this is the most common surgical region in the human and because this is also the suggested area in the standards (ASTM 2005).

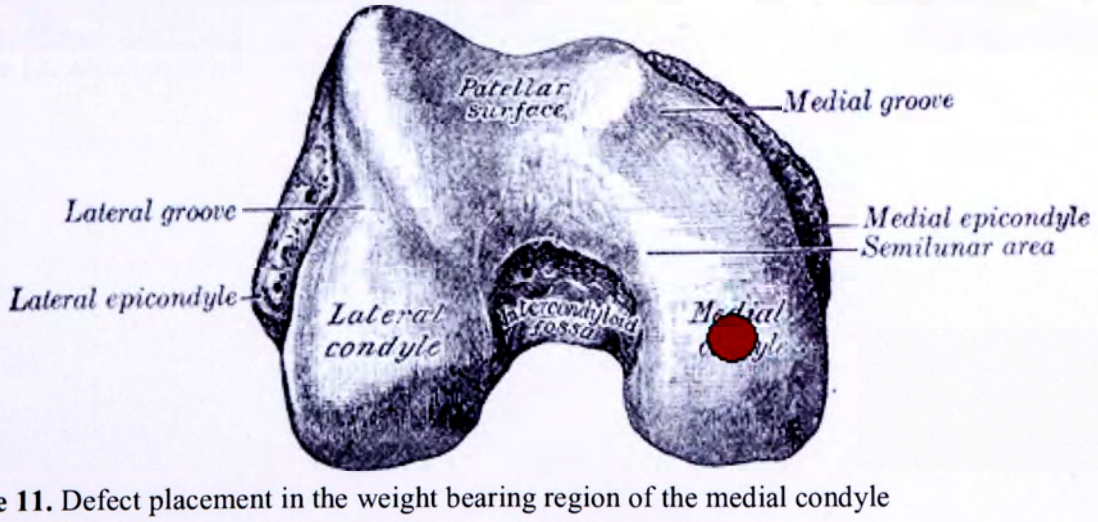


**Figure 11.** Defect placement in the weight bearing region of the medial condyle

The distal medial femoral condyle of the adult wether was exposed using a small incision medial to the patella tendon. Soft tissue layers above the joint were ablated using a diathermy to control bleeding (Figure 12). The patella was not reflected due to concerns of possible patella subluxation or dislocation upon weight bearing, and because it was simple to locate the condyle without reflecting the patella. The knee was maximally flexed to expose the weight bearing region of the femoral condyles and the defects were created taking great care not to damage the articular cartilage adjacent to the defect (Figure 13). The articular surfaces were frequently irrigated with saline solution while the joint was open.

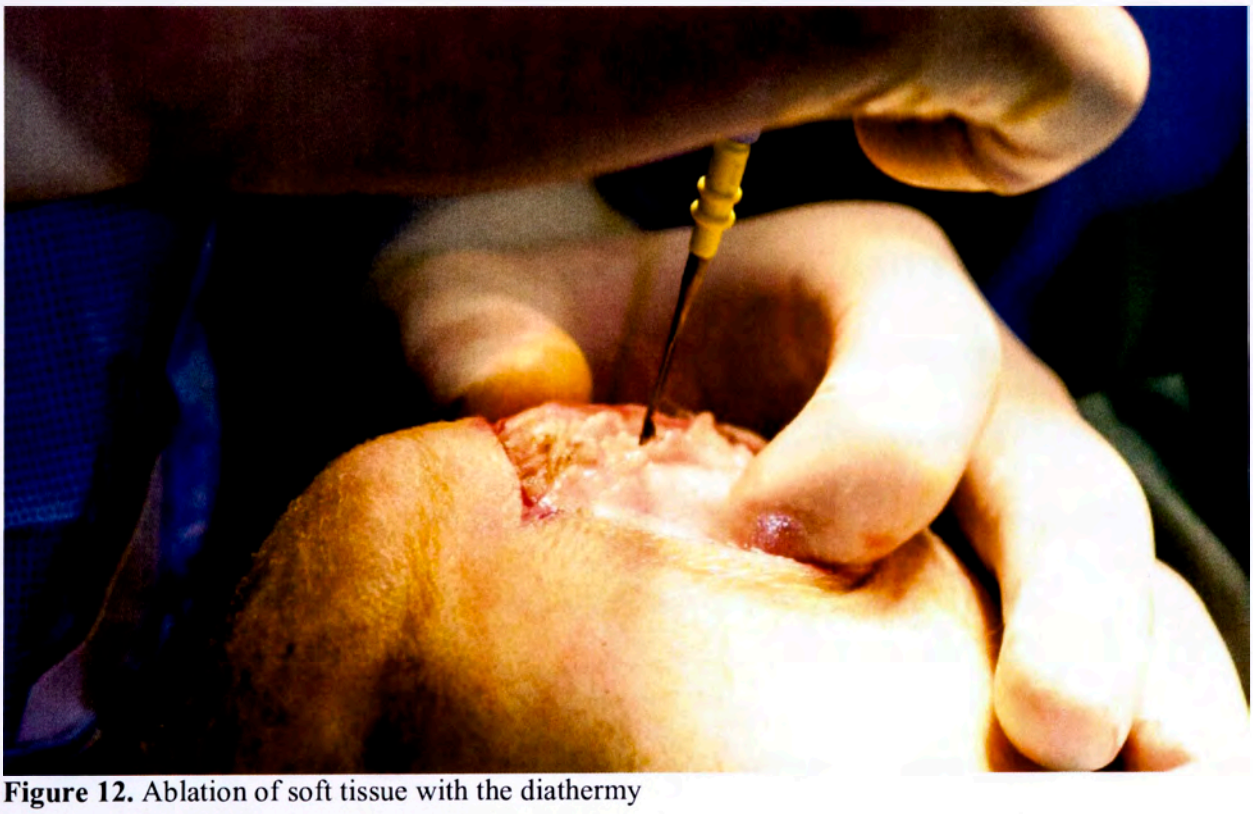

**Figure 12.** Ablation of soft tissue with the diathermy

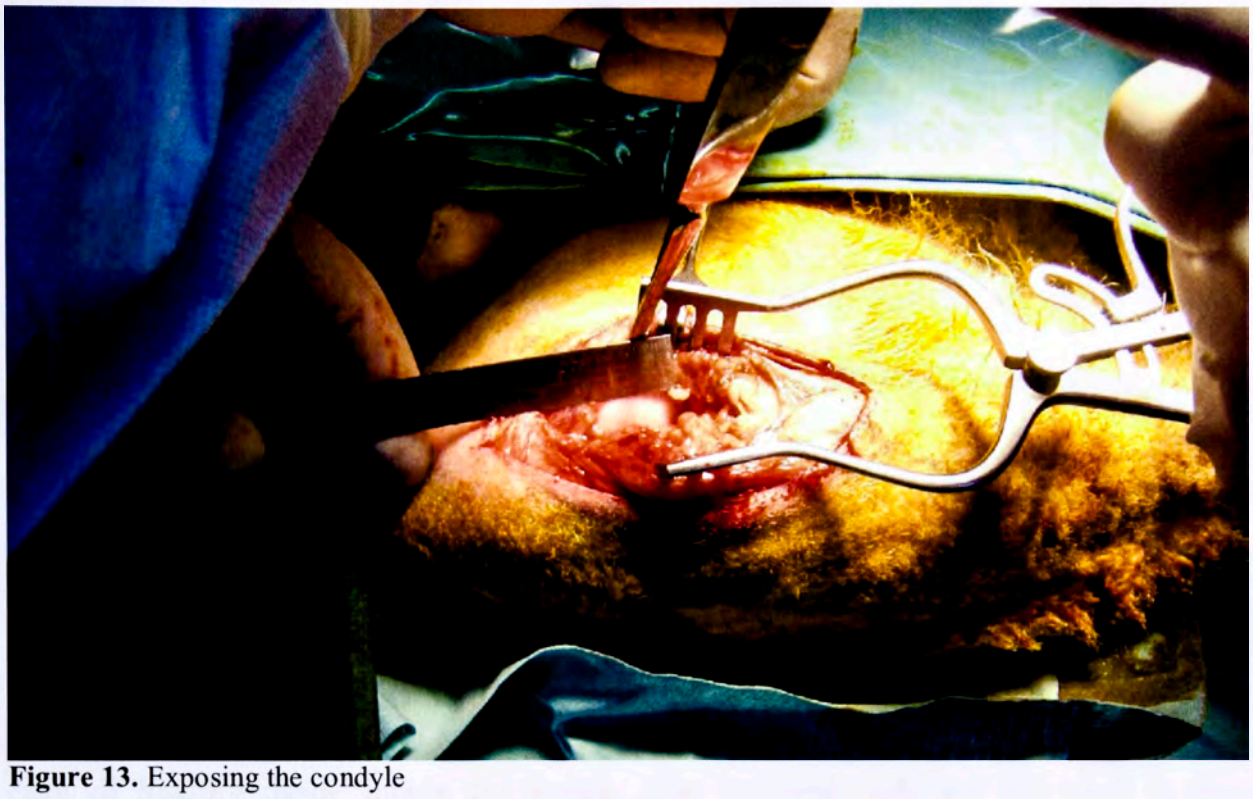

**Figure 13.** Exposing the condyle

The defects (6mm diameter, 6mm deep) were created with either a punch (OATS instrumentation, *Arthrex, Naples, USA*) or a surgical drill (Dyonics and Acufex instrumentation, *Smith & Nephew Endoscopy, Memphis, USA*). Each of these systems is treated in further detail in the following sections. Following creation, the empty defects were irrigated and given no further treatment. The synovial capsule and the skin were subsequently closed in layers with 3-0 Vicryl and 3-0 Dexon respectively and the wound sprayed with OpSite (*Smith & Nephew, Memphis, USA*).

The sheep were allowed full ambulation and weight bearing immediately after regaining consciousness. No casts, splints or bandages were applied to any of the joints. Animals were given postoperative analgesics and antibiotics once per day for 7 days post operation.

### 3.3.3 Group 1: Punch

The OATS (Osteochondral Autograft Transfer System, *Arthrex, Naples, USA*) instrumentation was used to create the punched defects in this study. As the name suggests, the OATS instrumentation is normally used in practice for osteochondral autografting procedures. In this procedure, grafts of healthy hyaline cartilage and the underlying subchondral bone are taken from a donor site in the non-weight bearing, or non-articulating regions of the knee and then transferred to the damaged region. The graft is obtained by hammering a cylindrical punch (the donor punch) through the cartilage and into the bone, then twisting and subsequently withdrawing to remove a core of healthy tissue inside the punch. The recipient hole for the graft is then prepared in a similar fashion, however, the recipient punch is 1mm smaller in diameter than the donor punch to allow for a tight press-fit when the graft is inserted. The core of damaged cartilage is disposed of. The graft, which is still inside the donor punch, is then driven into the recipient hole by lining up the punch with the hole and lightly tapping the graft with a long push-rod (known as a collared pin) which is inserted through the centre of the punch. Once the graft is driven into the recipient hole, the surgeon gently hammers it down until it is flush with the surface of the adjacent cartilage.

In this study, a 6mm recipient punch was used to create the defect. In a grafting procedure, the recipient punch is the same punch that would be used to prepare the defect in the region of the damaged cartilage. The core of bone and cartilage was removed and then the surgical site was closed. No grafting or further treatments were given. The OATS instrumentation is shown in Figures 14 to 17.

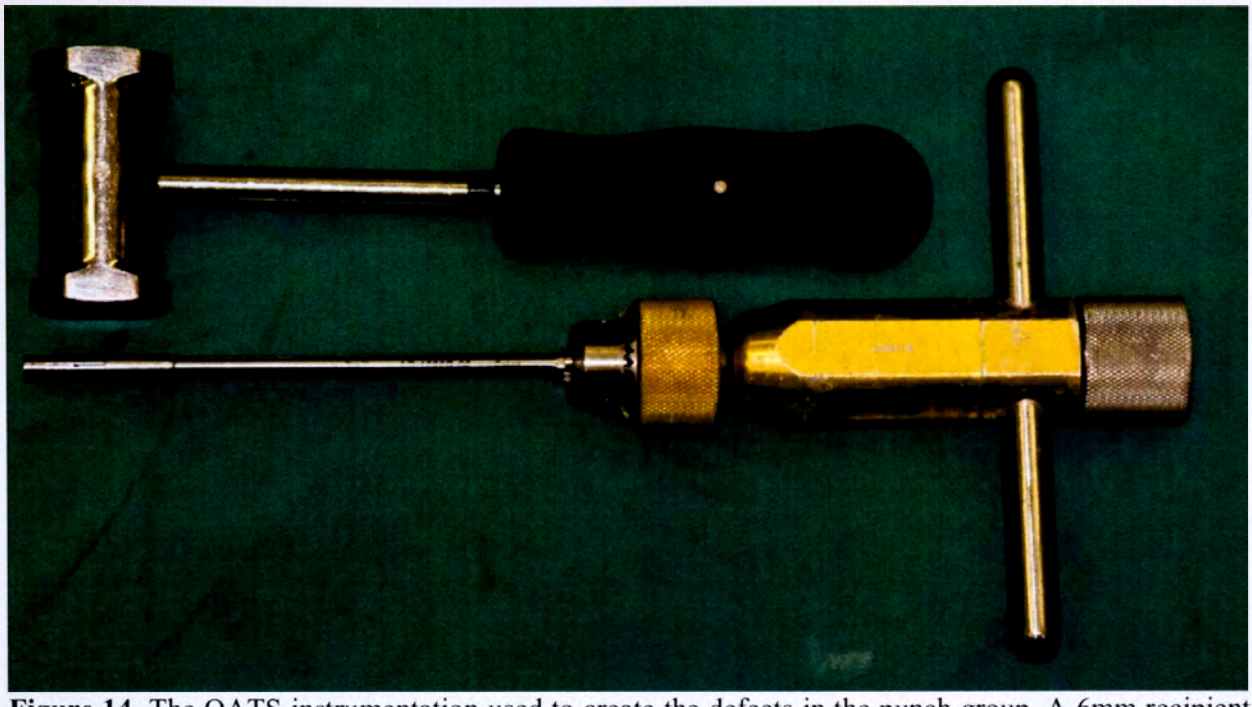

**Figure 14.** The OATS instrumentation used to create the defects in the punch group. A 6mm recipient punch is secured in a Jacob's chuck which is connected to an assembly to allow the punch to be hammered into the tissue and then the T-handle allows the unit to be twisted to break the bone and remove the tissue

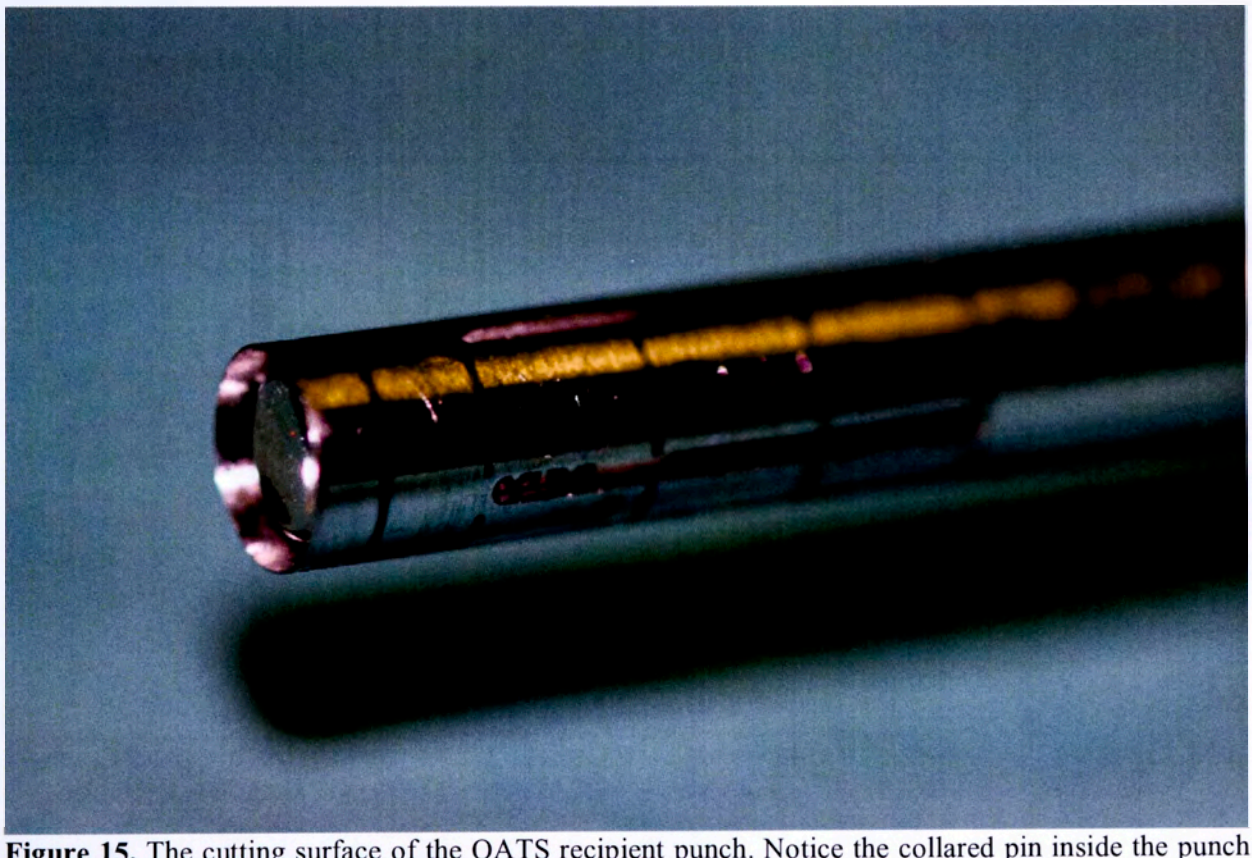

**Figure 15.** The cutting surface of the OATS recipient punch. Notice the collared pin inside the punch to allow for removal of the core of material and the graduations to mark the depth of the punch intra-operatively

**Figure 16.** To remove the material from the punch, the T-handle section of the assembly is removed to expose the end of the collared pin, a cover is placed over the pin to prevent bending and the pin is gently hammered to force the material out.

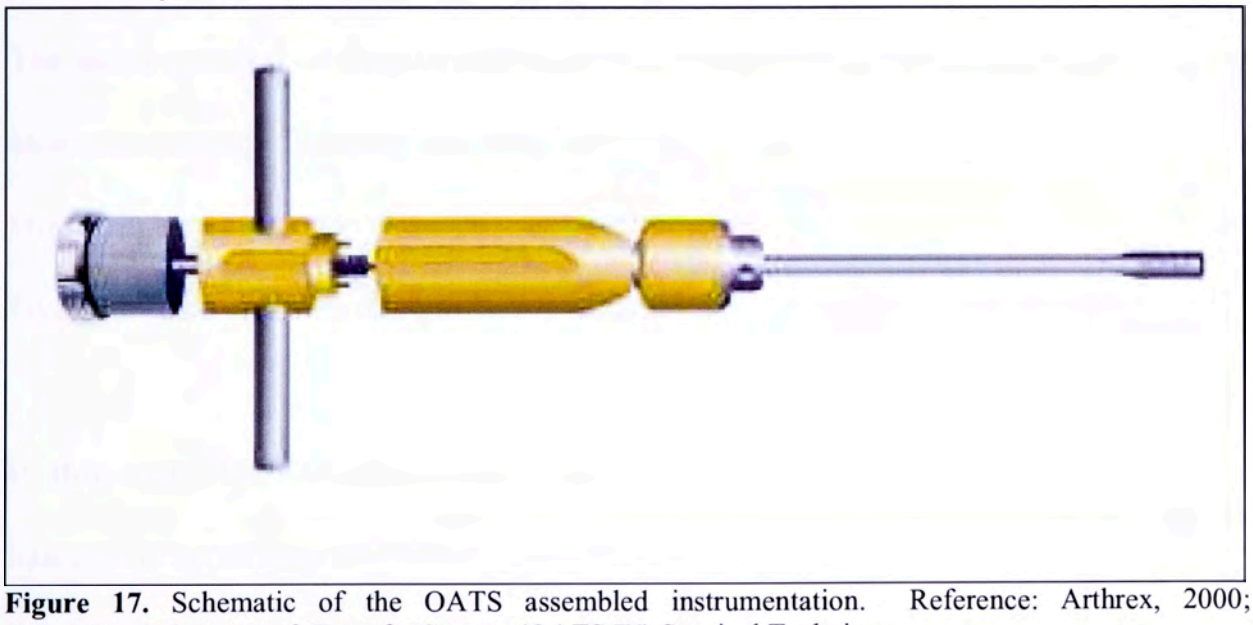

**Figure 17.** Schematic of the OATS assembled instrumentation. Reference: Arthrex, 2000; Osteochondral Autograft Transfer System (OATS ™) Surgical Technique

### 3.3.4 Group 2: Drill

The drilled defects were created using an electrically powered surgical drill (Dyonics Power, *Smith & Nephew Endoscopy, Memphis, USA*) with a cannulated drill bit (Acufex, *Smith & Nephew Endoscopy, Memphis, USA*). The power unit for the drill was set to the maximum revolutions per minute; 1200 rpm (Figure 18). The drill bit used was a 6mm cannulated endoscopic drill bit (Figure 19), which is most commonly used in reconstructive surgery of the anterior cruciate ligament (ACL). The only difference between this endoscopic drill bit and a conventional drill bit is the length of the cutting surfaces, otherwise known as the flutes. The endoscopic drill bit has very short flutes to avoid tunnel widening and damage to soft tissues in ACL reconstructions. This drill bit is designed to remove the fragmented tissue quickly rather than compact it, as can be seen with other cutting bits such as stepped routers. The quick removal of fragmented tissue is a favourable quality for a drill bit, as this increases cutting efficiency and may help reduce heat generation. A disadvantage of this drill bit is that the base of the hole produced is not square, which would be favourable for implants and grafts that have flat bottom surfaces.

In this study, the site of the defect was located and then a 2.35mm guide pin was hammered approximately 5-6mm into the subchondral bone. This was the minimum depth required for stabile fixation of the guide pin. The cannulated drill was then positioned over the guide pin and drilled down to a depth of 6mm (Figure 20). The drill was then withdrawn and the guide pin removed before closing up the surgical site. This arrangement of guide pin and cannulated drill was used to avoid damage to the adjacent cartilage from the drill bit skiving off the articular surface. Pilot studies and experience with other studies indicated that it was difficult to drill a clean hole in

articular cartilage using a standard, un-cannulated drill bit without some skiving on the surface. Even the most minor amount of skiving could cause premature degeneration of the adjacent cartilage, which would certainly influence the outcomes of this study.

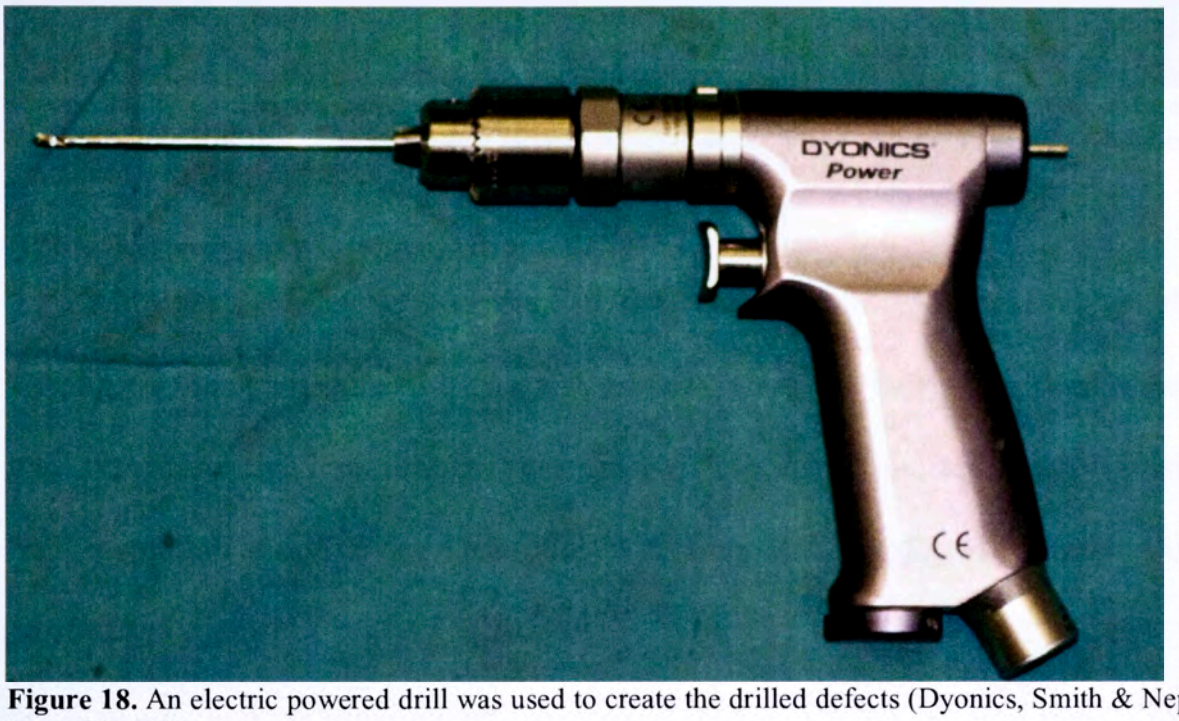


**Figure 18.** An electric powered drill was used to create the drilled defects (Dyonics, Smith & Nephew, Memphis, USA)

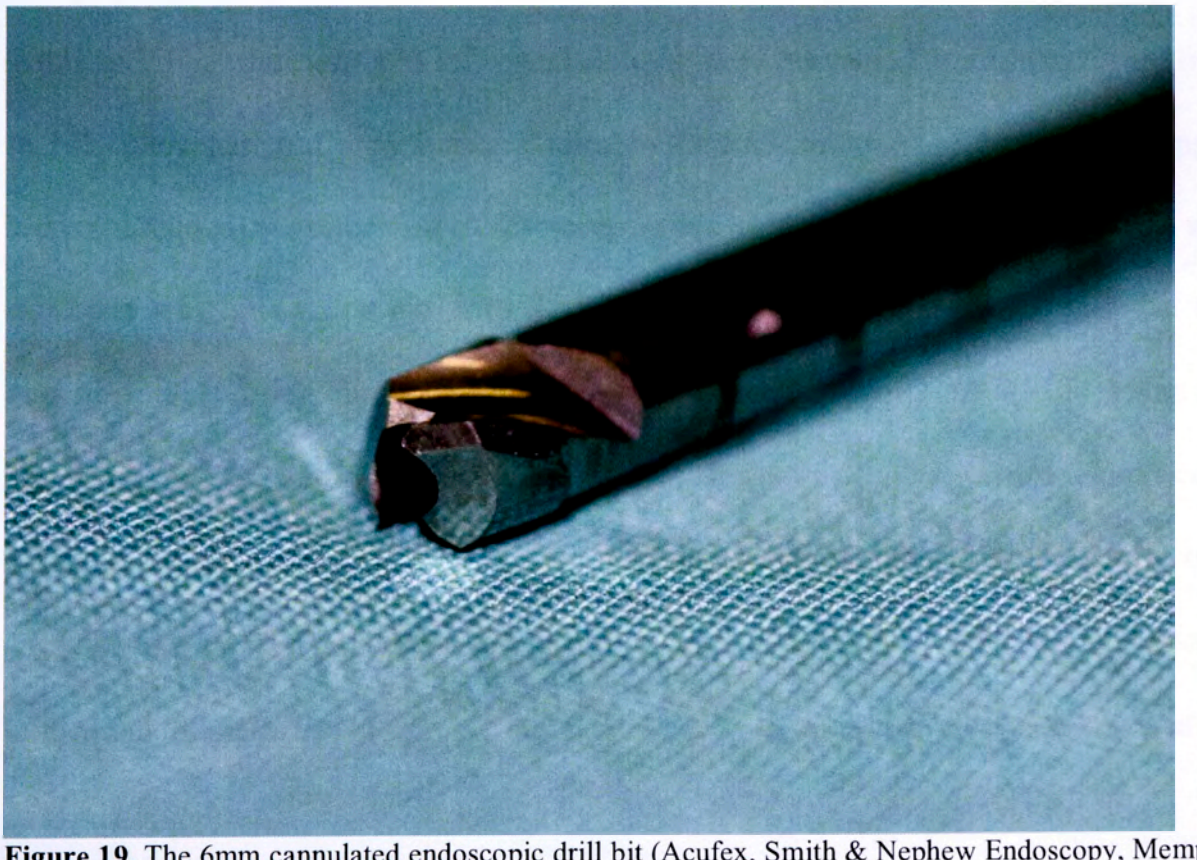

**Figure 19.** The 6mm cannulated endoscopic drill bit (Acufex, Smith & Nephew Endoscopy, Memphis, USA). Notice the two cutting surfaces and the graduations along the drill for monitoring the depth of the defect.

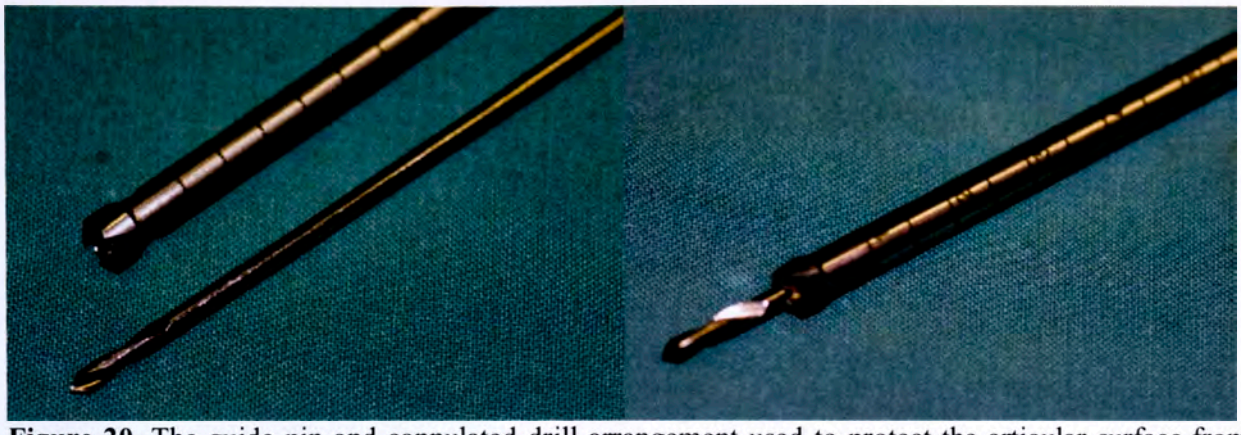

**Figure 20.** The guide pin and cannulated drill arrangement used to protect the articular surface from skiving of the drill bit. The guide pin is first secured in the bone and the cannulated drill is then positioned over the pin, constraining lateral motion of the drill bit.

### 3.3.5 Time zero radiographs

Two additional defects were created in the femoral condyle of a deceased sheep, serving as time-zero controls. These specimens were cut with a diamond wire saw into 1mm thick sections through the centre of the defect and radiographed using a high resolution x-ray device (Faxitron, Wheeling, IL) and digital cassettes (AGFA Australia, Sydney)

### 3.3.6 Histology

After sacrifice, the right and left distal femora were harvested and immediately fixed in 10% phosphate buffered formalin solution for a minimum of 48 hours. The samples were subsequently decalcified in formalin-formic acid solution for up to 4 weeks until the bone was able to be cut with a scalpel blade. The samples were then cut into superior and inferior blocks by making one cut through the centre of the defect and trimming to fit into regular histological cassettes (Figure 21). Macroscopic photographs of the cut sections were taken with a Canon digital SLR camera. Both superior and inferior halves of the sample were decalcified further and subsequently embedded in paraffin blocks, from which 5μm sections were cut and stained for analysis.

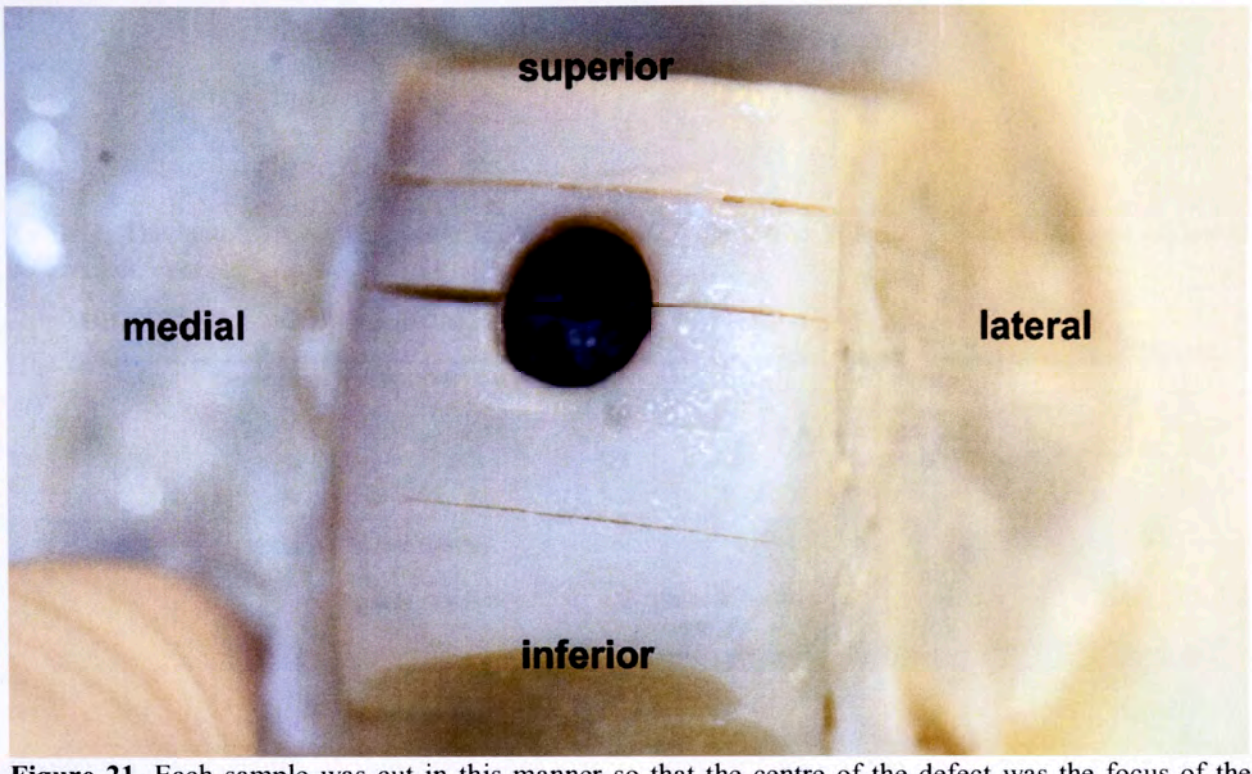


**Figure 21.** Each sample was cut in this manner so that the centre of the defect was the focus of the histological analysis.

Sections were stained with haematoxylin and eosin (H&E) for routine histology and Safranin-O for proteoglycans. Sections were analysed for the quality and quantity of repair tissue in the chondral and osseous regions of the defect, signs of degenerative changes in the adjacent cartilage and signs of bone resorption and remodelling. Histology was qualitatively analysed using the modified O'Driscoll 27 point scoring system proposed by Frenkel and co-workers (Table 2) (Frenkel, Bradica, Brekke, Goldman, Ieska, Issack, Bong, Tian, Gokhale, Coutts, & Kronengold 2005). In brief, this system scores the percentage hyaline cartilage, structural characteristics, and freedom from degenerative changes in the repair tissue and surrounding cartilage, reconstitution of subchondral bone, bonding of repair cartilage and positive Safranin-O staining.

**Table 2.** The histologic scoring scale for the empty defects is a modified O'Driscoll method proposed by Frenkel, et al.

**HISTOLOGIC SCORING SCALE**

| | | | Point value |
|---|---|---|---|
| I. | **Percentage hyaline articular cartilage:** | 80 - 100% | 8 |
| | | 60 - 80% | 6 |
| | | 40 - 60% | 4 |
| | | 20 - 40% | 2 |
| | | 0 - 20% | 0 |
| II. | **Structural Characteristics** | | |
| | **A. Surface regularity:** | Smooth and intact | 2 |
| | | Fissures | 1 |
| | | Severe disruption, fibrillation | 0 |
| | **B. Structural integrity:** | Normal | 2 |
| | | Slight disruption, including cysts | 1 |
| | | Severe lack of integration | 0 |
| | **C. Thickness:** | 100% of normal adjacent cartilage | 2 |
| | | 50 - 100% of normal cartilage, or thicker than normal | 1 |
| | | 0 - 50% of normal cartilage | 0 |
| | **D. Bonding to adjacent cartilage:** | Bonded at both ends of graft | 2 |
| | | Bonded at one end / partially at both ends | 1 |
| | | Not bonded | 0 |
| III. | **Freedom from Cellular Changes of Degeneration:** | Normal cellularity, no clusters | 2 |
| | | Slight hypocellularity, <25 chondrocyte clusters | 1 |
| | | Moderate hypocellularity / hypercellularity, >25% clusters | 0 |
| IV. | **Freedom fromDegenerative Changes in Adjacent Cartilage** | | |
| | Normal cellularity, no clusters, normal staining | | 3 |
| | Normal cellularity, mild clusters, moderate staining | | 2 |
| | Mild or moderate hypocellularity, slight staining | | 1 |
| | Severe hypocellularity, poor or no staining | | 0 |
| V. | **Reconstitution of Subchondral Bone** | | |
| | Complete reconstitution | | 2 |
| | Greater than 50% reconstitution | | 1 |
| | 50% or less reconstitution | | 0 |
| VI. | **Bonding of Repair Cartilage to Denovo Subchondral Bone** | | |
| | Complete and uninterrupted | | 2 |
| | <100% but >50% complete | | 1 |
| | <50% complete | | 0 |
| VII. | **Safranin-O Staining** | | |
| | Greater than 80% homogeneous positive stain | | 2 |
| | 40-80% homogeneous positive stain | | 1 |
| | Less than 40% homogeneous positive stain | | 0 |
| | | **Total Score:**_____ | |

**[TOTAL MAXIMUM SCORE: 27]**

### 3.3.7 Computed Tomography

Regular computed tomography and microCT were conducted on the medial femoral condyles of the animals at 52 weeks only. CT was performed using a Toshiba clinical CT scanner (Toshiba, Japan) with an axial slice thicknes of 0.5mm. MicroCt was performed with a Skyscan 1072 device, which is described in detail in Chapter X.

## *3.4 Results*

All animals were fully ambulating and weight bearing immediately after regaining consciousness. One of the animals in the 52 week group was culled early due to infection and was not replaced due to financial constraints. This animal was excluded from all analyses. During surgery, one of the defects in the punch group (sheep 1497 Left) was accidentally over-punched to a depth of 15mm. The defect was packed with an autograft of subchondral bone to a depth of 5mm and then tamped down to 6mm.

### 3.4.1 Time-zero radiographic appearance

Two time-zero defects were created to highlight the differences between the punch and drill on the defect geometry. Radiographs of 1mm thick sections show that there is minimal trauma to the surrounding cartilage in the punched defect (Figure 22). This contrasts with the drilled defect, in which major deformation of the cartilage layer is evident. Another significant factor is the geometry of the defect within the bony compartment. Both the punch and the drill provide vertical walls to the defect, however, significant differences are seen in the preparation of the base. In the case of the punched defect, the base is approximately flat, whereas the base of the drilled

defect follows the angle of the drill in such a way that the base is triangular. Profiles of the punch and cannulated drill bit are shown in Figure 22.

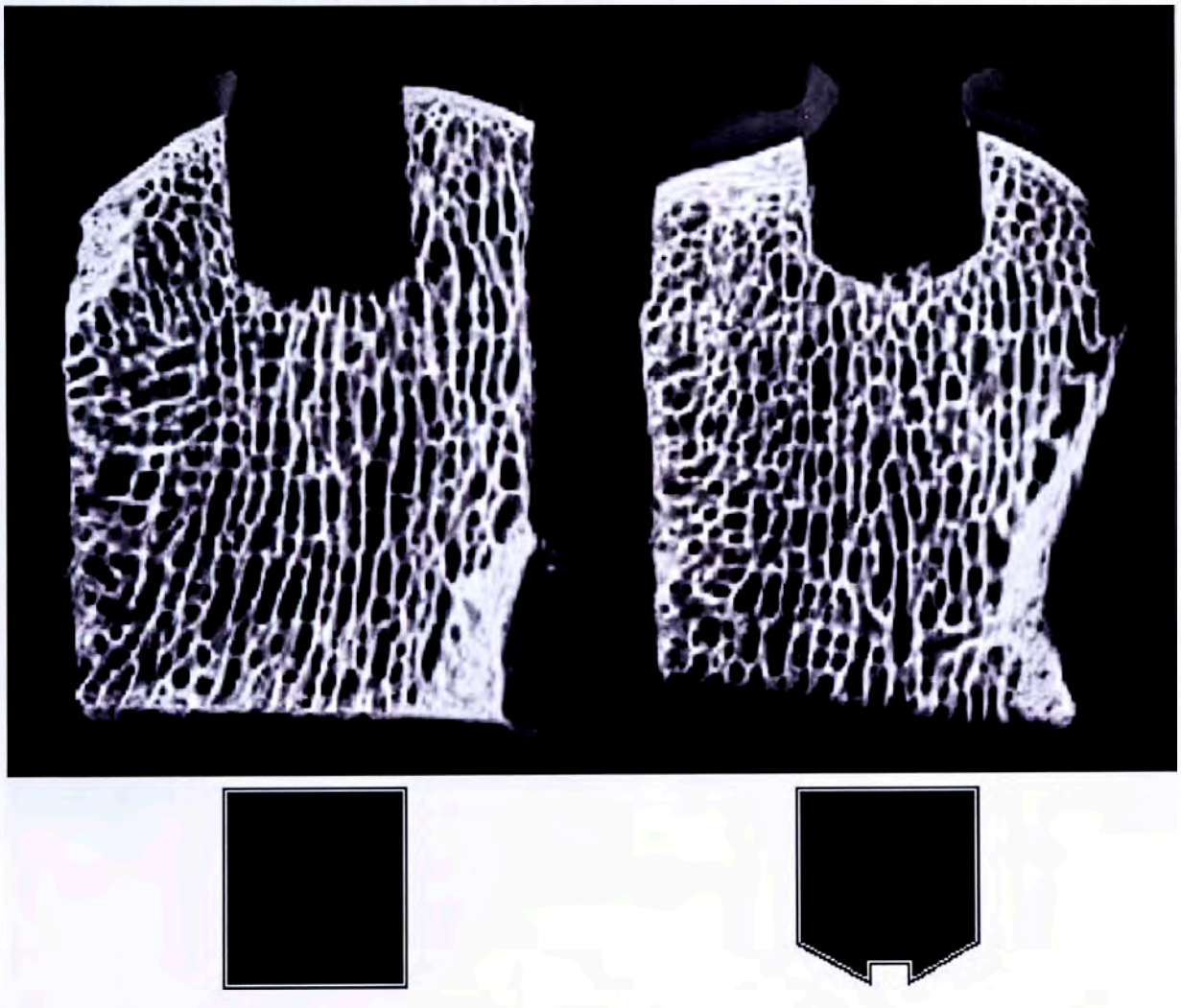

**Figure 22.** Top: Radiographs of 1mm thick sections of the punched (left) and drilled (right) defects showing minimal damage in the punch group, but severely deformed cartilage adjacent to the drilled defect. The punch provides an approximately flat base while the cannulated drill cuts a more triangular base. Bottom: Profiles of the instrument show that the geometry of the bony region of the defect closely follows the geometry of the instrument.

### 3.4.2 Intraoperative appearance of defects

Significant differences were noted between the punch and drill groups at the edges of the defects during surgery. Generally, the punched defects had very sharp and clearly defined edges to the defect with no obvious scoring or damage to the adjacent cartilage (Figure 23). In contrast, the drilled defects had a rougher appearance around the boundary of the defect. The cartilage immediately adjacent to the drilled defects appeared to be somewhat damaged, as indicated by a marked reduction in lustre (Figure 24).

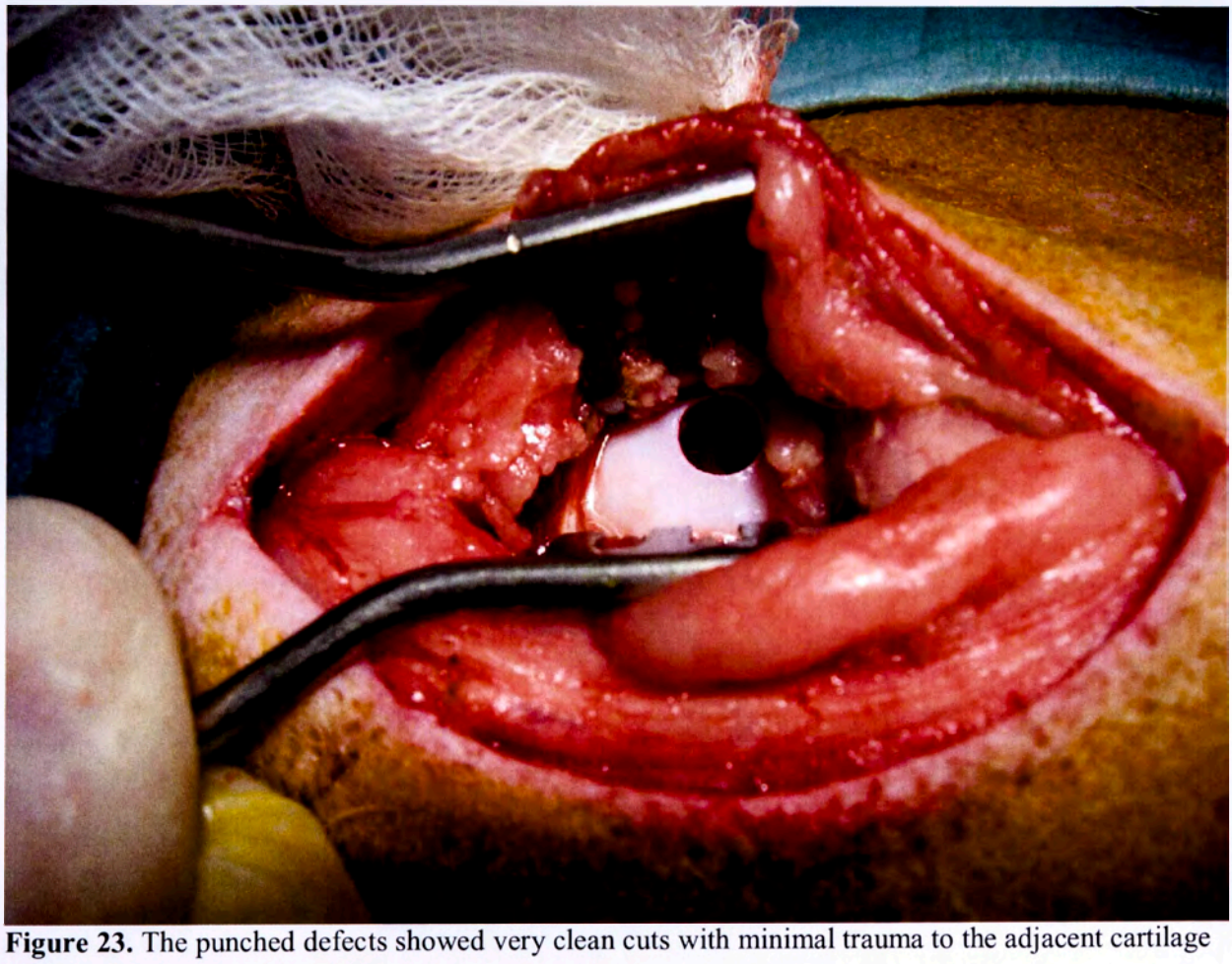

**Figure 23.** The punched defects showed very clean cuts with minimal trauma to the adjacent cartilage

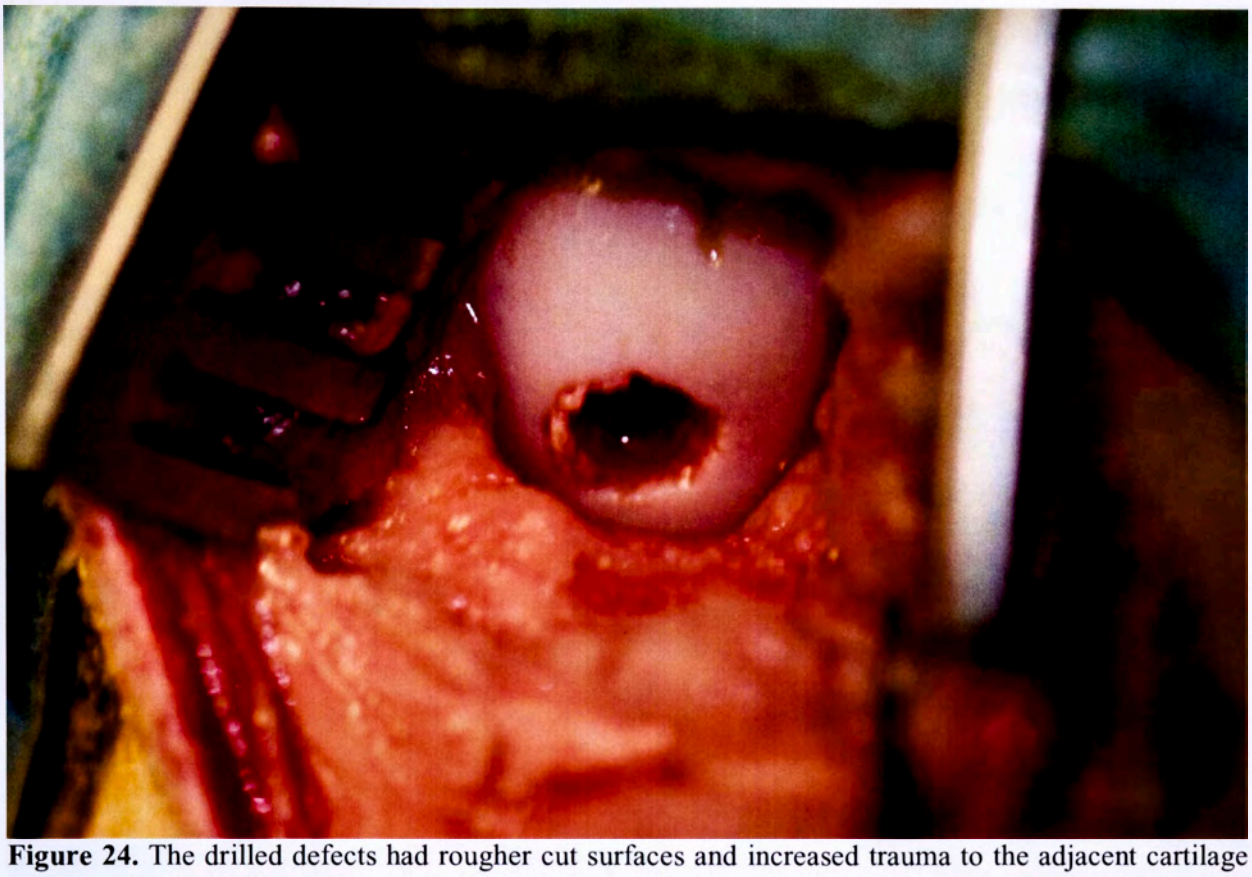

**Figure 24.** The drilled defects had rougher cut surfaces and increased trauma to the adjacent cartilage is noticed from macroscopic evaluation

### 3.4.3 Macroscopic Inspection

**4 weeks:** At the four week time point, none of the defects appeared healed and the fill of the defect with repair tissue was variable within the groups. The repair tissue did not appear to be of hyaline quality and had a rough, irregular surface indicating poor structural arrangement. Both the punch and drill group had similar appearance with large voids remaining within the defect and some obvious fissuring of the adjacent cartilage (Figure 25).

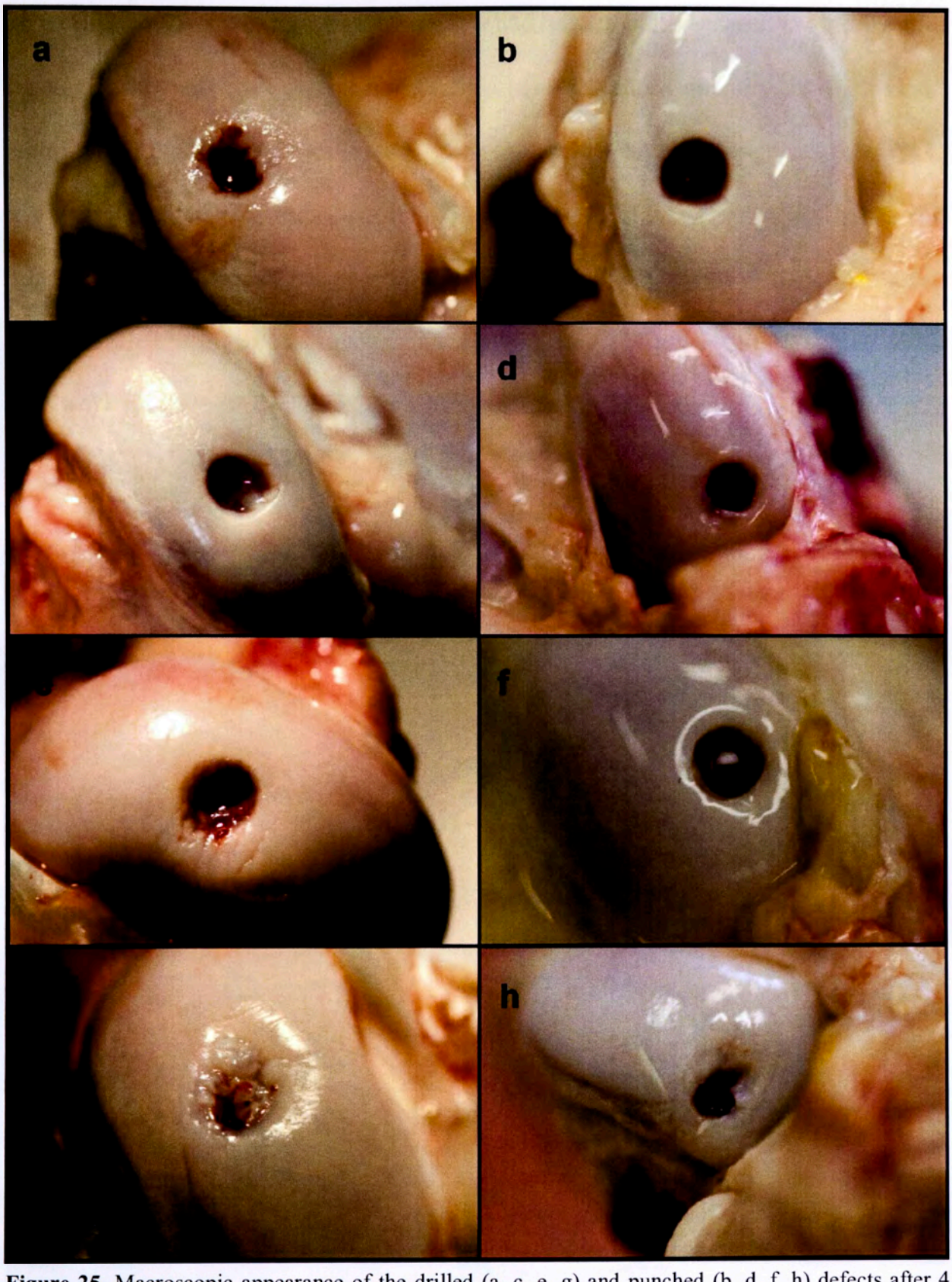


**Figure 25.** Macroscopic appearance of the drilled (a, c, e, g) and punched (b, d, f, h) defects after 4 weeks.

**26 weeks:** By 26 weeks, none of the defects had healed with a smooth layer of hyaline cartilage, although both groups appeared to have increased quantity of repair tissue compared to the four week defects. In general, the adjacent cartilage appeared smooth and healthy, albeit with the occasional fissure around the boundary of the defect. The punch group appeared to have increased fill of the defect compared to the drill group (Figure 26). The macroscopic appearance of the adjacent cartilage was similar to the four week group.

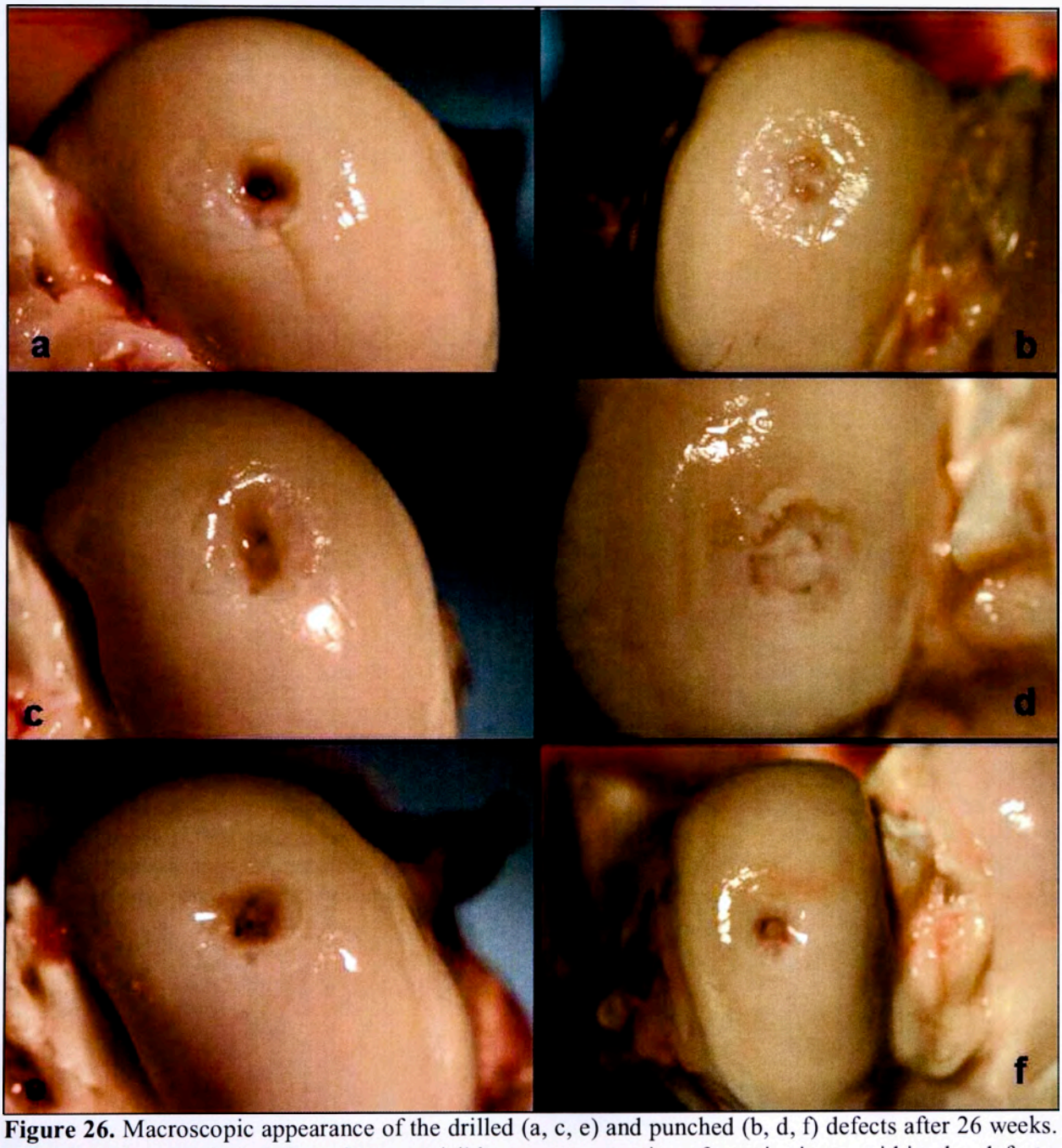


**Figure 26.** Macroscopic appearance of the drilled (a, c, e) and punched (b, d, f) defects after 26 weeks. Note that the punched defects have a visibly greater quantity of repair tissue within the defects, however none are fully healed.

**52 weeks:** Similar to the 26 week group, the 52 week defects were not healed with smooth layers of hyaline cartilage. However, the quantity of repair tissue appeared to increase from 26 to 52 weeks (Figure 27). Three out of four defects were filled with repair tissue to the level of the adjacent cartilage, although the repair tissue appeared poorly organised and of dubious quality. The adjacent cartilage did not appear to have degenerated any more than the 26 week group, however, some degeneration is noted superior to the defect in three out of four sites.

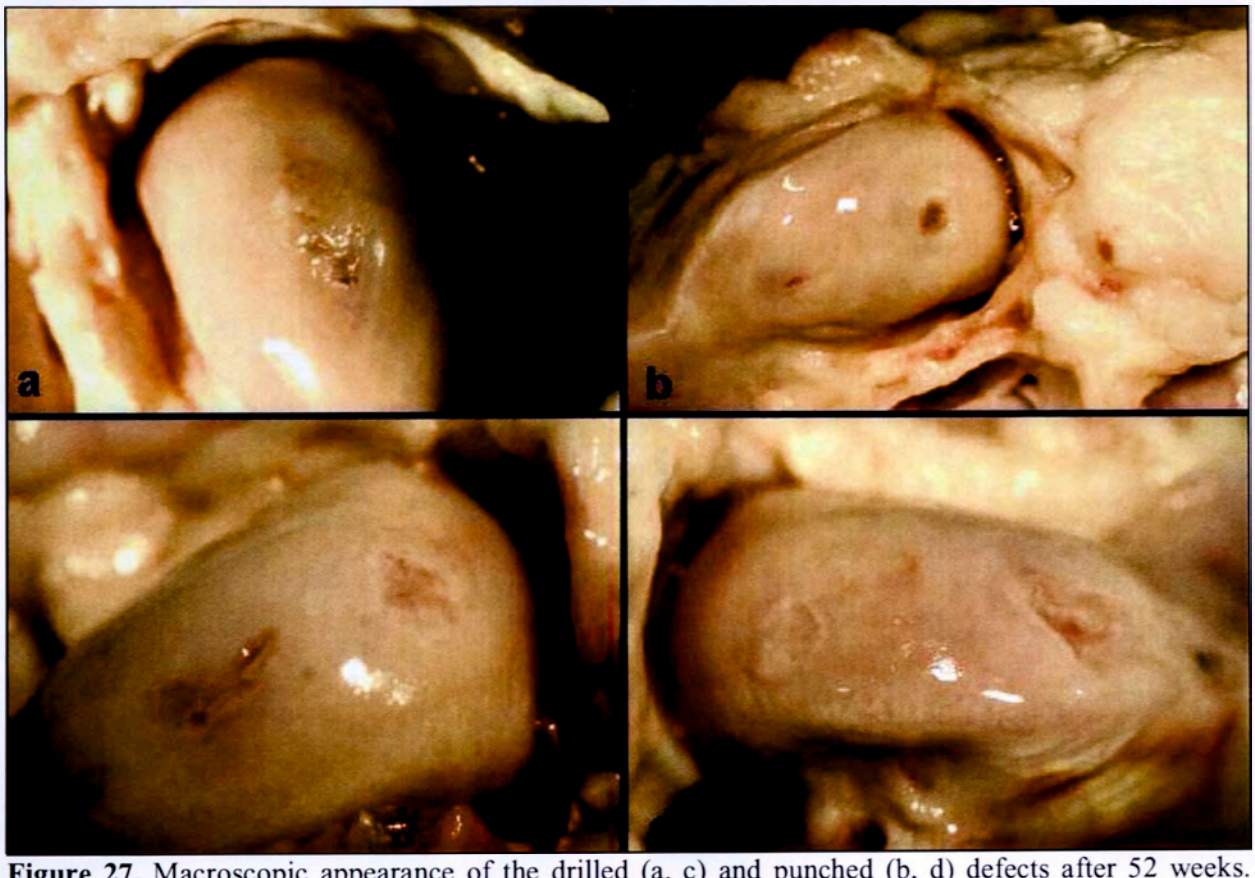


**Figure 27.** Macroscopic appearance of the drilled (a, c) and punched (b, d) defects after 52 weeks. Note that three of four defects have substantial amounts of disorganised repair tissue filling the defect. Also note the presence of secondary lesions superficial to the defect. The cause of these defects may be stray diathermy marks from the joint exposure.

### 3.4.4 Histology

**4 weeks:** Histology confirmed that none of the empty defects from either the punch or drill group had successfully healed with layers of hyaline cartilage and subchondral bone. Vacant space constituted the majority of most defects and in no case was the surface of the cartilage restored. In almost all cases, the subchondral bone compartment was either empty or only partially filled, with the punch group exhibiting larger voids than those observed with the drill group. The punch group showed an increased incidence of bone resorption (Figure 28), while the drill group showed a larger amount of new bone formation at the base of the defect. Apart from some new bone in the drill group, the most prevalent repair tissues within the defects were blood clot and loose fibrous tissue, with occasional islands of cartilage deep in the defect. Most of these cartilage islands appeared to have subsided from the surface. In general, the bone compartment appeared empty in the punch group, with more repair tissue, albeit of poor quality, being found in the drill group (Figure 29).

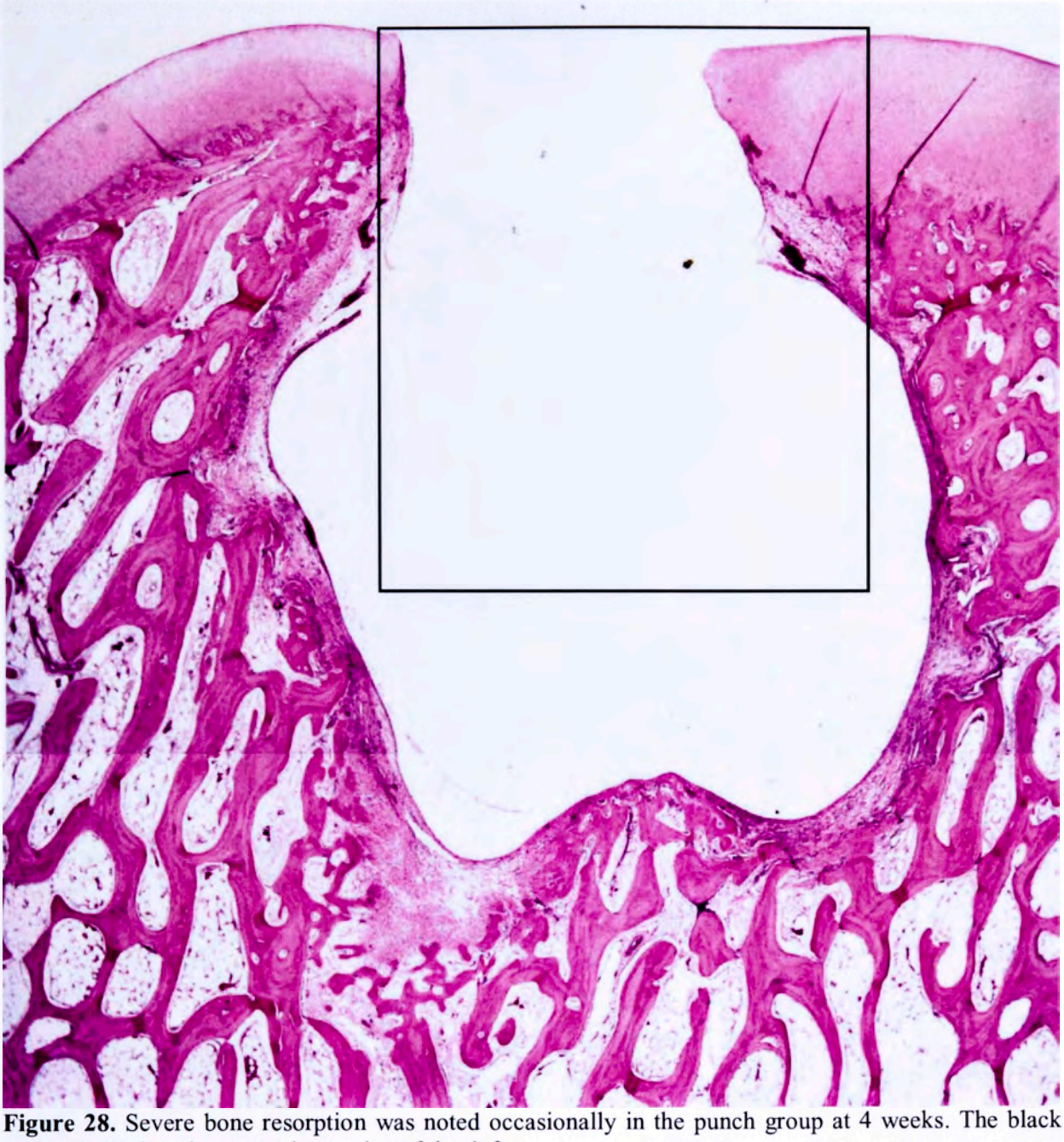

**Figure 28.** Severe bone resorption was noted occasionally in the punch group at 4 weeks. The black rectangle depicts the approximate size of the defect.

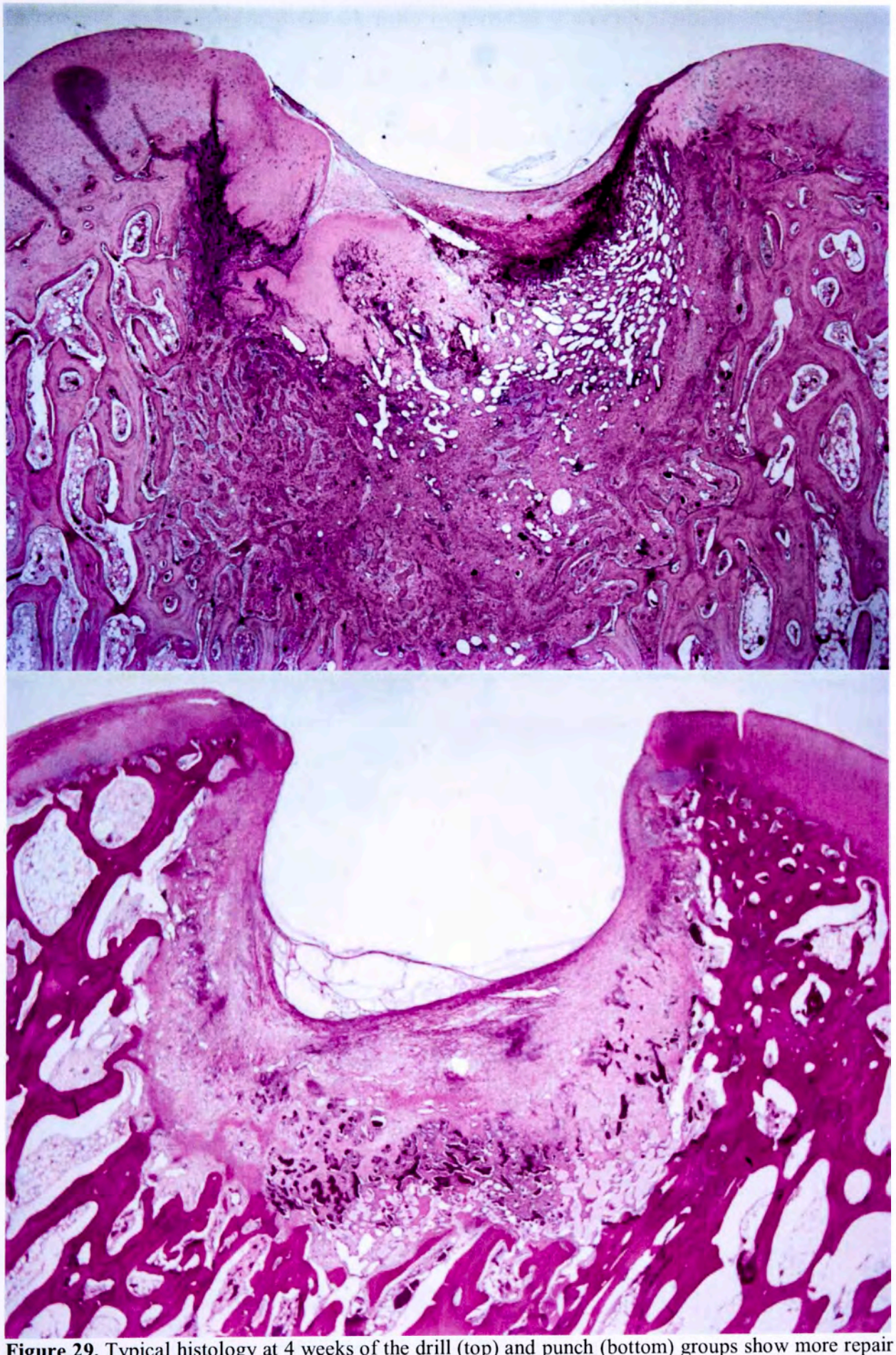

**Figure 29.** Typical histology at 4 weeks of the drill (top) and punch (bottom) groups show more repair tissue and more new bone formation in the drill group. Both images highlight degeneration of the surrounding cartilage in the form of fissures. The drill group also often had islands of cartilage in the defect, which may have subsided from the surface. Original magnification 12.5x.

In no case was the surface successfully restored at 4 weeks. Chondrocyte clustering was evident at the edge of the defects in both groups, providing evidence for a minimal healing response in the cartilage (Figure 30). In most cases, however, localised clustering was also accompanied by a regional decrease in cellularity. Minor fibrillations in the adjacent cartilage were noted occasionally in both the punch and drill group. Safranin-O stained sections revealed severe reduction in proteoglycan content in the cartilage at the boundaries of the defect, which was obvious in both drill and punch groups (Figure 31). The drill group showed some localised staining of the repair tissue, sometimes deep in the bone region, and also highlighted the loss of proteoglycans at the occasional surface fibrillations (Figure 31, top). Histological grading with the modified O'Driscoll scale revealed an average score of $4.5 \pm 1.7$ and $1.3 \pm 0.5$ for the drill and punch groups respectively.

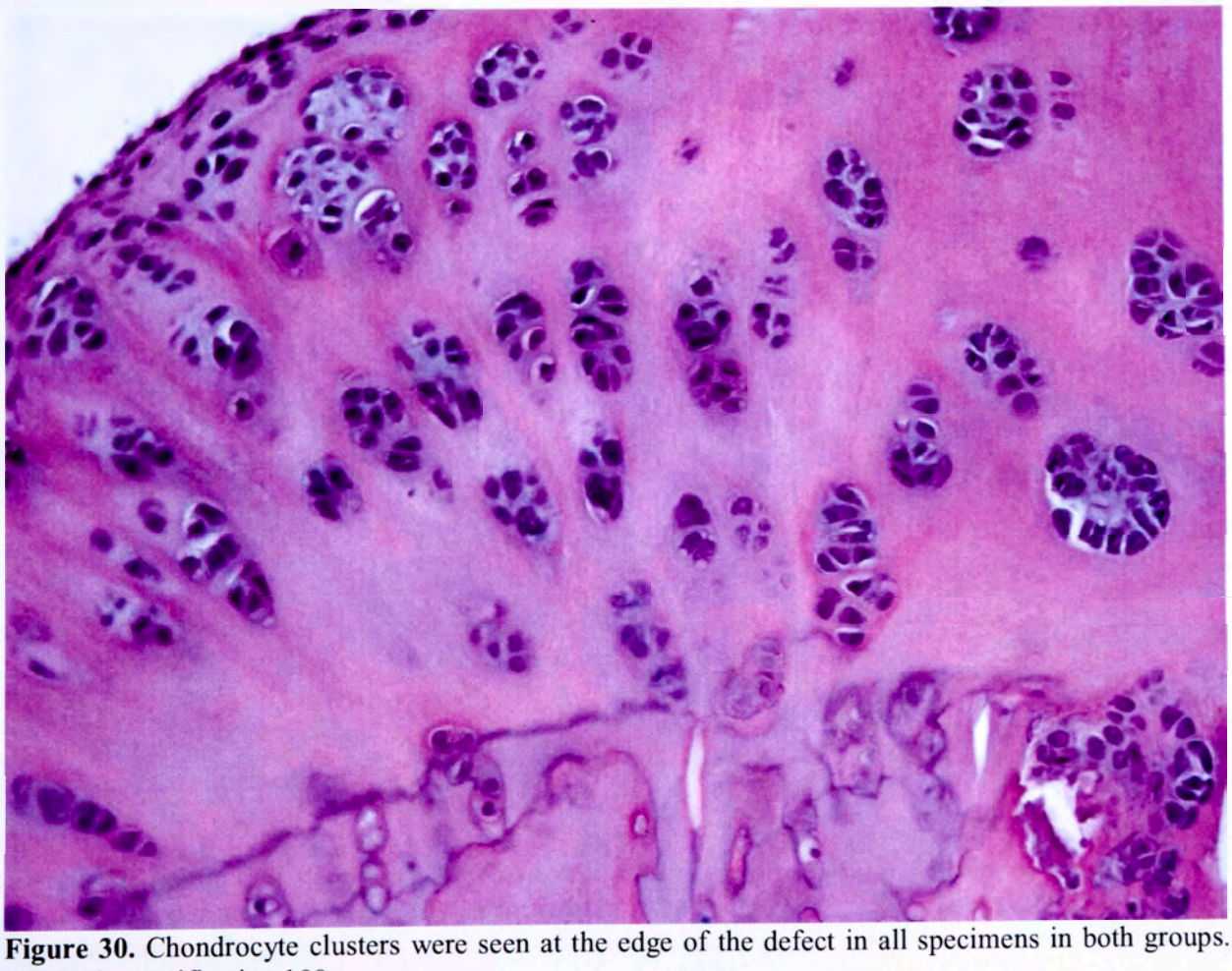

**Figure 30.** Chondrocyte clusters were seen at the edge of the defect in all specimens in both groups. Original magnification 100x.

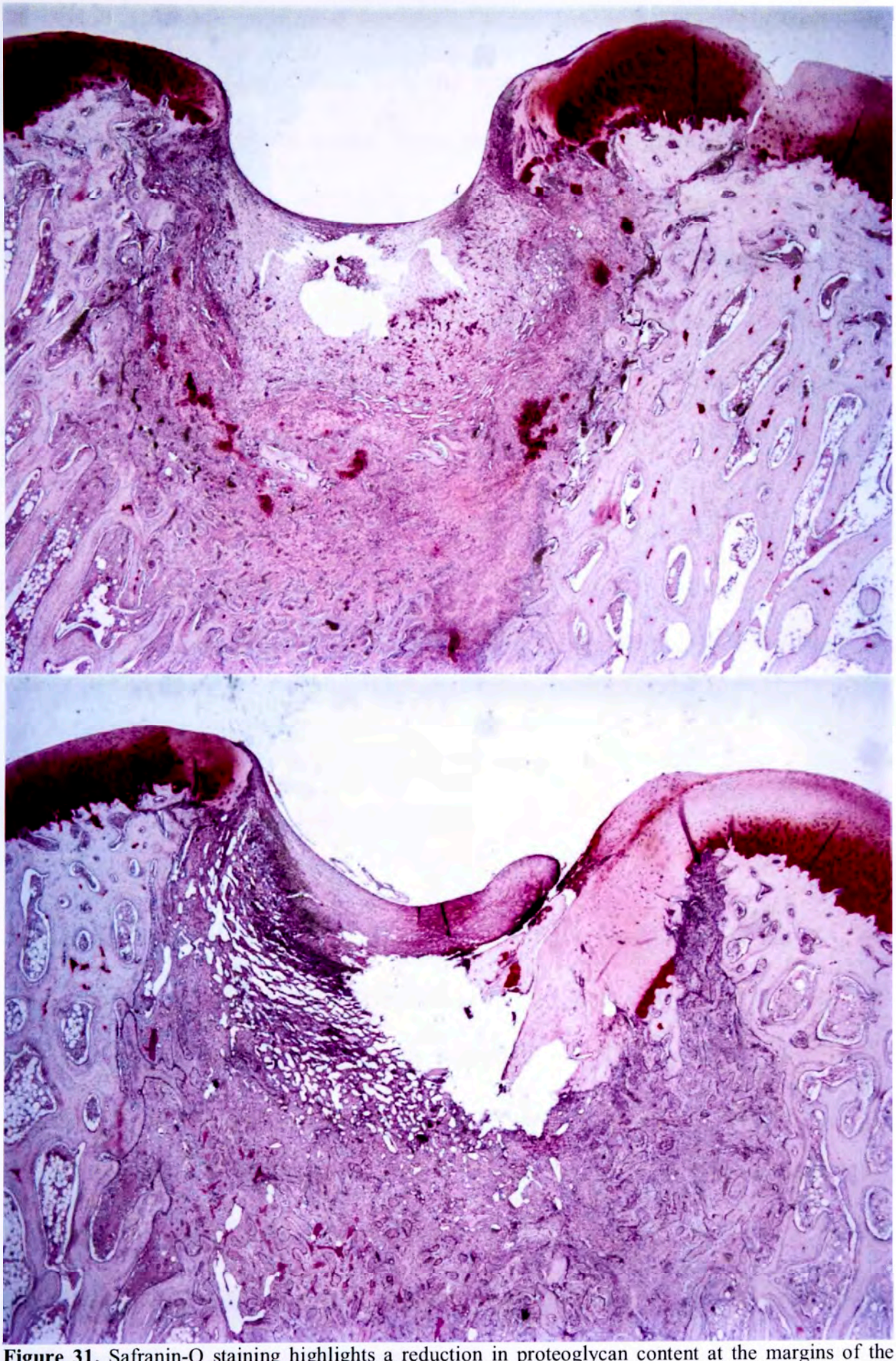

**Figure 31.** Safranin-O staining highlights a reduction in proteoglycan content at the margins of the defect and at a fissure approximately 3mm from the edge of the defect (top). In time, a fissure such as this may cause a large island of cartilage, with the underlying subchondral bone to subside into the defect (bottom).

**26 weeks:** Histology confirmed that neither of the groups had completed successful restoration of the empty defects with the original subchondral bone and hyaline cartilage layers, even by 26 weeks. There was marked improvement in both groups from 4 weeks to 26 weeks, particularly in the amount of repair tissue and the repair of the subchondral bone. This was most noticeable in the punch group where there was no evidence of bone resorption such as was occasionally noted at 4 weeks. In exactly half of the specimens, a subchondral bone bridge formed underneath the cartilage surface, leaving a large cyst deep in the defect (Figure 32).

In both groups, the repair tissue was generally well bonded to the adjacent cartilage and usually stained positively with Safranin-O, indicating a high concentration of proteoglycans. Again, this was more noticeable in the punch group. The surface was restored to a higher quality in the punch group when compared to the drill group, in which large crevices were still obvious. Nonetheless, a smooth and intact surface was not achieved in any of these untreated defects.

The appearance of the adjacent cartilage at 26 weeks was similar to that at 4 weeks, with chondrocyte clusters, some hypocellularity and occasional fissures/fibrillations. The adjacent cartilage did not appear to degenerate significantly from 4 to 26 weeks in either group. However, the cartilage adjacent to the drilled defects was of poorer quality than the punched defects with surface fibrillations and irregularities being more commonly seen in the drill group at 26 weeks (Figure 33). Histological grading with the modified O'Driscoll scale revealed an average score of $8.7 \pm 3.2$ and $11.7 \pm 4.0$ for the drill and punch groups respectively.

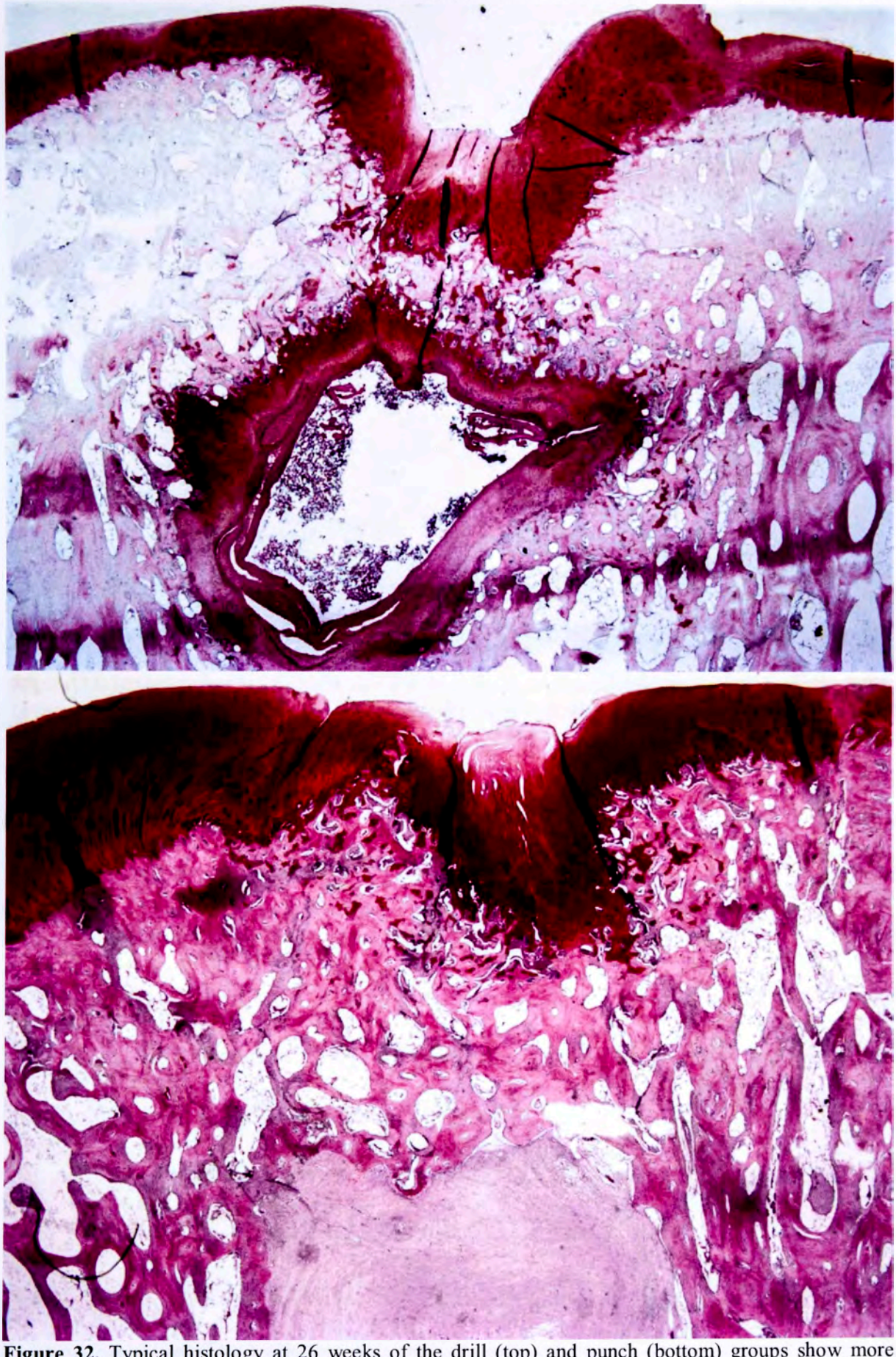

**Figure 32.** Typical histology at 26 weeks of the drill (top) and punch (bottom) groups show more repair tissue and more new bone formation in the punch group. The punch group also has a markedly smoother surface than the drill group. Note also that new subchondral bone has formed a bridge above the bottom of the defect, leaving a cyst underneath. Original magnification 12.5x.

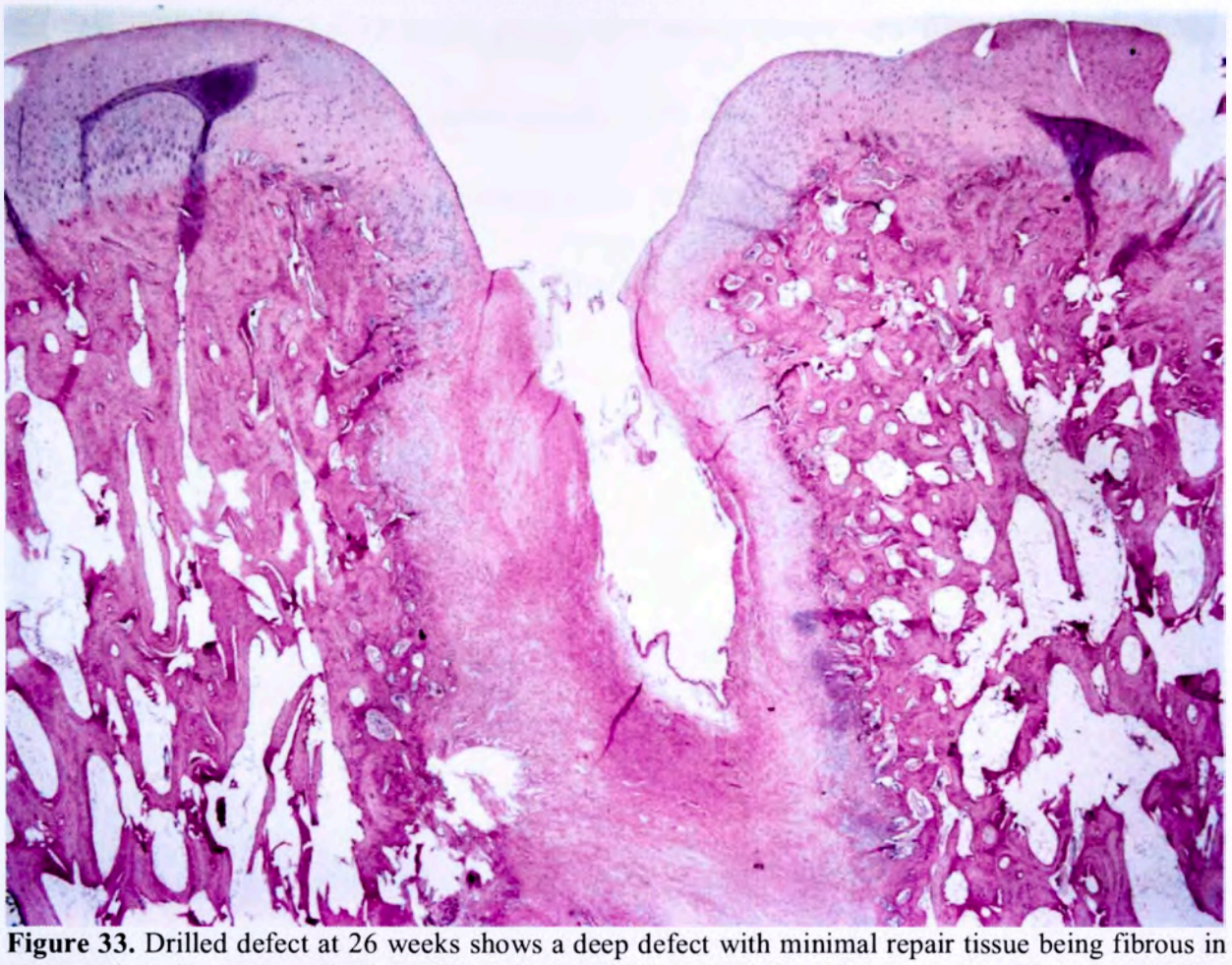

**Figure 33.** Drilled defect at 26 weeks shows a deep defect with minimal repair tissue being fibrous in nature. There is no reconstitution of the subchondral bone and deep fissures and surface irregularities are present in the adjacent cartilage.

**52 weeks:** Histology at 52 weeks again confirmed that the 6mm defects created with either a punch or a drill were not completely healed. However, healing had progressed well from the 26 week time point with the reconstitution of the subchondral and underlying cancellous bone in three out of four cases. Whilst the subchondral and cancellous bone was reconstituted to the normal height in the area of the defect, the structural organisation was irregular. This indicates that bone remodelling is not yet complete at 52 weeks (Figure 34). The neo-cartilaginous repair tissue was greater than 50% of the normal thickness of the cartilage, although the surface was severely irregular. On a cellular basis, this neo-cartilaginous repair tissue does not represent hyaline cartilage. The cells are positioned randomly, with local areas of hyper- or hypocellularity and there is frequent evidence of chondrocyte clustering (Figures 35 and 36).Where the cancellous and subchondral bone was not reconstituted (in one of

the four defects in the 52 week group) the repair tissue was fibrous in nature and presented similarly to the typical result after 26 weeks (Figure 37). Histological grading with the modified O'Driscoll scale revealed an average score of 16.0 ± 2.4 and 12.0 ± 6.4 for the drill and punch groups respectively.

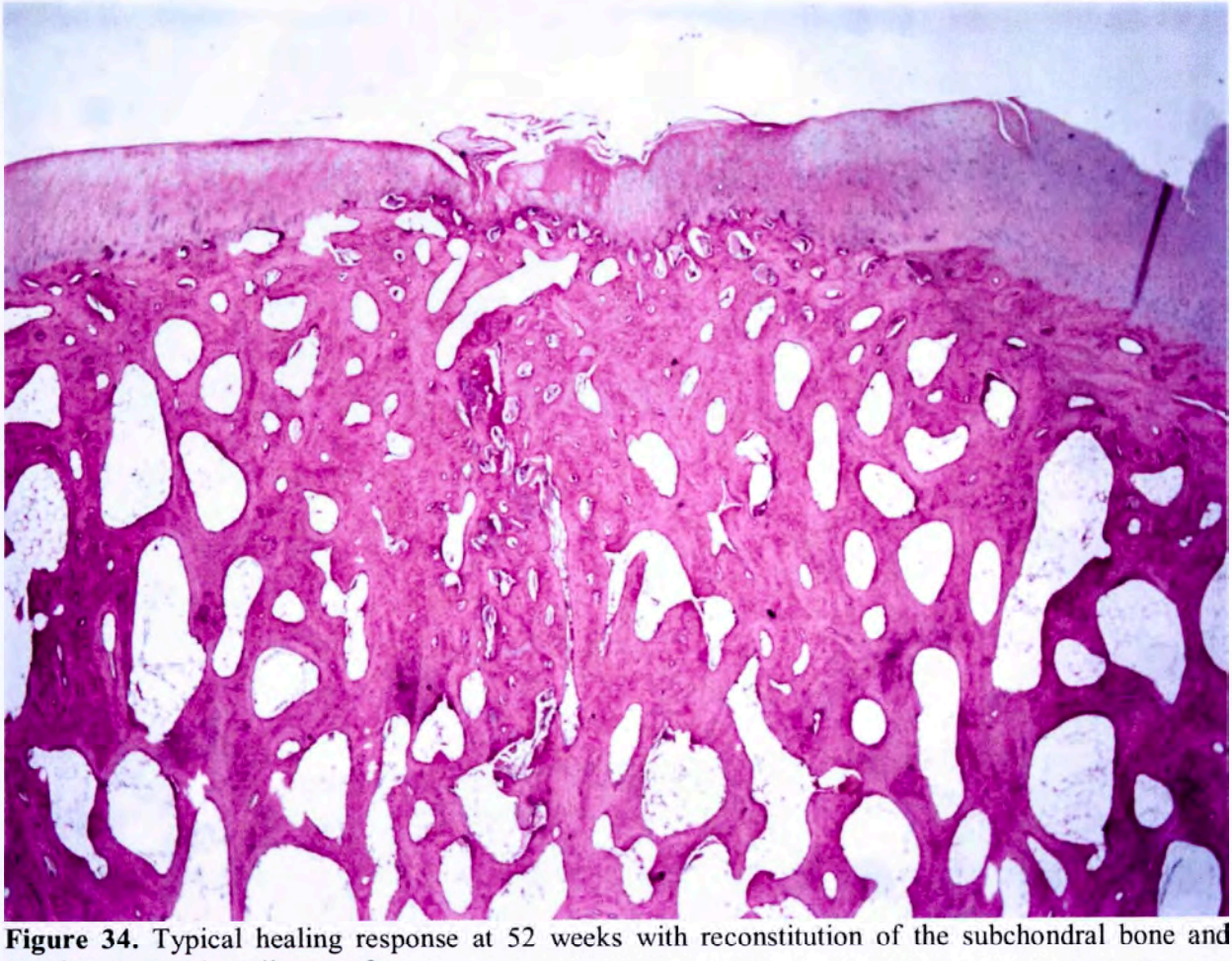

**Figure 34.** Typical healing response at 52 weeks with reconstitution of the subchondral bone and poorly structured cartilage surface.

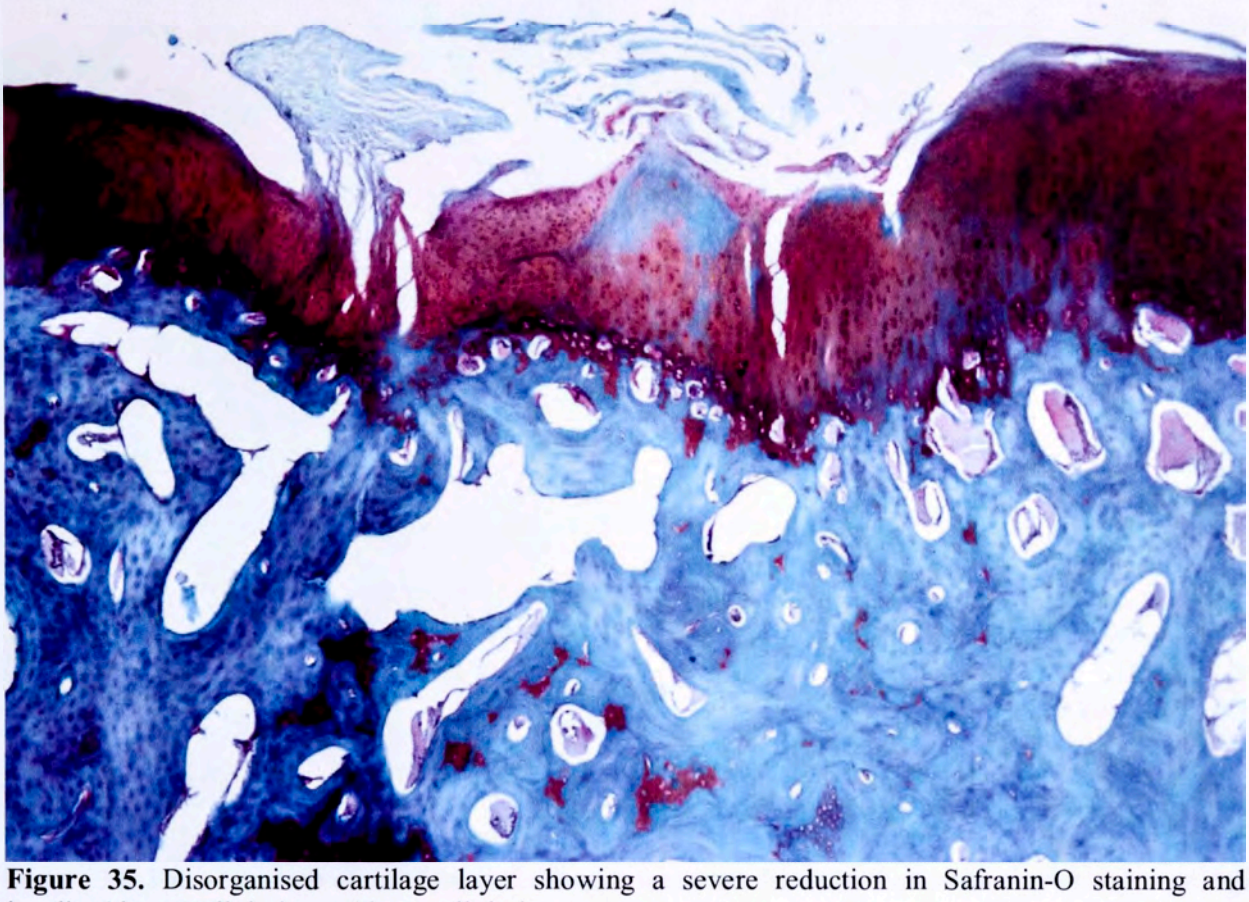

**Figure 35.** Disorganised cartilage layer showing a severe reduction in Safranin-O staining and localised hypercellularity and hypocellularity.

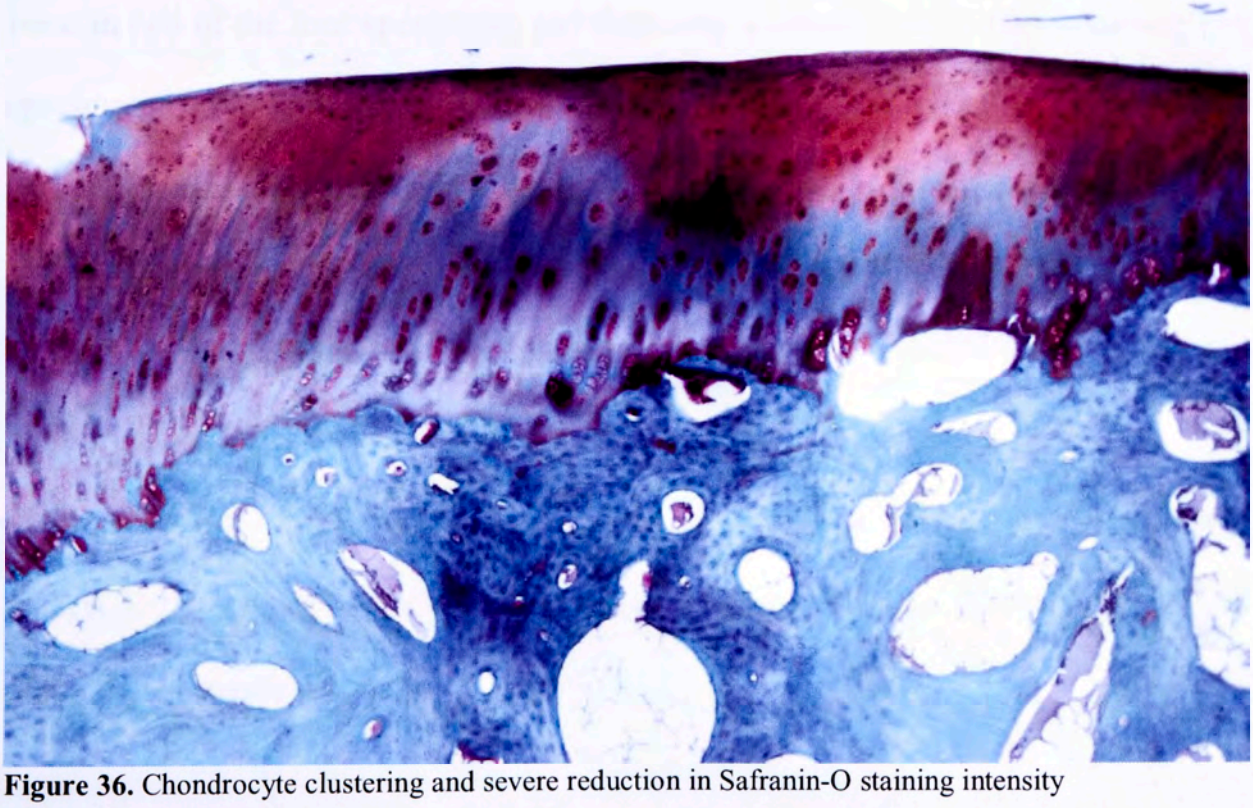

**Figure 36.** Chondrocyte clustering and severe reduction in Safranin-O staining intensity

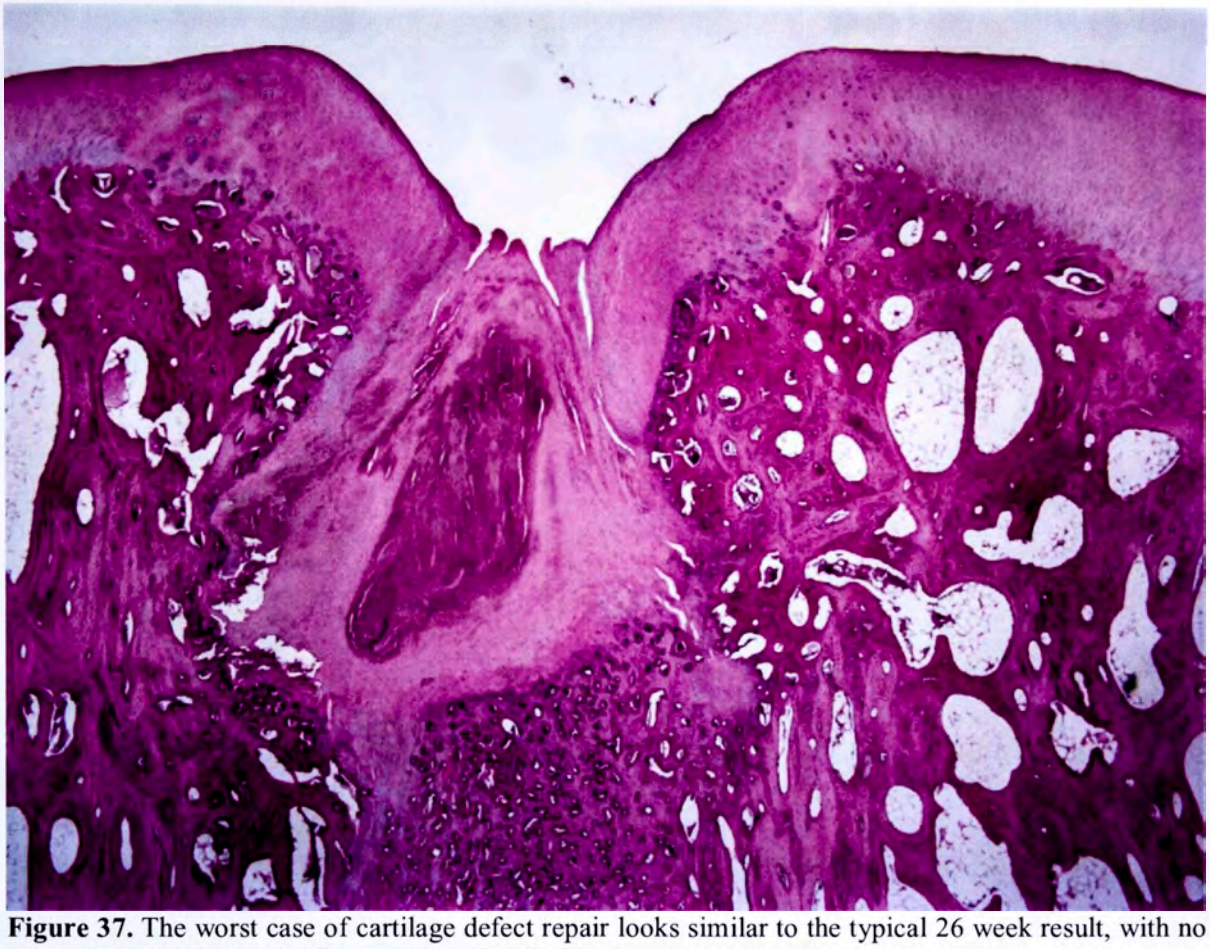

**Figure 37.** The worst case of cartilage defect repair looks similar to the typical 26 week result, with no reconstitution of the cancellous and subchondral bone.

### 3.4.5 Computed Tomography

Computed tomography at 52 weeks revealed poor reconstitution of the cancellous bone in two of the four specimens, and moderate reconstitution in the remaining two specimens. In those defects with less successful healing in the osseous regions, there was still some extent of new bone growth, however, it was not complete (Figure 38). In those defects which did fill with new bone, there were obvious changes to the surrounding cancellous bone, as evidenced by the local increase in signal on the radiograph, which may indicate increased bone density or increased volume of bone in the vicinity of the defect (Figure 39). From these CT scans it also appeared that the defects had progressed more deep than the original defect, suggesting some resorption of the bone beneath the defect.

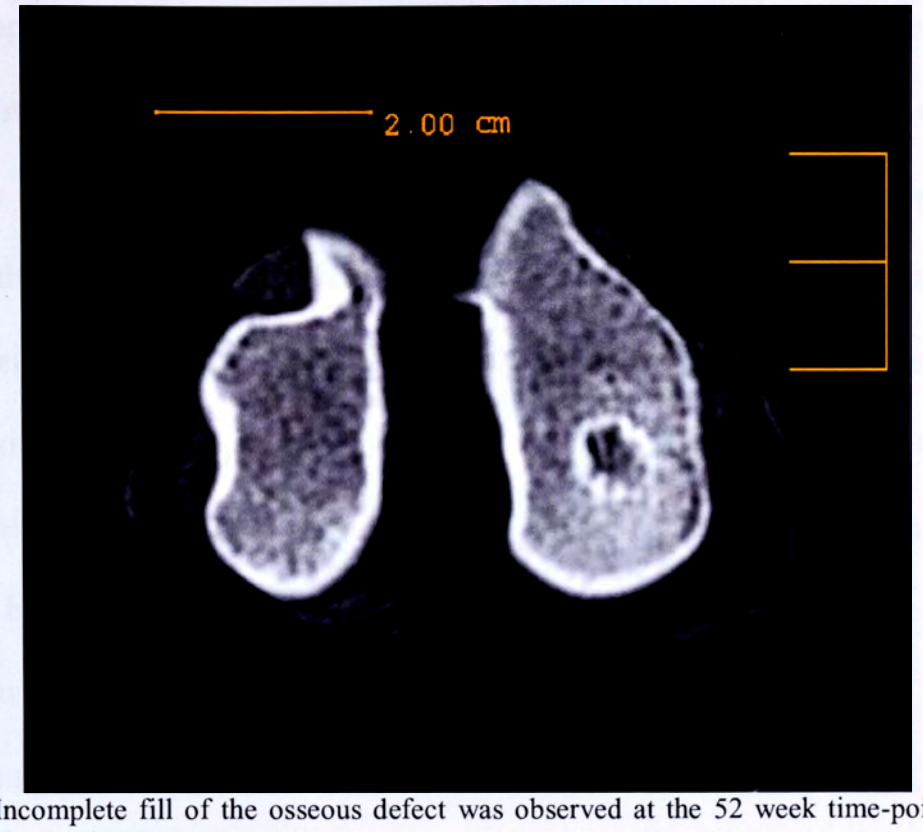


**Figure 38.** Incomplete fill of the osseous defect was observed at the 52 week time-point by regular computed tomography.

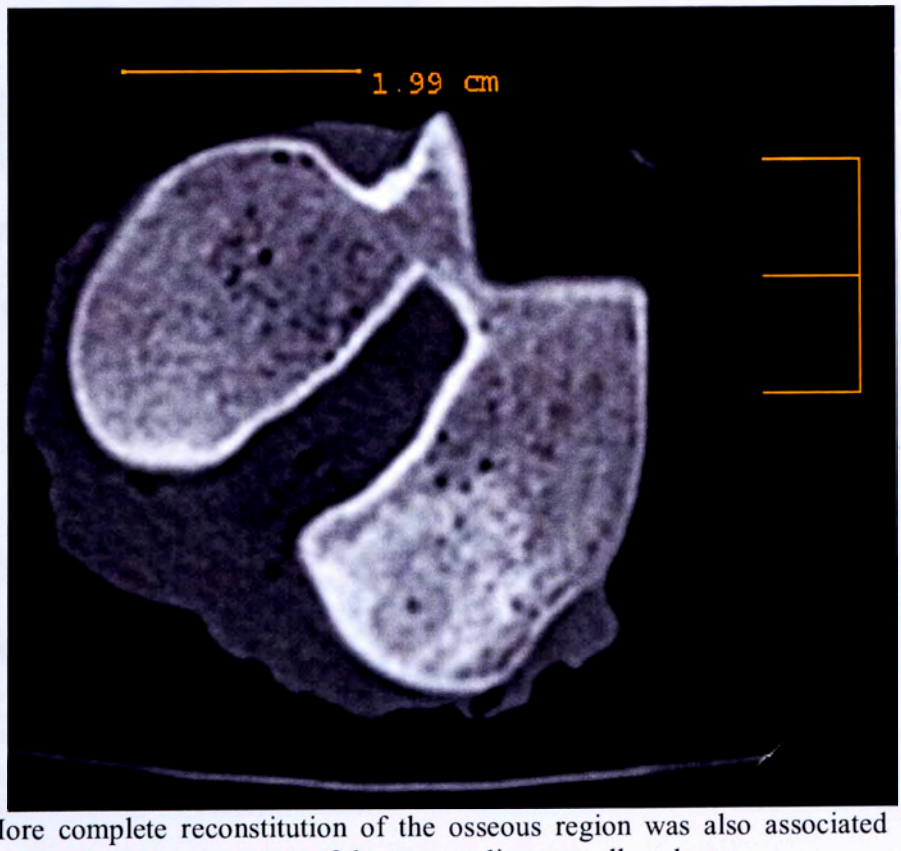


**Figure 39.** More complete reconstitution of the osseous region was also associated with observed changes in the radiographic appearance of the surrounding cancellous bone.

Micro-computed tomography at 52 weeks provided further evidence of the incomplete bone healing. On microCT it was evident that none of the osseous defects had completely filled with new bone, nor had bone remodelling been completed. Figure 40 shows that a defect that is partially filled with new bone, which near the articular surface seems close to the same density as the adjacent bone, but appears to be a lower density in the deeper regions. Importantly, the defect has become deeper than the original defect, which is suggestive of bone resorption in that area. The bone within the boundaries of the original defect, especially more deep, has the appearance of immature or woven-bone, which is evidences the observation that bony remodelling is not complete.

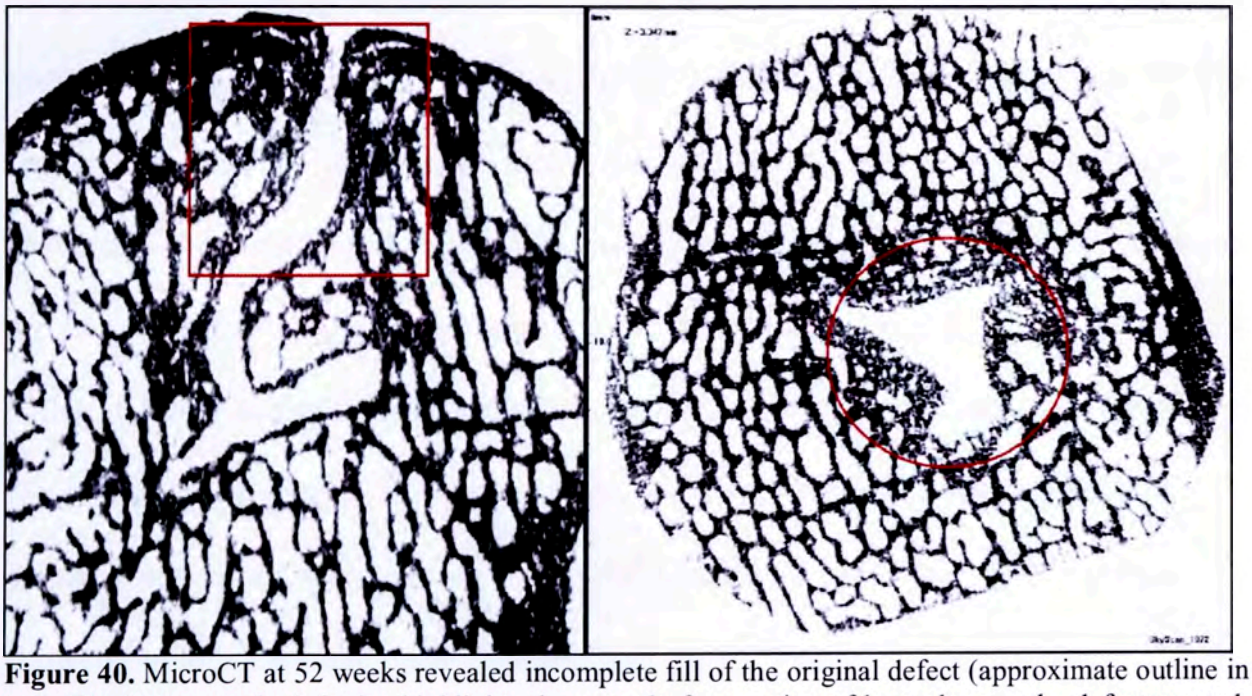

**Figure 40.** MicroCT at 52 weeks revealed incomplete fill of the original defect (approximate outline in red). The image on the left also highlights the extend of resorption of bone deep to the defect created, while the image on the right shows immature or woven bone inside the boundaries of the defect.

## 3.5 Discussion

The ideal treatment for cartilage lesions has yet to be revealed. While many studies have focussed on the specific treatment modality, there has been little exploration of the actual technique used to create the defect. Local tissue damage and the ensuing inflammatory reaction may play an important role in defect healing as well as the response to different treatment regimes. The primary aim of this study was not to treat a full thickness cartilage defect but rather to evaluate the biological effect of two different surgical methods of defect creation. This information will be valuable in both clinical and experimental scenarios where the surgical preparation of the defect may significantly influence the outcome of the repair or treatment options.

The intra-operative appearance of the drilled and punched defects was dissimilar, with the punch providing a much cleaner cut and more distinct margin to the defect at the surface of the cartilage. The drill produced a noticeably more ragged appearance around the edge of the defects and some damage to the adjacent cartilage was observed. These differences are due to the different mechanisms of cutting between the two systems, the punch is a clean vertical cut whereas the drill is a rotating cut which is likely to produce more abrasion and higher increases in temperature. These factors may contribute to increased trauma to the surrounding tissue in the drill group. These observations were supported by radiographs of time-zero defects which also showed obvious cartilage damage in the drill group. The punch also produces a flatter base than the drill and would therefore provide a larger contact area for an implant with a flat base. These differences may become important when implanting a rigid construct such as an osteochondral graft, or a semi-rigid construct such as a polymeric scaffold, using the press-fit method. When press-fitting an implant, intimate contact

with the adjacent tissue must be achieved and this will only be possible with precise geometry of both the walls and base of the defect.

Damage to the adjacent cartilage from the drill may be due to a local increase in temperature, inducing moisture loss in the cartilage or thermal necrosis of the tissue. Another possibility is the physical strain and abrasion of the cartilage as the drill rotates and removes chips of material. Chacon, et al showed that the design of the cutting faces of a drill significantly affects the heat generation within bone (Chacon et al. 2006) which we can assume would not be replicated to the same extent when using a punch. That being said, Huntley has reported that not all punches are created equal, with more acute angles of the cutting edge resulting in smaller margins of chondrocyte death (Huntley et al. 2005). Evans, et al. found that the viability of chondrocytes after harvesting osteochondral grafts was improved using a punch harvesting technique as opposed to a powered trephine. These researchers concluded that the power harvesting method produced a larger "zone of death" around the edge of the graft which may negatively impact the integration and clinical survival of the graft. They suggest that to preserve healthy chondrocytes in the cartilage graft, only manual harvesting methods should be used. This agrees with the current study, where a more positive healing response was associated with the punch method compared to the powered drill, especially in the early time points.

Our results demonstrate that after 4 weeks of healing all of the defects remained with a large central void and exposed subchondral bone deep into the defect. The subchondral and cancellous bone were not restored in any specimen and significant bone resorption was observed in approximately half of the specimens. On several

occasions the walls of the defects had collapsed and cartilage islands subsided from the surface into the base or walls of the defect. This may have caused an aberration in the scoring system at 4 weeks, since the hyaline tissue in the defect may have subsided from the surface rather than having been formed in the defect. This was also noted in Jackson's empty defect model in the goat (Jackson et al. 2001). Similarly to Jackson's goat model, our sheep model showed no evidence of extensive bone resorption at 26 weeks and indeed the reconstitution of the subchondral bone had progressed well by this time. This was most obvious in the punched defects. By 52 weeks, the subchondral bone was re-established and substantially remodelled back to a normal state in 75% of the defects.

However, CT and microCT revealed that none of the defects at 52 weeks were completely filled with bone, and that some resorption had occurred deep to the original defect. In addition, there were obvious changes in the radiographic appearance of the cancellous bone adjacent to the boundaries of the original defect, suggesting that stress distribution throughout the cancellous bone was different in response to the defect and that bone remodelling was active, but not yet complete.

Jackson also reports a similar finding to our subchondral bone bridge with a large cyst deep in the defect at 26 weeks. These observations strongly suggest that the reconstitution of the subchondral bone is paramount for the successful repair of a cartilage defect. A solid base is essential not only to provide support for the cartilage, but also to promote normal transmission of load through the joint such that the neo-cartilage experiences physiological loads (Braman et al. 2005;Raimondi & Pietrabissa 2005). This also supports the theory that implants consisting of very weak or

compliant materials, such as fibrin glue or collagen sponge, would not be effective as osteochondral replacements since they cannot transmit load to the surrounding cancellous bone. In accordance with Wolff's Law of bone remodelling, such implants would not prevent bone resorption nor promote bone growth and the restoration of the cartilage layer could not proceed with satisfaction.

Another factor that may contribute to the resorption of bone within these empty defects is fluid-induced osteolysis. The pressure of fluid, and in particular synovial fluid, around cancellous bone has been observed to induce osteolysis and contribute to implant loosening in animal models (Aspenberg & Van, V 1998;Van, V et al. 1998). As the sheep knee in the current model is loaded and unloaded, the synovial fluid is forced into the defect and repetitive cycles may cause accumulative damage that eventually progresses as osteolysis. Whether this observed action is due to fluid pressure alone, or from molecular components of the synovial fluid (including potential wear debris) is unknown at this stage.

Whilst the drill group in this study appeared to have superior fill of the defect at 4 weeks, by 26 weeks the punched defects were superior in all aspects. The bone restoration was more complete, the cartilage surface smoother and nearer to the normal height and the staining with Safranin-O more homogenous throughout the neo-cartilage. Cellular activity in the surrounding cartilage at 4 weeks presented as localised chondrocyte clustering accompanied by regional decreases in cellularity. This suggests that the future maintenance of the extracellular matrix may be jeopardised. At 26 weeks, degeneration of the adjacent cartilage was somewhat improved in the punched defects but remained unchanged in the drilled defects from 4

to 26 weeks. However, in no case was the untreated, empty defect repaired successfully with a smooth hyaline cartilage surface on top of a structurally integral base of subchondral bone. Since all other aspects of the surgery were identical, the differences noted between the punch and drill groups can be attributed to the instrumentation used to create the defect.

With the loss of the third animal at 52 weeks giving a reduced sample size of two, it is difficult to interpret differences between the groups at this time point. However, the subchondral and cancellous bone layers were reconstituted, albeit not entirely remodelled, in three of four defects, which was not seen in any of the 26 week animals. At 52 weeks, the adjacent cartilage appeared on histology to be similar, if not somewhat improved, when compared to the 26 week groups.

Histological grading with the modified O'Driscoll scale revealed a significant difference between the drill and punch group at 4 weeks (P=0.014) but not at 26 or 52 weeks (Figure 41). The 52 week punch group is marred by large standard deviation due to the small number of animals in this cohort, after the complication with the third animal in a group which was already small in number. For this reason, the data is re-plotted without the drill and punch groups (Figure 42). In this case, the collective 26 week defects were significantly improved compared to the collective 4 week defects (P=0.001) and the 52 week defects were almost significantly improved compared to the 26 week defects (P=0.06). With increased sample size, it is likely that significance would be established.

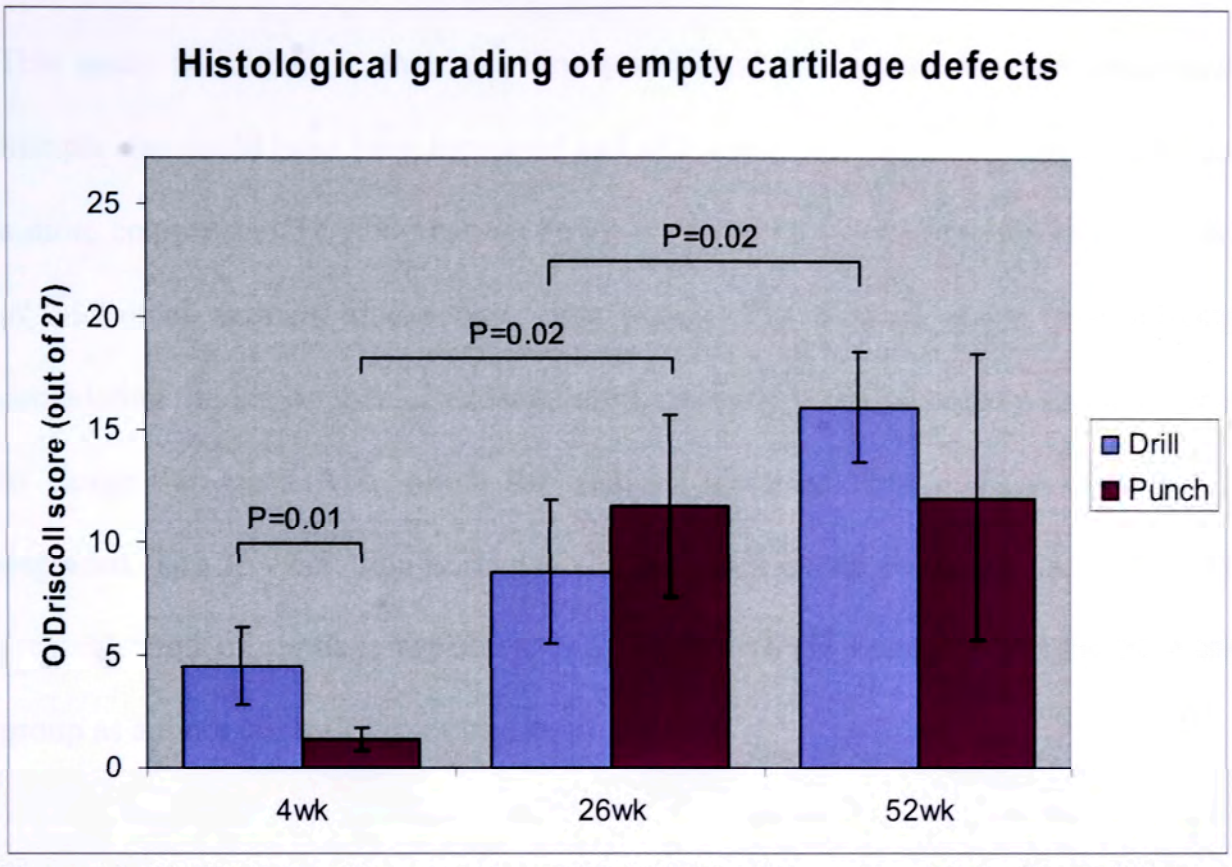


**Figure 41.** Histological grading using the modified O'Driscoll score revealed significant differences between the punch and drill at 4 weeks, the punch group from 4 to 26 weeks and the drill group at 52 weeks compared to 4 and 26 weeks. Large standard deviations in the 52 week punch group were due to one underperforming defect and only a small sample size.

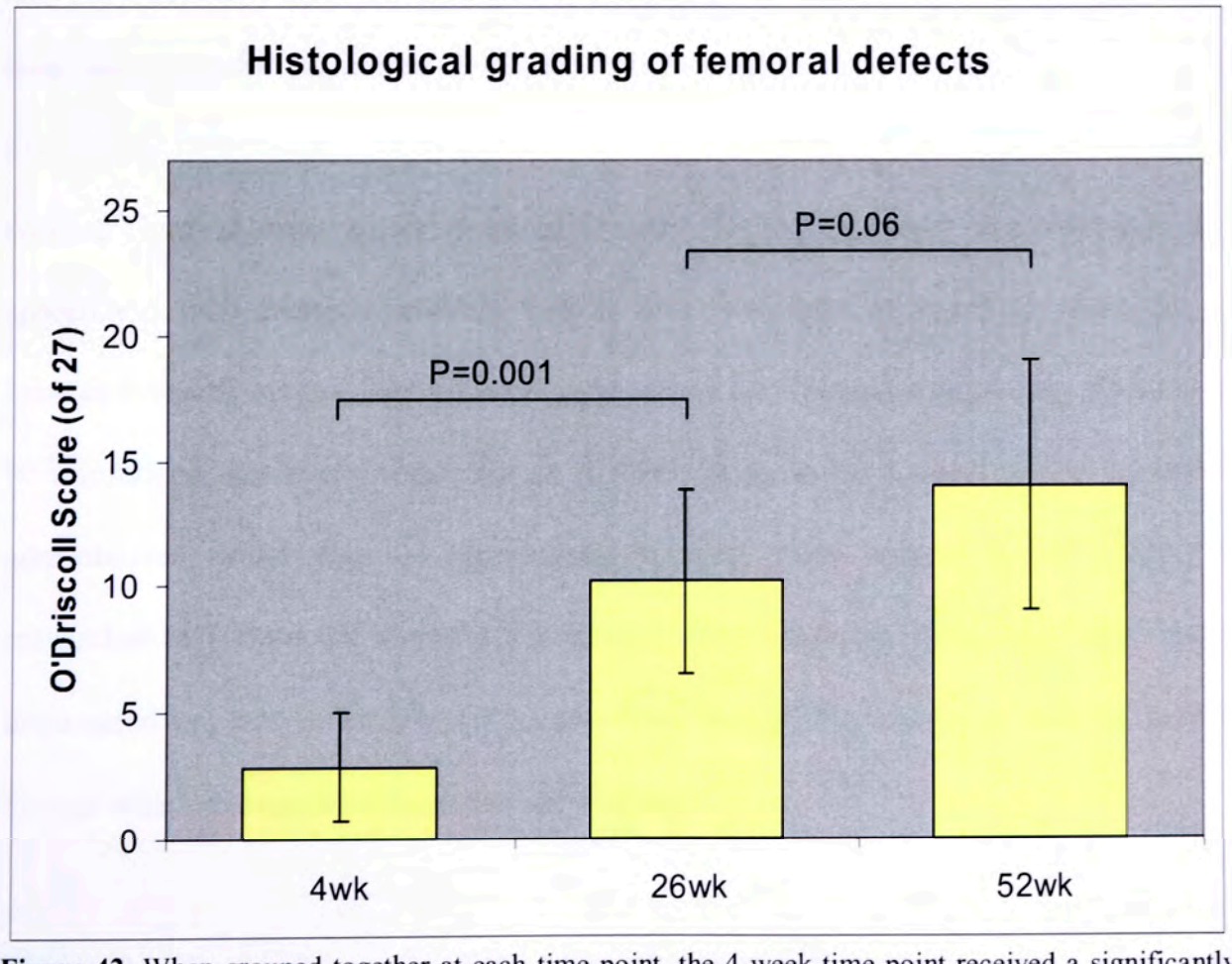


**Figure 42.** When grouped together at each time point, the 4 week time point received a significantly lower score than the other groups. The 52 week time point showed a trend of being improved over the 26 week time point (P=0.06), which may have become significant with increased sample size.

This study is limited in that only one punch and drill geometry were examined. Sample size could have been increased and additional time points included to provide a more comprehensive examination, however, financial constraints prevented the use of additional animals at the later time points. The 4 week group was selected considering the importance of understanding the early phase of healing and to be able to gauge the speed with which the adjacent cartilage may become damaged or degraded. The 26 week time point was chosen based on the minimum time suggested for evaluation of cartilage repair methods by the ASTM standard and the 52 week group as a more clinically relevant late time point.

This study has thus shown that creating a full thickness cartilage defect with a punch provides a superior healing response to the same approach using a drill. At the early time point, the drill causes more aggressive spontaneous healing with a greater fill of the defect, albeit with mostly fibrous tissue. In contrast the less aggressive punch method elicits minimal repair tissue at 4 weeks. Hence the punch technique provides researchers with greater control of their in vivo evaluation of a specific treatment, at least in the early stages. This is favourable where the spontaneous healing effect is to be minimised, since any repair tissue is more likely to be a result of the treatment administered rather than of spontaneous healing. Such control would allow the researcher to isolate the active component of their implant, which may be a tissue engineered implant, cultured cells or any other biological component such as growth factors which are most active in the early stages.

This study has also shown that 6mm defects in the weight bearing region of the sheep medial femoral condyle do not spontaneously repair with hyaline cartilage even after

52 weeks. The repair tissue at 26 and 52 weeks was predominated by fibrous tissue and disorganised neo-cartilage, not of the high quality of normal hyaline cartilage. These defects were often associated with underlying cancellous bone resorption, defect wall collapse and degeneration of the adjacent cartilage, which highlights the need for new treatment modalities for osteochondral defects. Finally, this study has highlighted the need for more thorough reporting of the surgical technique in the creation of full thickness cartilage defects.

# 4.0 Damage to the proximal tibial condyle and meniscus following an untreated osteochondral defect on the medial femoral condyle

## *4.1 Introduction*

The previous section of this study dealt with the healing of osteochondral defects on the medial femoral condyle of sheep. Macroscopic observations of damage to the meniscus and tibial articular cartilage opposite the defect in the 26 week animals prompted this second study using the same animals. It has previously been shown that major interventions such as metallic resurfacing can have a degradative affect on the articular cartilage that it articulates against (Kirker-Head et al. 2006; Custers et al. 2007). Furthermore, the susceptibility of articular cartilage to abrasive damage has been highlighted in a study that showed degradation in articular cartilage after repairing the meniscus with sutures (Yasunaga et al. 2001). It is also known that osteochondral defects significantly alter the stress and contact area across a joint (Braman et al. 2005), which may also play a role in damaging the surface opposing a defect. For these reasons, the tibial cartilage and meniscus opposing an osteochondral defect in the femur were analysed at 26 and 52 post operative weeks.

## *4.2 Methods*

### 4.2.1 Macroscopic Assessment

Immediately following sacrifice, the proximal tibial condyles and menisci were harvested from the animals in the 26 and 52 week groups of the previous study. Macroscopic damage to the tibial cartilage was assessed using a modified Outerbridge scale (Table 3).

**Table 3.** Modified Outerbridge scale for macroscopic assessment of cartilage

| Outerbridge Score | Appearance |
|---|---|
| 0 | Normal |
| 1 | Minor roughening of the superficial zone |
| 2 | Extensive roughening and/or deep fissures in small areas <1cm2 |
| 3 | Extensive roughening and/or deep fissures in large areas >1cm2 |
| 4 | Erosion to subchondral bone |

### 4.2.2 Histology

Both tibial condyles and menisci were fixed in cold phosphate buffered formalin for a minimum of 48 hours, after which time the tibiae were decalcified in 10% formic acid-formalin solution for approximately 4 weeks, or until soft enough to be cut with a blade. The tibiae were grossly sectioned into three blocks in the coronal plane through the region opposing the defect on the femur (Figure 43). The menisci in the same region were similarly sectioned. As before, samples were embedded in paraffin blocks, sectioned to 5μm slices and stained with Haematoxylin & Eosin. The tibial sections were also stained with Safranin-O and Fast Green, which stain the proteoglycans and bone respectively. Sections from each of the three tibial blocks were graded using the 14 point Mankin scale (Table 4), whereas the meniscal sections were analysed subjectively for structural damage or degenerative changes. Quanititative data was analysed using a one way analysis of variance with SPSS for Windows, with a significance level of P=0.05.

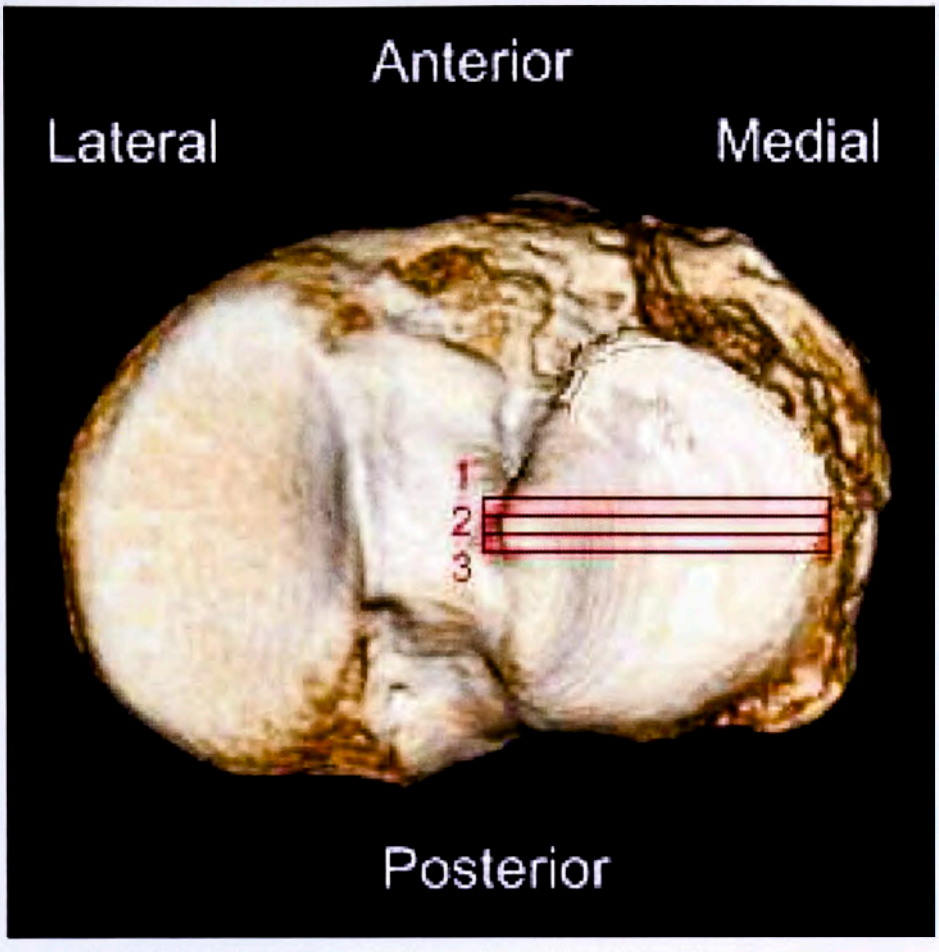


**Figure 43.** The medial tibial plateau was grossly sectioned into three blocks

**Table 4.** The Mankin scale is a 14 point histological grading system that quantifies the quality of articular cartilage with respect to the structure, cellular characteristics and proteoglycan content

| **Mankin Scale**<br>Histologic and Histochemical Grading of Articular Cartilage | |
|---|---|
| **I. Structure** | **Score** |
| a. Normal | 0 |
| b. Surface irregularities | 1 |
| c. Pannus and surface irregularities | 2 |
| d. Clefts to middle zone | 3 |
| e. Clefts to deep zone | 4 |
| f. Clefts to calcified cartilage | 5 |
| g. Complete disorganisation | 6 |
| **II. Cells** | |
| a. Normal | 0 |
| b. Diffuse hypercellularity | 1 |
| c.Chondrocyte clustering | 2 |
| d. Hypocellularity | 3 |
| **III. Safranin-O staining** | |
| a. Normal | 0 |
| b. Slight reduction | 1 |
| c. Moderate reduction | 2 |
| d. Severe reduction | 3 |
| e. No dye noted | 4 |
| **IV. Tidemark integrity** | |
| a. Intact | 0 |
| b. Crossed by blood vessels | 1 |

## *4.3 Results*

### 4.3.1 Macroscopic Assessment

At 26 and 52 weeks, macroscopic grading using the Outerbridge scale revealed an average score of 1 out of a possible 4 (range 0 to 3). Most specimens received a score of 0 or 1, with one outlying site (drilled defect at 26 weeks) given an Outerbridge score of 3. There were no statistical differences detected between groups within each time point or between the two time points.

### 4.3.2 Histology

**26 weeks:** Histology confirmed that all tibiae at 26 weeks exhibited some form of structural degeneration and degenerative changes in the cellular aspect of the cartilage. Most commonly, this damage presented as an occasional deep fissure in the medial spline of the plateau, where the meniscus does not cover the tibial plateau. Commonly, some localised loss of Safranin-O staining was noticed, usually around these fissures (Figure 44) but also occasionally on the central region of the plateau. Cellular changes such as localised hypercellularity or occasional small areas of hypocellularity were noticed in most specimens, although chondrocyte clustering and widespread hypocellularity was rarely encountered. Blood vessels were observed to cross the tidemark in 30% of the tibiae at 26 weeks. In general, there was no observable difference between the drill and punch group, and this is reflected in the average Mankin scores of $6.4 \pm 1.7$ and $6.2 \pm 3.6$ respectively. When grouping the 26 week specimens together, the average Mankin score was $6.3 \pm 2.5$.

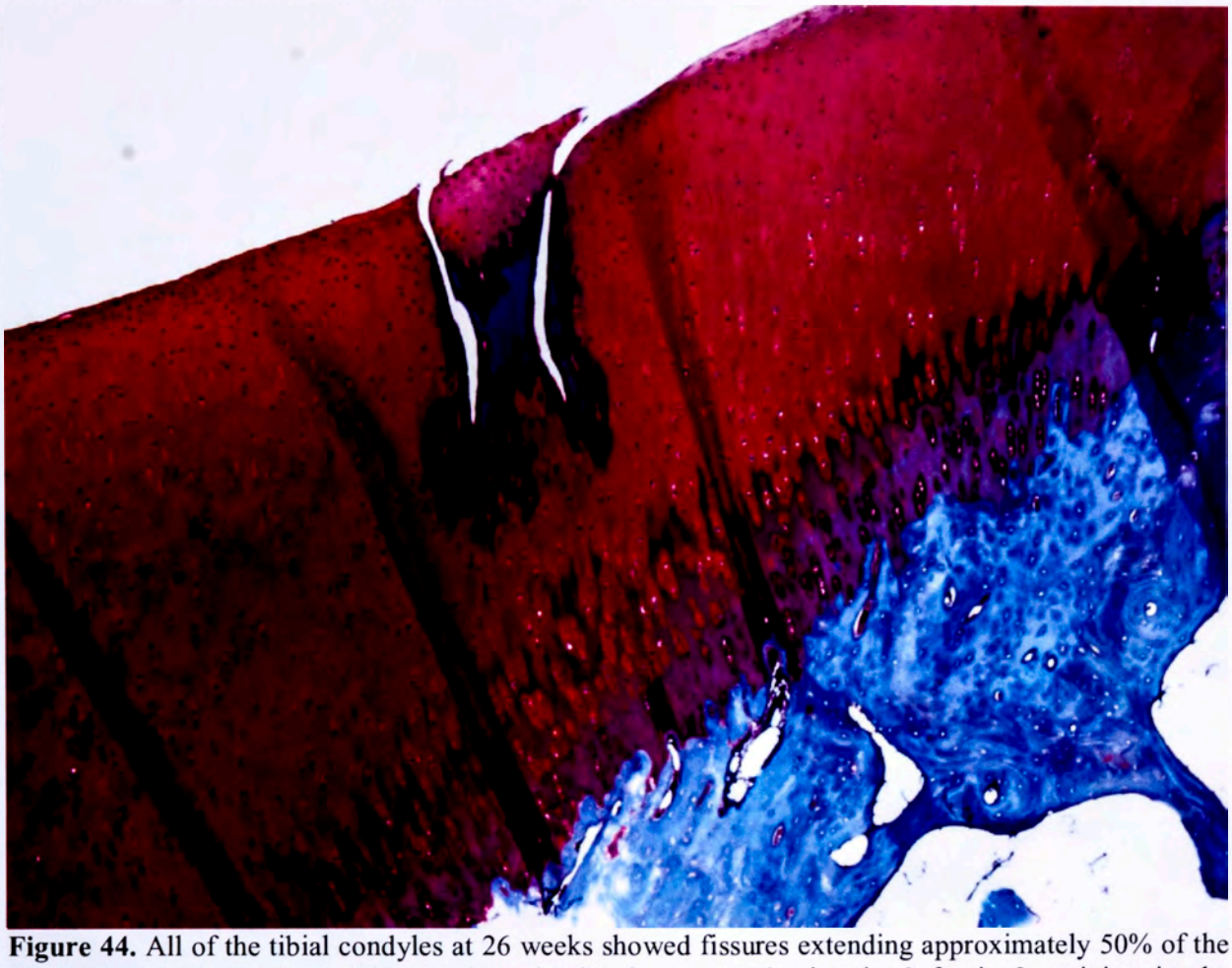

**Figure 44.** All of the tibial condyles at 26 weeks showed fissures extending approximately 50% of the thickness of the cartilage. This section clearly shows a reduction in Safranin-O staining in the immediate vicinity of the fissures.

The subchondral bone plate was observed to increase in thickness in four out of six tibial plateaux at this time point (Figure 45). There was no correlation between punch and drill groups. The structure of the cancellous bone and thickness of the trabeculae was difficult to analyse, however, subjectively they did not appear to be significantly different to the normal state.

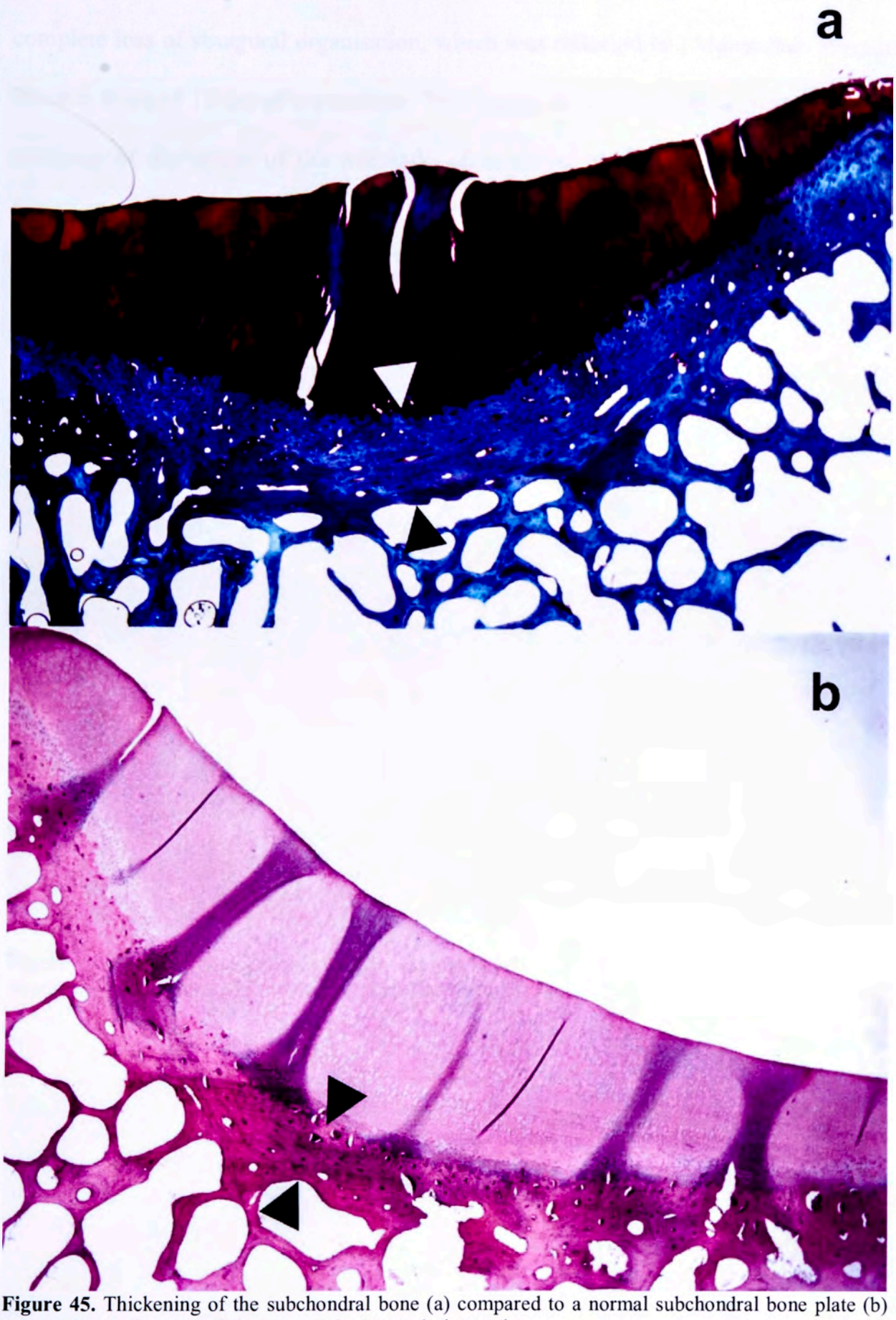


**Figure 45.** Thickening of the subchondral bone (a) compared to a normal subchondral bone plate (b) was evident in four out of six cases at the 26 week time point

In one case, where the meniscus was severely damaged, the tibial cartilage suffered complete loss of structural organisation, which was reflected in a higher than average Mankin score of 12 out of a maximum 14 (Figures 46 and 47). This site also showed evidence of disruption of the tidemark, chondrocyte clustering and large areas of hypocellularity.

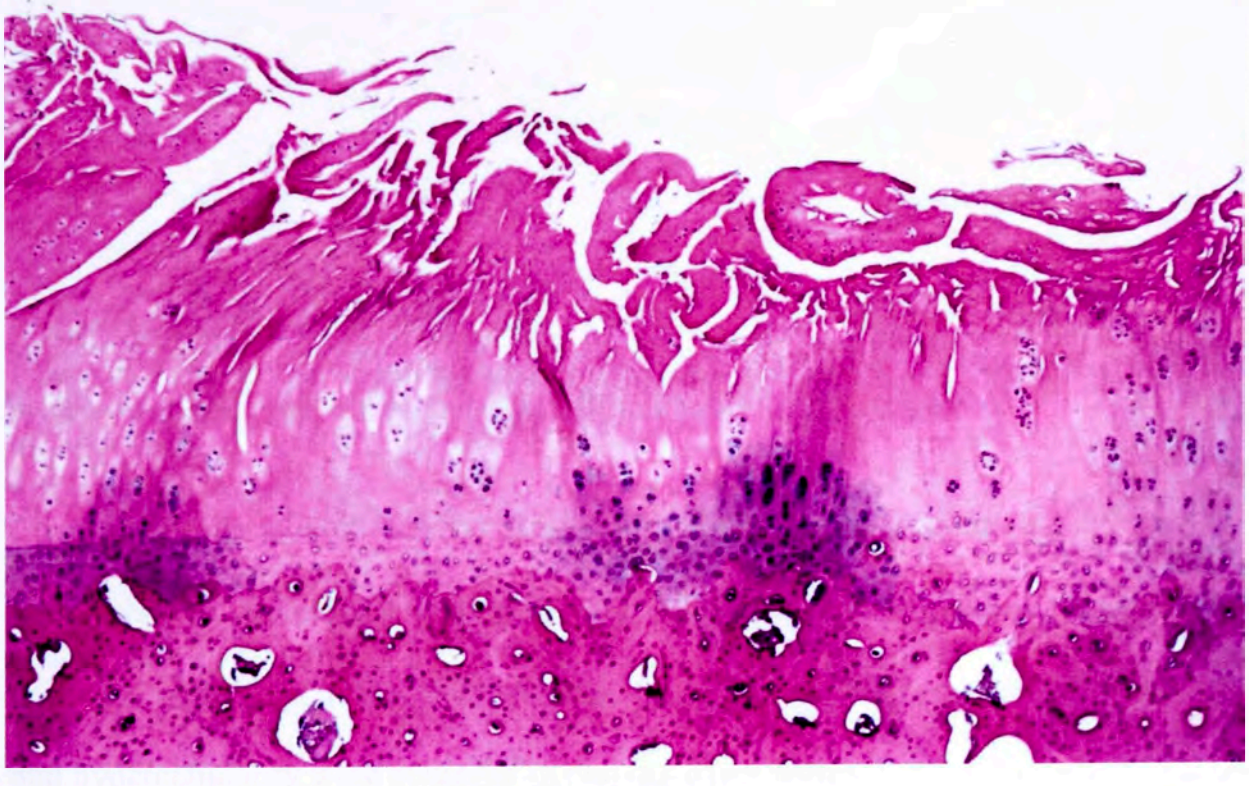

**Figure 46.** Complete disorganisation of the articular cartilage is accompanied by significant cellular degeneration in the form of chondrocyte clustering and hypocellularity

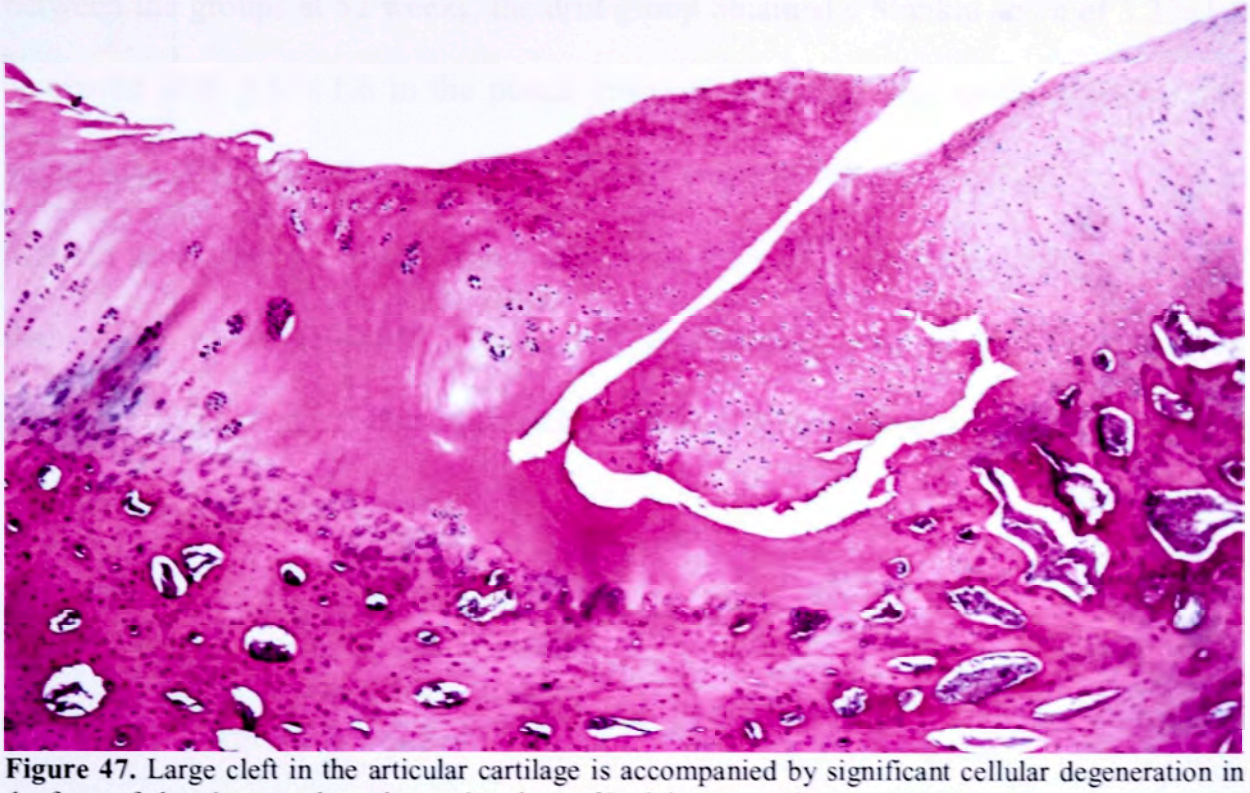

**Figure 47.** Large cleft in the articular cartilage is accompanied by significant cellular degeneration in the form of chondrocyte clustering and regions of both hypo- and hypercellularity

Five out of six medial menisci experienced some fissuring of the surface, one of which showed extensive structural damage. This meniscus corresponded to the worst case of degeneration in the tibial cartilage. Local regions of increased staining density and hypercellularity were observed in two out of six menisci.

**52 weeks:** Histology of the medial tibial condyles at 52 weeks showed damage in similar areas to the 26 week group. Minor surface irregularities were noted in the central and lateral regions of the plateau, with occasional deep clefts in the medial spline (Figure 48 and 49). However, the damage to the tibial cartilage at 52 weeks appeared to be reduced in comparison to the 26 week group. In general, the 52 week tibiae had similar structural damage and Safranin-O staining, but reduced cellular changes when compared to the 26 week tibiae (Figure 50). Similarly to the 26 week

specimens, blood vessels were observed to cross the tidemark in 30% of the tibiae at 52 weeks. Although small sample numbers make it difficult to interpret the results in between the groups at 52 weeks, the drill group obtained a Mankin score of 3.2 ± 1.8 compared with 5.0 ± 1.6 in the punch group (Figure 51). This result is statistically significant (P=0.03). When grouping the 52 week specimens together, the average Mankin score was 4.1 ± 1.8, which shows cartilage of a significantly higher quality than at 26 weeks (P=0.01) (Figure 52). Additionally, one of four sites showed evidence of subchondral bone thickening, which is a substantially reduced occurrence compared to the 26 week group.

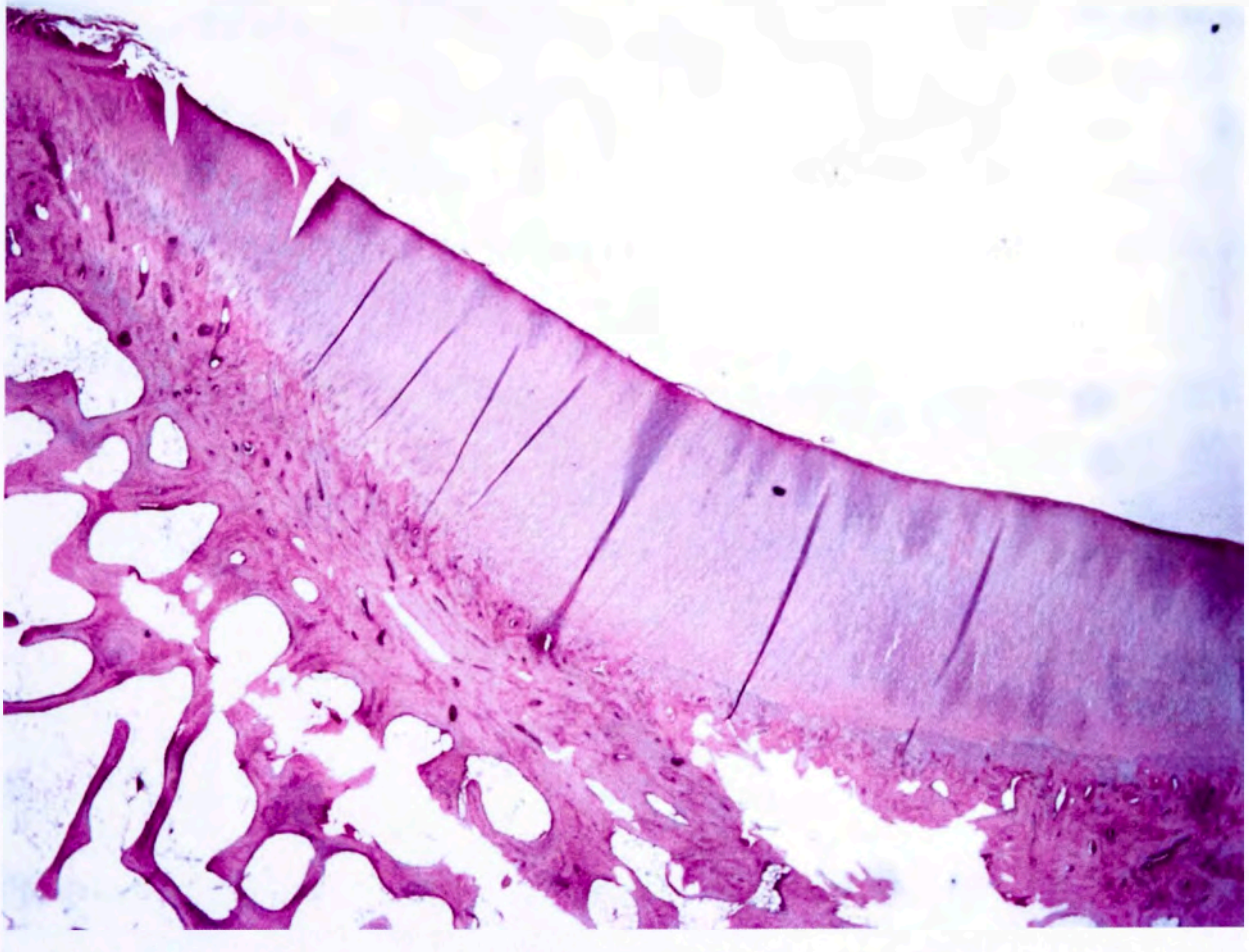

**Figure 48.** A typical section at 52 weeks shows minor surface irregularities and occasional fissures high on the medial spline

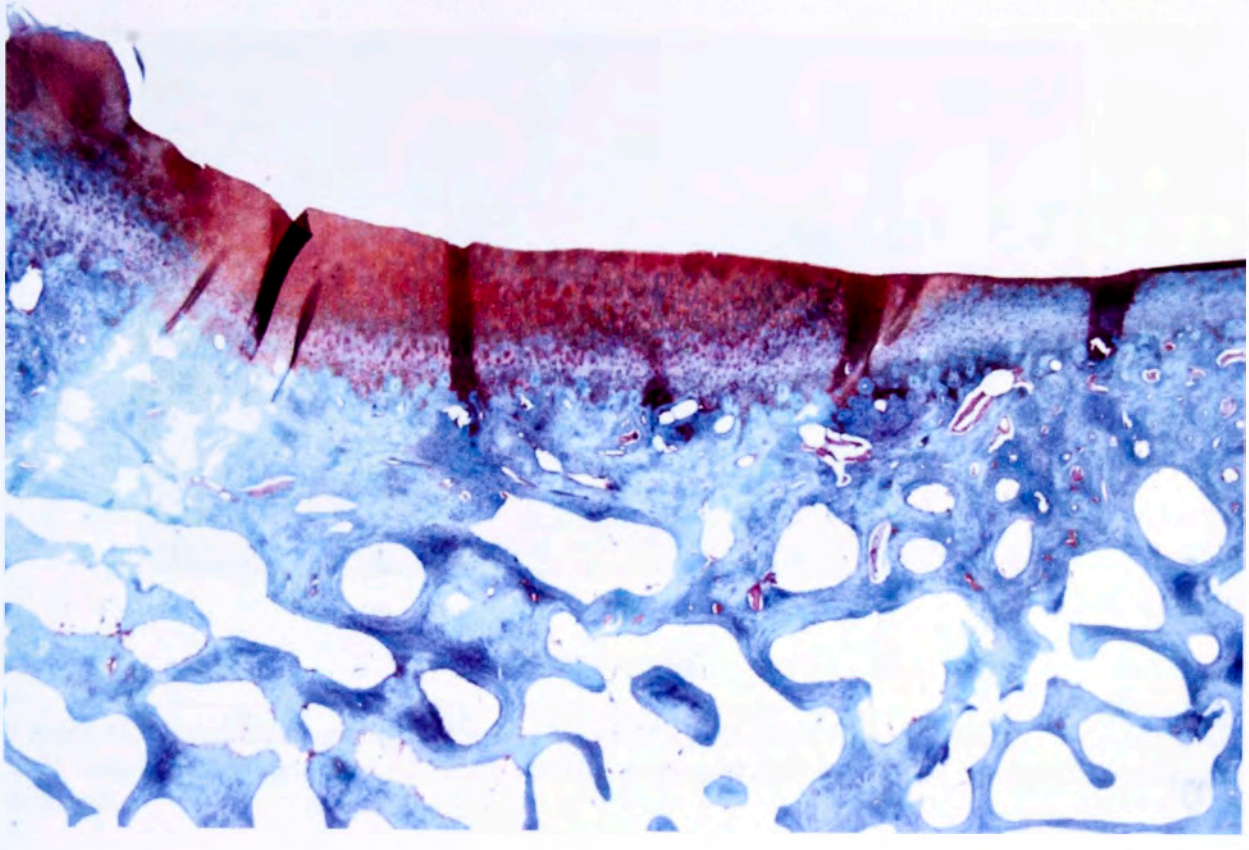

**Figure 49.** A typical 52 week specimen showing surface irregularities and moderate reduction in Safranin-O staining

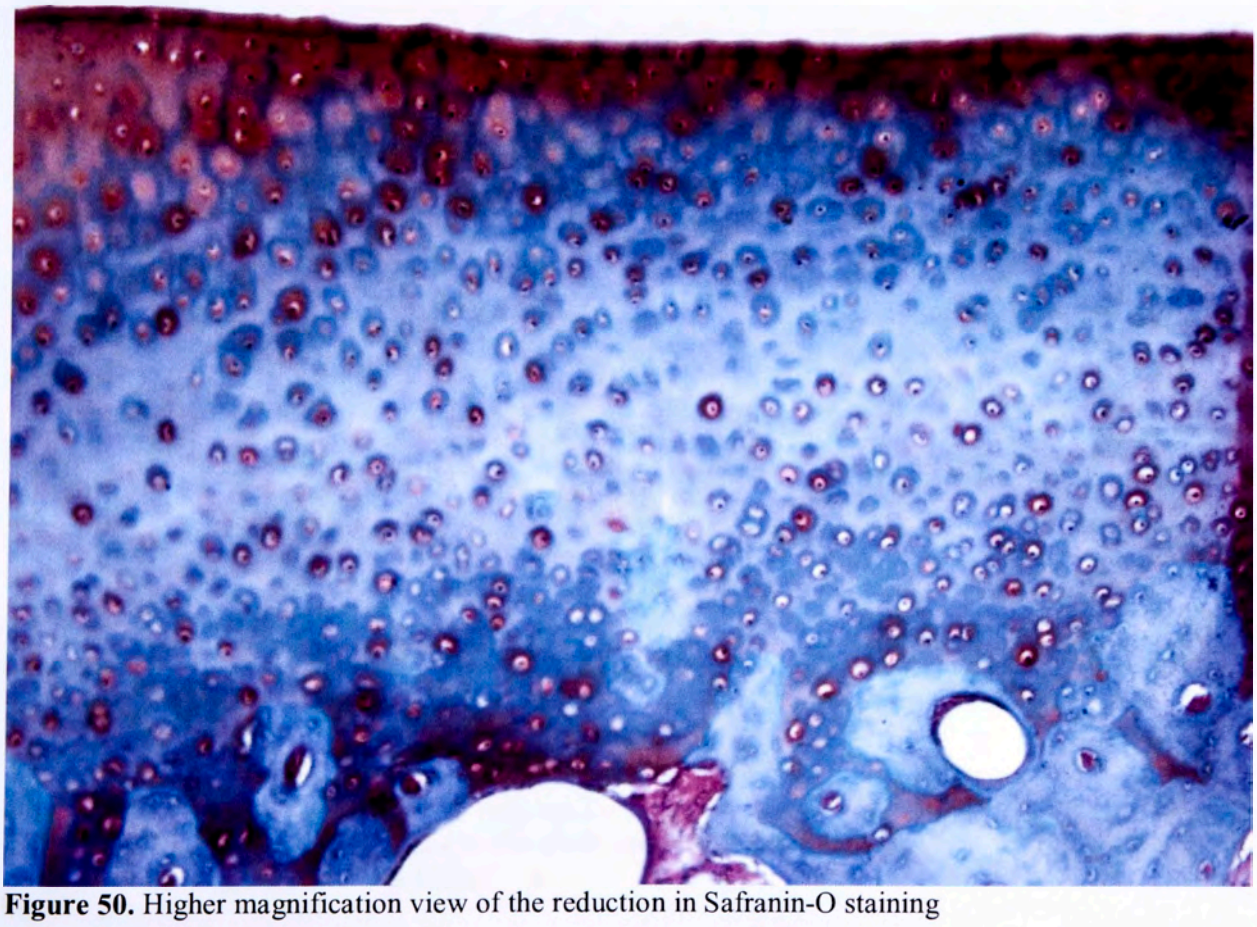

**Figure 50.** Higher magnification view of the reduction in Safranin-O staining

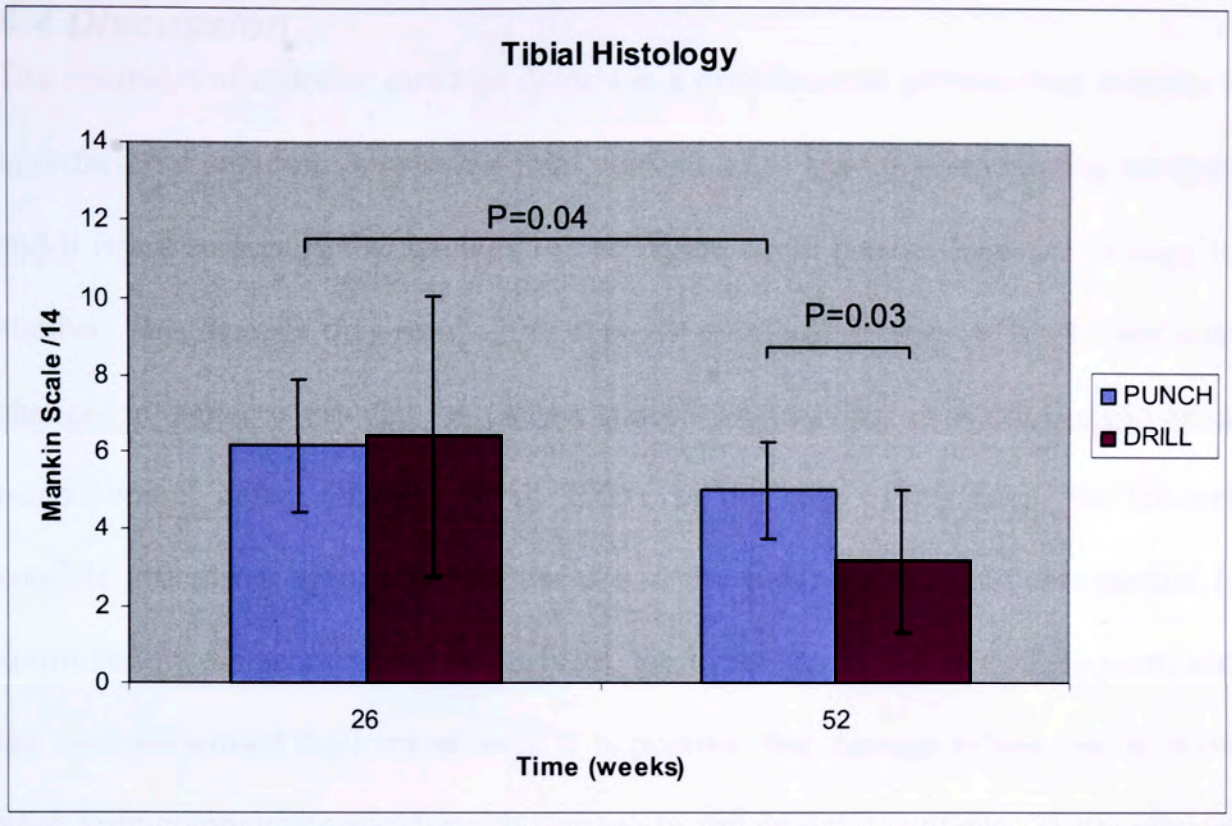


**Figure 51.** Quantitiative grading of the tibia revealed significant differences between the punch group at 26 weeks and both groups at 52 weeks. Also the punch and drill group at 52 weeks were significantly different.

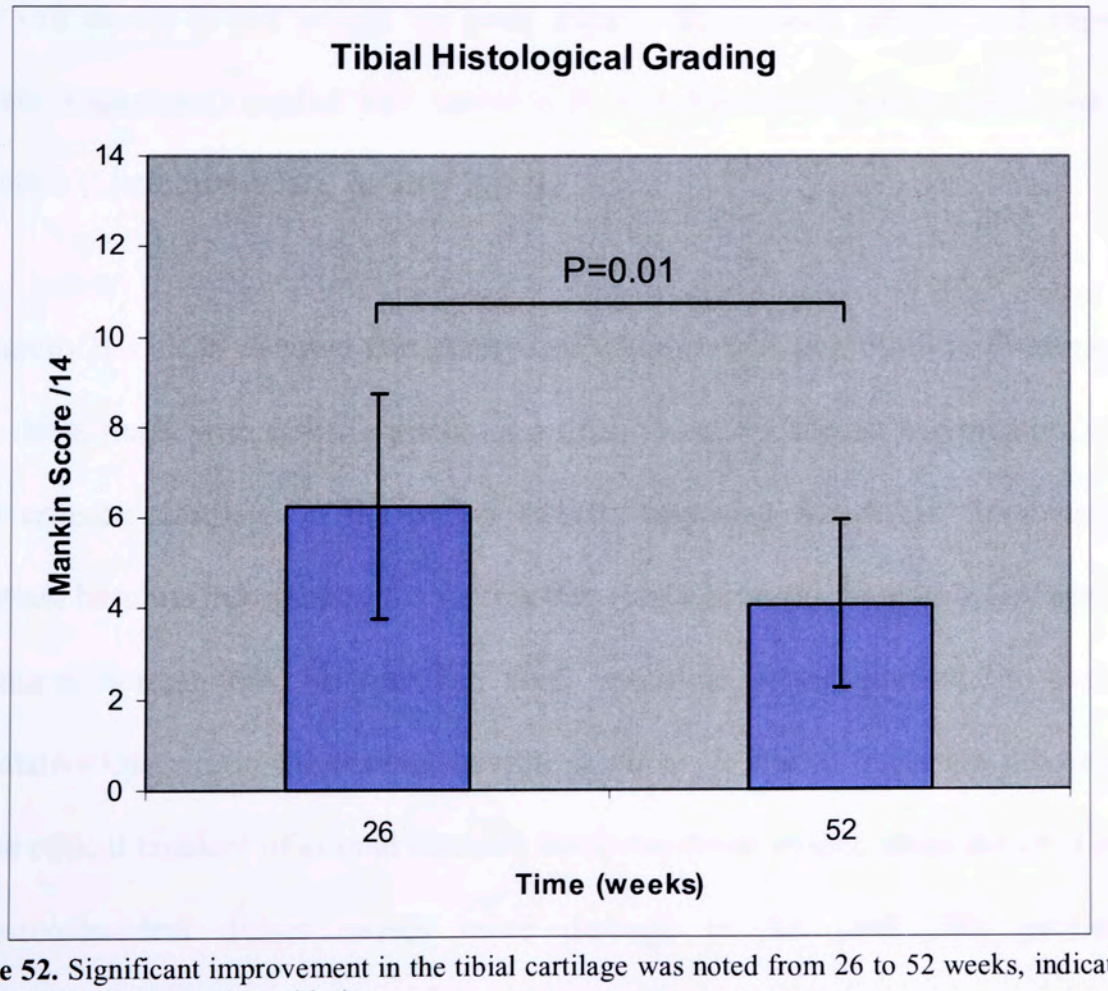


**Figure 52.** Significant improvement in the tibial cartilage was noted from 26 to 52 weeks, indicating a reversal of the degeneration with time.

## 4.4 Discussion

The treatment of articular cartilage defects is a multifactorial problem that requires a multifactorial solution. A synovial joint consists of at least two articulating surfaces and it is not surprising that damage to one region could potentially cause damage in another. This damage may result from abrasive or adhesive wear, or from significant changes in contact areas and joint stress concentrations, such as in rim loading of an osteochondral defect (Braman et al. 2005). In the case of the knee, the femoral condyle articulates against the meniscus and the tibial condyle and this motion is controlled by the geometry of the surfaces, the ligaments in and around the joint, and the muscles around the joint as well. It is possible that damage to any one of these knee joint components could cause damage to the articular cartilage. In the clinical environment, articular cartilage injuries often occur in association with damage to other soft tissues in and around the knee, namely the menisci, anterior and posterior cruciate liagaments, medial and lateral collateral ligaments, joint capsule and the synovium (Shelbourne, Jari, & Gray 2003).

This study has clearly shown that empty osteochondral defects, 6mm in diameter and 6mm deep, made with either a punch or a drill, cause significant degeneration in the tibial articular cartilage in the region directly opposing the defect. This result is important baseline information for studies that create an osteochondral defect and then administer a treatment, because the ideal treatment would prevent or slow the degradative changes in the counter-bearing surfaces. It is also important information for the ethical conduct of animal research using the sheep model, since the creation of an osteochondral defect causes more damage to the joint than previously acknowledged.

An important finding is that the degeneration noted macroscopically and by histology at 26 post operative weeks did not progress out to 52 weeks. In fact, at the later time point there was a reversal in the damage to the tibial cartilage. This is possibly related to the quality of the healing response on the femur, which was significantly improved between 26 and 52 weeks. It might be expected that the tibial cartilage would be damaged less, and given a greater chance to heal when articulating against a smoother, more normal surface than when articulating against a poorly healed osteochondral defect. Another possibility is that the healing response in both the femur and tibia is a slow process that requires more than 26 weeks. This is supported by the standards, which suggest a minimum study duration of 6 months to achieve maximum potential for osteochondral healing (ASTM 2005).

# 5. Repairing an established osteochondral defect with a metallic resurfacing device

## *5.1 Abstract*

This chapter of the thesis outlines a new animal model for osetochondral defects and the efficacy of a new device indicated for treating focal cartilage lesions. The HemiCAP cartilage resurfacing device has previously been trialled in a healthy knee model in the goat in which the results were excellent (Kirker-Head et al. 2006). However, this model attracted criticism for the reason that this type of device would never be implanted into a pristine knee joint and the chondro-protective qualities seen in that model may not be replicated in a more hostile environment, such as a joint that has already sustained damage. For this reason, a model of an established osteochondral defect was developed to simulate a diseased joint and a more challenging environment in which to test the device.

Whilst the repair of the femoral defect is certainly of interest, the primary focus of this study is on the ability of the device to protect the opposing tibial articular cartilage surface from further damage. The damage to the cartilage is assessed by macroscopic inspection, mechanical testing and histology, and any changes to the bone are assessed by microCT and histology.

## *5.2 Introduction*

Focal cartilage lesions may present clinically from blunt or repetitive trauma, osteochondritis dissecans (OCD) or avascular necrosis (AVN). Such full thickness cartilage lesions are known to progress to severe joint degeneration and osteoarthritis, however, the treatment strategy varies with the age and level of activity of the patient.

Typically, an elderly patient with large grade IV cartilage lesions in the knee would be indicated for total joint replacement surgery. Although this is not the case for younger patients, who would be expected to outlive more than one knee replacement prosthesis. Patients who are yet to reach skeletal maturity (as determined by closure of the epiphyseal plates) respond positively to conservative treatments such as microfracture, where the repair tissue is often a much higher quality than in adults (Cain & Clancy 2001). Patients who are adults up to approximately 45 years of age may be treated with techniques such as mosaicplasty and autologous chondrocyte implantation, with the quality of the repair declining with the age of the patient.

Unicompartmental prostheses are implants that replace one femoral condyle, one tibial condyle and the meniscus in between. Most commonly it is the medial side of the knee that is replaced (Collier et al. 2006). As such, the medial side of the knee articulates synthetic material against synthetic material, whereas the lateral compartment of the knee remains normal, with cartilage articulating against cartilage. The advantage of unicompartmental knee arthroplasty (UKA) over total knee arthroplasty (TKA) is the preservation of some bone stock in the knee which can delay the use of revision components when a TKA is performed later on. Other advantages include shorter operative times, less blood loss, quicker recovery and increased range of motion (Springer et al. 2006).

UKA was originally indicated for low-demand patients older than 70 years of age, however, good results in comparison to high tibial osteotomy have broadened the indications to include younger patients (Vince & Cyran 2004). Recently though, Collier, et al. found that the clinical success of UKA was reduced significantly with

younger patients. UKA also has the complication of bone loss on the tibia that requires augmentation with either bone graft or metallic implants in 57-77% of conversions to TKA (Barrett and Scott 1987; Springer et al. 2006). The average life of a UKA before conversion to TKA is 8.3 to 9 years (Collier et al. 2006; Springer et al. 2006), although this has improved markedly from the early results of 47 months (Barrett & Scott 1987).

Middle-aged patients from approximately 40 to 60 years of age are limited in the available treatments for osteochondral lesions because they are too old for the biological/conservative treatments, but too young to be considered for TKA or UKA. In these patients there is a need for a bridging prosthesis that removes pain and restores functionality to the joint for long enough to prolong the introduction of a total joint replacement until the patient reaches a more appropriate age. One such implant is the hemicondylar prosthesis.

Hemicondylar prostheses, or resurfacing prostheses, involve the replacement of part of one condyle with a synthetic material, which then articulates against cartilage on the counter-bearing surface. The advantages of this approach include less invasive surgery, shorter hospital stay, less constrictive rehabilitation and also the preservation of healthy bone and cartilage tissues throughout the majority of the joint. Since the metallic component does not articulate against polyethylene, such as in UKA, the issue of UHMWPE wear debris-induced implant loosening is mitigated. Metallic resurfacing implants have been used in the femoral head of the hip (Siguier et al. 2001), the femoral condyles of the knee (Hodge 1991;Kirker-Head, Van Sickle, Ek, &

McCool 2006), the tibial condyles of the knee (Springer et al. 2006) and the patella (Harrington 1992).

Kirker-Head, et al. have previously studied one such metallic resurfacing device in the physiologically normal medial femoral condyle of the goat. However, it is important that the performance of the device is tested in a clinically relevant model because a healthy joint may react differently to the implant than a diseased joint. The current study builds on the knowledge gained from the Kirker-Head study by introducing the metallic resurfacing device into a knee with an established osteochondral defect rather than a pristine joint. As such, the current study introduces a new model for osteochondral defect repair that is more clinically relevant and a more challenging environment to test the efficacy of the resurfacing device.

The previous model tested the hypothesis that the metallic resurfacing device would not degrade the healthy articular cartilage on the tibia. In contrast, the established osteochondral defect model developed in the current study tests the hypothesis that the resurfacing device would not accelerate the damage in cartilage already damaged by the established defect on the femur. The results of the resurfacing component are compared to control knees which were given the established defect without being treated with the resurfacing device. As such, this preclinical study is a strong indicator of the expected clinical performance of the device because the model is more clinically relevant.

## 5.3 Methods

### 5.3.1 HemiCAP™ resurfacing device

The HemiCAP resurfacing device consists of two components; an anchor screw component and an articulating component that are engaged with a taper-lock (Figure 53). Since the sheep femoral condyle is much smaller than the comparative site in the human, the implants from this study were selected from the Great Toe™ range of HemiCAP implants. These implants are smaller than the femoral implants although the materials and surgical technique are otherwise identical. The Co-Cr articulating component is available in a range of geometries that allows the surgeon to choose, intra-operatively, the best fit with the native curvature of the joint surface. The different articulating components vary by different radius of curvature in both the superior-inferior and medial-lateral directions, although the overall diameter of the component is the same. The articulating component is available in a range of sizes, however, in this study each implant was 12mm in diameter with various curvatures to match the native condyle. The articulating surface is highly polished to lower the coefficient of friction and reduce protein adsorption onto the surface, whilst the undersurface is roughened to improve bone ongrowth for stable fixation. In this study, each anchor screw was 8mm at the widest point and 12mm in length. The anchor screw component is constructed from titanium alloy (Ti6Al4V).

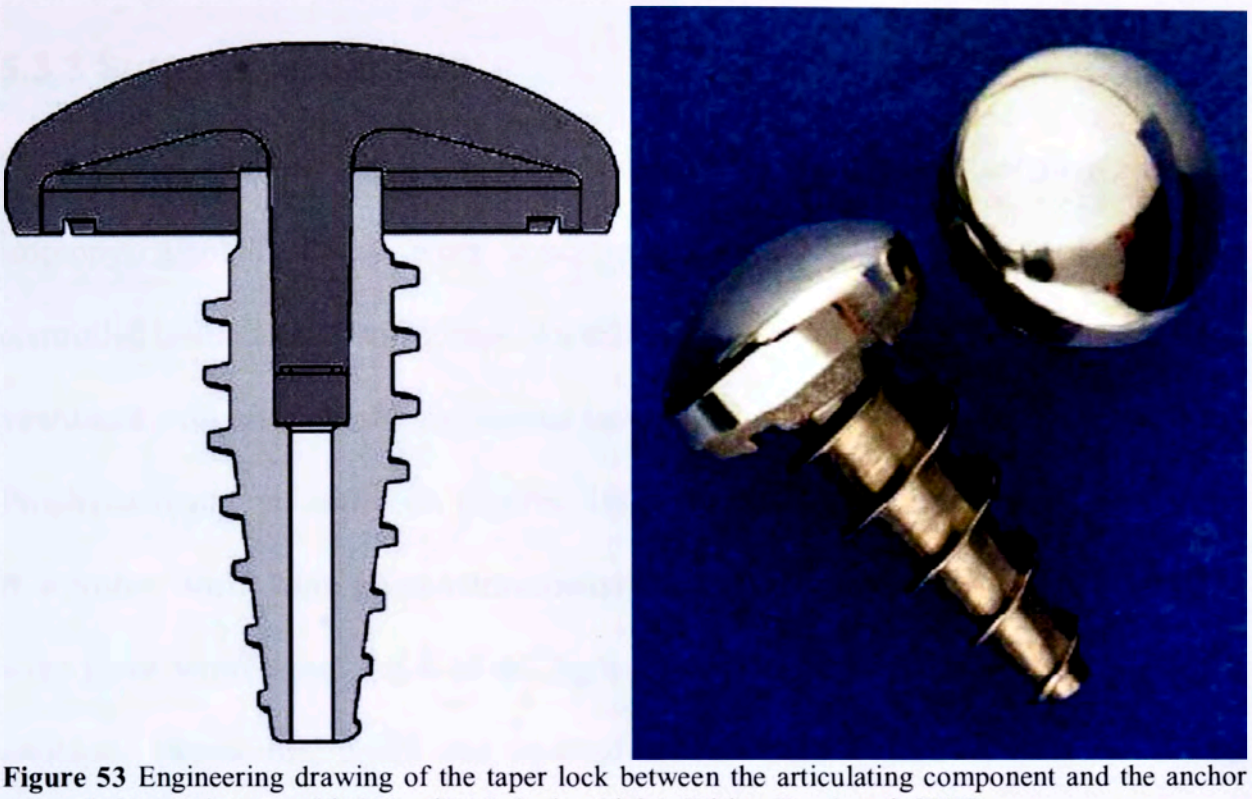

**Figure 53** Engineering drawing of the taper lock between the articulating component and the anchor screw (left) and the assembled HemiCAP device (right) (Kirker-Head et al. 2006)

### 5.3.2 Animals

Adult crossbred wethers of age 18 months were used in this study. The sheep were allowed continuous access to water and were fed a diet of chaff and hay once per day. All animals were transported to the holding cells in Level 4 Samuels Building, UNSW and allowed to acclimatise for at least 3 days before surgery. The sheep were fasted overnight before surgery and remained at Samuels Building for at least 1 week postoperatively before being transported to deep cover pens at the Biological Resource Centre, Little Bay. Animal ethics were obtained from the Animal Care and Ethics Committee (ACEC), University of New South Wales.

### 5.3.3 Surgical preparation

The surgical site was shaved and cleaned with an iodine scrub solution and 70% isopropyl alcohol. Sheep were anaesthetised with an injection of Zoletil and controlled inhalation of isofluorane. An endotracheal tube was inserted and the animal ventilated with anaesthesia maintained using isofluorane (2-3%) and 100% oxygen. Prophylactically, an antibiotic (Keflin, 1000mg) and an anti-inflammatory/analgesic (Carprofen, 4mL) were given intravenously. Crystalloid fluids (Hartmann's solution) were given intravenously at 4-10 mL/kg/h prior to and during surgery. A long acting antibiotic (Benacillin, 5mL) was injected intramuscularly prior to surgery. During surgery, a dedicated anaesthetist continually monitored the animal for respiration, heart rate, jaw tone, membrane colour and other vital signs (including oxygen saturation).

### 5.3.4 Study Design

This study involves a two-stage, bilateral surgical model of an established osteochondral defect and subsequently resurfacing with the HemiCAP device. The first stage is the bilateral creation of 9mm defects in the medial femoral condyle, followed by a 5 week wait to develop a chronic defect environment in the knee. The second stage is to re-operate and treat one knee with the HemiCAP resurfacing device. The defect in the other knee remains untreated as a contralateral control. A total of 26 defects, from 13 sheep were allotted to five different groups, as outlined in Tables 5 and 6. A further 5 knees were sourced from non-operated animals to act as time zero controls.

A sample size of five was selected from a sample size calculation based on detecting differences of 2 points on the histological grading scale. The following assumptions were made:

Average value of sample 1 = 6
Average value of sample 2 = 8
Standard deviations = 2
Confidence interval = 5%
Power = 50%

Increasing the power to 70% would have required a sample size of nine which was prohibitive due to the cost of the animals.

**Table 5. Study Design**

| | Empty | HemiCAP |
|---|---|---|
| **Surgery 1**<br>5 week | n=6 | |
| **Surgery 2**<br>6 week<br>26 week | n=5<br>n=5 | n=5<br>n=5 |

**Table 6.** Study design flowchart for the two-stage bilateral established osteochondral defect model

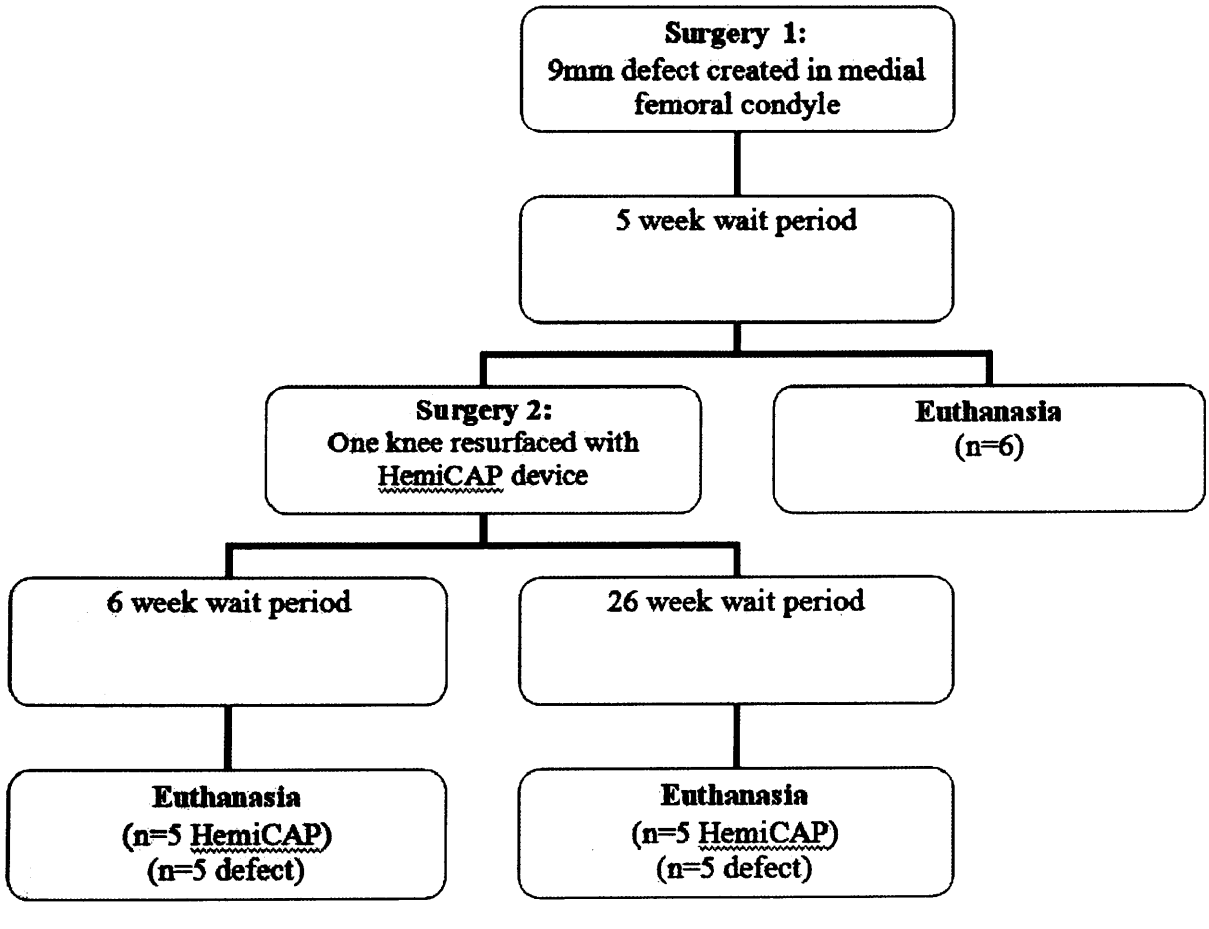

### 5.3.5 Surgery 1: Defect Creation

The first stage in this model was to create an osteochondral defect using a surgical punch (OATS instrumentation, Arthrex, FL) in each of the left and right medial distal femoral condyles, for a total of 2 defects per animal. These defects were 9mm in diameter by 6mm deep and were located in the weight bearing region of the femoral condyle (Figure 54). The medial condyle was chosen as it is the most common area treated with the HemiCAP™ in clinical practice.

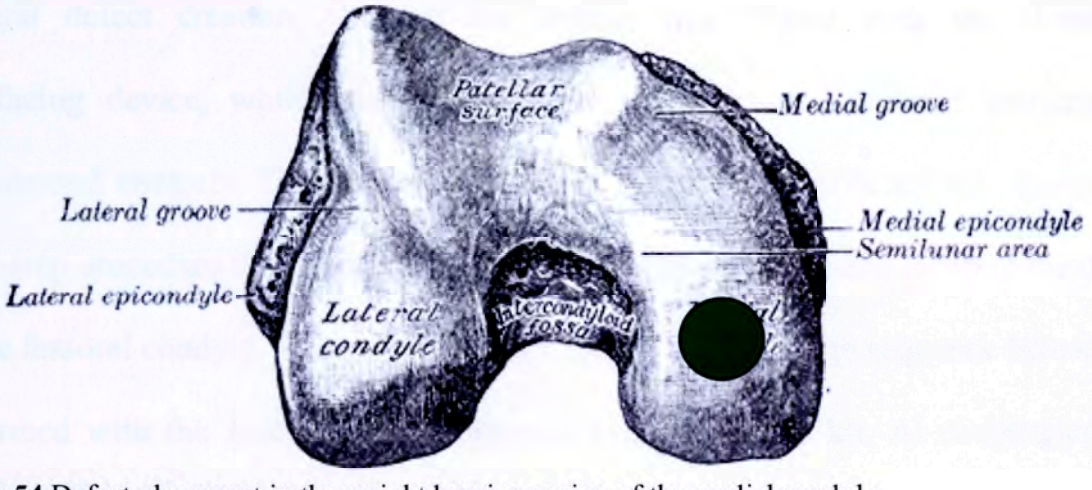


**Figure 54** Defect placement in the weight bearing region of the medial condyle

The surgical exposure was identical to that described in Chapter 3. Briefly, a small incision was made medial to the patella tendon and soft tissue layers were ablated using a diathermy to control bleeding. The patella was not reflected due to concerns of possible patella subluxation upon weight bearing, and because it was simple to locate the condyle without reflecting the patella. The knee was maximally flexed to expose the weight bearing region of the femoral condyle and the defects were created with a punch taking great care not to damage the articular cartilage adjacent to the defect. The articular surfaces were frequently irrigated with saline solution while the joint was open. After the defect was created with a 9mm punch, the joint was closed in layers and the animals were allowed full ambulation immediately post operation.

After 5 weeks, ten of the animals were operated on a second time with a resurfacing device in one knee. The remaining three animals were euthanized at the 5 week time point to serve as controls for the level of damage in the joint at the time that the other animals were treated with the HemiCAP device.

### 5.3.6 Surgery 2: Cartilage defect resurfacing

The second surgical procedure was conducted unilaterally, 5 weeks after the initial bilateral defect creation. One of the defects was treated with the HemiCAP resurfacing device, whilst the defect in the other knees remained untreated as contralateral controls. The surgical procedure to implant the HemiCAP device is a multi-step procedure that begins by opening the joint as before and locating the defect on the femoral condyle. The procedure, as depicted by the image sequence below, was performed with the Arthrosurface approved instrumentation kit. At completion, the edges of the HemiCAP resurfacing device should be flush or slightly recessed when compared to the native cartilage. An unacceptable result is for the device to be implanted proud of the surrounding cartilage although proper use of the instrumentation and correct choice of implant geometry reduce the likelihood of this scenario eventuating. The HemiCAP surgical procedure is summarised in Figures 55 to 57 and clearly outlined in the Appendices.

After the second surgical procedure to implant the HemiCAP device into the femoral condyles, the animals were returned to housing in deep litter pens with daily exercise in the paddock. The 26 week animals were returned to the paddock on a fulltime basis after approximately 4 weeks. Five animals were euthanized after 6 weeks and the remaining five animals were euthanized 26 weeks after the second operation. Each of

these animals received the established osteochondral defect 5 weeks prior to the HemiCAP implantation, so the three time points examined are thus 5, 11 and 31 weeks from the initial defect creation. For clarity, the groups are shown again in Table 7.

**Table 7.** Established cartilage defect and resurfacing experimental group allocation

| **Time from first surgery** | **Time from second surgery** | **Left** | | **Right** | |
|---|---|---|---|---|---|
| 5 weeks | n/a | defect | n=3 | defect | n=3 |
| 11 weeks | 6 weeks | HemiCAP | n=5 | defect | n=5 |
| 31 weeks | 26 weeks | defect | n=5 | HemiCAP | n=5 |

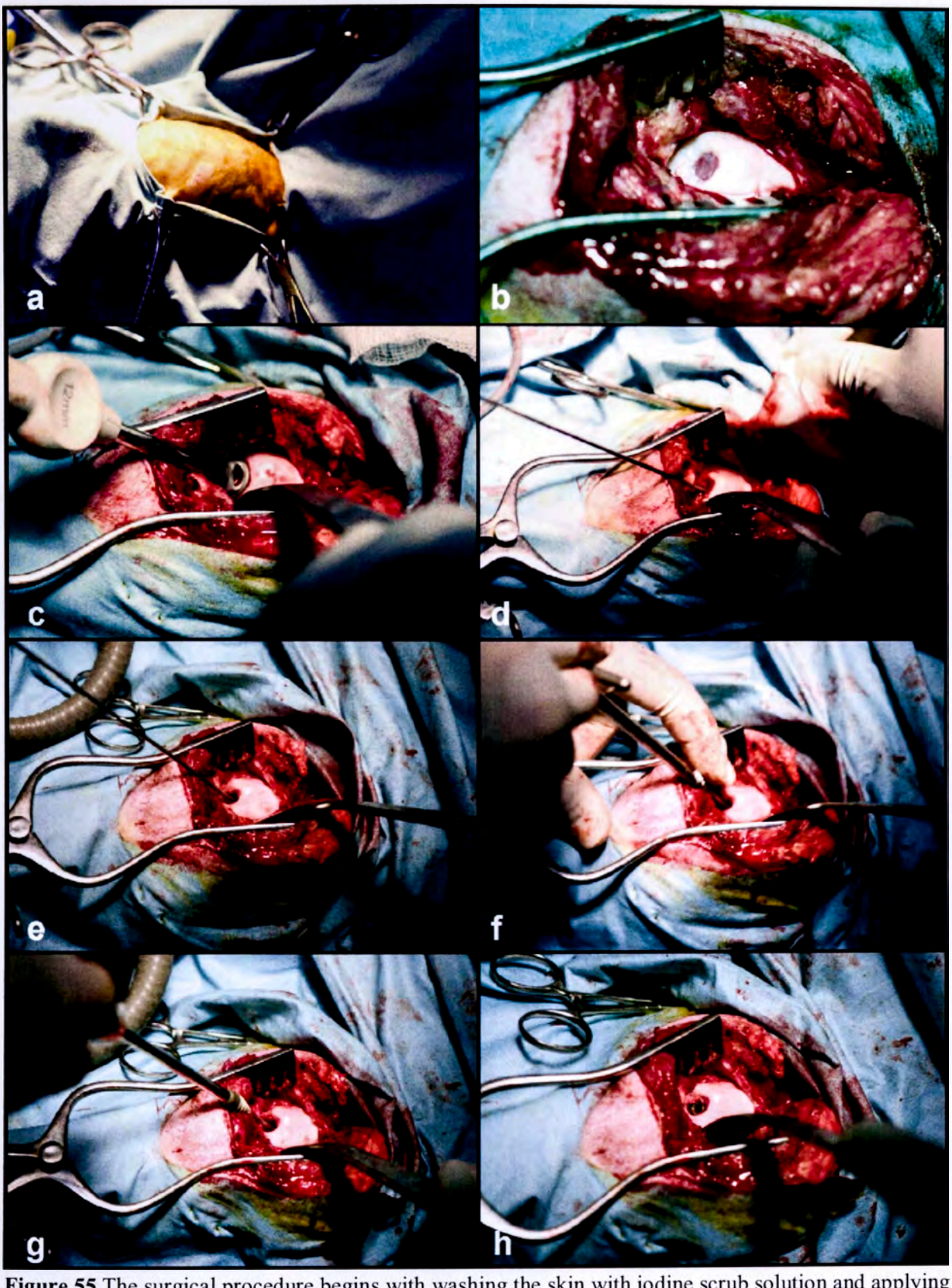


**Figure 55** The surgical procedure begins with washing the skin with iodine scrub solution and applying drapes to establish a sterile surgical field (a). The 5 week old defect is located using the same approach as in the original surgery (b) and the drill guide is positioned over the centre of the defect, perpendicular to the surface (c). A k-wire is drilled into the defect (d) and the defect is drilled with a pilot hole for the screw (e). The pilot hole is tapped (f) and the screw inserted (g). The screw is recessed into the bone at the correct height for the cap, as determined by depth gauges on the instrumentation (h).

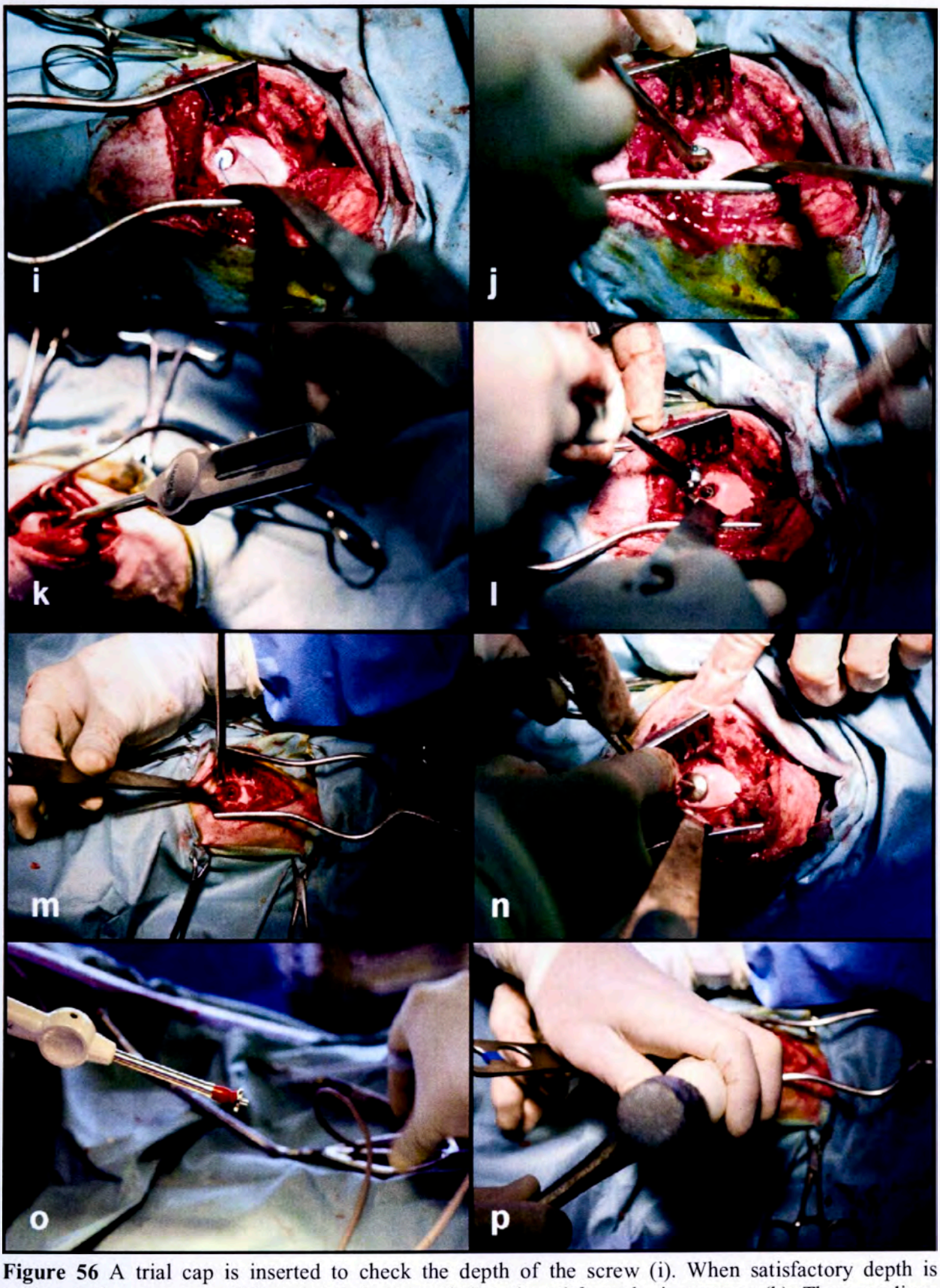


**Figure 56** A trial cap is inserted to check the depth of the screw (i). When satisfactory depth is achieved, the curvature of the condyle is mapped (j) and read from the instrument (k). These readings determine the selection of articulating component. A circular scalpel prepares the cartilage surface, removing any rough edges from drilling (l). The bed base is prepared for the articulating component with a size specific bur (m). A trial articulating component is inserted to check the curvature of the implant with respect to the condyle (n). The articulating component is attached to suction and implanted into the screw (o). Finally, the surgeon impacts the articulating component into the screw to engage the morse taper lock (p)

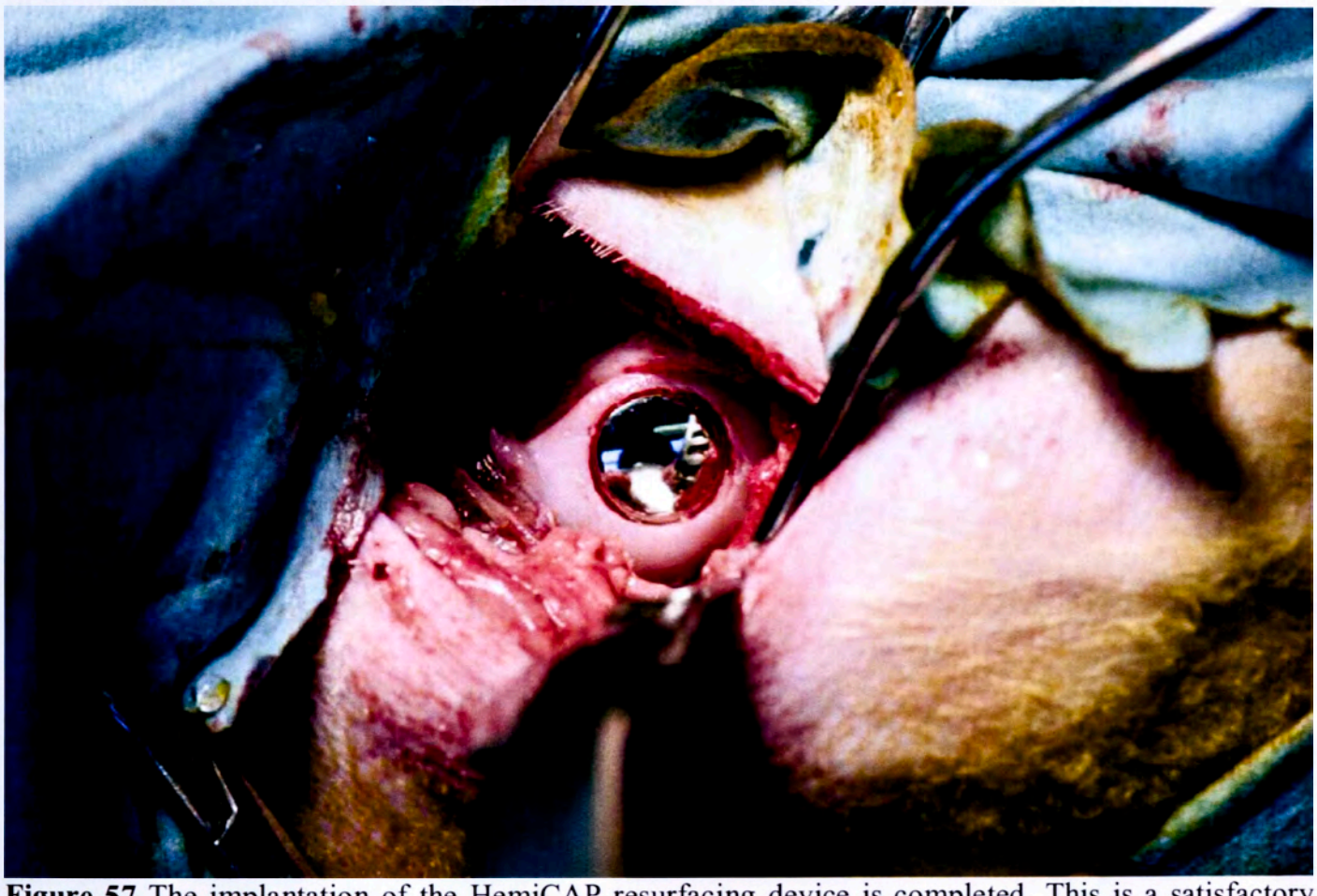

**Figure 57** The implantation of the HemiCAP resurfacing device is completed. This is a satisfactory result with the implant being slightly recessed in comparison to the native cartilage.

### 5.3.7 Macroscopic assessment

After sacrifice, the hind limbs were harvested and immediately frozen until required for analysis. The knee joint was meticulously dissected taking great care not to damage the cartilage surfaces or the menisci. The medial and lateral menisci were inspected for visible structural damage and the tibial plateaux were inspected for degenerative changes in the cartilage and for osteophyte formation.

**Defect group:** The distal femora (with empty defects) were visually inspected for signs of degenerative changes in the adjacent cartilage and on the lateral condyle, osteophyte formation and the quality and quantity of repair tissue within the defect.

**HemiCAP group:** The distal femora (with resurfacing device) were visually inspected for signs of degenerative changes in the adjacent cartilage and on the lateral condyle, and osteophyte formation. The implant was assessed for fixation, congruency with the cartilage surface and for the quality of the neocartilage formed over the perimeter of the articulating component.

After macroscopic inspection, the femora and menisci were immediately fixed in cold phosphate buffered formalin for a minimum of 48 hours. The tibial plateaux were subsequently analysed by dynamic mechanical indentation and micro computed tomography.

### 5.3.8 Dynamic mechanical indentation

The tibial plateaux were harvested, wrapped in gauze soaked with phosphate buffered saline solution and transported on ice to the Royal North Shore Hospital for dynamic mechanical indentation testing. A custom-made, validated dynamic probe was used to non-destructively indent the articular cartilage surface at a frequency of 30Hz

(Appleyard et al. 2001;Appleyard, Burkhardt, Ghosh, Read, Cake, Swain, & Murrell 2003).

**Dynamic arthroscopic indentation probe**

The equipment for the articular cartilage indentation comprises of a handheld probe with a long stainless steel beam, at the tip of which is a nonporous indenter probe. The beam has strain gauges attached that allow force and beam deflection to be monitored. The indenter probe at the tip is oscillated with amplitude of ±0.03mm at a frequency of 30Hz to remove noise, such as the shake of the operator's hand, from the data collection and to facilitate dynamic mechanical testing. The tip of the probe is carefully aligned perpendicular to the cartilage surface and the operator applies a load to the surface via the cantilever beam. The strain gauge system alerts the operator when a sufficient load has been applied and the data is collected and averaged over a period of 0.25s. The data recorded is the dynamic stiffness magnitude, dP/dH, and the phase lag φ.

This indentor system is similar to another developed by Lyrra, et al (Artscan 1000, Artscan Oy, Espoo, Finland) (Figure 58). The systems are almost identical, although the Artscan 1000 uses a constant applied displacement, whereas the system used in the current study imparts a dynamic displacement of the same amplitude, but at a frequency of 30Hz to filter out noise from the operator.

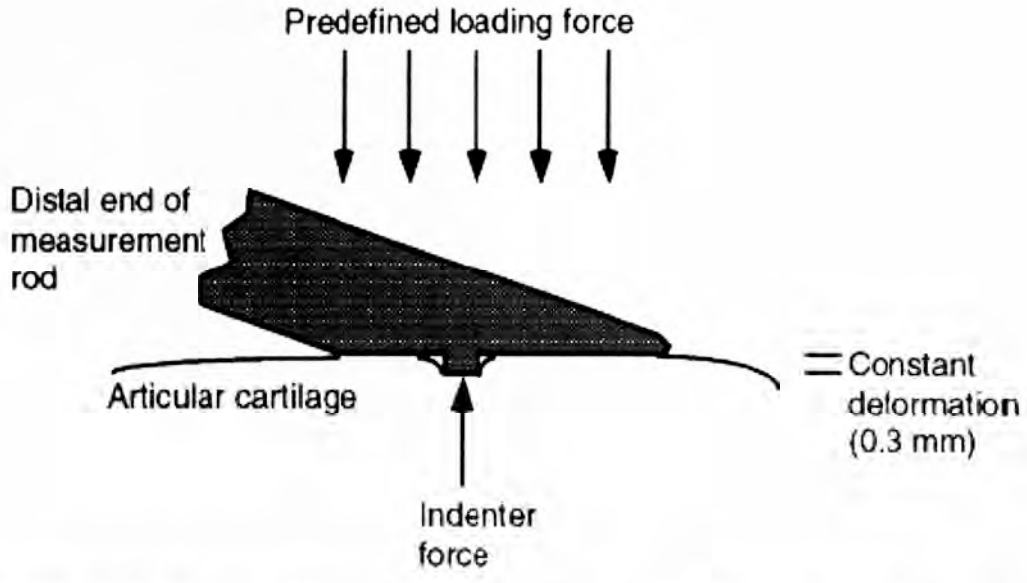


**Figure 58.** Schematic diagram of how the indentor system works. This is the static system, although the dynamic system works off the same principles.

**Data analysis**

The dynamic stiffness data is subsequently transformed into dynamic shear modulus which is calculated from the equation:

$G^* = dP/dH^*(1-v)/4ak$ (Appleyard et al. 2003)

Where G* is the effective modulus, dP/dH is the dynamic stiffness, v is the Poisson's ratio, a is the indentor radius and k is the theoretical correction function, described by Hayes, et al. in 1972.

The theoretical correction function, k, is a method of incorporating the relationship of the tip area and the cartilage thickness to transform structural properties, such as stiffness, into material properties such as modulus. The correction function was calculated from the data supplied by Hayes (Table 8), assuming a Poission's ratio of 0.5 (Hayes et al. 1972). The Hayes data was plotted and a curve was fitted to get an equation for the line (Figure 59).

**Table 8.** Theoretical correction function was calculated from the Hayes data set assuming a Poisson's ratio of 0.5

| *a/h* | $\nu = 0{\cdot}30$ | $\nu = 0{\cdot}35$ | $\nu = 0{\cdot}40$ | $\nu = 0{\cdot}45$ | $\nu = 0{\cdot}50$ |
|---|---|---|---|---|---|
| 0·2 | 1·207 | 1·218 | 1·232 | 1·252 | 1·281 |
| 0·4 | 1·472 | 1·502 | 1·542 | 1·599 | 1·683 |
| 0·6 | 1·784 | 1·839 | 1·917 | 2·031 | 2·211 |
| 0·8 | 2·124 | 2·211 | 2·337 | 2·532 | 2·855 |
| 1·0 | 2·480 | 2·603 | 2·789 | 3·085 | 3·609 |
| 1·5 | 3·400 | 3·629 | 3·996 | 4·638 | 5·970 |
| 2·0 | 4·335 | 4·685 | 5·271 | 6·380 | 9·069 |
| 2·5 | 5·276 | 5·754 | 6·586 | 8·265 | 13·00 |
| 3·0 | 6·218 | 6·829 | 7·923 | 10·26 | 17·86 |
| 3·5 | 7·160 | 7·906 | 9·274 | 12·32 | 23·74 |
| 4·0 | 8·100 | 8·983 | 10·63 | 14·45 | 30·75 |
| 5·0 | 9·976 | 11·13 | 13·35 | 18·80 | 48·47 |
| 6·0 | 11·84 | 13·27 | 16·07 | 23·23 | 71·75 |
| 7·0 | 13·70 | 15·41 | 18·79 | 27·69 | 101·27 |
| 8·0 | 15·55 | 17·53 | 21·49 | 32·15 | 137·7 |

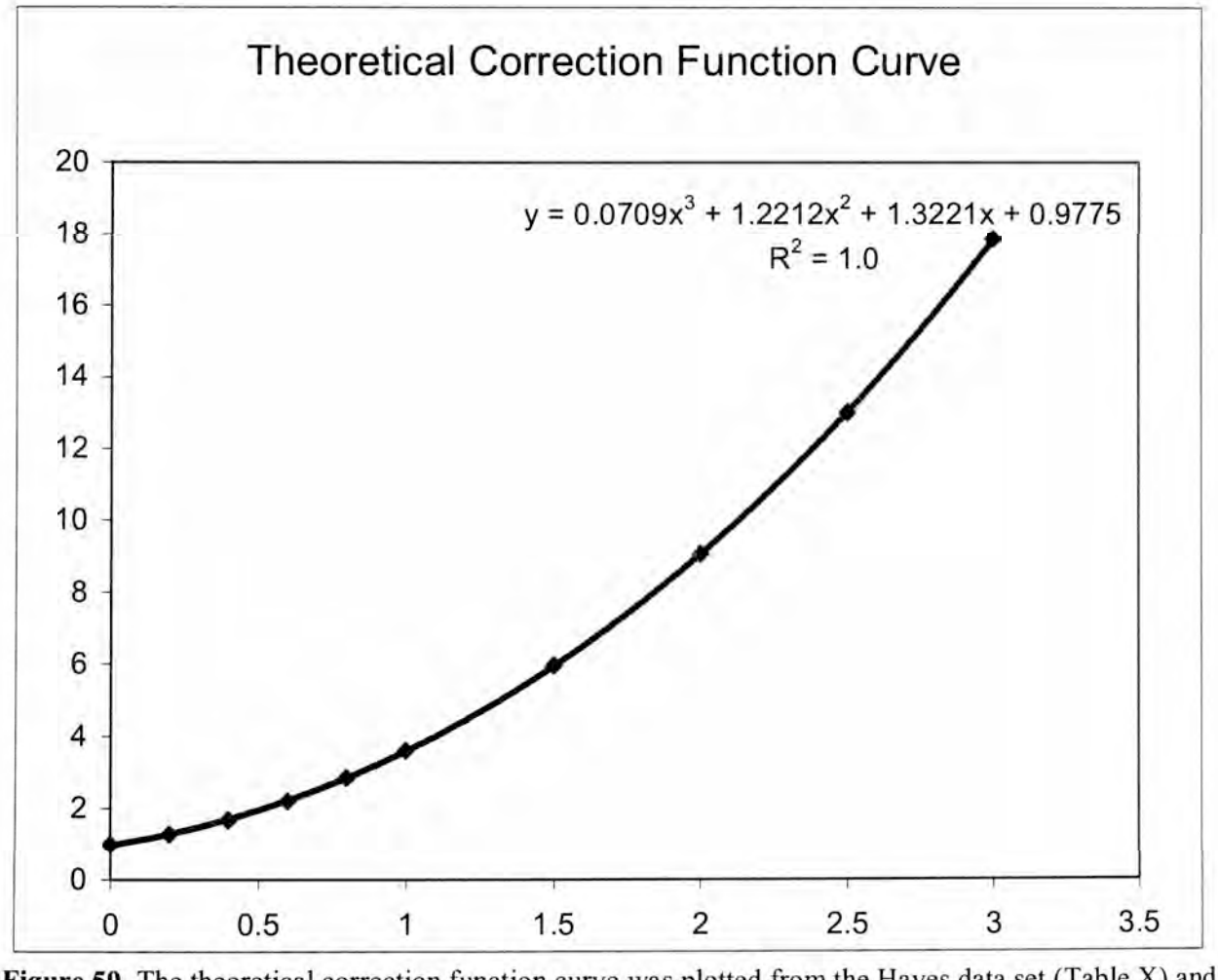


**Figure 59.** The theoretical correction function curve was plotted from the Hayes data set (Table X) and a third order polynomial curve fit resulted in the theoretical curve function equation, where x is the indentor radius divided by the cartilage thickness

The resulting equation can be described as:

$k = 0.0709(a/h)3 + 1.2212(a/h)2 + 1.3221(a/h) + 0.9775$

where k is the correction function and a/h is the indentor radius divided by the cartilage thickness.

The value for correction function, k, is then used in the original equation for the dynamic shear modulus $G^* = dP/dH^*(1-v)/4ak$.

The accuracy and reliability of this system has been validated (Appleyard et al. 2001). The accuracy of the system in measuring dynamic shear modulus was validated by comparing with a calibrated, commercially available indentation system (Micro Fourier Rheometer) and an excellent correlation ($R^2$=0.96) was found between the two systems. The interoperator and intraoperator reliability of the system was determined with five different operators measuring elastomeric materials of known material properties. It was found that the system was reliable ($R^2$=0.79) for the dynamic stiffness, however, the reliability of the phase lag measurements was poor ($R^2$=0.09).

Each tibia was cut with a bandsaw to a thickness of approximately 20mm, which is below the level of the growth plate. The tibial plateaux were then glued to a stage and marked with permanent ink at five locations on both the medial and lateral condyles. The central point was visually determined as the centre of the condyle and each of the four peripheral points were measured 5mm from the central point in the anterior, medial, posterior and lateral directions (Figure 60). Each point was then indented three times with the dynamic probe to allow averaging from three points in the

subsequent analyses (Figure 61). In this process, the condyle is exposed to the air for a period of 1 to 2 minutes, although moisture was retained within the cartilage by covering it with wet gauze when not being indented.

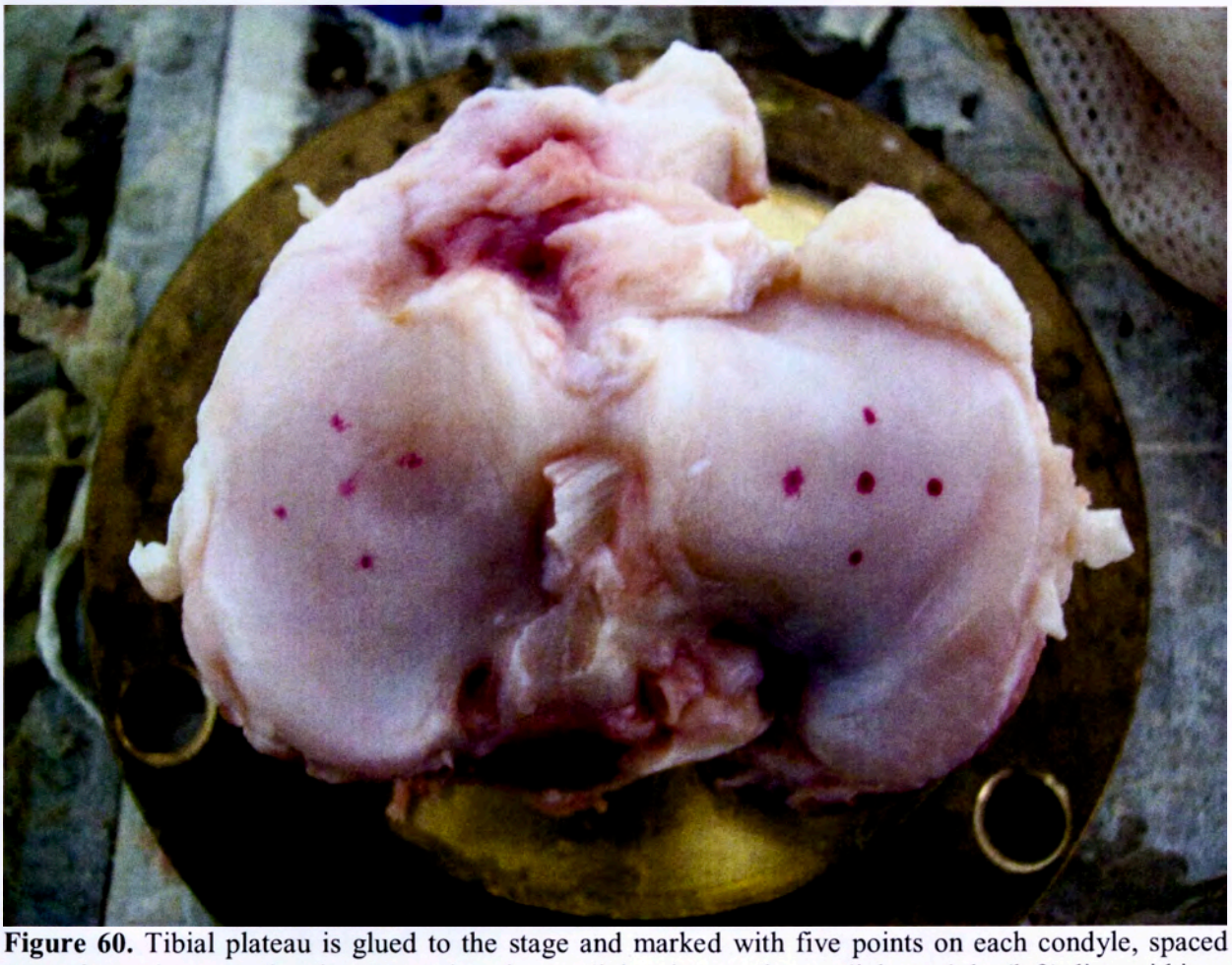

**Figure 60.** Tibial plateau is glued to the stage and marked with five points on each condyle, spaced 5mm from the central point. Note that the medial point on the medial condyle (left) lies within a damaged region of cartilage.

**Figure 61.** Dynamic mechanical testing with the indentor probe

After the indentation testing was completed three times at each point, the thickness of the cartilage was measured using a needle probe. Cartilage thickness is required to transform displacement to strain, and stiffness into elastic modulus. The needle probe consists of a vertically mounted needle, connected to a calliper with a digital readout. To ensure that the thickness measurement was taken perpendicular to the cartilage surface, the specimen was secured on a custom made stage that uses a ball and socket joint to vary the angle in all three axes of rotation (Figure 62). The specimen was positioned under the needle, the angle altered such that the cartilage surface was perpendicular to the needle and then the needle was brought down until it touches the surface. At this point the readout on the needle probe was zeroed and then the needle was lowered through the cartilage until it impacted with the hard subchondral bone plate below. The measured distance is the thickness of the cartilage at that point.

Thickness measurements were taken singularly because of the destructive nature of the test.

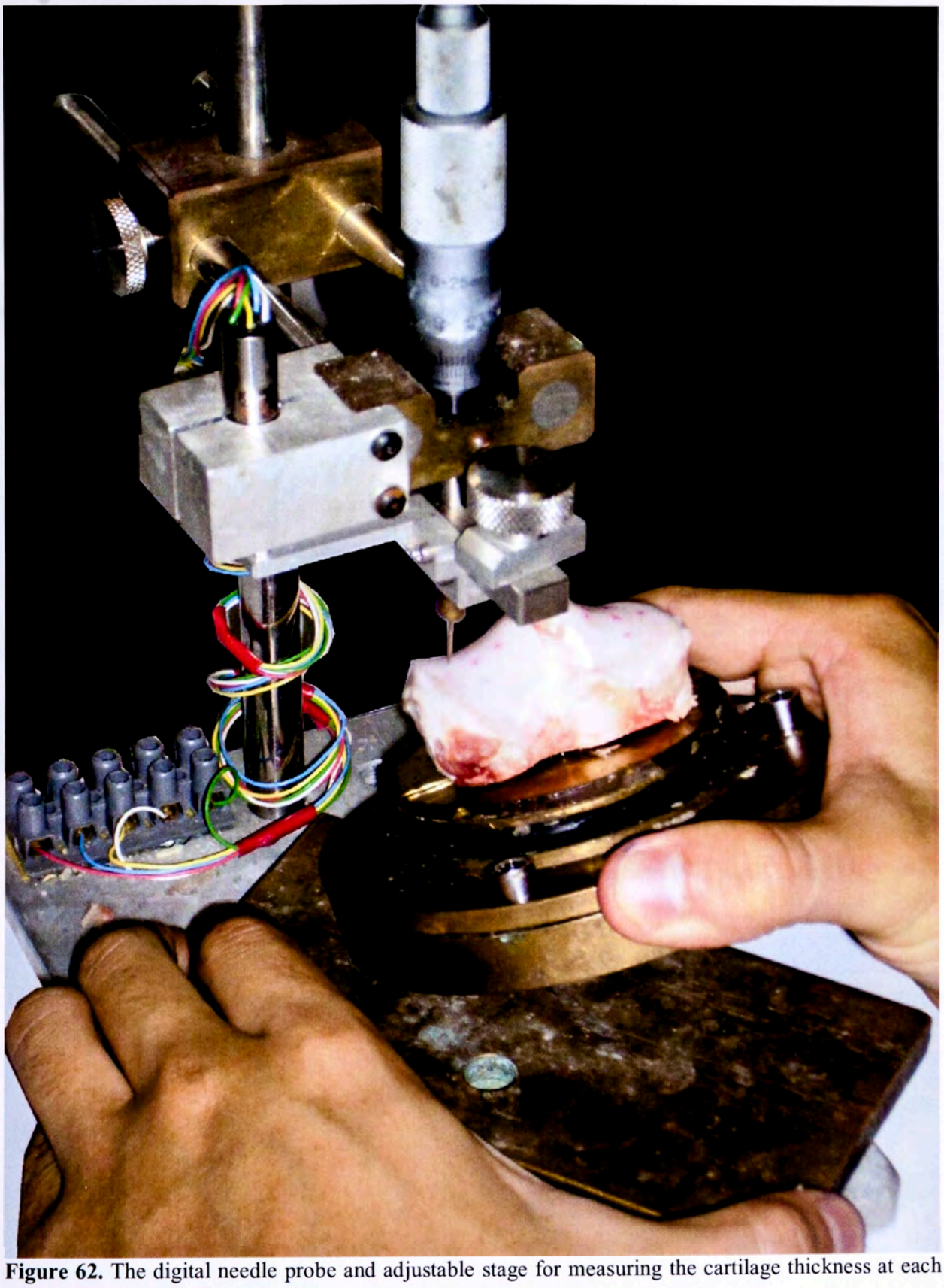

**Figure 62.** The digital needle probe and adjustable stage for measuring the cartilage thickness at each of the 10 testing locations

### 5.3.9 Micro computed tomography

Immediately after dynamic indentation testing, the tibial condyles were fixed in cold phosphate buffered formalin solution for a minimum of 48 hours. The medial condyles were trimmed to fit inside a specimen container, 25mm in diameter, which is approximately the largest sample size permitted in the microCT chamber. Each condyle (n=4) was then imaged using a Skyscan 1072 machine (Skyscan, Belgium) using rotational steps of 0.9degrees, exposure time of 5.7s and averaging from two frames. Images were then reconstructed and analysed using the Skyscan range of software.

Typical cancellous bone structural properties were calculated from a rectangular volume of interest 8mm wide by 4mm high by 3.8mm deep, in between the subchondral bone and the growth plate (Figure 63), as described in Chapter 6. The parameters calculated from microCT were Percentage Bone Volume, Bone Surface to Volume Ratio, Trabecular Thickness and Trabecular Separation.

The subchondral bone thickness was measured using the method described in Chapter 6. Briefly, the data set was recut in the coronal plane and the edge of the subchondral bone was detected by drawing a line of best fit. The subchondral bone plate thickness was measured along the length of the plateau at intervals of 50 pixels (approximately 1mm) (Figure 63).

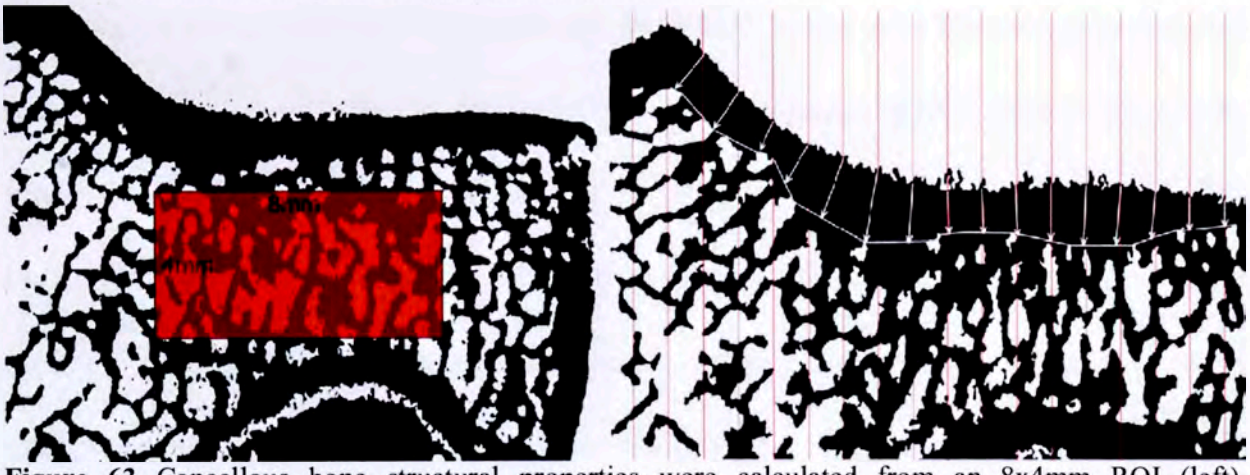

**Figure 63** Cancellous bone structural properties were calculated from an 8x4mm ROI (left). Subchondral bone thickness was measured at 50 pixel intervals (right)

### 5.3.10 Histology

After microCT of the medial tibial condyles, the proximal tibiae and distal femora were subsequently decalcified in 10% formalin-formic acid solution for up to 4 weeks until the bone was able to be cut with a scalpel blade. The femoral samples were sectioned through the centre of the defect in the coronal plane and then into 4 blocks, with block 2 and 3 being inside the boundaries of the defect and blocks 1 and 4 being on the superior and inferior periphery respectively (Figure 64).

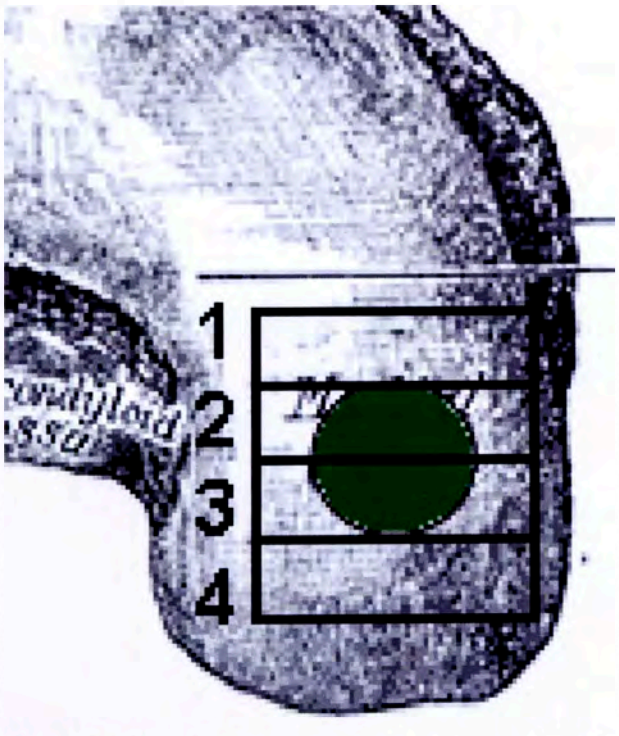


**Figure 64** Gross dissection of the femoral defects with blocks 2 and 3 within the boundaries of the defect

The medial tibial condyles were grossly sectioned in the area directly opposing the femoral defect or resurfacing device. Sections were made in the coronal plane into three blocks (Figure 65). Additionally, one section was taken from a corresponding location in the lateral femoral and tibial condyles. The medial and lateral menisci were cut radially through the central region to provide two sections for analysis from each specimen (Figure 66). In the 31 week group, a sample of synovium was also harvested and fixed in formalin solution. Each specimen was subsequently embedded in paraffin blocks, from which 5μm sections were cut and stained for analysis.

Femoral sections with empty defects were graded quantitatively using the modified O'Driscoll score proposed by Frenkel, et al. Medial tibial condyles of all animals were graded quantitatively using the Mankin scale. Statistical differences were determined using ANOVA with a significance level of $p<0.05$ using SPSS for Windows.

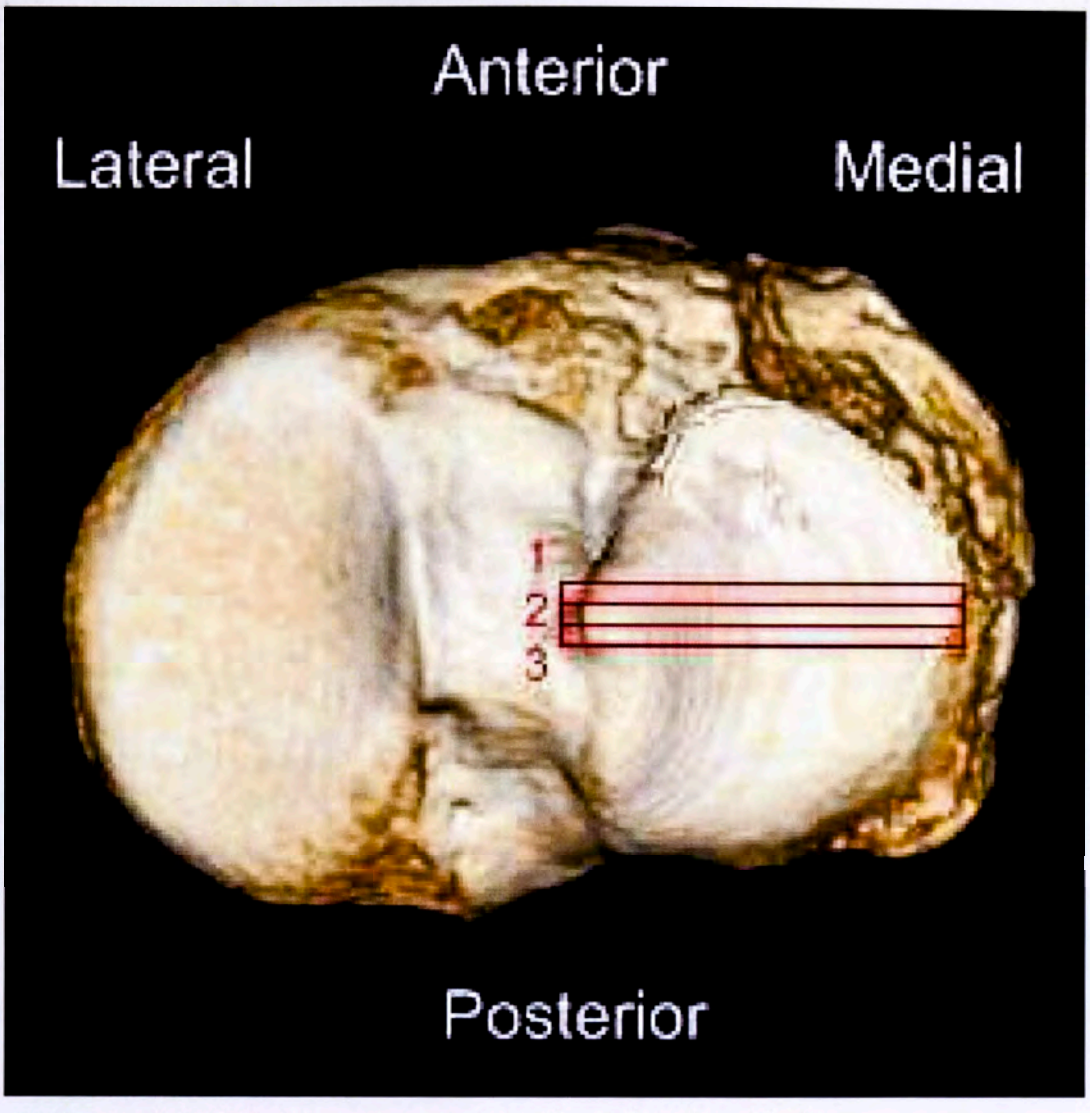


**Figure 65** The medial tibial plateau was grossly sectioned into three blocks

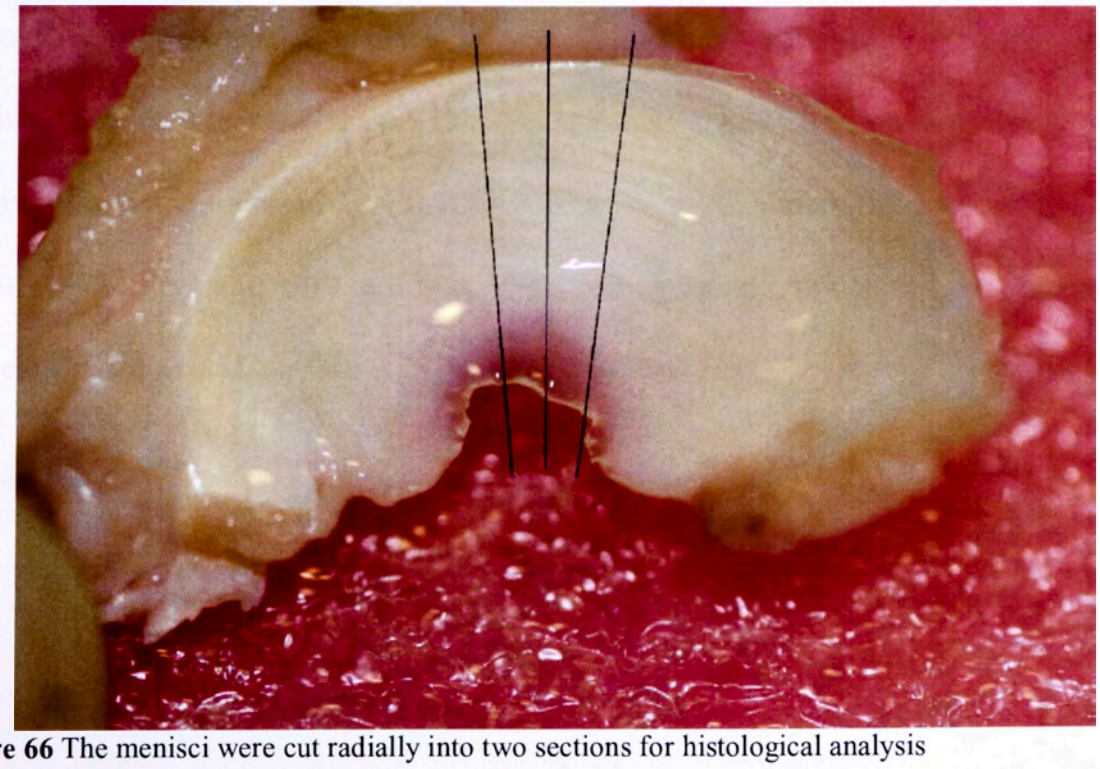

**Figure 66** The menisci were cut radially into two sections for histological analysis

**Hard tissue processing**

The notable exception in the histological preparation was that the medial femoral condyles with the HemiCAP resurfacing device were not decalcified. Instead, small biopsies of the neo-cartilage were taken from the medial and lateral boundaries and fixed in formalin for routine paraffin histology (in the 31 week group only). The remainder of the specimen was fixed in formalin, dehydrated stepwise through alcohol (70, 80, 90, 95, 100, 100%) for a minimum of 24 hrs in each solution. Specimens were then infiltrated with methyl methacrylate (MMA) under vacuum for 2 hrs and at atmospheric pressure for an additional 12 hrs minimum. A strong oxidising agent (Percadox-16) was mixed into a fresh quantity of MMA at a concentration of 5g/L to act as the catalyst for the polymerisation. The samples were then subjected to vacuum for another 2 hrs and left to polymerise in a water bath at 30degC. Polymerisation to polymethyl methacrylate (PMMA) was typically completed within two or three days.

A single 0.5mm section was taken from each specimen embedded in PMMA using a Buehler Linear Precision saw. The section was taken through the centre of the articulating component in the sagittal plane, running down the axis of the screw (Figure 67). These 0.5mm sections were radiographed, polished and stained with Stevenel's Blue and Van Giesen's or with Toluidine Blue.

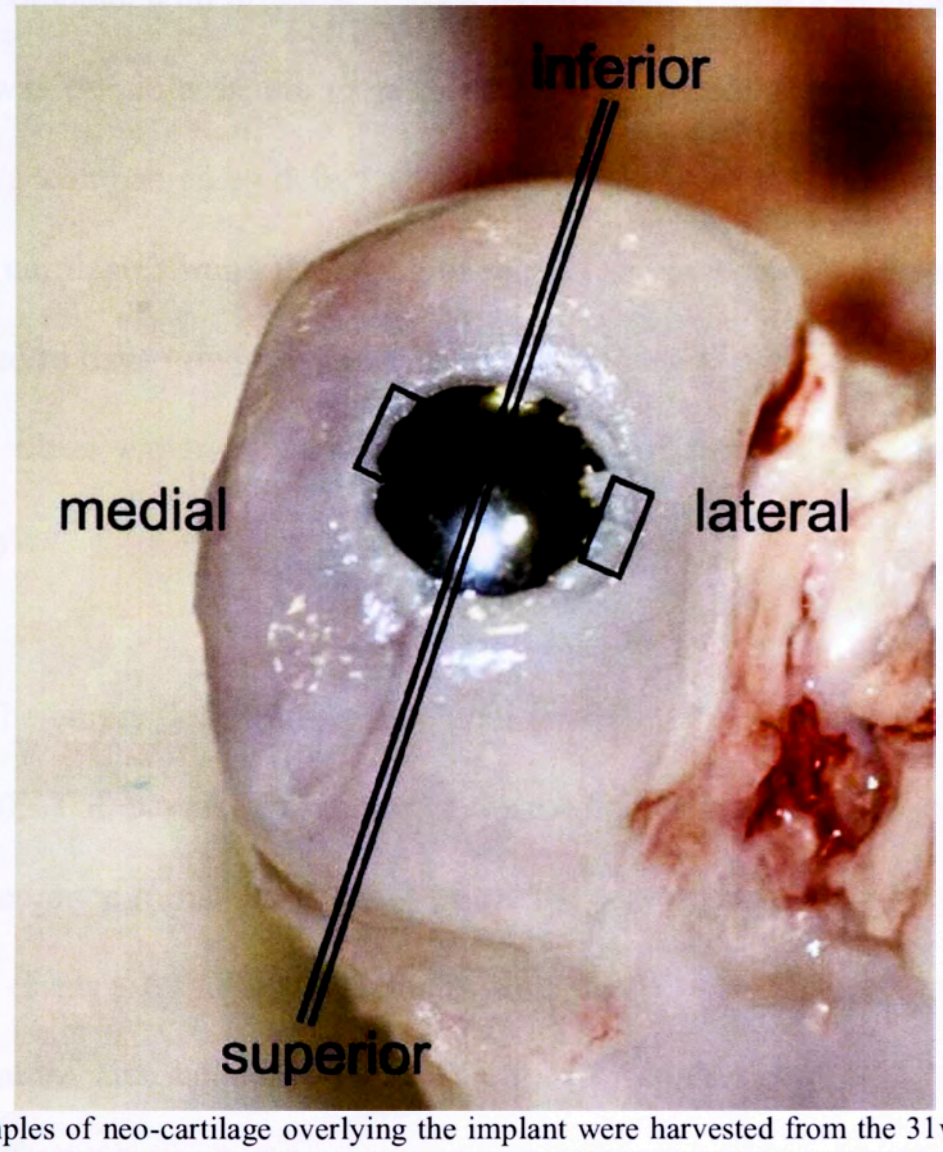


**Figure 67** Samples of neo-cartilage overlying the implant were harvested from the 31wk group in the medial and lateral regions bounded by the rectangles. The PMMA embedded condyle was sectioned in the sagittal plane as depicted by the two lines.

## *5.4 Results*

### 5.4.1 Macroscopic assessment

**5 weeks:** All animals were assessed at the time of the second surgery at which time all defects were obvious with minimal fibrous repair tissue within. Detailed macroscopic assessment was possible on the animals culled at 5 weeks (Figure 68). Two of six defects were accompanied by defect wall collapse and four (67%) showed fissuring of the adjacent cartilage around the edges of the defect. Two of the six medial menisci were observed to have minor degradation at the thinnest part of the white zone, whilst three of six tibiae experienced minor roughening of the articular cartilage in the medial condyle.

**11 weeks:** The empty defect group exhibited one case (20%) of defect wall collapse, two cases (40%) of extensive fissuring of the medial femoral cartilage and four cases (80%) of osteophyte formation or other geometric remodelling of the medial aspect of the condyle (Figure 69). Repair tissue within the femoral defects appeared to be fibrous in nature although none were filled with repair tissue to the level of the adjacent cartilage. Minor damage was noted in one of five menisci. Minor roughening of the tibial articular cartilage was evident on the medial condyle in five cases (100%) and extensive fissures were seen in two cases (40%).

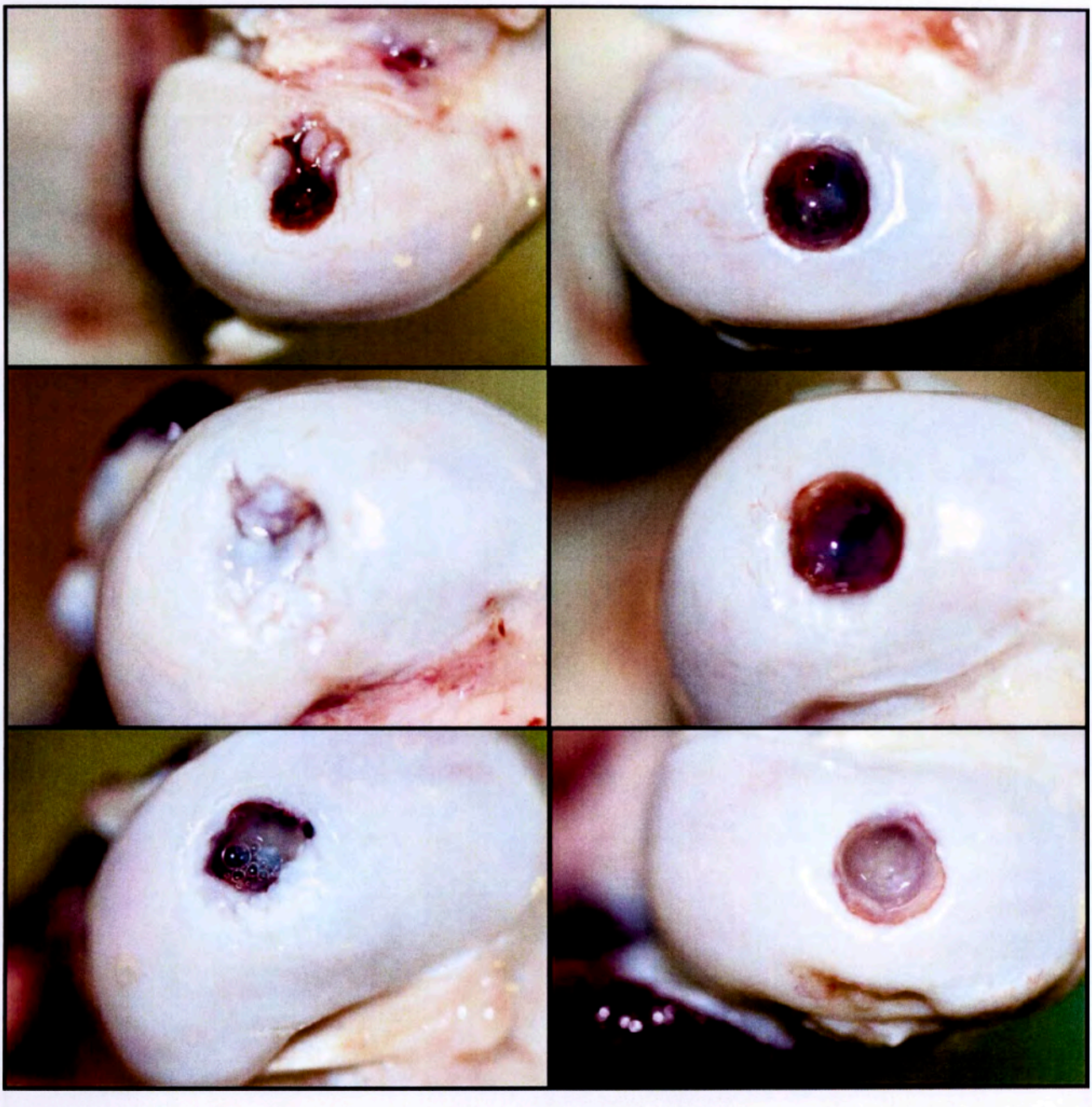

**Figure 68** Macroscopic appearance of empty femoral defects after 5 weeks

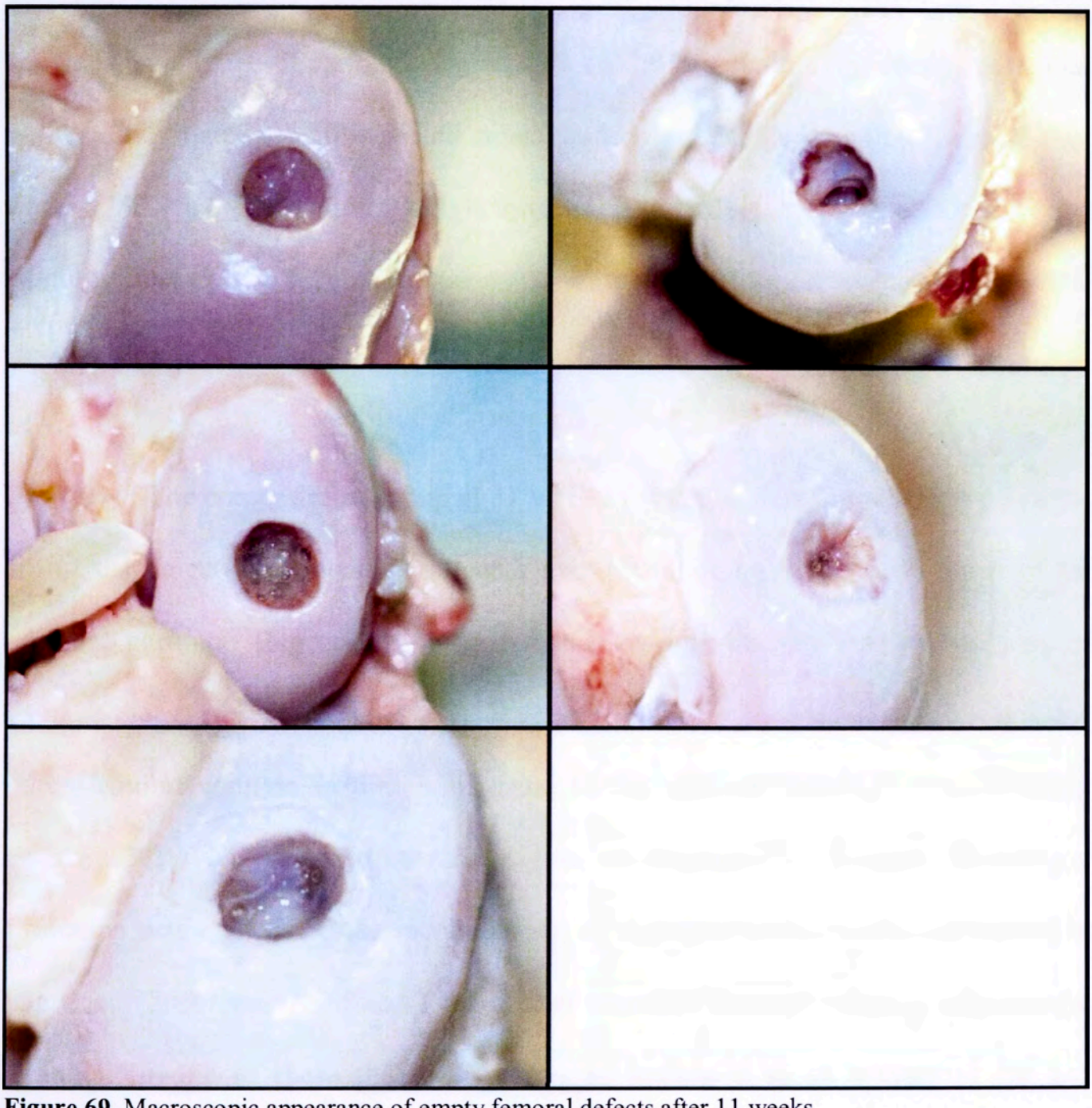

**Figure 69.** Macroscopic appearance of empty femoral defects after 11 weeks

All implants in the resurfaced group were well fixed, with no motion obvious on manual palpation. All implants were partially covered around the perimeter with smooth, white neo-cartilage in continuity with the surrounding cartilage (Figure 70). One of four medial femoral condyles exhibited fissuring and three (75%) had osteophyte formation on the medial aspect of the condyle. One trochlear groove also showed a small area of cartilage degradation on the lateral side. One medial meniscus was severely damaged although all others had no noticeable damage. Three of four tibiae (75%) exhibited minor roughening of the cartilage, two of which also had fissuring. Osteophyte formation was noted on the medial aspect of the tibial condyle in one case (25%).

**31 weeks:** The empty defect group at 31 weeks showed a marked improvement in the fill of the defect with repair tissue with four (80%) being filled to the level of the adjacent cartilage (Figure 71). One femoral condyle had an extensive region of damage that corresponded to a stray diathermy mark in the original surgery and one other femoral condyle exhibited fissuring in the adjacent cartilage. One trochlear groove (20%) had a small, central region of degenerative changes. Osteophyte formation was evident on the medial aspect of the femur in four cases (80%) and in one case (20%) on the tibia. Two medial menisci showed evidence of damage, although in one of these the damage can be attributed to an accidental cut and subsequent repair during the first surgery. All five tibiae displayed some roughening of the cartilage with two (40%) of these being moderate in severity and one (20%) exhibiting more extensive fissuring of the cartilage surface.

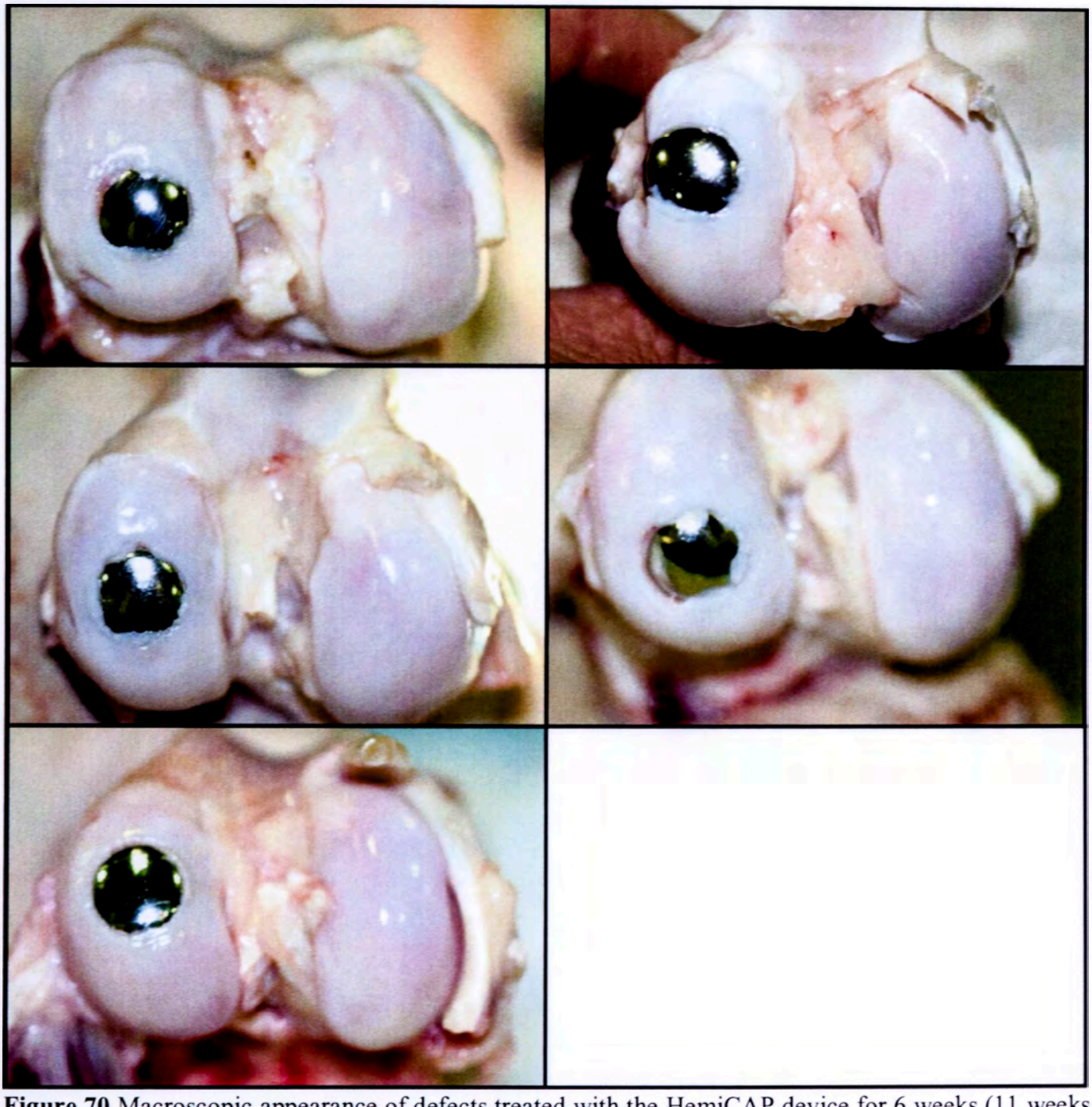

**Figure 70** Macroscopic appearance of defects treated with the HemiCAP device for 6 weeks (11 weeks since initial surgery)

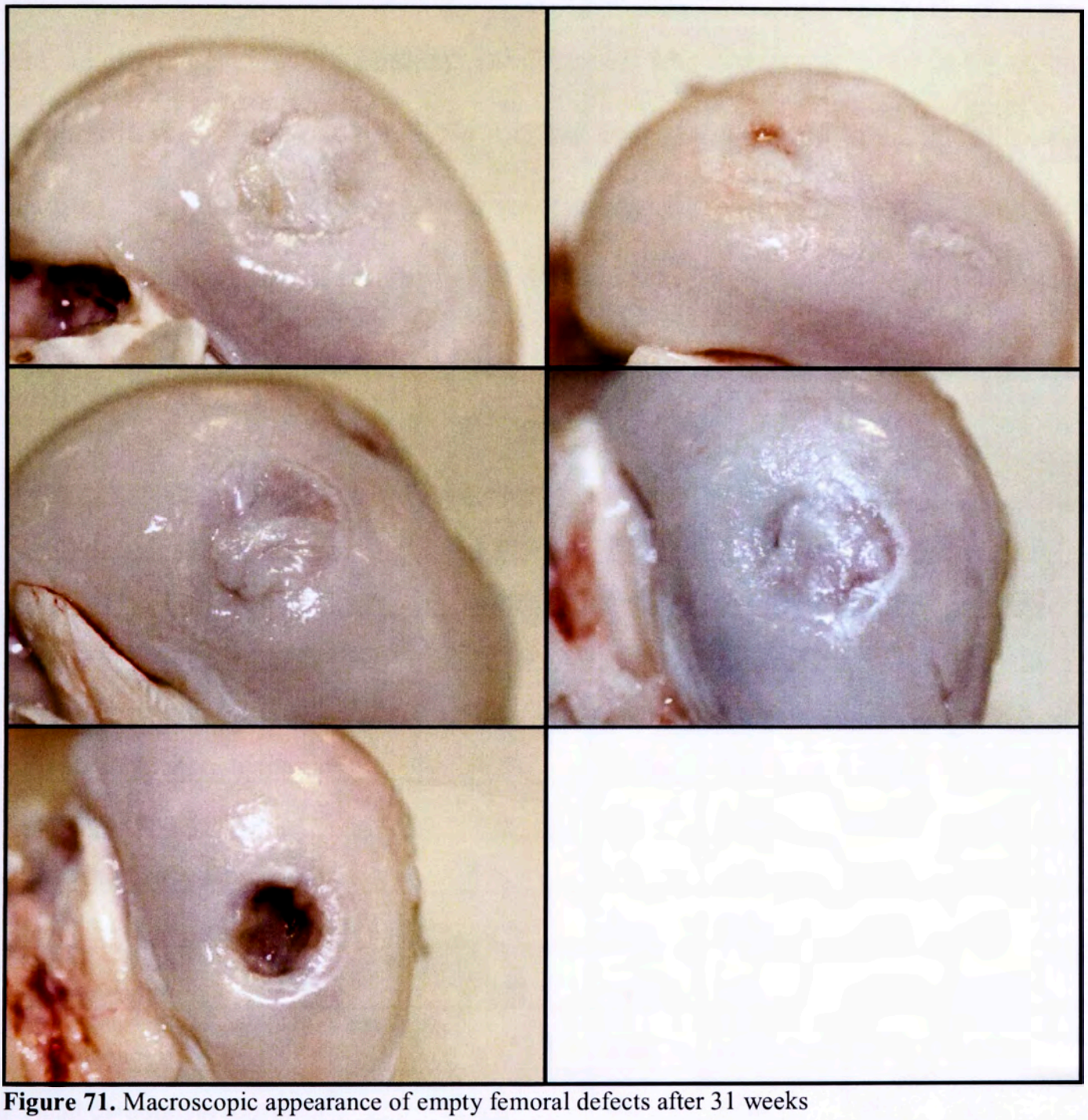

**Figure 71.** Macroscopic appearance of empty femoral defects after 31 weeks

All resurfacing implants were partially covered with progressively more repair tissue around the perimeter, when compared to the earlier time point (Figure 72). The repair tissue also appeared to be thicker. Osteophyte formation on the medial condyle was evident in 100% of cases whilst 40% had some fissuring of the femoral cartilage around the defect and degeneration was noted in one trochlear groove. On harvest of the neocartilage over the implant, calcification was noted above the level of the implant in one case (Figure 73). No menisci appeared to be damaged in this group. Two of five tibiae experience minor roughening of the cartilage and a further two tibiae had more extensive roughening and/or fissures. These results are summarised in Table 9.

**Table 9.** Summary results from macroscopic assessment of the femur, meniscus and tibia

| Group | 5 week | 11 week | | 31 week | |
|---|---|---|---|---|---|
| | Defect | Defect | HemiCAP | Defect | HemiCAP |
| Femoral fissuring/degradation | 67% | 50% | 25% | 40% | 40% |
| Defect collapse | 33% | 25% | n/a | 0% | n/a |
| Femoral osteophyte formation | 17% | 100% | 75% | 80% | 100% |
| Femoral repair tissue | 0% | 0% | 100% | 80% | 100% |
| Trochlea groove degeneration | 0% | 0% | 25% | 20% | 20% |
| Meniscal damage | 33% | 25% | 25% | 40% | 0% |
| Minor tibial articular cartilage degeneration | 50% | 100% | 75% | 100% | 80% |
| Extensive tibial articular cartilage degeneration | 0% | 50% | 50% | 20% | 40% |
| Tibial osteophyte formation | 0% | 0% | 20% | 20% | 0% |

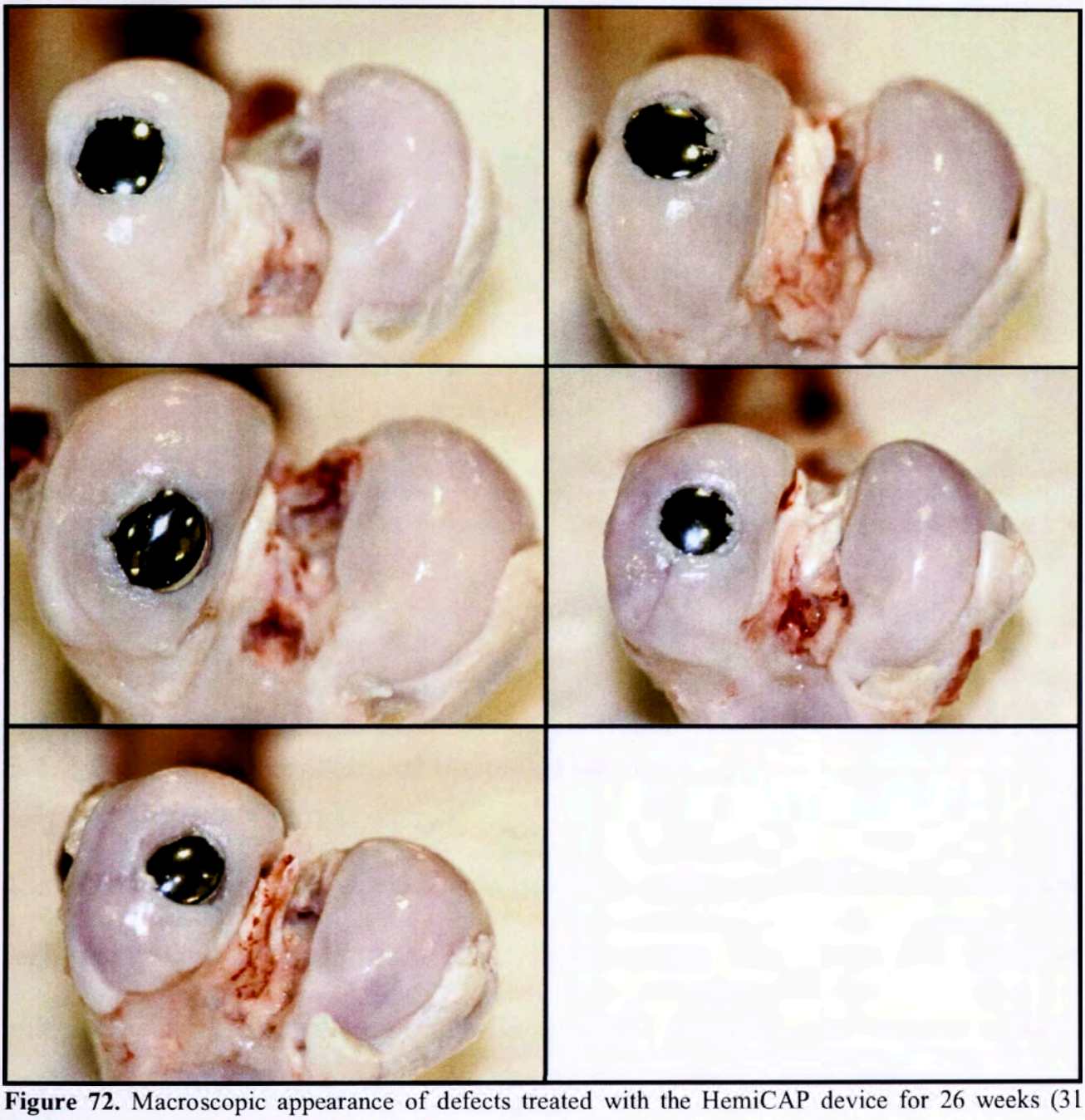

**Figure 72.** Macroscopic appearance of defects treated with the HemiCAP device for 26 weeks (31 weeks since the initial surgery)

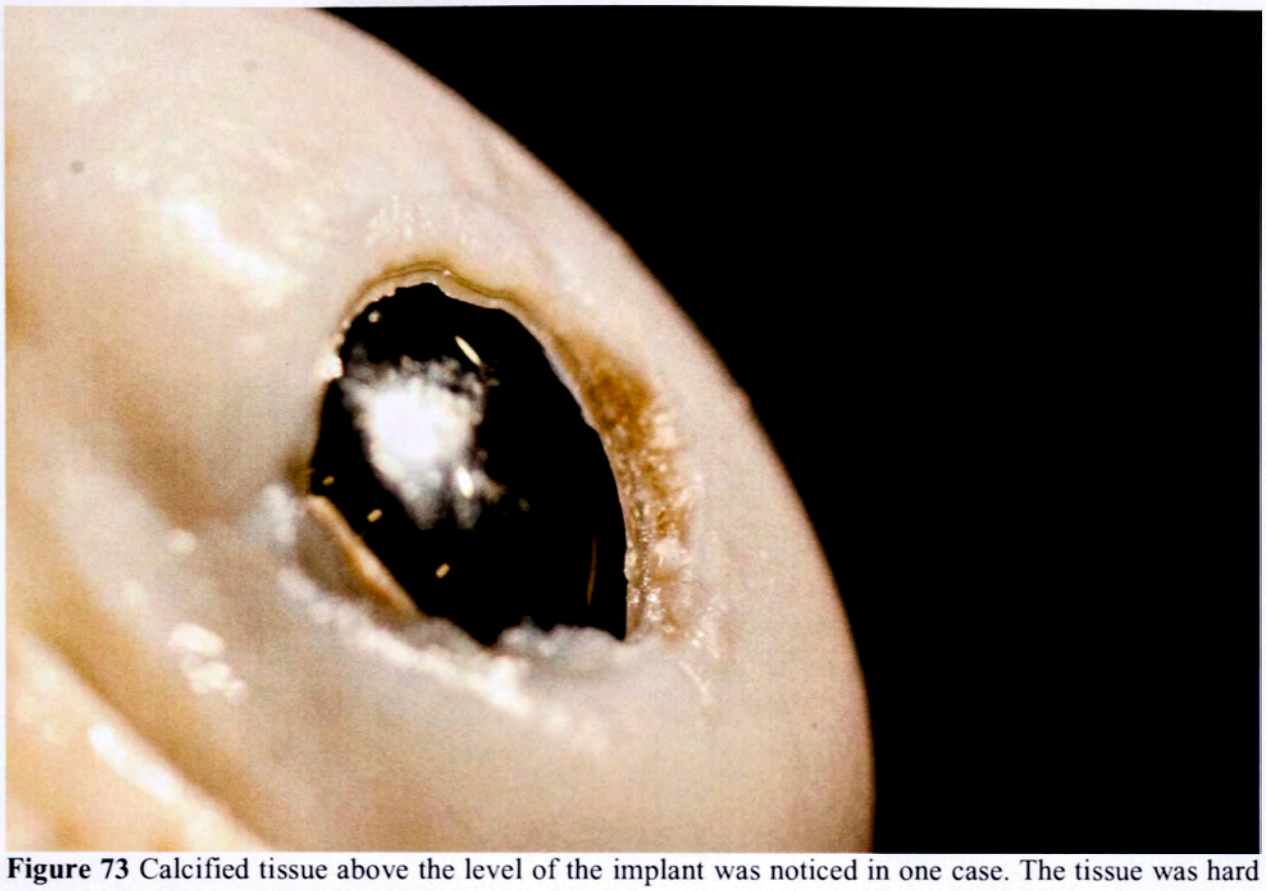

**Figure 73** Calcified tissue above the level of the implant was noticed in one case. The tissue was hard to cut with a scalpel. A cartilage layer approximately 0.5mm thick was covering the calcified tissue

## 5.4.2 Dynamic mechanical indentation

### Effective shear modulus

The effective shear modulus was calculated at 10 points across the tibial plateau and each point was averaged from three measurements. The results are displayed graphically in Figures 74 to 77. To simplify the reporting, and because of large variation across the topography of the plateau, these data points are also reported as the average value for each condyle (Table 10) and Figure 78.

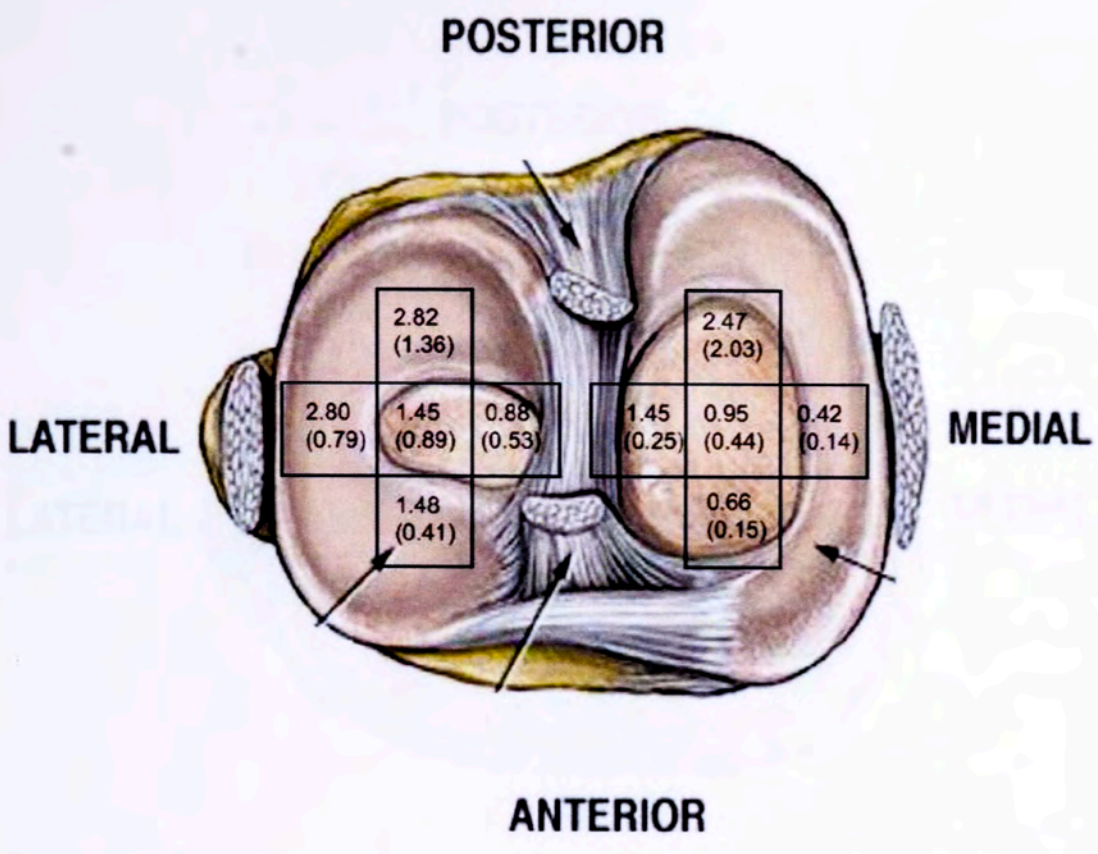


**Figure 74.** Effective shear modulus of the articular cartilage in the HemiCap group at 5 weeks, based on location. Note that the HemiCap device was located on the medial femoral condyle.

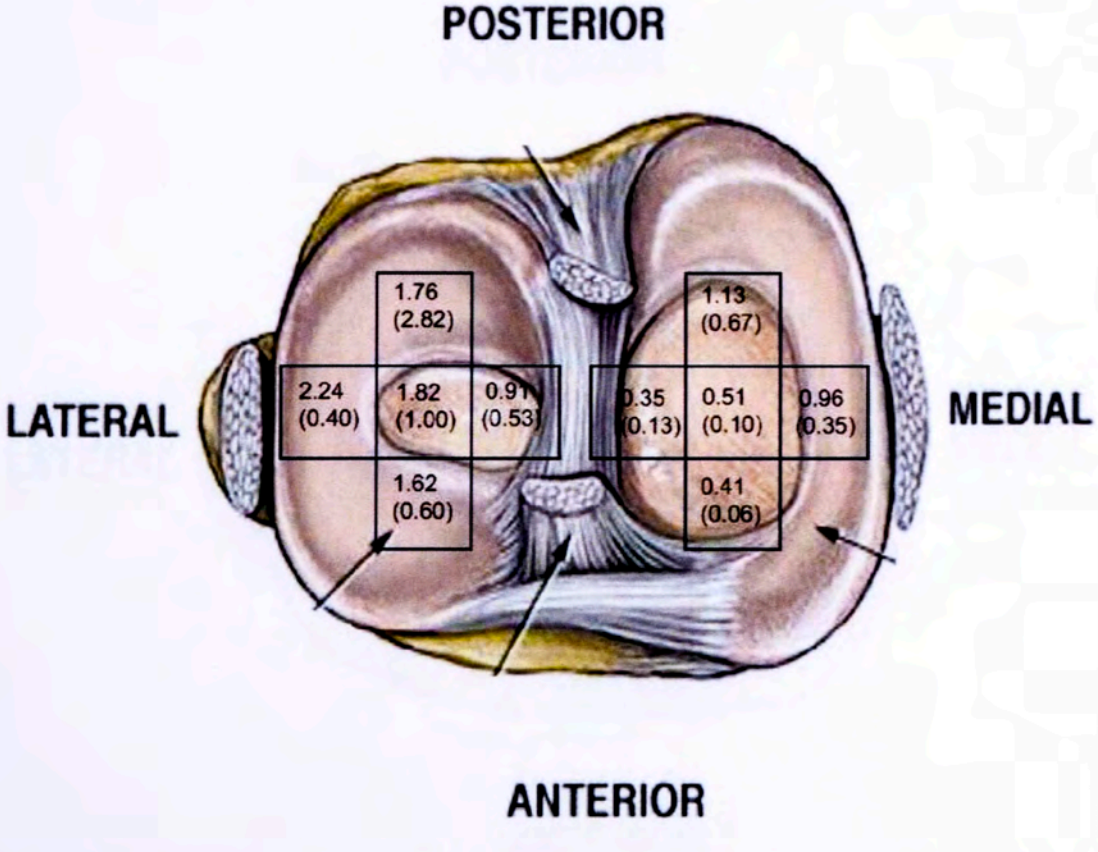


**Figure 75.** Effective shear modulus of the articular cartilage in the empty defect group at 5 weeks, based on location. Note that the empty defect was located on the medial femoral condyle.

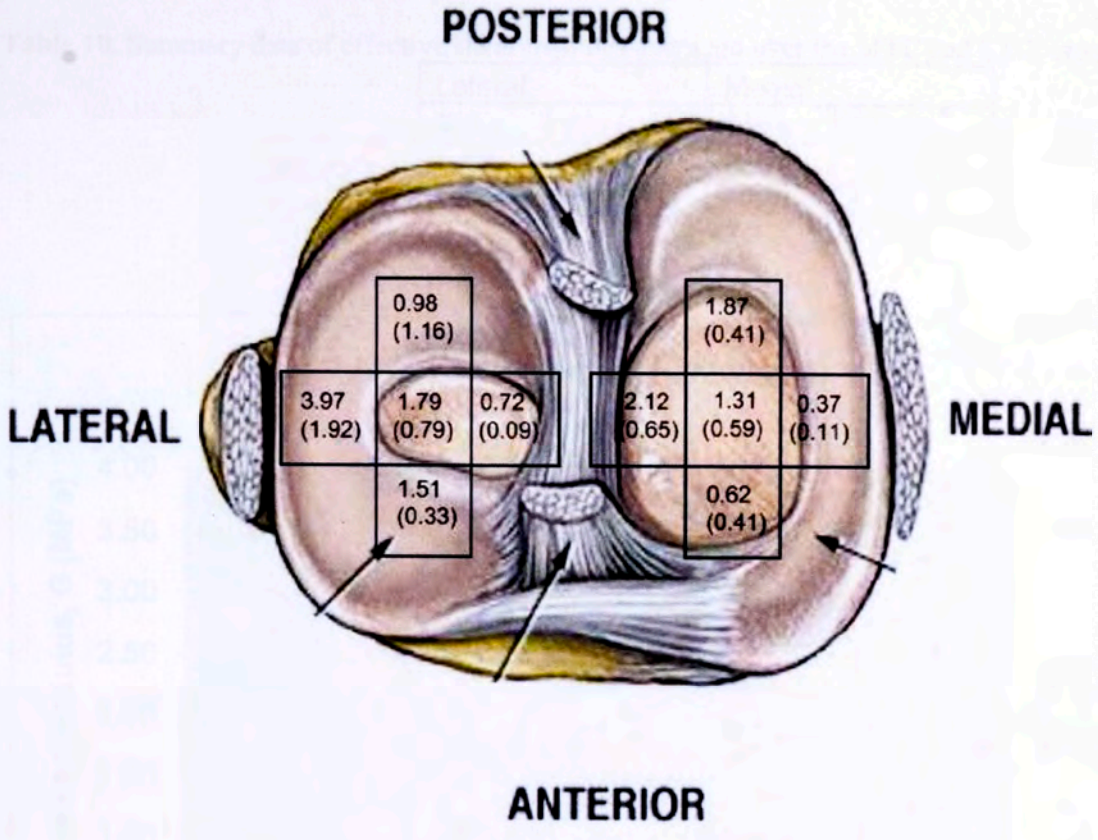


**Figure 76.** Effective shear modulus of the articular cartilage in the HemiCap group at 31 weeks, based on location. Note that the HemiCap device was located on the medial femoral condyle.

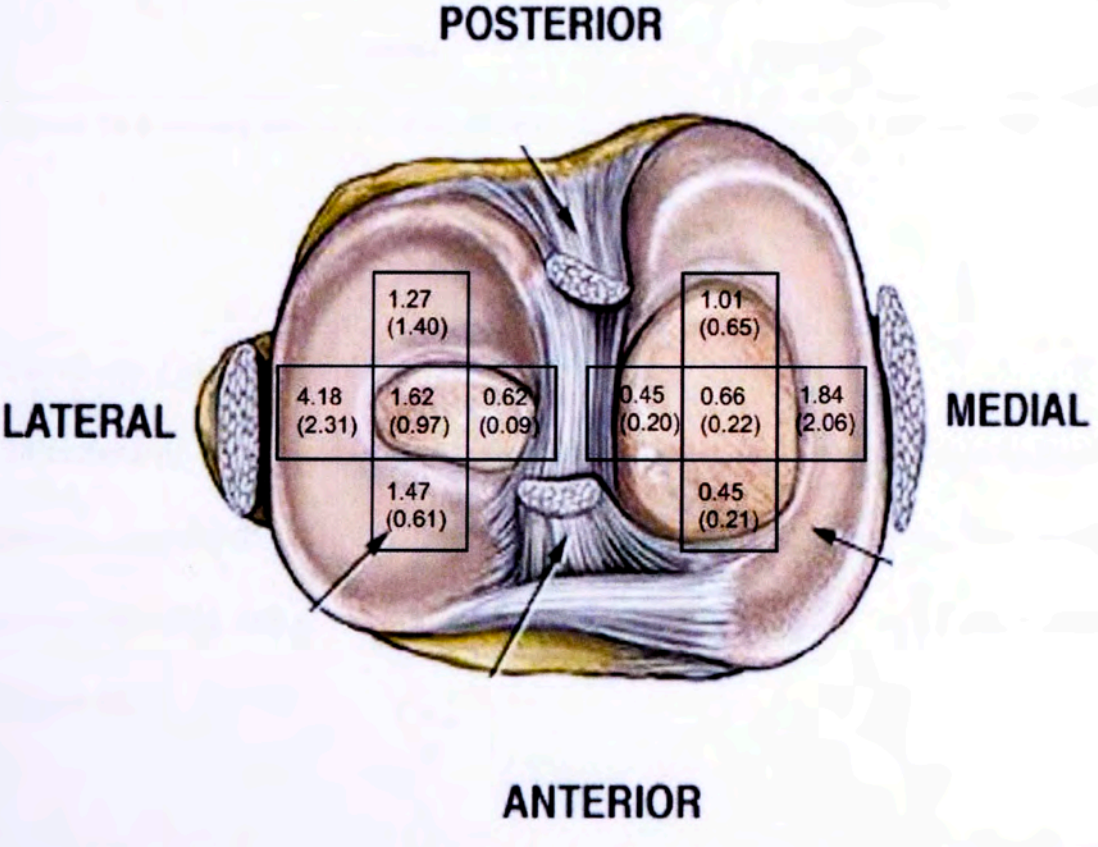


**Figure 77.** Effective shear modulus of the articular cartilage in the empty defect group at 31 weeks, based on location. Note that the empty defect was located on the medial femoral condyle.

**Table 10.** Summary data of effective shear modulus averaged over the MTC and LTC, units MPa.

| | Lateral | | Medial | |
|---|---|---|---|---|
| | 5wks | 31wks | 5wks | 31wks |
| Empty | 1.67 | 1.83 | 0.67 | 0.89 |
| HemiCAP | 1.99 | 1.79 | 1.37 | 1.26 |

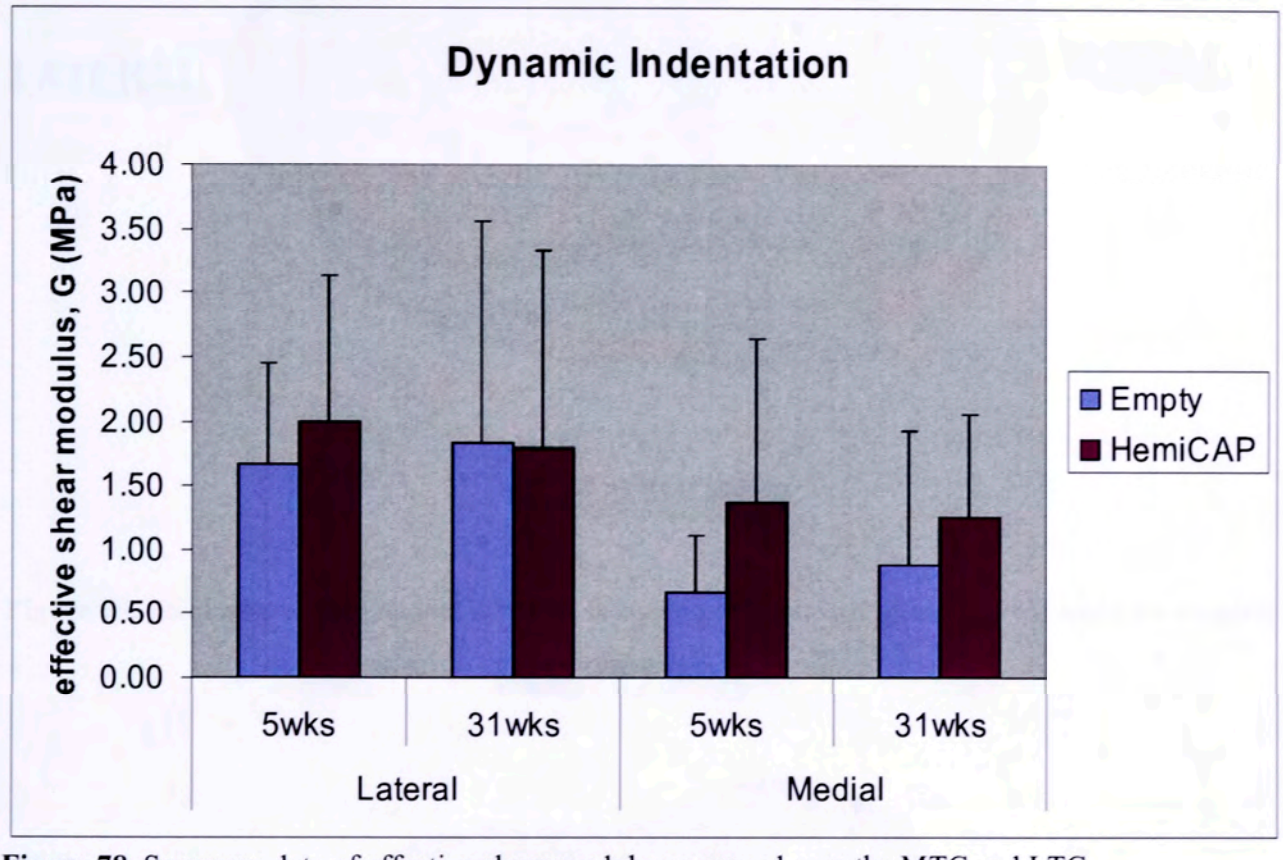


**Figure 78.** Summary data of effective shear modulus averaged over the MTC and LTC

## Cartilage Thickness

Thickness of the articular cartilage was measured at the same 10 points on the tibial plateau. Again, to simplify for the large topgraphical variations, the average values across the tibia are presented in Table 11 and Figures 79 to 82 and summarised in Figure 83.

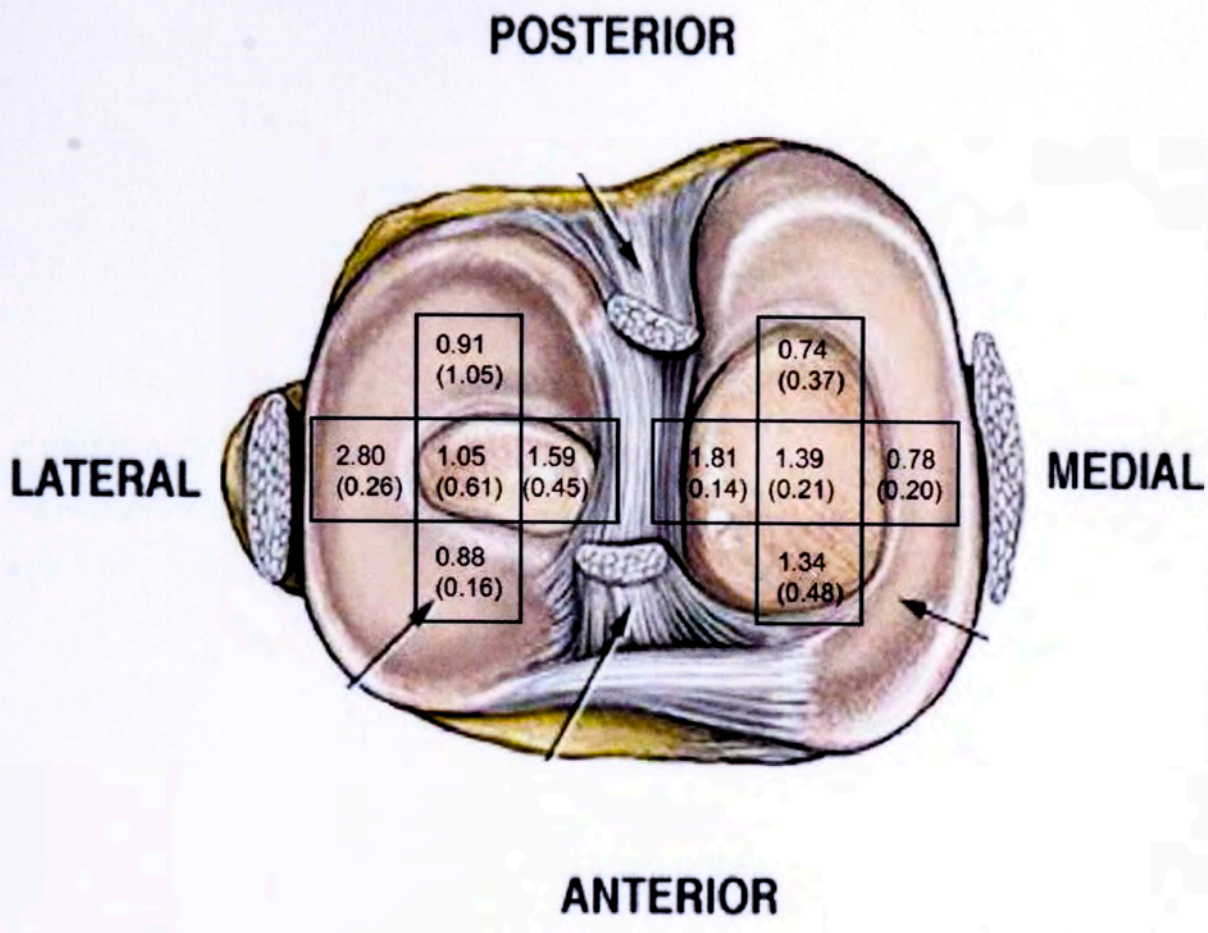


**Figure 79.** Thickness of the articular cartilage in the empty defect group at 5 weeks, based on location.

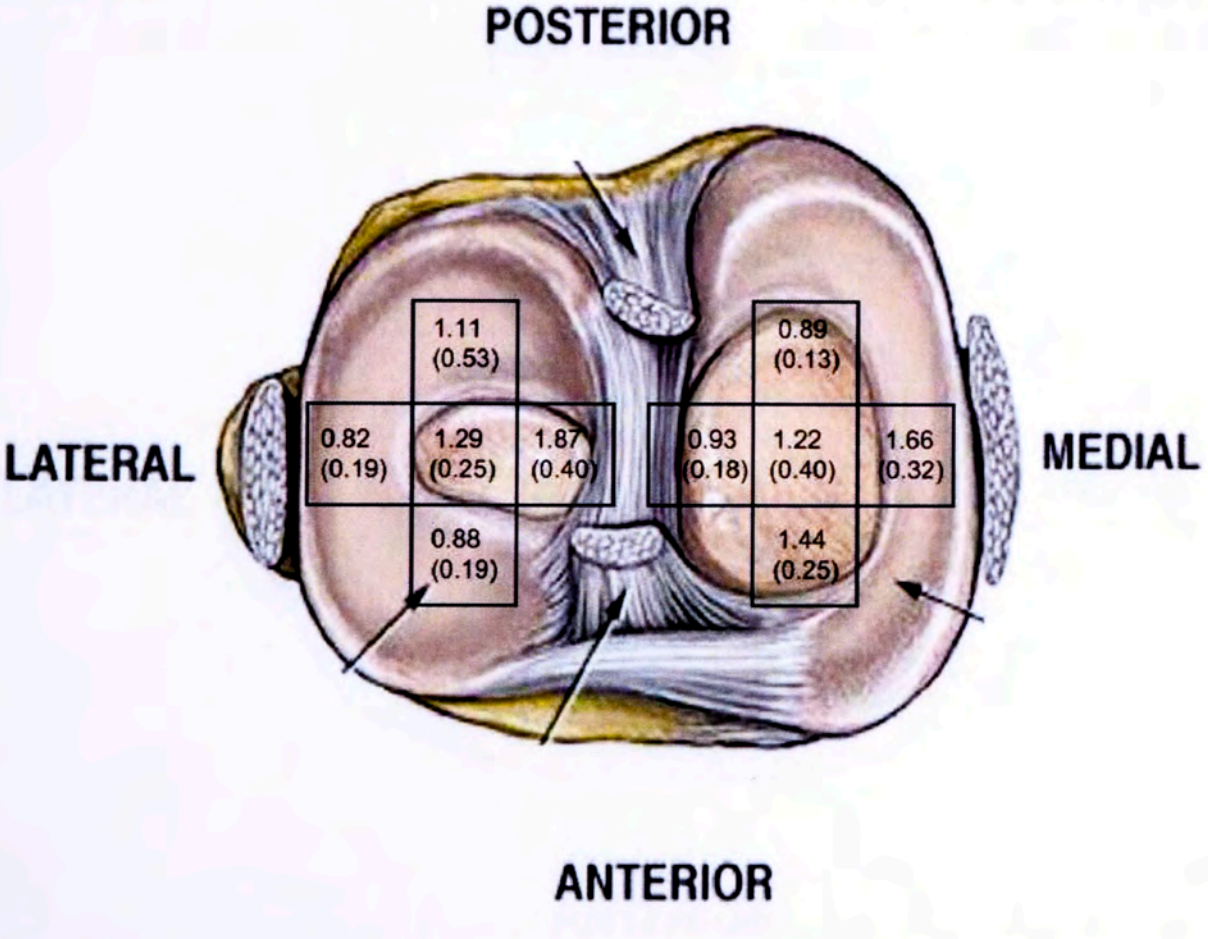


**Figure 80.** Thickness of the articular cartilage in the HemiCap group at 5 weeks, based on location.

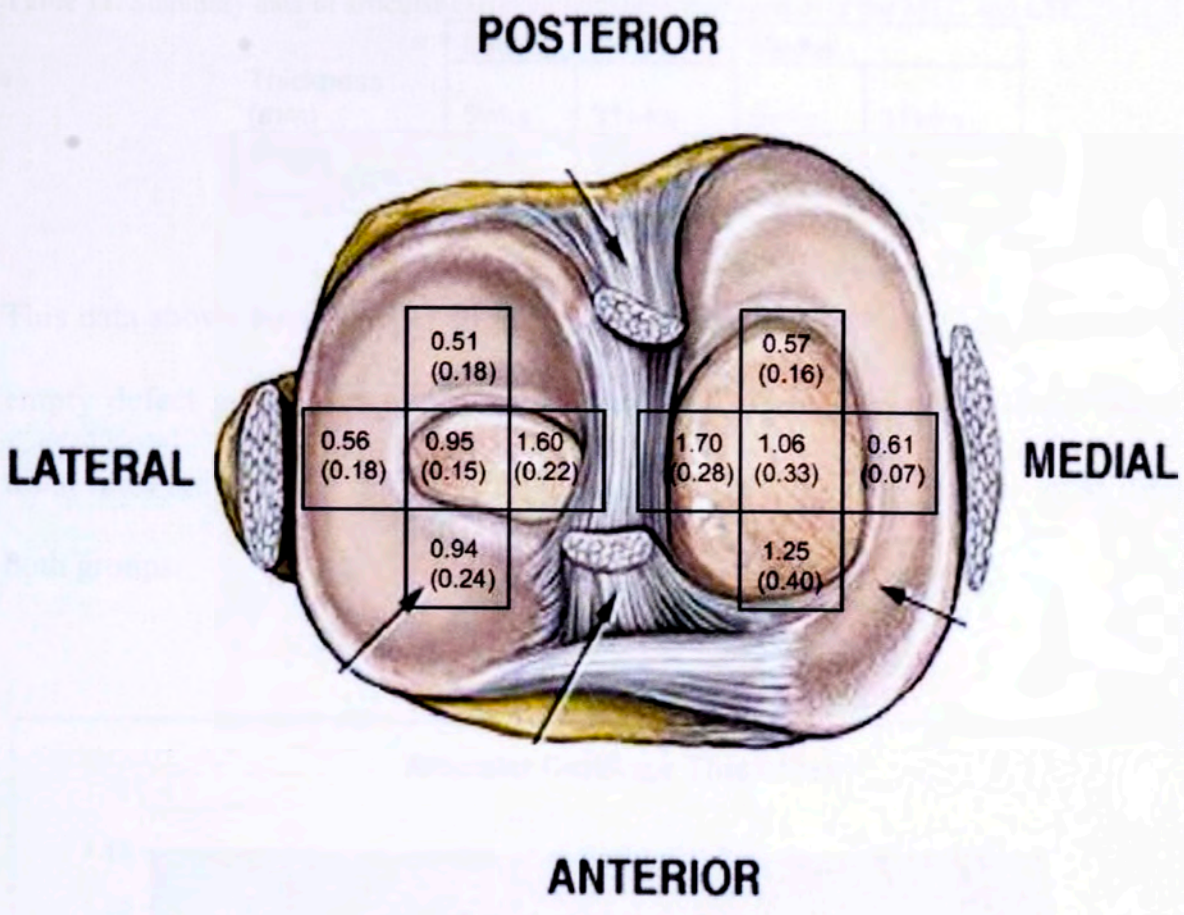


**Figure 81.** Thickness of the articular cartilage in the empty defect group at 31 weeks, based on location.

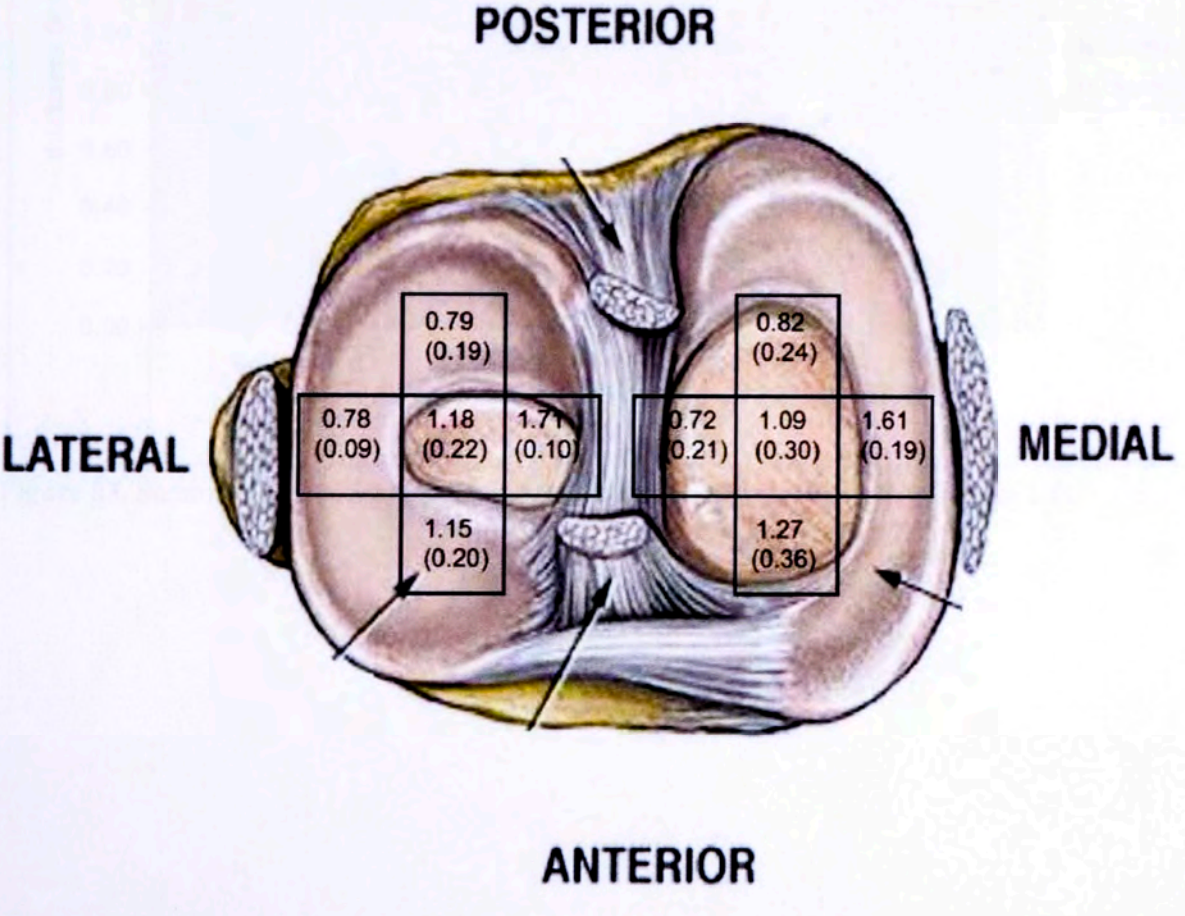


**Figure 82.** Thickness of the articular cartilage in the HemiCap group at 31 weeks, based on location.

**Table 11.** Summary data of articular cartilage thickness averaged over the MTC and LTC.

| Thickness (mm) | Lateral | | Medial | |
|---|---|---|---|---|
| | 5wks | 31wks | 5wks | 31wks |
| Empty | 0.99 | 0.91 | 1.21 | 1.04 |
| HemiCAP | 1.19 | 1.12 | 1.23 | 1.10 |

This data shows no statistical differences between the tibial cartilage thickness in the empty defect group compared to the HemiCAP treated group, however, there is a trend for a reduction in thickness on the medial condyle from 5 weeks to 31 weeks in both groups.

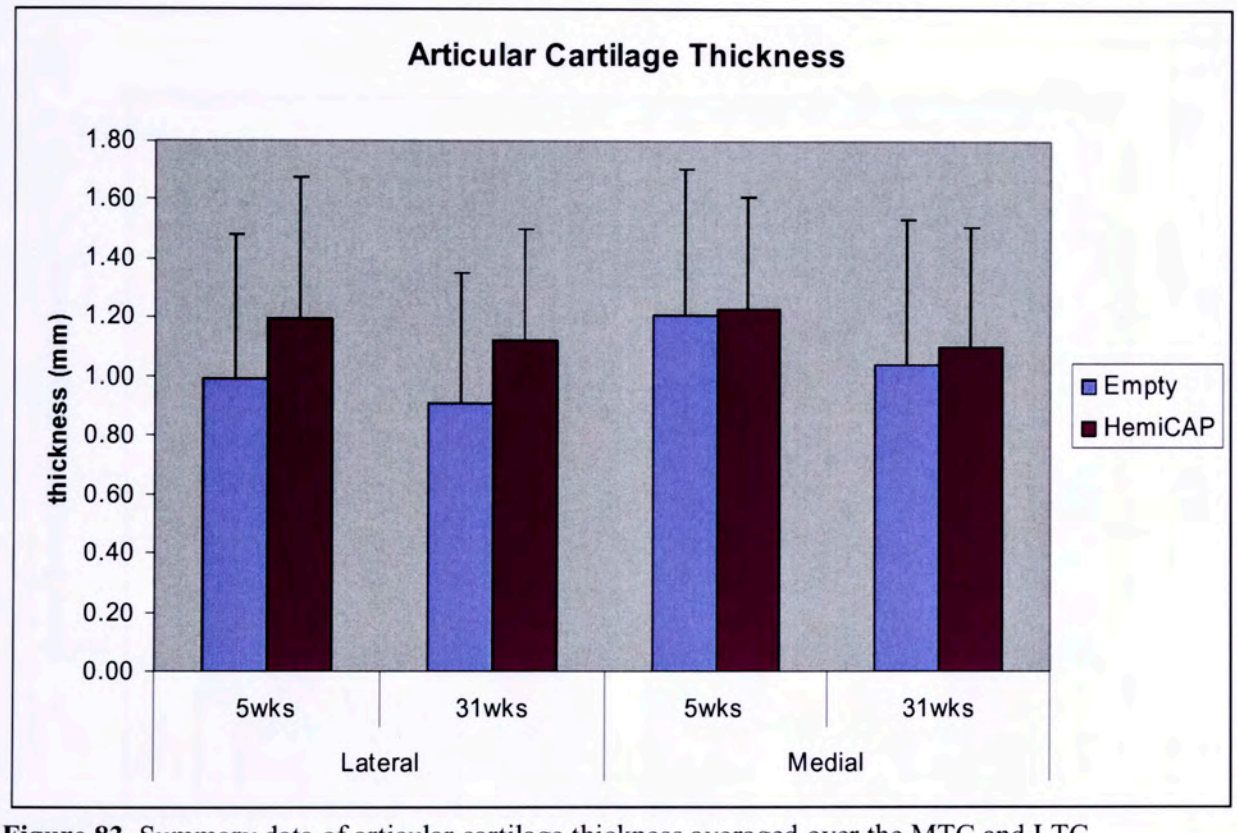


**Figure 83.** Summary data of articular cartilage thickness averaged over the MTC and LTC.

### 5.4.3 Micro computed tomography

Micro computed tomography of the cancellous bone revealed no significant differences for any of the parameters studied between the HemiCAP group and the empty defect group at either of the time points. Significant differences were noted in the percentage of bone (Figure 84), trabecular thickness (Figure 86) and trabecular number (Figure 87) between the 5 wk group when compared to the other time points. All quantitative parameters at 31 weeks tended towards similarity with the non operated controls (Figure 85, Figure 86).

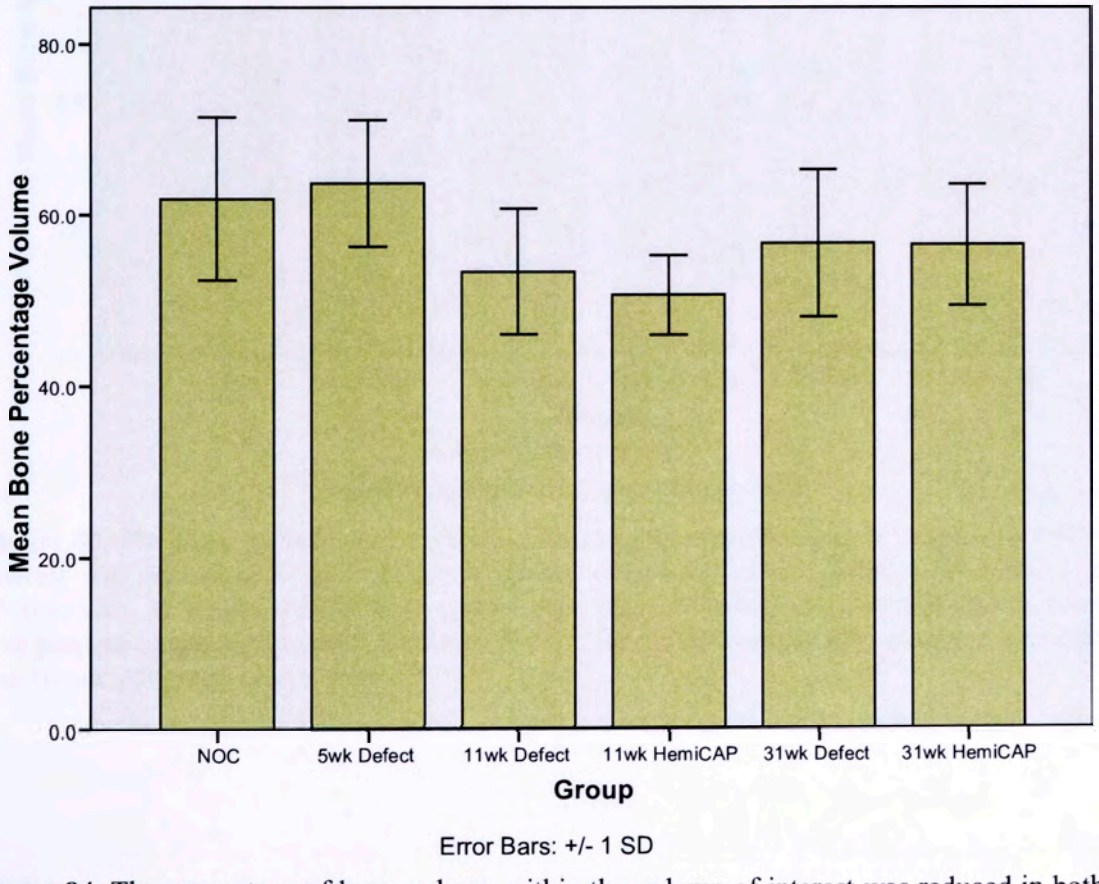


**Figure 84.** The percentage of bone volume within the volume of interest was reduced in both 11 week groups compared to the normal medial tibial plateau, although the difference was not significant. By 31 weeks, the changes in mean bone percentage had resolved back to baseline levels.

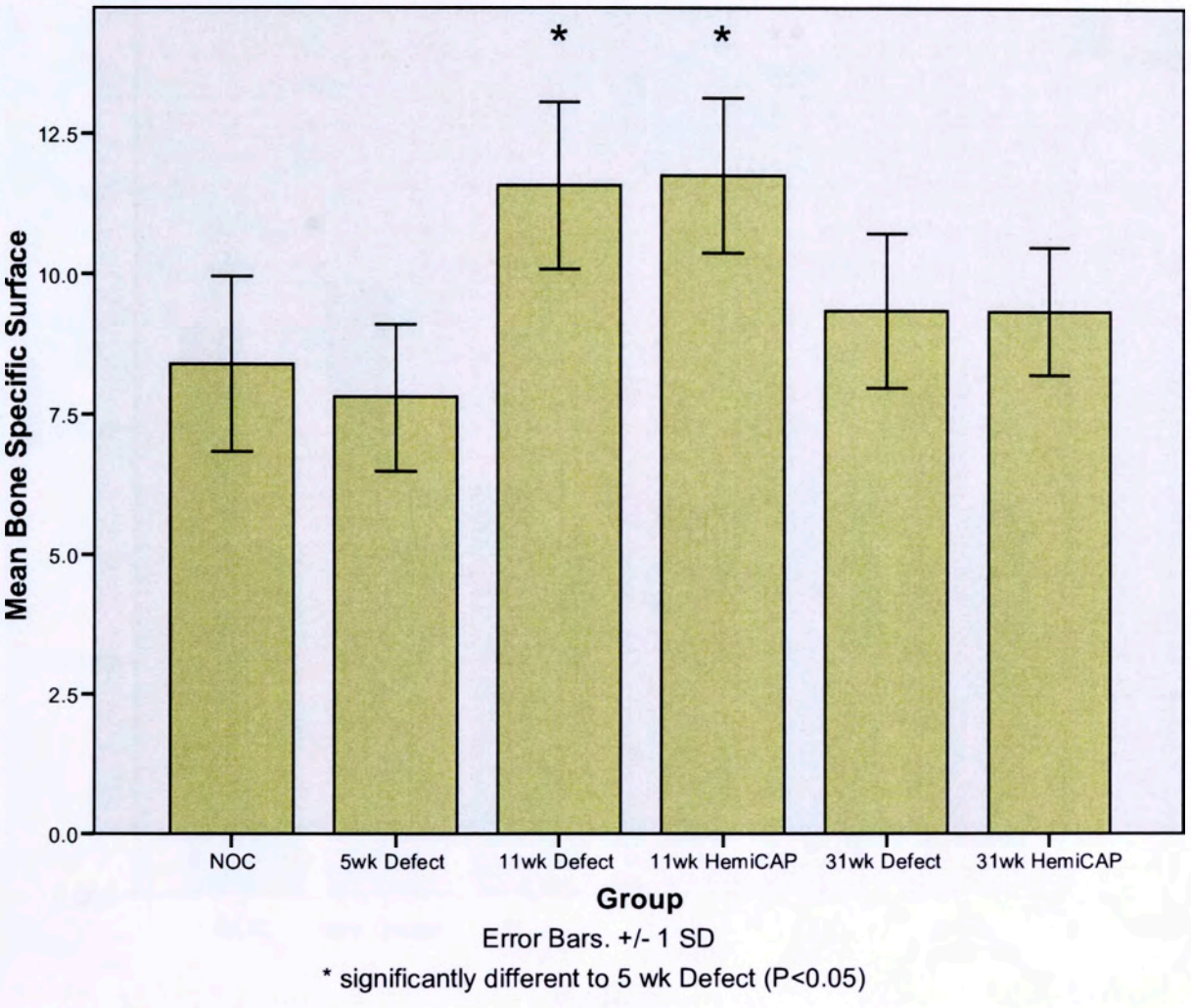


**Figure 85.** The bone specific surface (ratio of bone surface area to bone volume) within the volume of interest was increased in both 11 week groups compared to the medial tibial plateau at 5 weeks ($P<0.05$). By 31 weeks, the changes in mean bone specific surface had resolved back to baseline levels and were no longer significantly different. No significant differences were detected between the defect and HemiCAP group at any time.

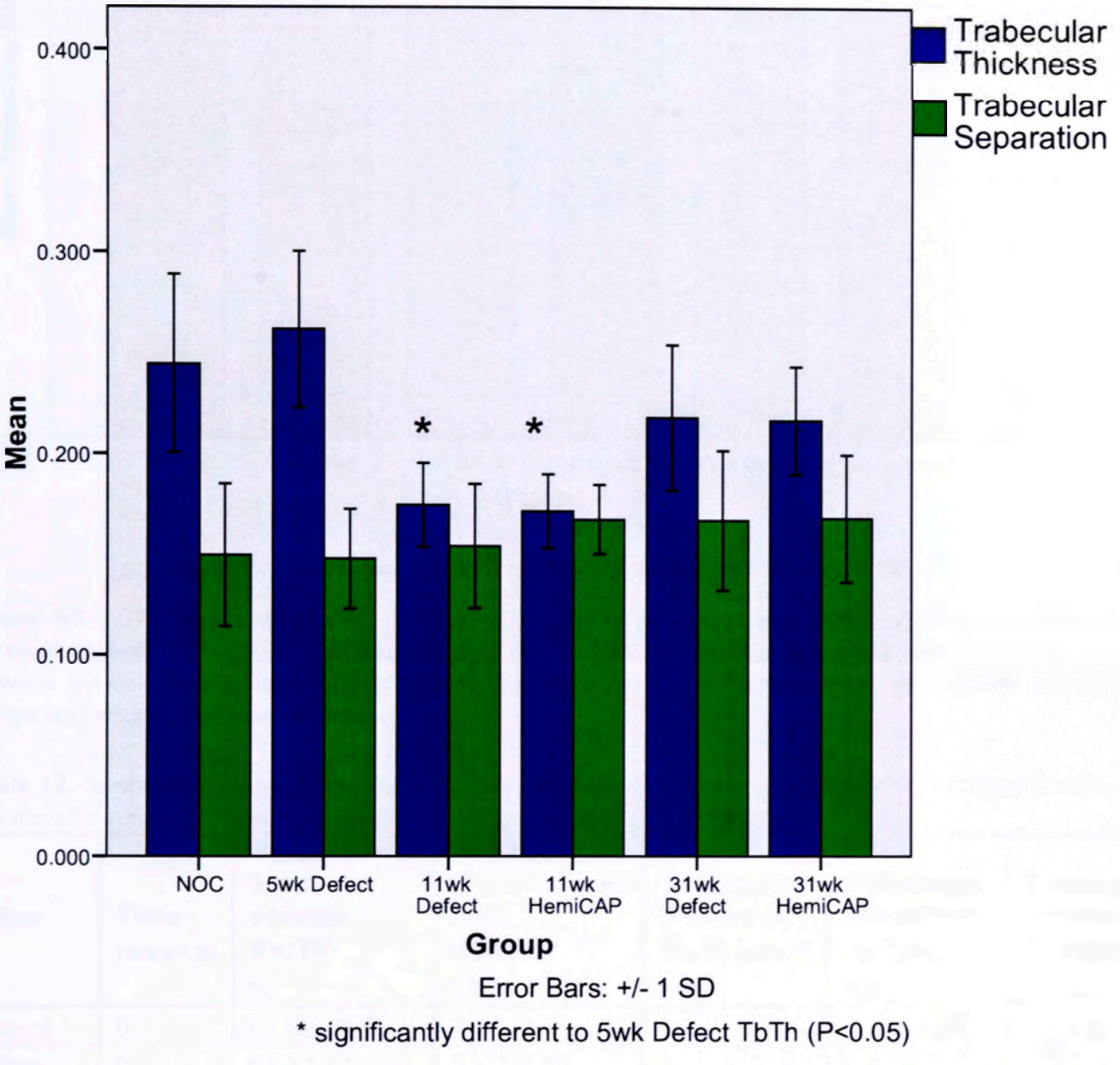


**Figure 86.** The trabecular thickness in both 11 week groups was significantly less than the value at 5 weeks ($P<0.05$) however there were no differences between the defect and HemiCAP groups. The difference between 5 and 11 weeks had mostly resolved back to baseline levels by 31 weeks and were no longer significant. The trabecular separation remained unchanged between all groups at each time.

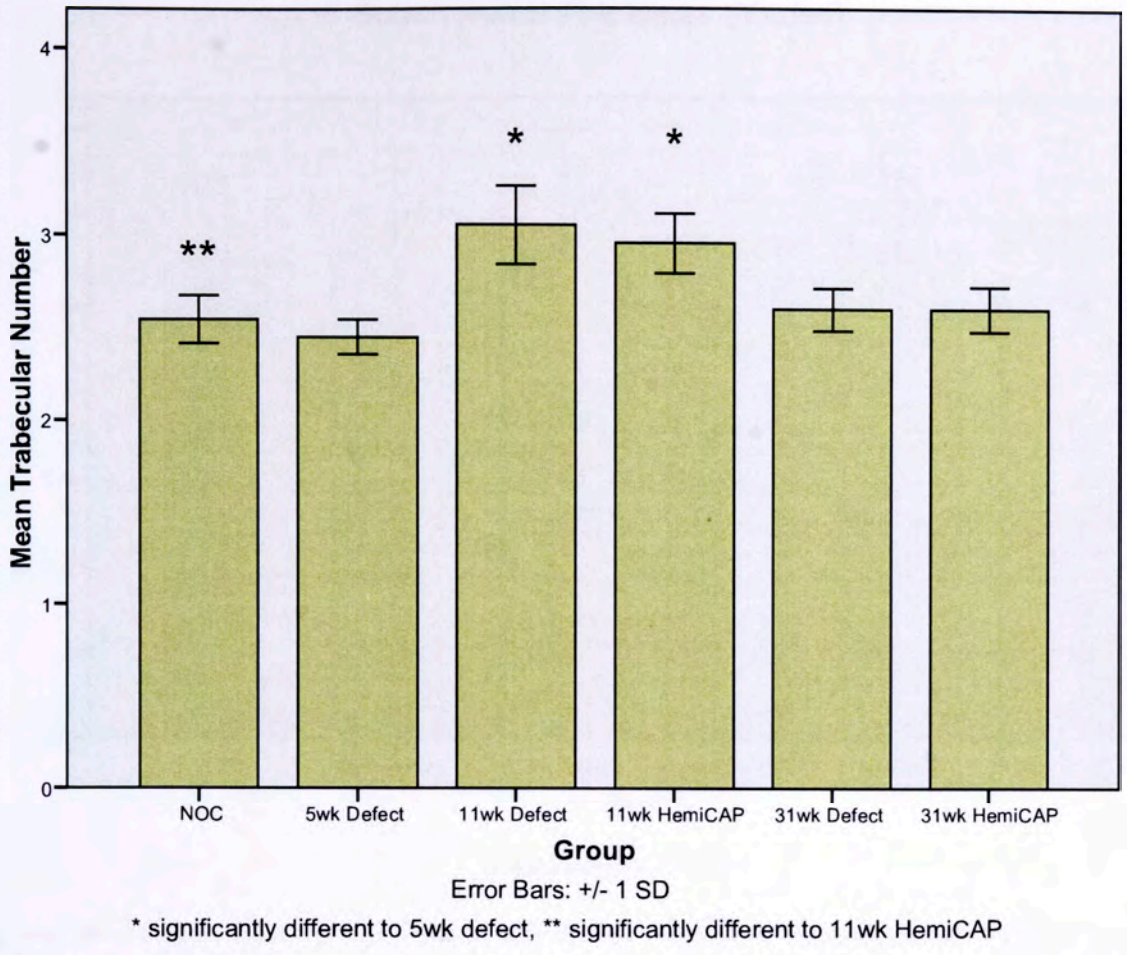


**Figure 87.** The mean trabecular number (the number of trabeculae per mm) was significantly increased in both 11 week groups compared to the 5 week group. However there were no differences between the defect and HemiCAP groups at any time. At 31 weeks, the trabecular number for both groups had returned to baseline levels.

**Table 12.** Summary of quantitative microCT of the cancellous bone on tibiae opposite either a defect or a metallic resurfacing implant on the femur; mean (standard deviation)

| Group | Time (weeks) | Percent bone volume BV/TV % | Bone surface / volume ratio BS/BV 1/mm | Trabecular thickness Tb.Th(pl) mm | Trabecular separation Tb.Sp(pl) mm | Trabecular number Tb.N(pl) 1/mm |
|---|---|---|---|---|---|---|
| Control | 0 | 61.89 (9.5) | 8.40 (1.6) | 0.245 (0.04) | 0.150 (0.04) | 2.54 (0.13) |
| Defect | 5 | 63.71 (7.4) | 7.80 (1.3) | 0.262 (0.04) | 0.148 (0.02) | 2.45 (0.10) |
| Defect | 11 | 53.34 (7.4) | 11.58 (1.5) | 0.175 (0.02) | 0.154 (0.03) | 3.05 (0.21) |
| HemiCAP | 11 | 50.59 (4.7) | 11.76 (1.4) | 0.172 (0.02) | 0.168 (0.02) | 2.96 (0.16) |
| Defect | 31 | 56.64 (8.6) | 9.35 (1.4) | 0.218 (0.04) | 0.167 (0.03) | 2.60 (0.12) |
| HemiCAP | 31 | 56.42 (7.1) | 9.34 (1.1) | 0.217 (0.03) | 0.168 (0.03) | 2.60 (0.12) |

Measurements of subchondral bone thickness of each of the medial tibial condyles revealed a trend of increasing thickness from the normal state to the 5 week group and further to the 11 week group before returning back to basal levels at 31 weeks (Figure 88 to 90). This was especially true for the central and lateral regions of the medial condyle, although this trend did not reach statistical significance.

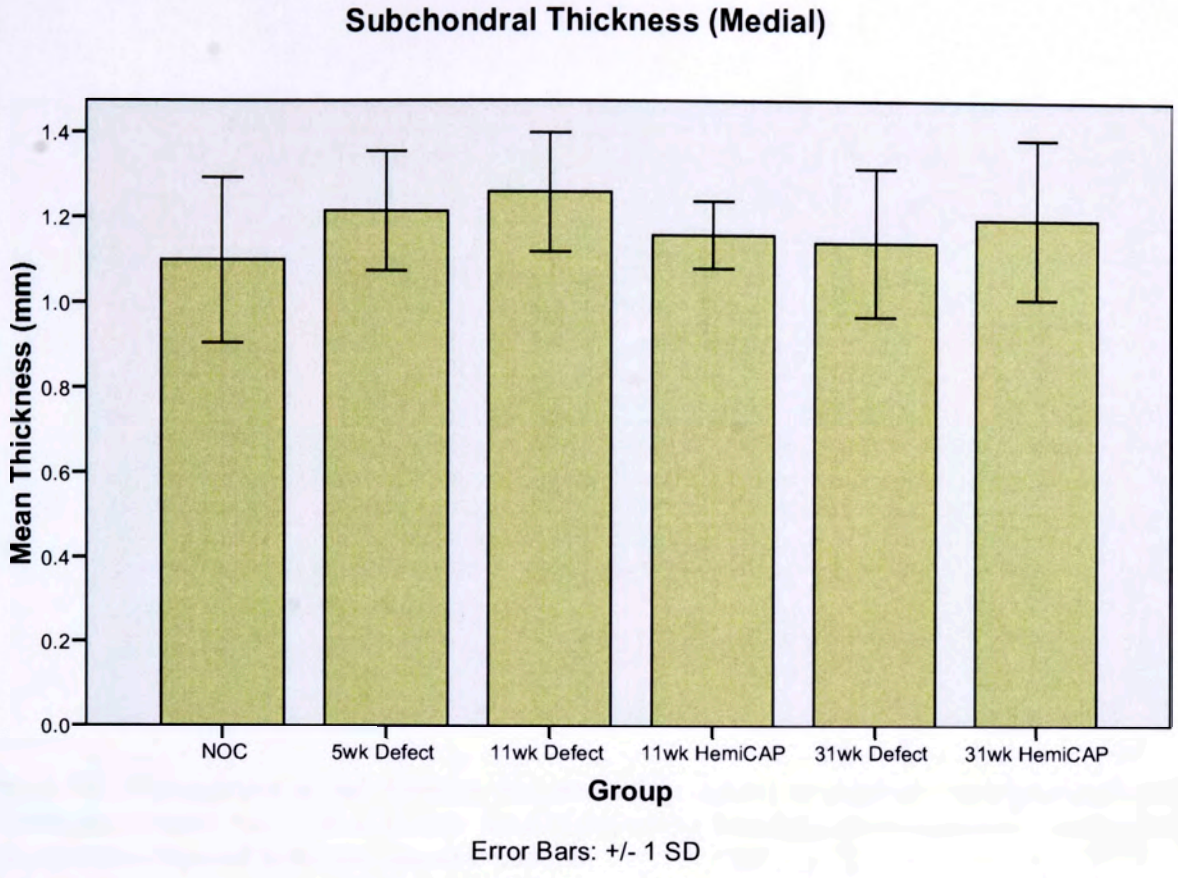


**Figure 88.** Measurement of subchondral thickness revealed no significant differences between any groups in the medial zone

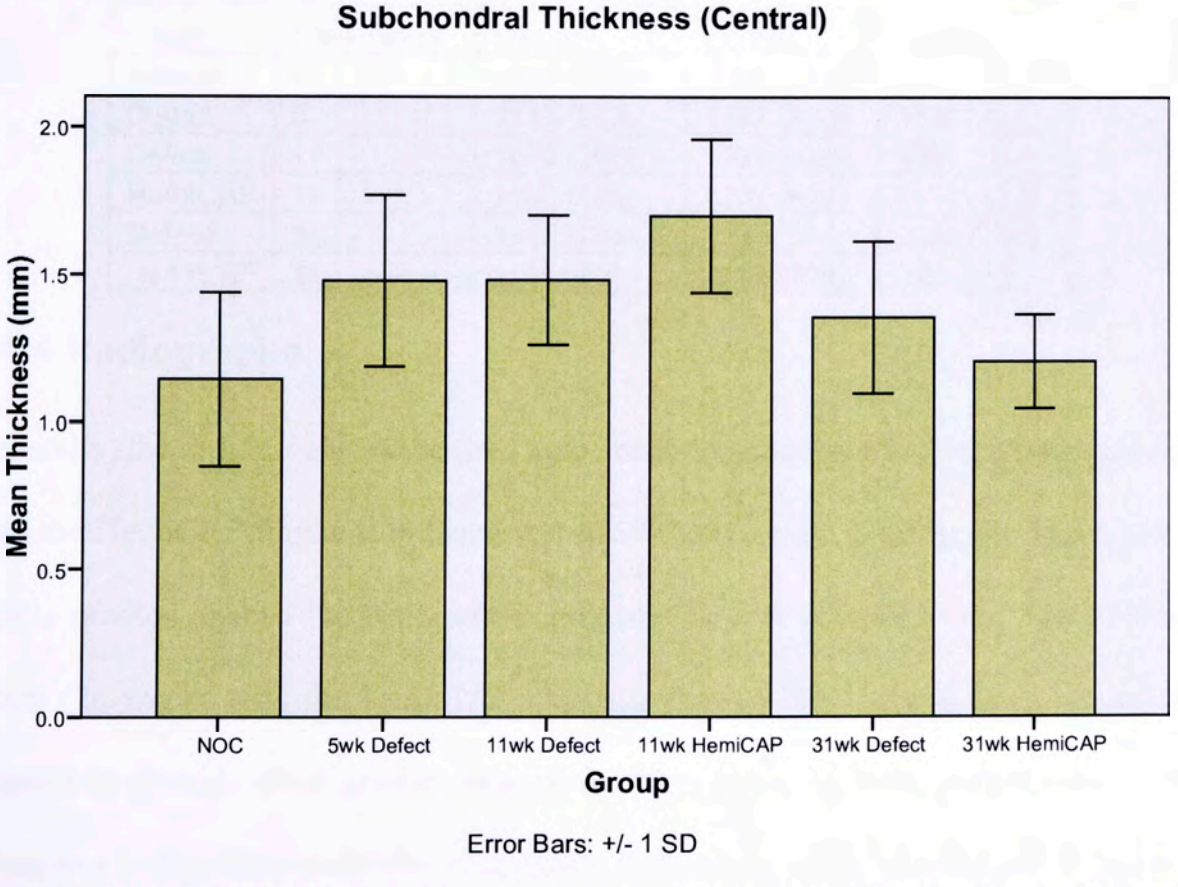


**Figure 89.** Measurement of subchondral thickness in the central region revealed no significant differences between any groups. However, a definite trend of increasing thickness was noted in the 5 week and 11 week groups compared to the non operated control, which was mostly resolved by 31 weeks.

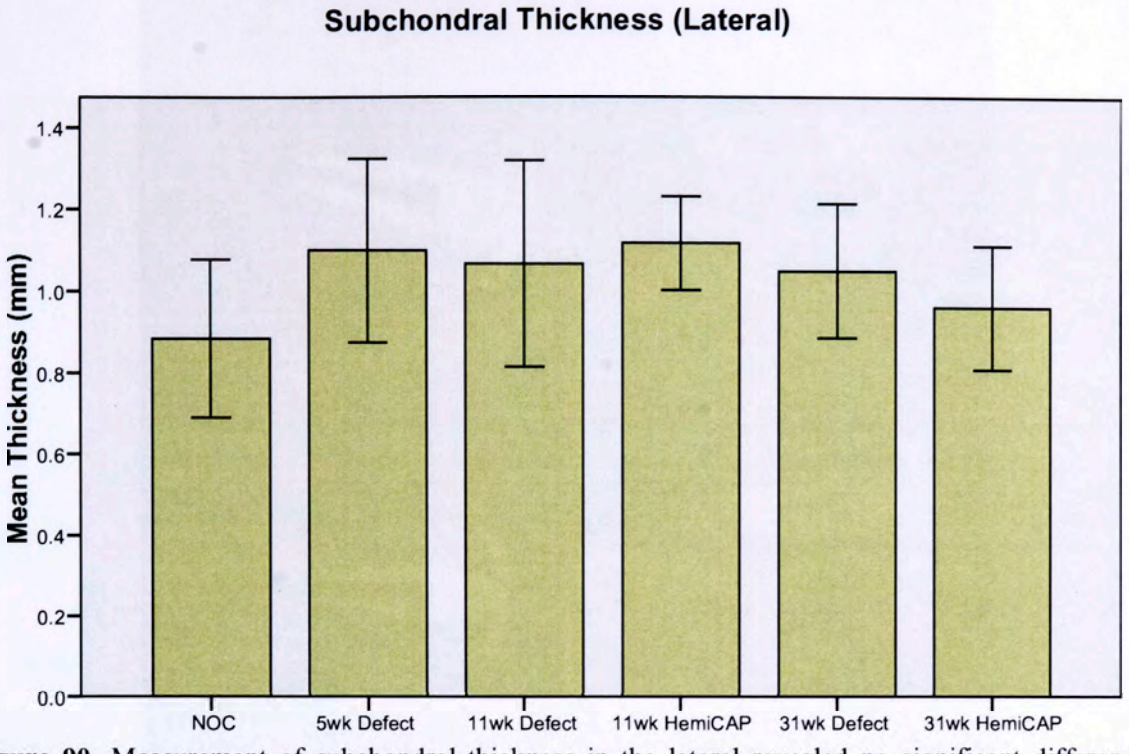


**Figure 90.** Measurement of subchondral thickness in the lateral revealed no significant differences between any groups. However, a definite trend of increasing thickness was noted in the 5 week and 11 week groups compared to the non operated control

**Table 13.** Summary of the subchondral bone thickness (μm) measured with the microCT method. The values in parentheses correspond to the standard deviation.

| Group | Time (wks) | Medial | Central | Lateral |
|---|---|---|---|---|
| Normal | 0 | 1098 (292) | 1140 (412) | 883 (301) |
| Defect | 5 | 1215 (273) | 1497 (390) | 1099 (418) |
| Defect | 11 | 1260 (285) | 1481 (340) | 1067 (363) |
| HemiCAP | 11 | 1160 (305) | 1700 (390) | 1118 (352) |
| Defect | 31 | 1142 (274) | 1335 (364) | 1050 (281) |
| HemiCAP | 31 | 1196 (305) | 1212 (298) | 960 (249) |

### 5.4.4 Radiographs

Generally, the radiographs of the time zero specimen and the 11 week group (6 weeks with the HemiCAP implant) indicate that the initial fixation is adequate. The screw is tightly pressed against the walls of the prepared hole in all specimens. The 31 week group (26 weeks with the HemiCAP implant) showed bone remodelling around the implant to provide even greater fixation in most cases. In both groups, some void space was still evident under the articulating component where the original defect was created. One case at 31 weeks showed bone osteolysis around the threaded portion of the implant (Figure 91).

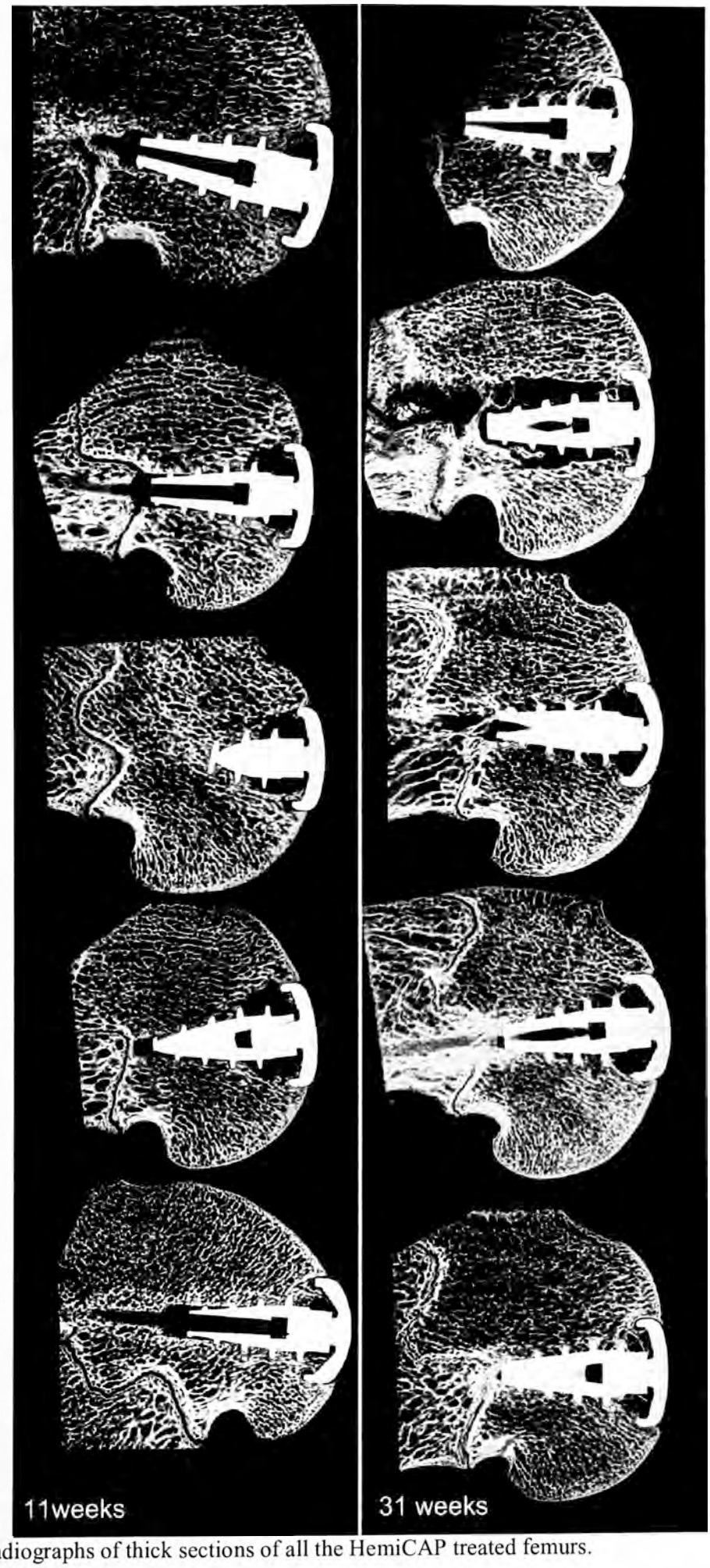


**Figure 91** Radiographs of thick sections of all the HemiCAP treated femurs.

**11 weeks:** Radiographs of thick sections through the femora treated with the HemiCAP implant showed bone abutting against the threaded portion of the screw. This confirmed the result form manual palpation that the implant was securely fixed into the bone. Some new bone was noted around the screw threads, although bone deposition and remodelling was not complete, with evidence of the k-wire and drill holes still remaining. The osseous portion of the original osteochondral defect was still evident in all cases (Figure 92). The presence of the defect made no difference to the stability of the device. The surface of the implant was congruent with the level of the adjacent cartilage.

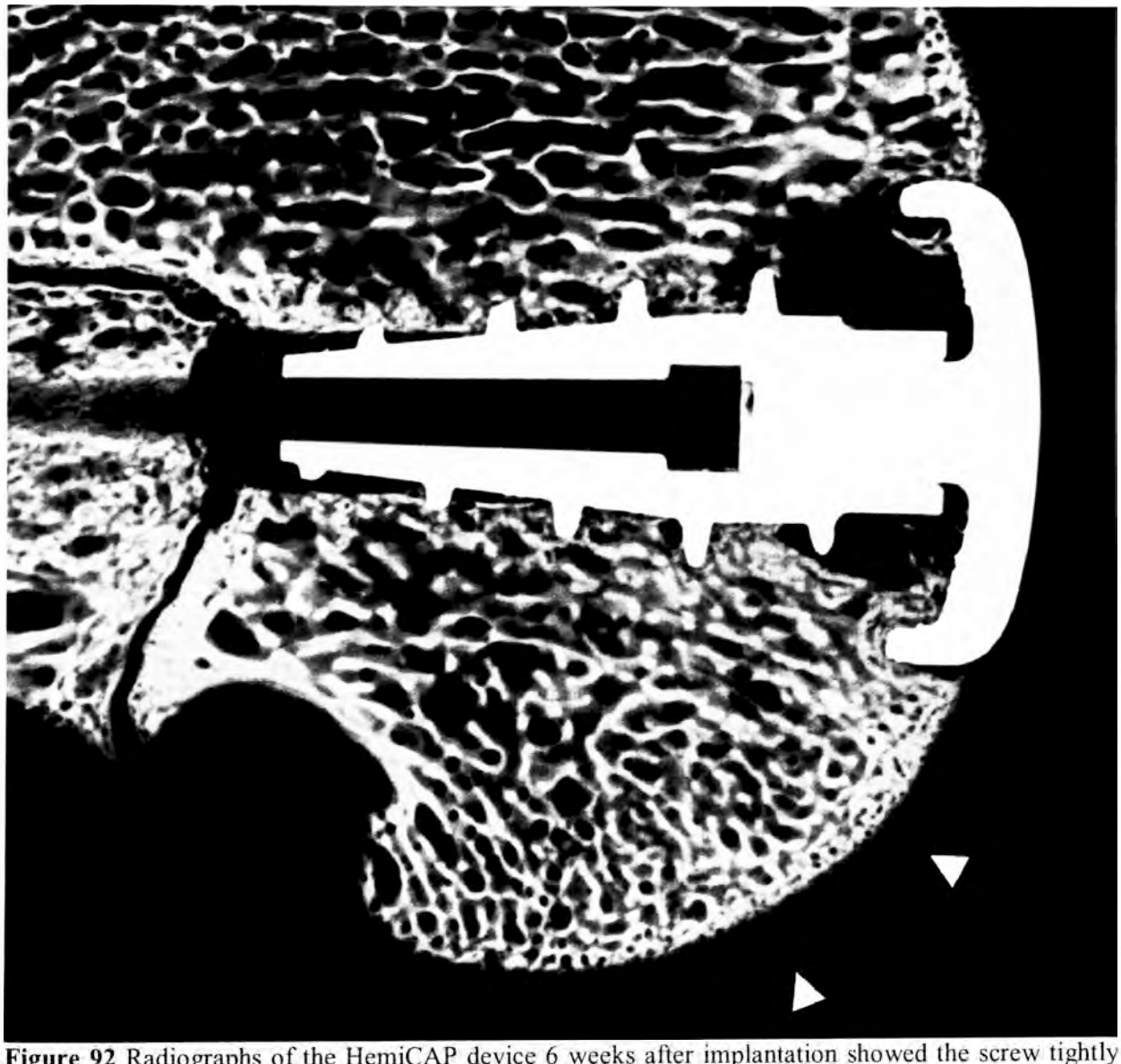

**Figure 92** Radiographs of the HemiCAP device 6 weeks after implantation showed the screw tightly fixed within the bone. New bone formation around the screw is incomplete and the original bone defect remains underneath the cap. The epiphyseal plate is clearly not fused, indicating the animal has not yet reached skeletal maturity. The layer of cartilage is faintly visible (arrowheads), showing excellent congruency with the surface of the device.

**31 weeks:** In four out of five animals, the HemiCAP resurfacing device was well fixed in the condyle with generous new bone abutting the screw threads, as confirmed by Faxitron radiographs of thick sections. Remodelling of the bone around the implant was noticeable with the mature bone being concentrated around the threads (Figure 93). Evidence of the holes from the k-wire used to implant the device were occasionally faintly visible, although the hole from the drill was completely remodelled. The original bone defect was still evident with mature bone partially filling the void space on one side at least (Figure 94). In some specimens, bone had grown into the cannulated region of the screw. Two of five implants had evidence of radiolucency around the lip underneath the articulating component and both of these also had calcified tissue above the level of the implant (Figure 94 and 95). One specimen in the 31 week group showed extensive bone osteolysis around the threaded portion of the device (Figure 95) although the implant appeared well fixed by manual manipulation.

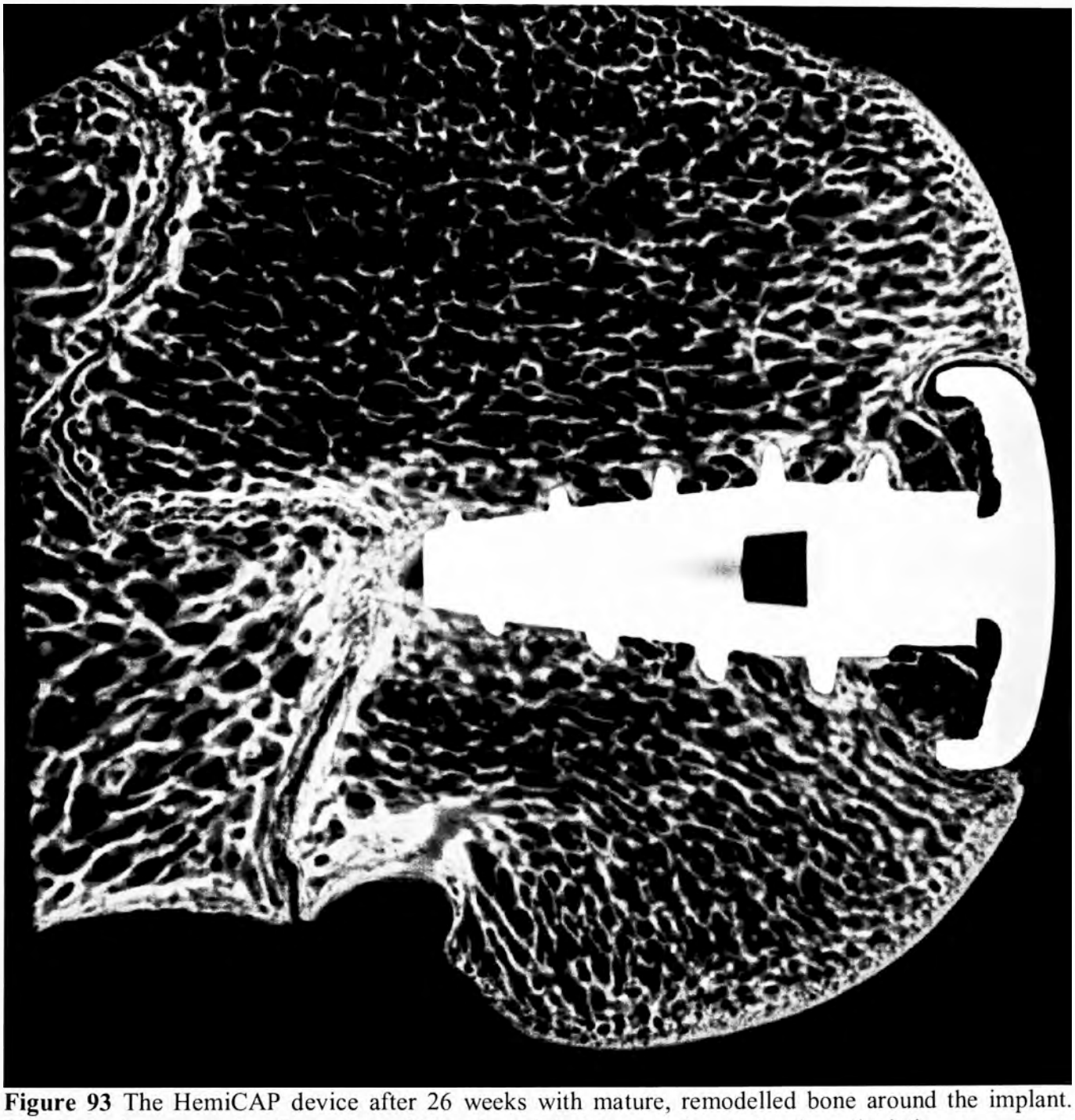

**Figure 93** The HemiCAP device after 26 weeks with mature, remodelled bone around the implant. This is the best example of new bone filling the original bone defect under the articulating component. A region of rediolucency is noted around the lip of the articulating component (top) and a small quantity of bone growing over the implant.

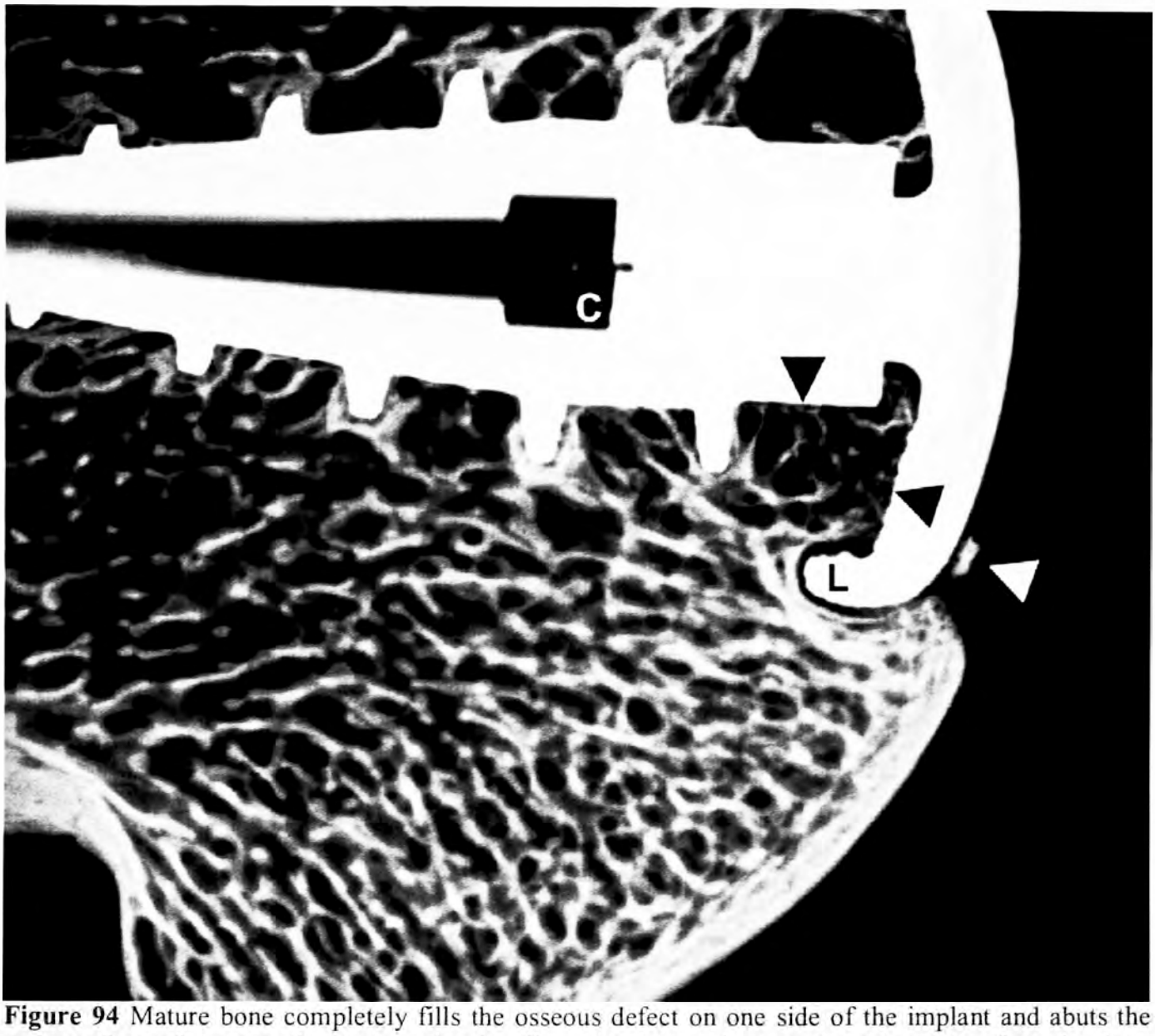


**Figure 94** Mature bone completely fills the osseous defect on one side of the implant and abuts the undersurface of the cap (black arrowheads). Bone is also evident on the other side of the implant, although to a lesser extent. Mature bone is concentrated around the screw threads indicating good fixation. A small quantity of calicified tissue is evident in the cannulated portion of the screw (C). A small island of calcified tissue was found above the level of the implant (white arrowhead) above a region of radiolucency around the lip of the articulating component (L).

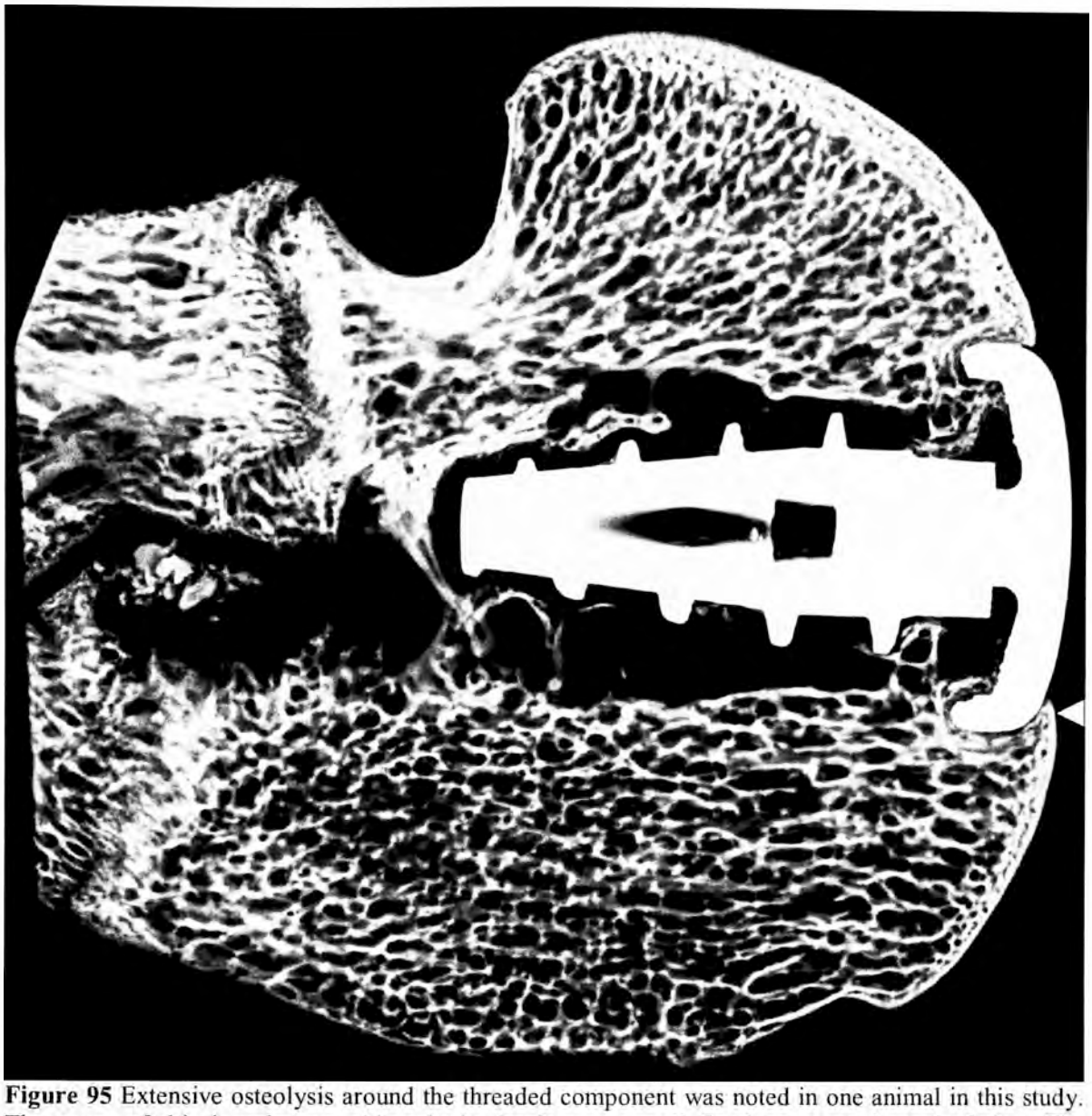

**Figure 95** Extensive osteolysis around the threaded component was noted in one animal in this study. The cause of this is unknown although the implant was well fixed on manual manipulation. The implant may possibly have subsided, as evidenced by the level of the subchondral bone plate above the surface of the device (arrowhead).

**Time zero:** A single specimen was prepared at time zero to assess the initial fixation of the implant and to visualise the size of the original osteochondral defect (Figure 96). The implant was well fixed with the threaded portion in firm contact with the cancellous bone. The osseous portion of the osteochondral defect extended approximately to the depth of the first thread. Minimal bone was abutting the underside of the articulating component at time zero, although the lip of the

articulating component had intimate contact with the subchondral and cancellous bone.

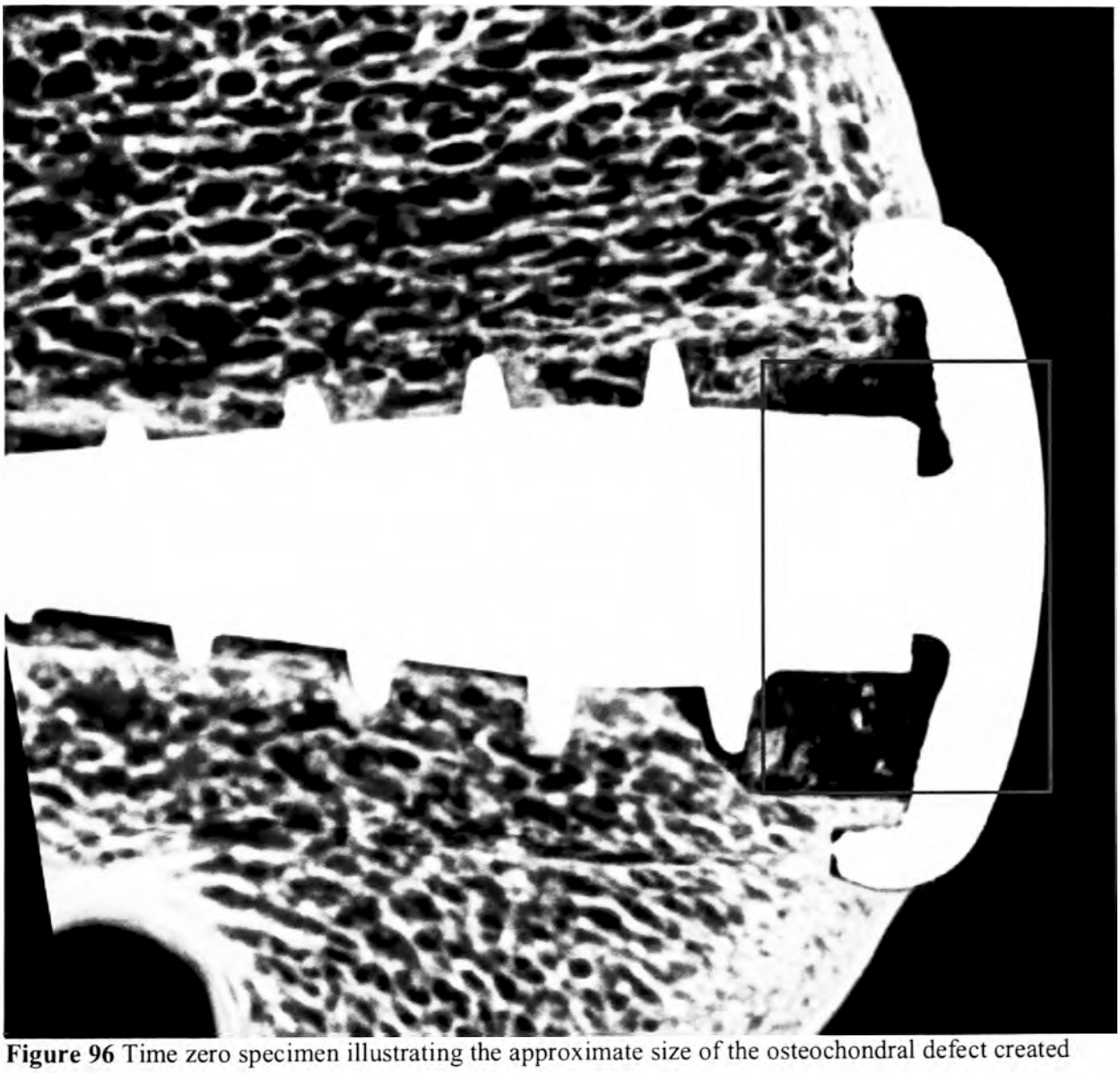

**Figure 96** Time zero specimen illustrating the approximate size of the osteochondral defect created

### 5.4.5 Histology

**5 weeks:** At five weeks, none of the empty femoral defects were healed. A small amount of fibrous repair tissue and blood clot were evident in the defect (Figure 97). Bone deposition was minimal, however, there was also no evidence of extensive resorption either along the walls or the base of the defects. The adjacent cartilage showed signs of degeneration such as extensive chondrocyte clustering, deep fissures and reduced Safranin-O staining intensity. Wall collapse and the subsequent flow of articular cartilage from the surface into the defect were noted (Figure 98). Due to the lack of repair tissue and bone healing, histological grading on the femur was not possible, so a score of zero on the O'Driscoll scale is assumed in this group.

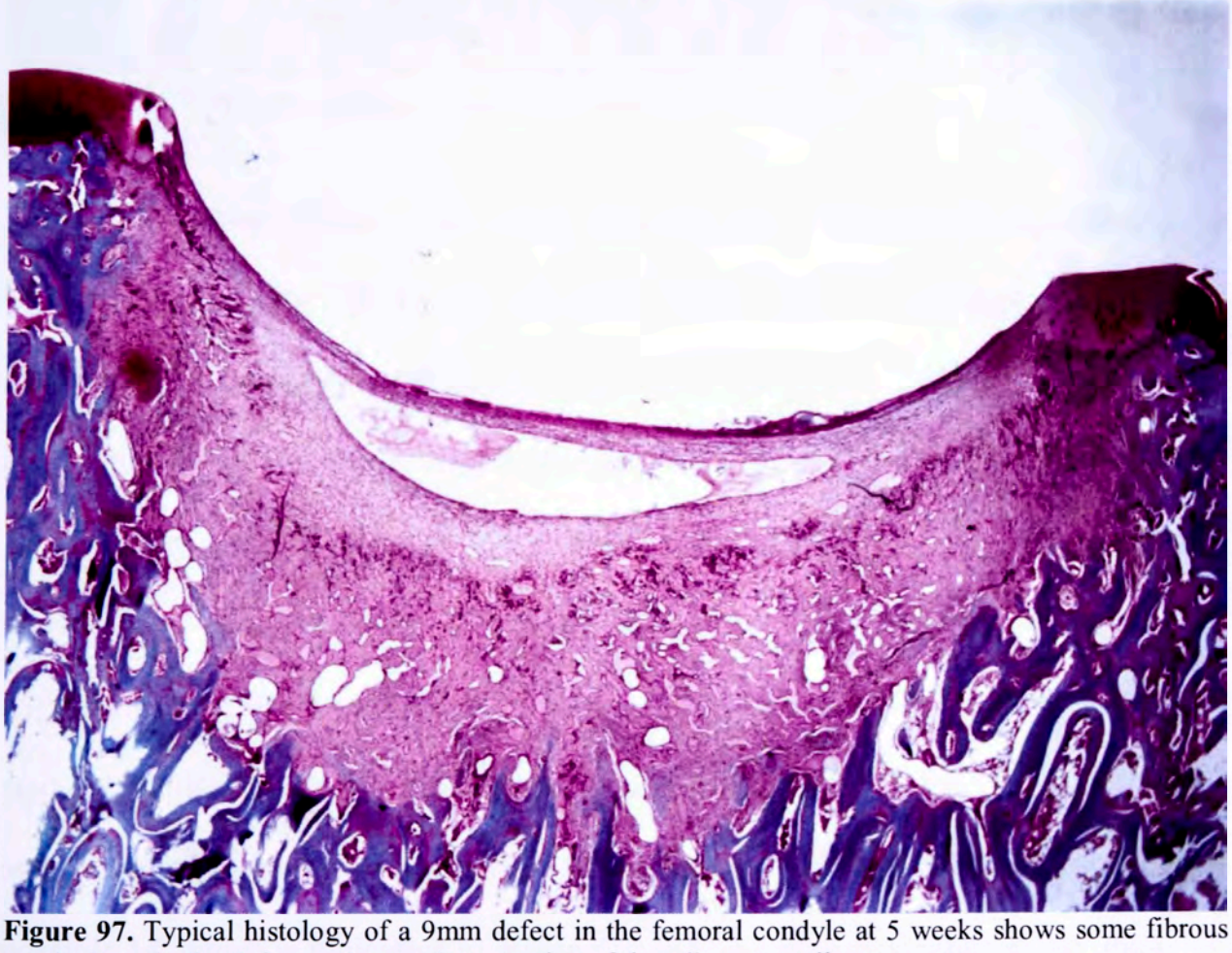

**Figure 97.** Typical histology of a 9mm defect in the femoral condyle at 5 weeks shows some fibrous repair tissue in the defect and some degeneration of the adjacent cartilage

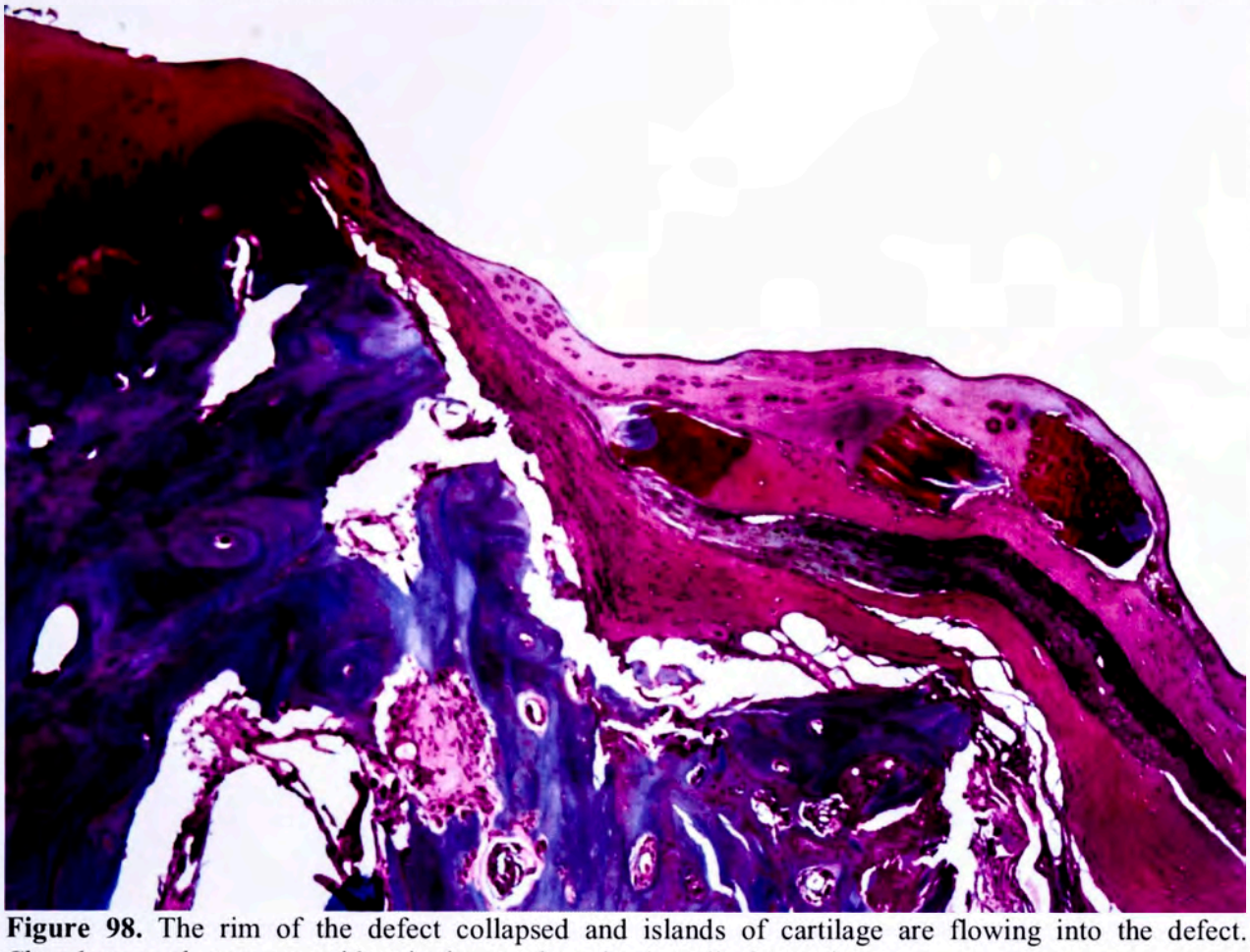

**Figure 98.** The rim of the defect collapsed and islands of cartilage are flowing into the defect. Chondrocyte clusters are evident in the poorly stained cartilaginous tissue.

The medial tibial condyles opposing the defect were minimally damaged after 5 postoperative weeks. In four out of six specimens the cartilage surface was occasionally interrupted by fissures extending to the middle or deep zone, although structural integrity was maintained (Figure 99). The other two tibiae showed some surface irregularities without deep fissures. Generally the appearance of the chondrocytes was normal, with only occasional localised regions of minor hypercellularity. Half of the specimens exhibited minor reduction on Safranin-O staining, whilst the other half showed intense, homogenous staining (Figure 100). The average Mankin score for the tibial sections at 5 weeks was 4.50 ± 1.3 out of a possible 14, which is indicative of minor damage on a structural and cellular basis.

**Figure 99** Typical tibial section at 5 weeks shows fissures extending beyond the superficial zone

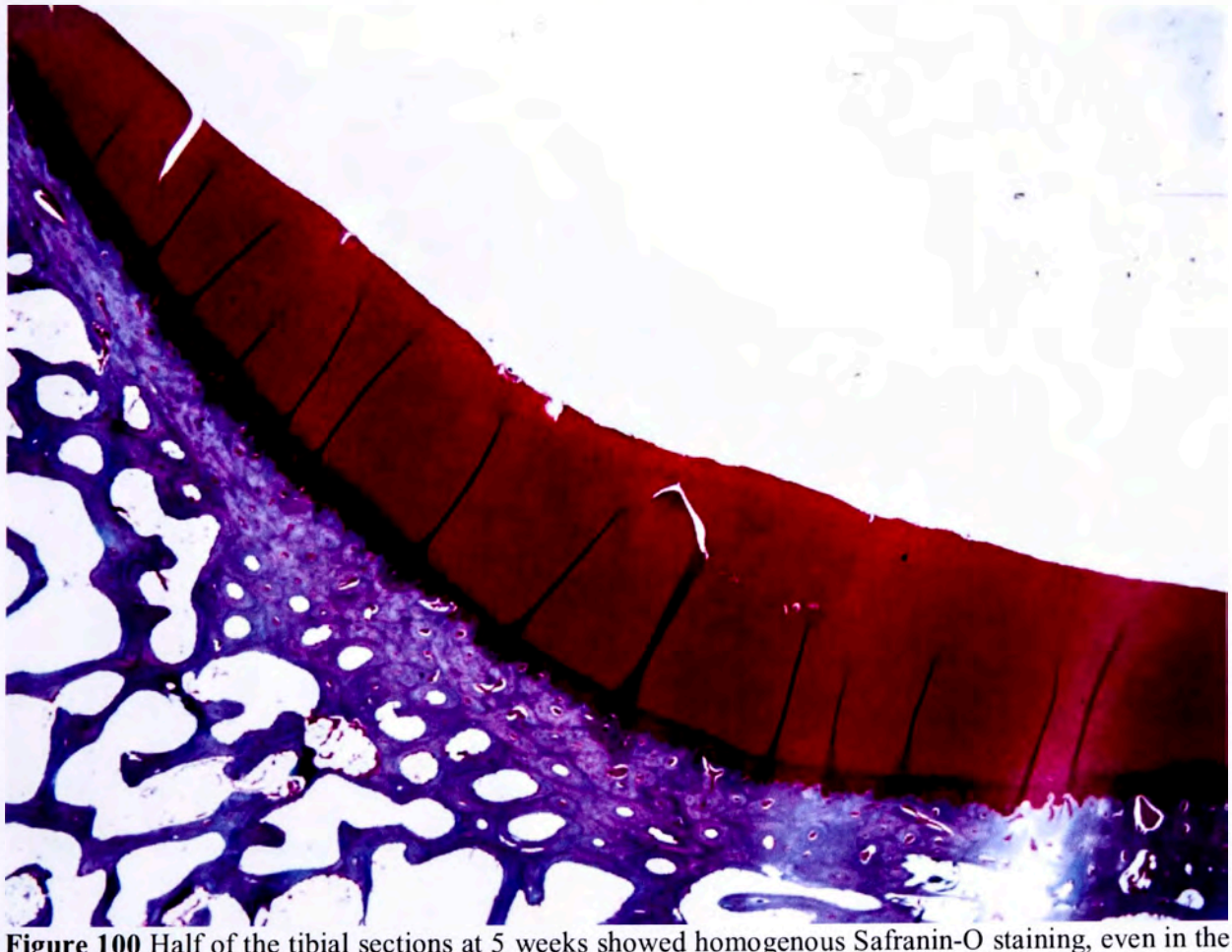

**Figure 100** Half of the tibial sections at 5 weeks showed homogenous Safranin-O staining, even in the presence of structural damage. This section also indicated possible subchondral bone thickening.

**11 weeks:** The empty femoral defects at 11 weeks were healed with a high degree of variability. Three of the defects (60%) were partially filled with repair tissue (Figure 101), one of which was almost to the level of the adjacent cartilage, although the repair tissue was fibrous in both the osseous and chondral regions of the defect (Figure 102). The remaining two defects (40%) were essentially empty (Figure 103). Reconstitution of the cancellous and subchondral bone was not noted and three of five specimens showed evidence of bone resorption along the walls of the defect (Figure 104). Commonly, chondrocyte clustering and loss of Safranin-O staining was noted in the adjacent cartilage (Figure 105). Histological grading using the O'Driscoll scale revealed average scores of 1.80 ± 1.5 for the empty defects, which indicates very low quality repairs across the board (Figure 111).

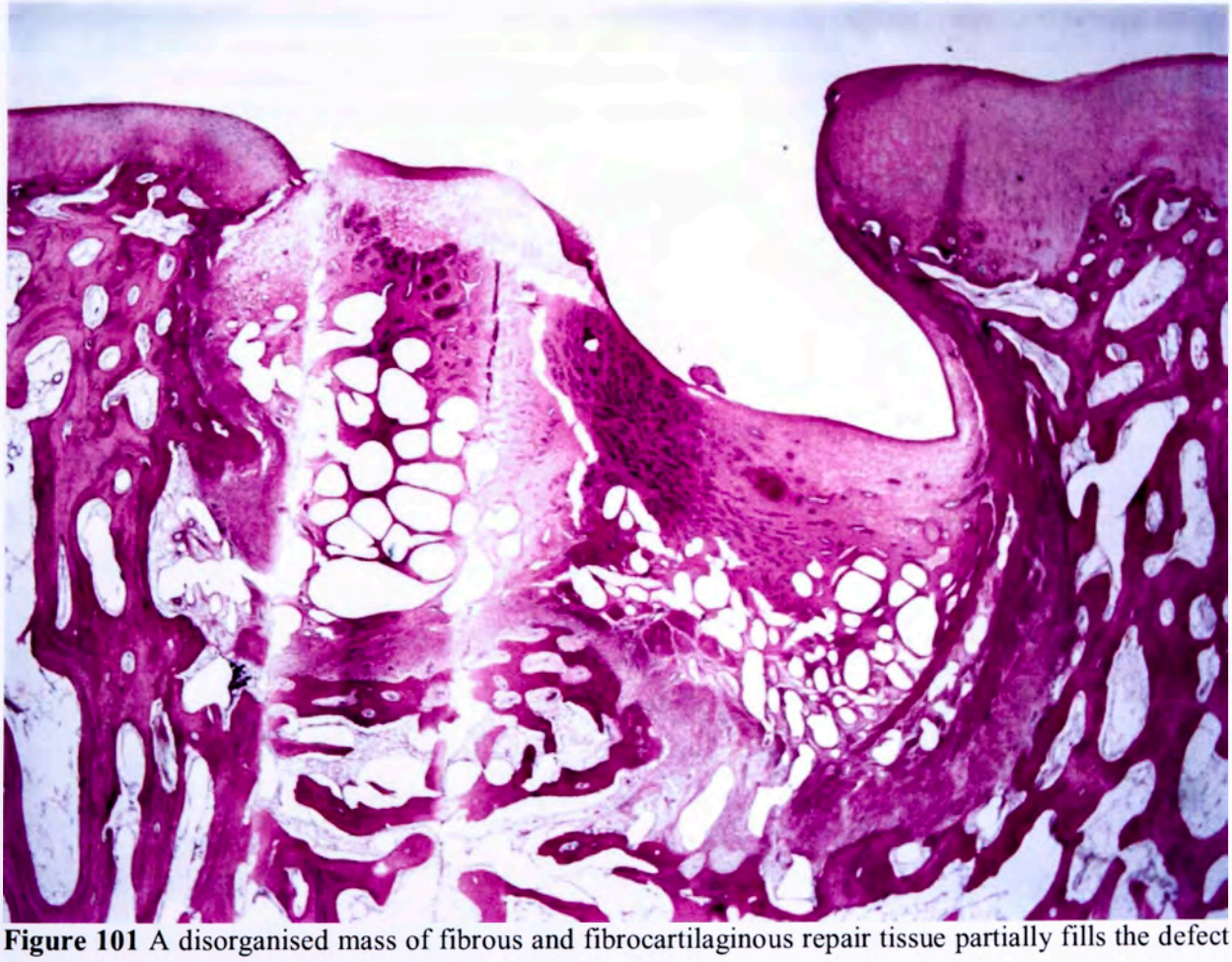

**Figure 101** A disorganised mass of fibrous and fibrocartilaginous repair tissue partially fills the defect space

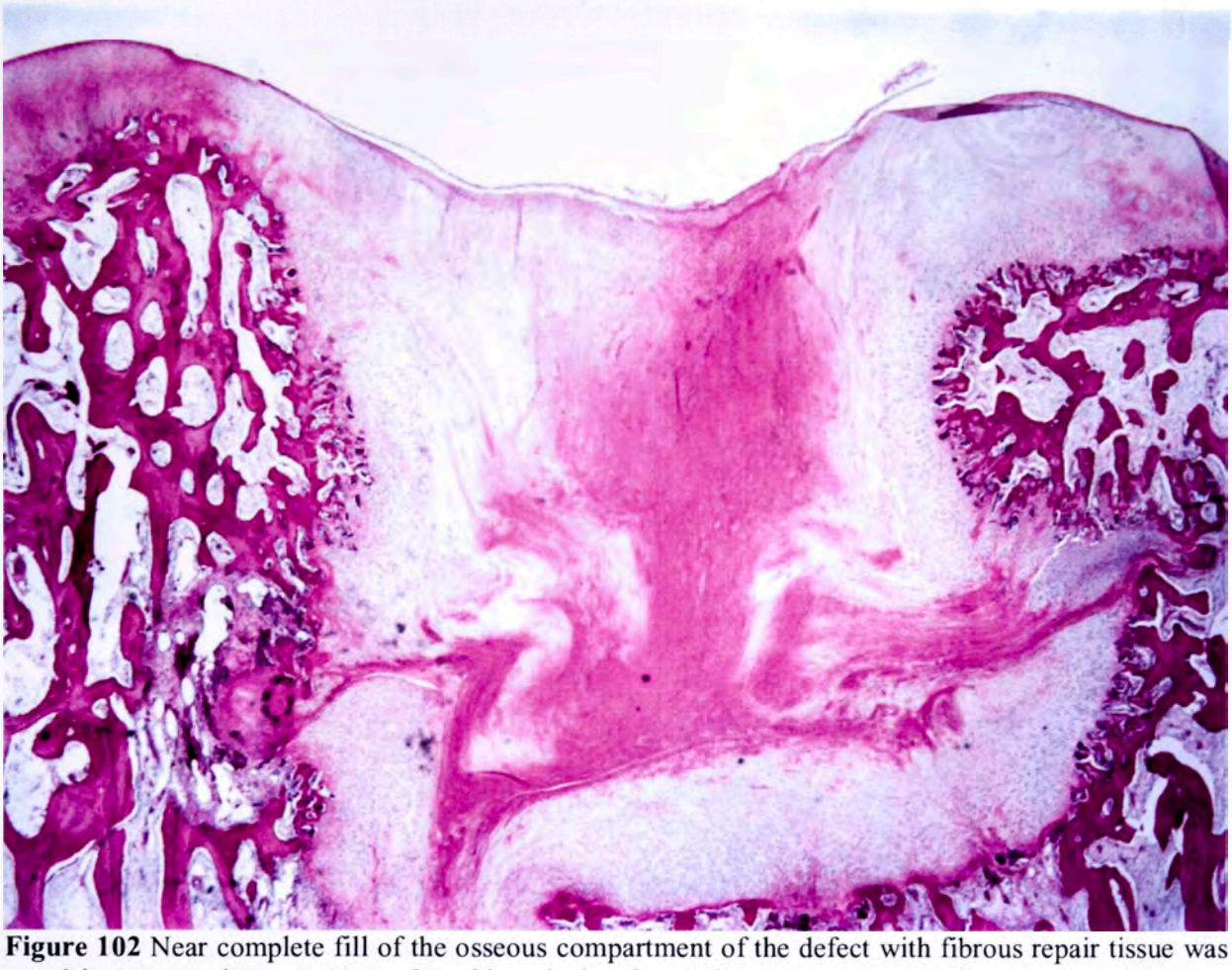

**Figure 102** Near complete fill of the osseous compartment of the defect with fibrous repair tissue was noted in one specimen at 11 weeks, although the chondral compartment remains mostly void space. Also obvious is intensive osteoclastic activity on the walls of the defect.

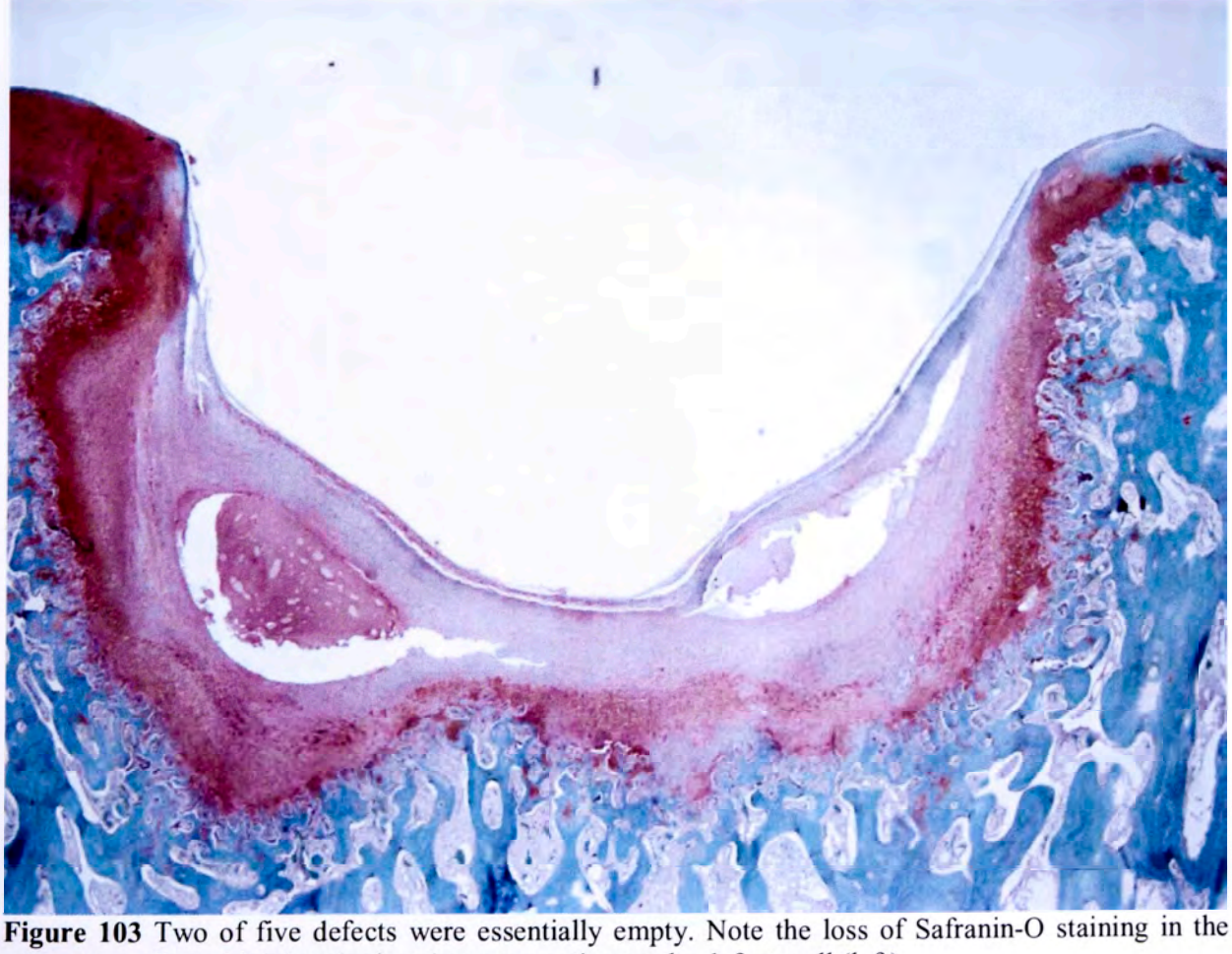

**Figure 103** Two of five defects were essentially empty. Note the loss of Safranin-O staining in the adjacent cartilage (right) and minor bone resorption on the defect wall (left)

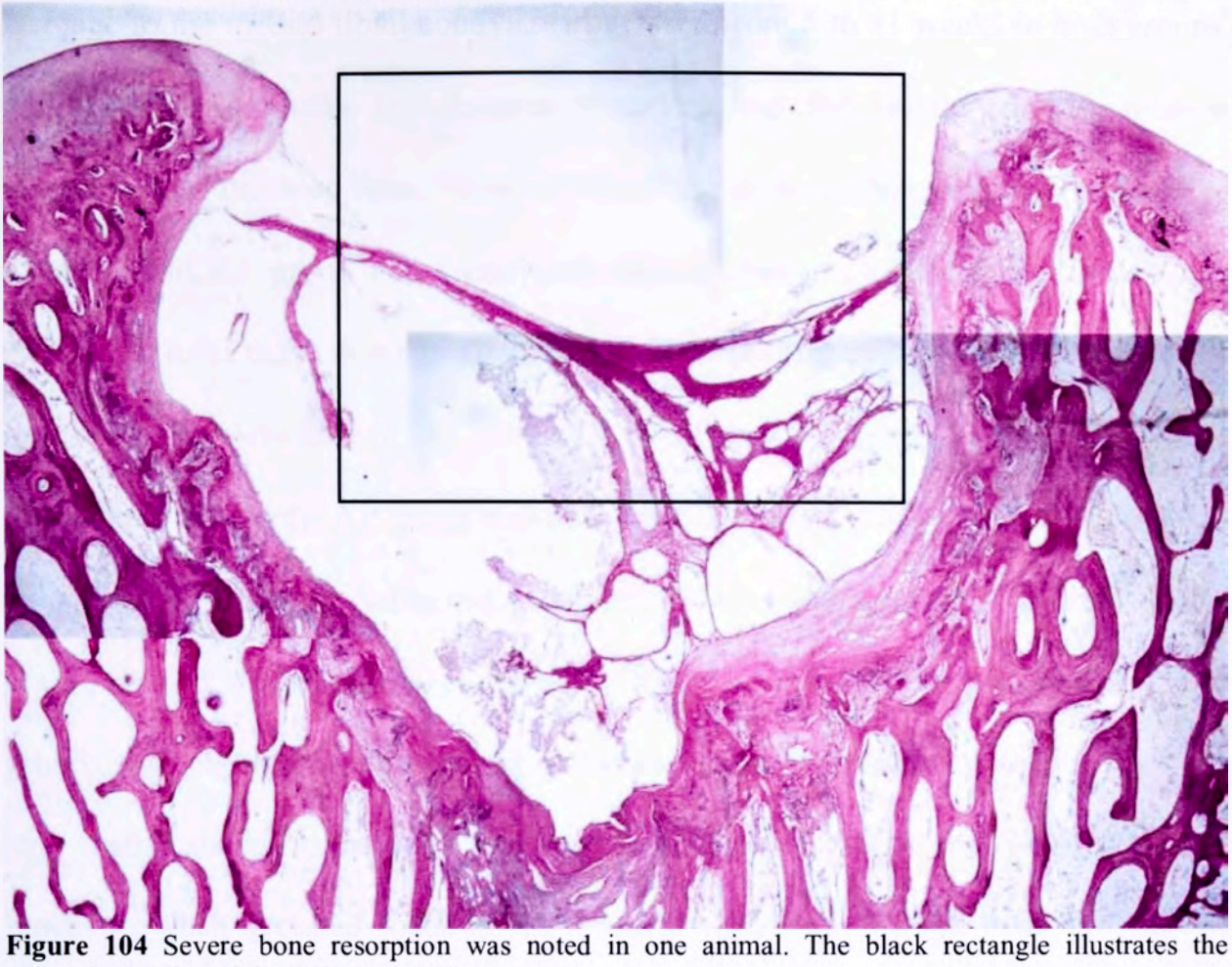

**Figure 104** Severe bone resorption was noted in one animal. The black rectangle illustrates the approximate size of the defect created.

**Figure 105** Extensive chondrocyte clustering accompanied by regional loss of Safranin-O staining in the native cartilage adjacent to the defect

Damage to the medial tibial condyles progressed from 5 to 11 weeks in both groups. All tibiae at 11 weeks had fissures extending into the middle zone, with most extending into the deep zone. Three of five tibiae in the defect group and one of five in the HemiCAP group had significant cellular changes, as noted by chondrocyte clusters. Two of these tibiae in the defect group were also accompanied by regions of hypocellularity which was not noticed in the HemiCAP group at this time. Three tibiae from the HemiCAP group and four from the defect group showed moderate to extensive reduction in Safranin-O staining. Histological grading with the Mankin scale revealed scores of 6.87 ± 2.4 and 7.67 ± 1.76 for the HemiCAP and defect groups respectively. The HemiCAP group and the empty defect group did not have any significant differences between them at the 11 week time point (P=0.28), however, when grouped together there was a significant change from the 5 week group (P=0.002).

**31 weeks:** The empty femoral defects at 31 weeks were filled with progressively more repair tissue than the 5 or 11 week groups. One of five defects healed with hyaline cartilage overlying reconstituted subchondral bone, although the cartilage showed extensive chondrocyte clustering suggestive of early degeneration (Figures 106 and 107). A large cyst was obvious deep to the defect, and much deeper than the surgically created defect. One of the remaining four defects had partially reconstituted the subchondral bone and an irregular surface of hyaline cartilage was present (Figure 108). The remaining three defects were poorly repaired, albeit slightly better than the 11 week group. Three of five specimens showed cellular degeneration in the adjacent cartilage in the form of moderate to severe hypocellularity, chondrocyte clustering and/or reduction in Safranin-O staining. Histological grading using the O'Driscoll

scale revealed an average score of 8.50 ± 6.6 out of a possible 27 for the empty defects.

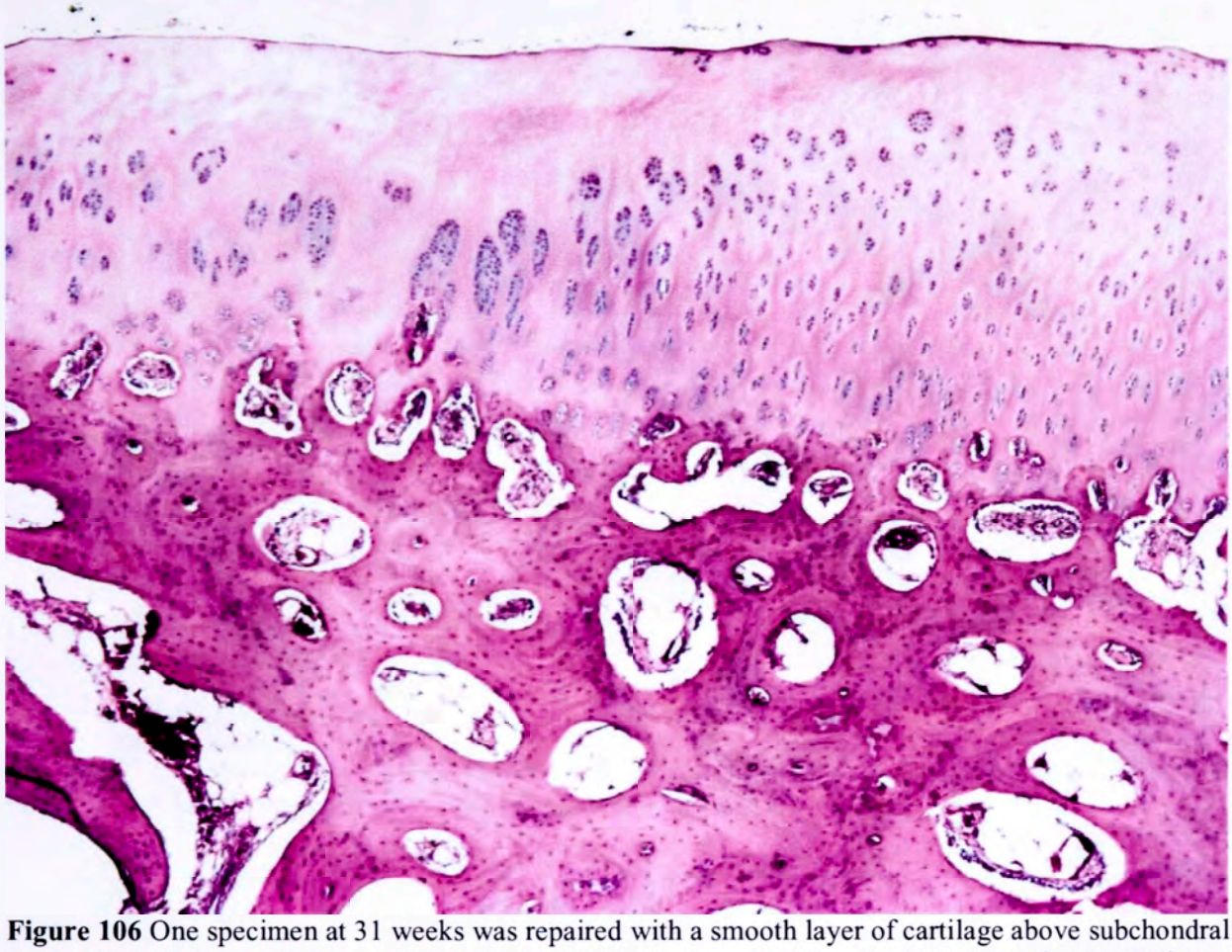

**Figure 106** One specimen at 31 weeks was repaired with a smooth layer of cartilage above subchondral bone, although signs of degeneration are noted as extensive chondrocyte clustering. Blood vessels are also seen to penetrate from the subchondral bone and the tidemark is not re-established. This image is taken from the centre of the defect.

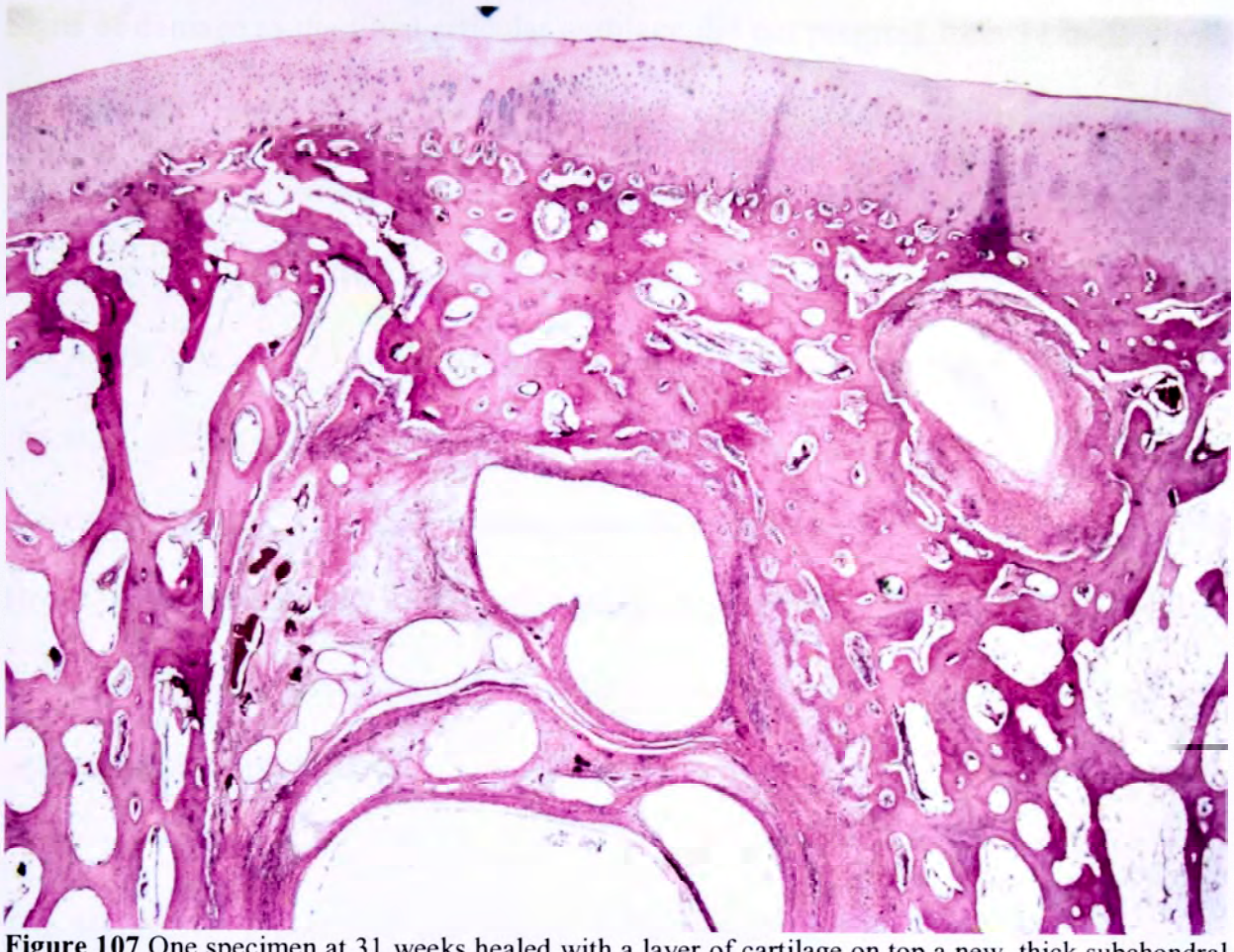

**Figure 107** One specimen at 31 weeks healed with a layer of cartilage on top a new, thick subchondral bone plate. A large cyst is obvious in the bone beneath the defect.

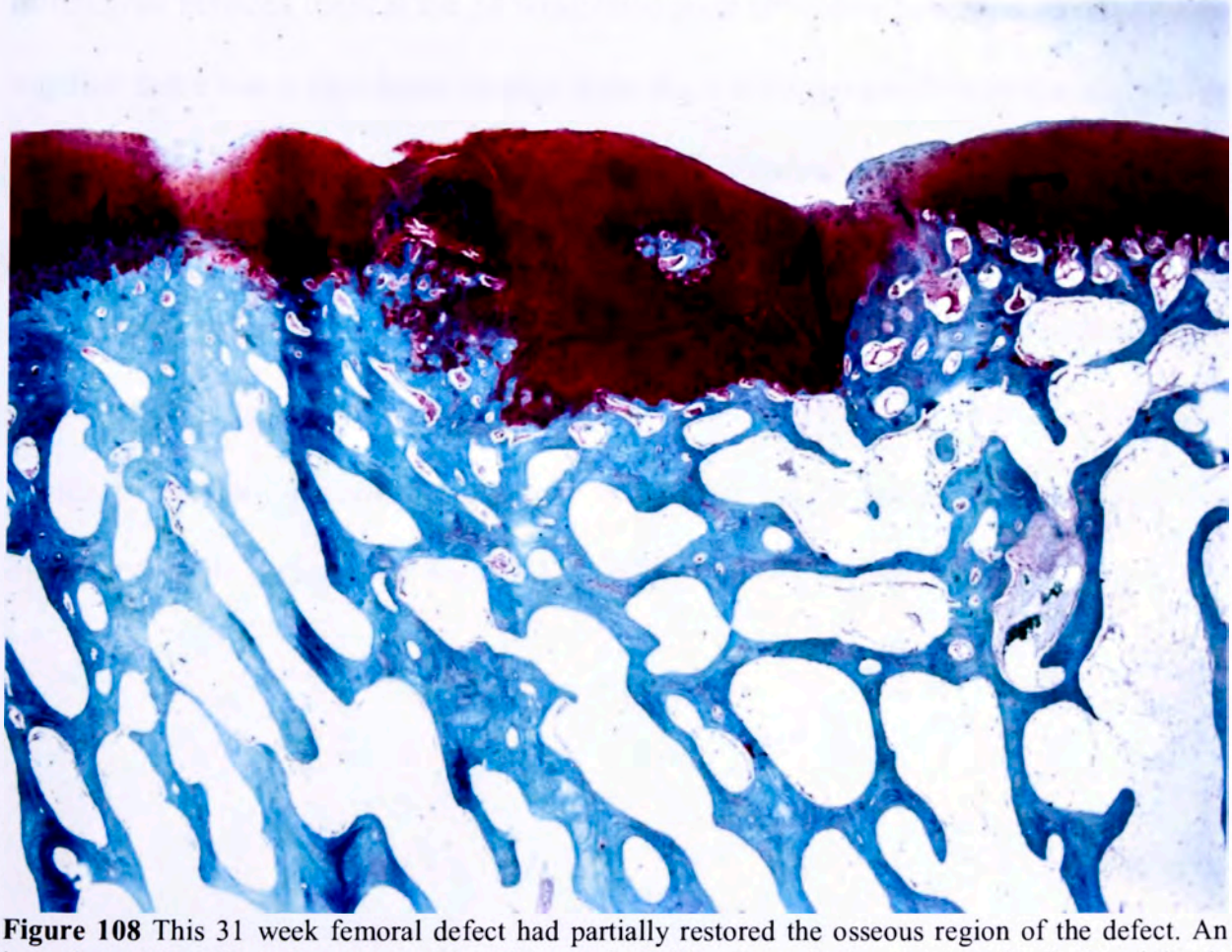

**Figure 108** This 31 week femoral defect had partially restored the osseous region of the defect. An irregular cartilage layer is present with an island of calcified tissue in the centre. Safranin-O staining is modestly reduced on the right hand side of the image.

Signs of damage to the tibial articular cartilage did not progress from 11 to 31 weeks in either the HemiCAP or the defect group. Rather, the damage appeared to be partially recovered in both groups. The structural damage to the cartilage was similar to the previous group, with one or more fissures extending into the deep zone in most specimens (Figure 109). Cellular signs of degeneration were noted in one of five specimens in the HemiCAP group and two of five in the defect group. Moderate to extensive loss of Safranin-O staining was likewise noted in one specimen in the HemiCAP group and two in the defect group (Figure 110). Histological grading with the Mankin scale revealed scores of $5.87 \pm 1.8$ and $6.07 \pm 2.27$ for the HemiCAP and defect groups respectively.

The HemiCAP group and the empty defect group did not have any significant differences between them at the 31 week time point ($P=0.44$), however, when grouped together there was a significant change from the 5 week group ($P=0.045$) but not from the 11 week group ($P=0.08$), although it may have reached significance with increased sample size. Hence the trend observed by histological grading of the tibia was that damage was indeed detected 5 weeks after the introduction of a defect on the femur, this damage progressively increased out to 11 weeks (6 weeks with the HemiCAP device or without it) and then began to recover by 31 weeks (Figure 112). No differences were detected between the HemiCAP and empty defect groups.

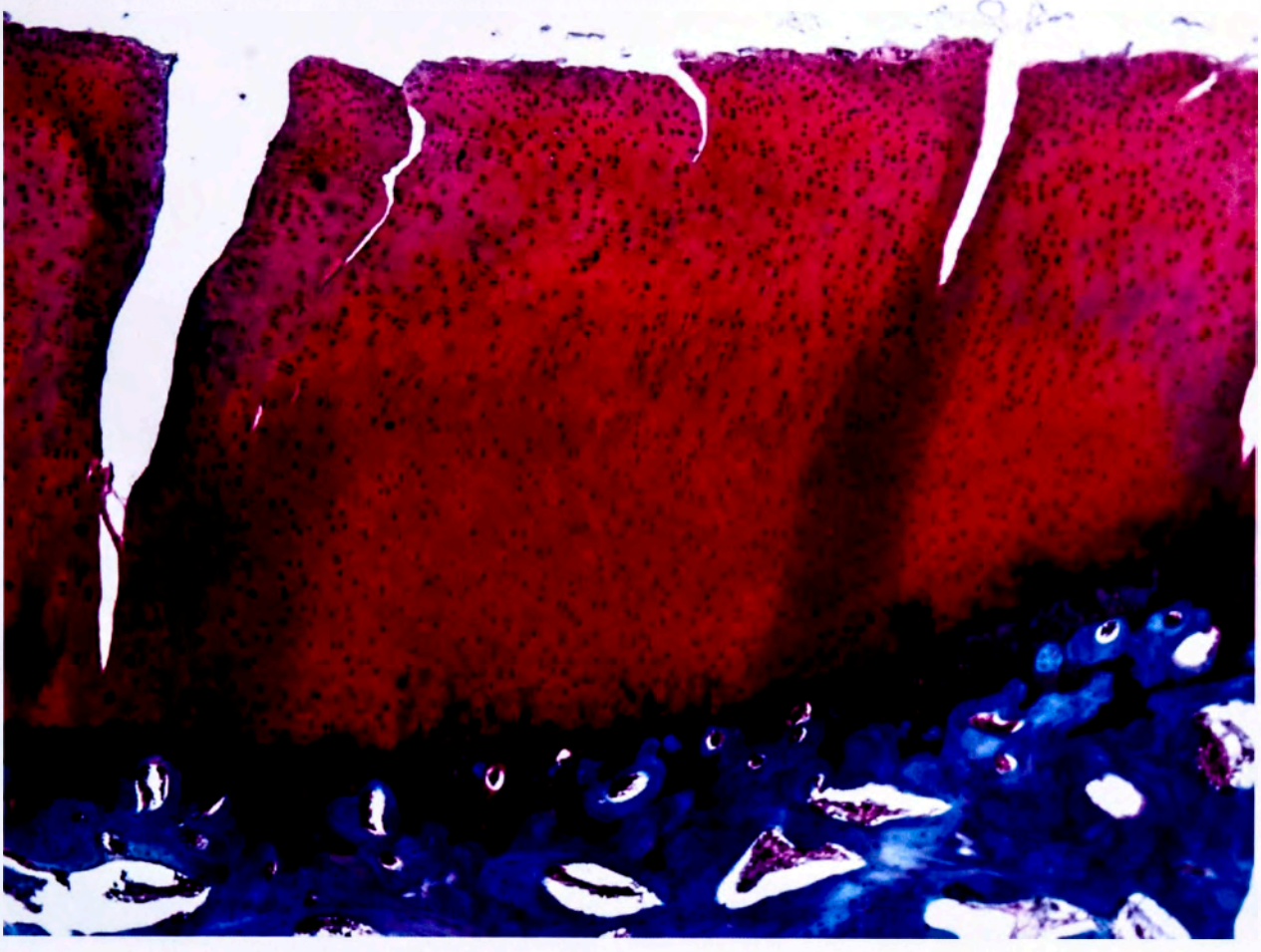

**Figure 109** Structural damage in the form of fissures extending into the middle and deep zones accompanied by moderate hypercelluarity in a tibia from the 31wk HemiCAP group. Safranin-O staining intensity is essentially normal, with some very minor reduction in intensity along the large fissure.

**Figure 110** Extensive loss of Safranin-O staining accompanied by chondrocyte clusters and a large region of hypocellularity in a tibia from the 31wk defect group.

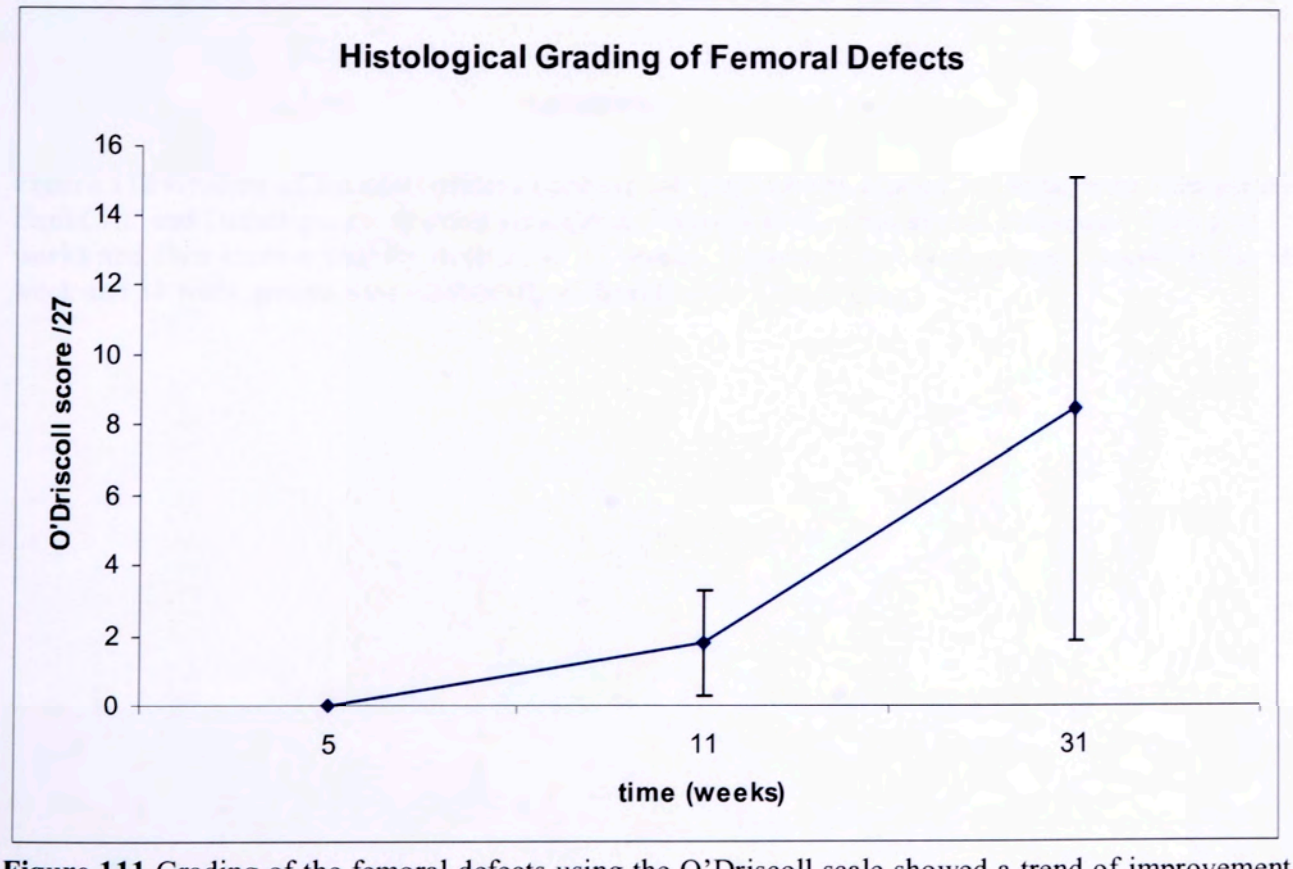


**Figure 111** Grading of the femoral defects using the O'Driscoll scale showed a trend of improvement out to 31 weeks, although with large variation in the results as shown by the large standard deviations

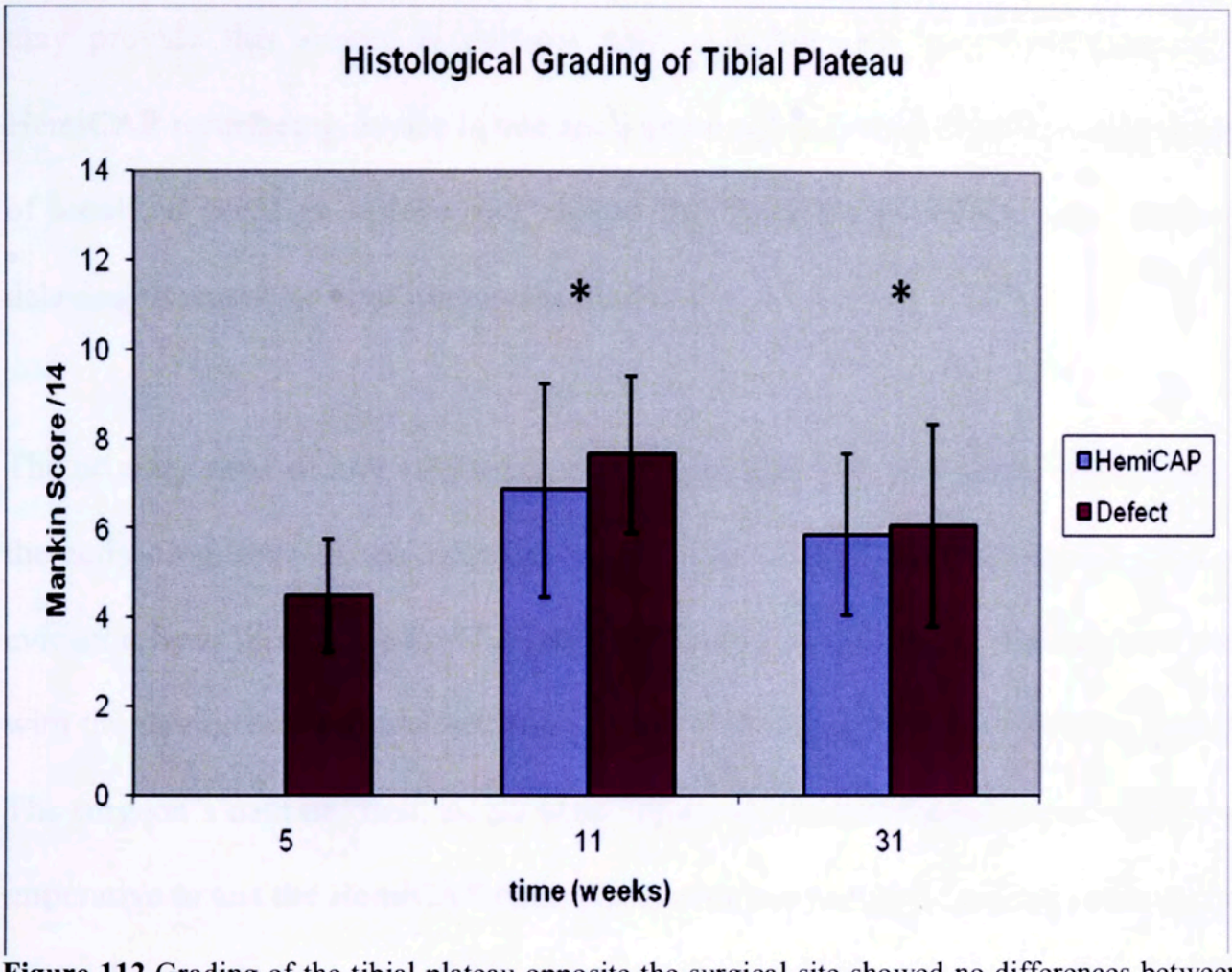


**Figure 112** Grading of the tibial plateau opposite the surgical site showed no differences between the HemiCAP and Defect groups at either time point. Damage to the tibia tended to increase from 5 to 11 weeks and then recover slightly from 11 to 31 weeks. * denotes that when grouped together, the 11 week and 31 week groups were statistically different to the 5 week group.

## 5.5 Discussion

A subset of patients exists that are considered to be too old for biological treatment of focal full thickness cartilage lesions, yet too young for end-stage treatments such as total knee arthroplasty. The recent introduction of partial joint resurfacing devices may provide this subset of patients with a medium to long term solution. The HemiCAP resurfacing device is one such treatment that aims to reduce the symptoms of localised cartilage lesions and restore the functionality of the joint, meanwhile delaying the need for total joint arthroplasty.

The primary aims of any joint surgery are to reduce pain and improve mobility, and the early clinical evidence seems to be in favour of the HemiCAP device. Anectodal evidence from the early adopting orthopaedic surgeons suggests that patients treated with the device recover uneventfully and are able to quickly return to daily activities. The surgeon's oath of "first, do no harm" must also be remembered and therefore it is imperative to test the HemiCAP device to ensure that the hard metallic surfaces do not cause increased damage to the counter-bearing surfaces of the tibia. It is not economic, nor moral, to implant a device that reduces pain on one condyle at the expense of accelerated degeneration on another because this degeneration will in turn lead to increased pain and a reduction in joint mobility. Hence, the oath of "do no harm" would be broken.

The two modalities that are available to test the efficacy of the HemiCAP device are preclinical (animal) models and clinical results. Unfortunately we are unable to gather clinical outcomes such as patient-reported pain and quality of life scores from animal models, and we are seldom able to collect sufficient histological data from human

patients to adequately document the success or failure of a device. For this reason, it will be necessary to collect clinical outcomes from human patients and to gather biological data from animal model endpoints. Generalised clinical outcomes may be collected from patients using visual analogue scales (VAS) for the level of pain, or the short form 36 (SF-36) for measurement of quality of life. Several other clinical scales are also available such as the Knee Score, the Oxford Knee Score and the Bristol Knee Score. In fact, the early clinical studies for the HemiCAP partial resurfacing device were conducted in Australia, and 90 partial resurfacing devices have been implanted through the end of 2007. The National Joint Replacement Registry Annual Report 2008 (Australian Orthopaedic Association) reports a revision rate of 16.5% after 2 years with HemiCAP, compared to 4.5% for unicompartmental knee replacements and 2.1% for total knee replacements. This may imply that the early clinical results of the HemiCAP device are inferior to other joint replacement devices, however, without in depth analysis of the clinical factors (such as patient demographics, diagnosis for surgery, etc.) it is not possible to comment, and it is outside of the scope of this thesis to do so. The current study focuses solely on the research endpoints from an ovine model and one limitation is that VAS and SF-36 data could not be collected from the sheep.

This study has used the traditional endpoints of radiographs and histology to compare the effects on the counter-bearing surfaces of the tibia and meniscus from chronic osteochondral defects treated with a metallic resurfacing device or osteochondral defects that were not given any treatment. In addition, a novel mechanical indentation device was employed to compare the mechanical properties of the articular cartilage

and a micro tomographic analysis was conducted on the tibial subchondral and cancellous bone opposite the surgical site.

The first interesting finding is that the 9mm osteochondral defects on the femur were relatively well healed after 31 weeks. This is in stark contrast to the 6mm defects presented previously in Chapter 3 in which a similar degree of healing was not noted until 52 weeks postoperative. These defects were created with the same instrumentation and in the same weight bearing location, so the explanation for a larger defect healing more quickly than a smaller defect is difficult to comprehend. Perhaps one possibility is that the larger defects suffered more from defect wall collapse or from adjacent cartilage flowing into the defect, giving a false impression of newly formed tissue in the defect, although it is difficult to make such claims from the histology. Similarly to the previous study with 6mm defects, deep cysts were discernible in femora that otherwise looked well healed after 31 weeks. The cancellous and subchondral bone were generally reconstituted above the cyst, so it is not known whether these cysts would eventually be infiltrated with new bone, or if they would remain indefinitely. The same result was found in the Jackson goat model of spontaneous healing.

Macroscopic inspection of the tibial cartilage surface and the menisci revealed no significant differences between the two groups (HemiCAP and empty defect) at any time point, which is encouraging information supporting the claim that the HemiCAP device does not cause any greater damage to the joint as a whole when compared to not treating the defect. Another interesting finding is that osteophyte formation was found on most medial femoral condyles at both 11 and 31 weeks (indicating

significant changes in the profile of load distribution through the condyle), however, they were seldom found on the tibial condyles. This could therefore be an indicator that the changes to the load distribution on the tibia have not reached the required threshold to initiate bone remodelling.

Structural damage to the articular cartilage on the tibia was noted at 5 weeks and progressed to 11 weeks. At 5 weeks, the damage was not normally associated with changes to the intensity of Safranin-O staining indicating that the damage to the cartilage might be traumatic rather than being degenerative on a cellular basis at this early stage. The damage to the cartilage was accompanied by a reduction of Safranin-O staining at 11 and 31 weeks, indicating a reduction in concentration of proteoglycans. Hence, the traumatic injury to the cartilage is followed by degenerative changes. A reduction in proteoglycan concentration is problematic in cartilage because the interaction of proteoglycans, the extracellular matrix and the entrapped fluid provide the tissue with its compressive strength and load bearing capacity.

Radin and Rose reported that changes in the subchondral bone can lead to the progression of damage in the overlying articular cartilage layer (Radin & Rose 1986a). In particular they highlighted that repetitive loading above a defined joint force can lead to increased stiffness in the subchondral bone which can then influence the health of the cartilage layer. Where Radin and Rose have reported that changes in the subchondral bone can lead to damaged cartilage, the findings in this thesis also support the opposite pathway; that damaged cartilage can lead to changes in the subchondral bone. This has also been reported by Cake, et al who found significant

changes in the subchondral bone of the tibia 6 months after a meniscectomy was performed (Cake et al. 2000).

It must be noted that the HemiCAP device is not the only device that has been used as a partial joint resurfacing device. In a case study of one patient, Hodge found that a cobalt chrome device (similar to the HemiCAP device) implanted in the distal femoral condyle had good clinical scores after 30 years in vivo. Given the substantial differences in elastic modulus for cobalt chrome and articular cartilage (approximately 200GPa vs approximately 1MPa) it comes as a surprise that the metallic implant can perform adequately as a cartilage replacement. For that reason, implants with mechanical properties more similar to articular cartilage have also been employed as cartilage replacements. One such resurfacing implant made of a cylindrical plug of polyvinyl alcohol hydrogel was shown to give improved clinical knee scores after 6 months, but not by 12 months (Lange et al. 2006). Inadequate anchoring of the implant within the bone and breakdown of the material were two of the reasons for failure of this resurfacing device.

Perhaps the clinical success of the metallic resurfacing device is partly due to the overgrowth of neocartilage that was documented both in the present study and the previous study by Kirker-Head. This neocartilage was noted in the present study at the earliest time point of 6 week post-implantation and progressively increased in area and volume out to 26 week pos-implantation of the HemiCAP device. This extensive growth of cartilage is above and beyond the quantity of neocartilage produced in the empty defects and is most likely due to the load sharing between the metallic device and the adjacent cartilage. In comparison, the empty defect does not allow any form

of load transfer by nature of the fact that it's empty and there are no structures to carry any load. It is not known if the neocartilage would eventually completely overgrow the metallic device, however, this had not occurred by the longest time point of 26 weeks in the current study and 52 weeks in the Kirker-Head study.

The results of this study show that a metallic resurfacing device implanted in the medial femoral condyle generally has a similar impact on the tibial cartilage and bony tissues when compared to an untreated osteochondral defect. The finding that knees with untreated defects and knees treated with the HemiCAP device were not significantly different from a histological viewpoint suggests that the HemiCAP device did not protect the tibial cartilage from damage in this model. However, at the least, the HemiCAP device does not accelerate degeneration of the joint.

It is important to note that the model used in this study is not perfectly analogous to the defects treated clinically by this type of device. Typically, the HemiCAP device would be used to treat a focal chondral defect and not usually an osteochondral defect and therefore the results from this study should not be directly extrapolated to the clinical condition. However, the osteochondral defect in this study was selected based on the previous work (Chapter 3-5) that showed an osteochondral defect in the femur could initiate degradation of the tibial cartilage. Since the HemiCAP had already previously been evaluated in a pristine knee, our goal in this study was to evaluate it in a challenging model of pre-existing trauma to the tibial cartilage.

This study is limited by not being able to measure clinical outcomes, such as reduction in knee pain. In the sheep model, it is not possible to measure the extent of

pain relief that the HemiCAP device may, or may not, provide. Although macroscopic, histological and radiographic data from this study suggest that it does no further harm compared to not treating the defect at all.

An important next step in validating the efficacy of the HemiCAP device would be to conduct a clinical trial, which Arthosurface initiated in September 2005. The clinical trial will gather patient reported pain scores with a final follow up after 24 months. Preliminary data was presented at the American Academy of Orthopaedic Surgeons annual meeting in San Diego in 2007 which reported 87% improvement in pain and 84% improvement in function at an average follow up of 11 months. If the HemiCAP device does provide pain relief and restoration of joint mobility, as suggested by the preliminary clinical data, then it might be a successful bridging prosthesis for those patients who fall in the age bracket of 40-50 years old who are still too young to receive a total joint replacement.

# 6. Method for micro computed tomographic analysis of tibial subchondral bone plate and cancellous bone

## *6.1 Equipment*

Micro computed tomography (microCT) was performed with a Skyscan model 1072 high resolution device (Skyscan, Belgium). In this application, the Skyscan 1072 is operated with an 80kV x-ray source running at a current of 100μA, with a digital camera of 1024x1024 resolution. Together, three dimensional data may be captured with a resolution of the order of 5μm.

The device functions by placing the specimen on a stage in between the x-ray source and the camera. Magnification of the specimen is achieved by decreasing the distance between the x-ray source and the specimen, and thus increasing the distance between the specimen and the camera. Three dimensional data is acquired by rotating the specimen stepwise through 180 or 360 degrees and taking x-ray exposures at each increment. Typically, angle increments of either 0.45 or 0.9 degrees are selected, giving a total of 400 or 200 images respectively, with the typical 180 degree specimen rotation. These "shadow images" are akin to regular radiographs, although the computing hardware and software is able to collect the images from each angle and reconstruct them into cross sectional images. The resulting cross sectional images can then be used to reconstruct a three dimensional model. The minimum scan time for the Skyscan 1072 is approximately 55 minutes.

## *6.2 Sample preparation*

Proximal tibiae from the sheep hind leg were harvested, carefully removing the menisci and other soft tissues. The medial tibial condyles were isolated and trimmed to fit inside a specimen container with diameter 25mm (Figure 113). This was

approximately the largest specimen that the x-ray chamber could accommodate. The specimens were fixed in cold phosphate buffered formalin solution prior to microCT analysis to maintain the cellular appearance in subsequent histological analyses. All specimens were scanned in solution to avoid dehydration and to reduce heat build up from the constant x-ray source during the scan.

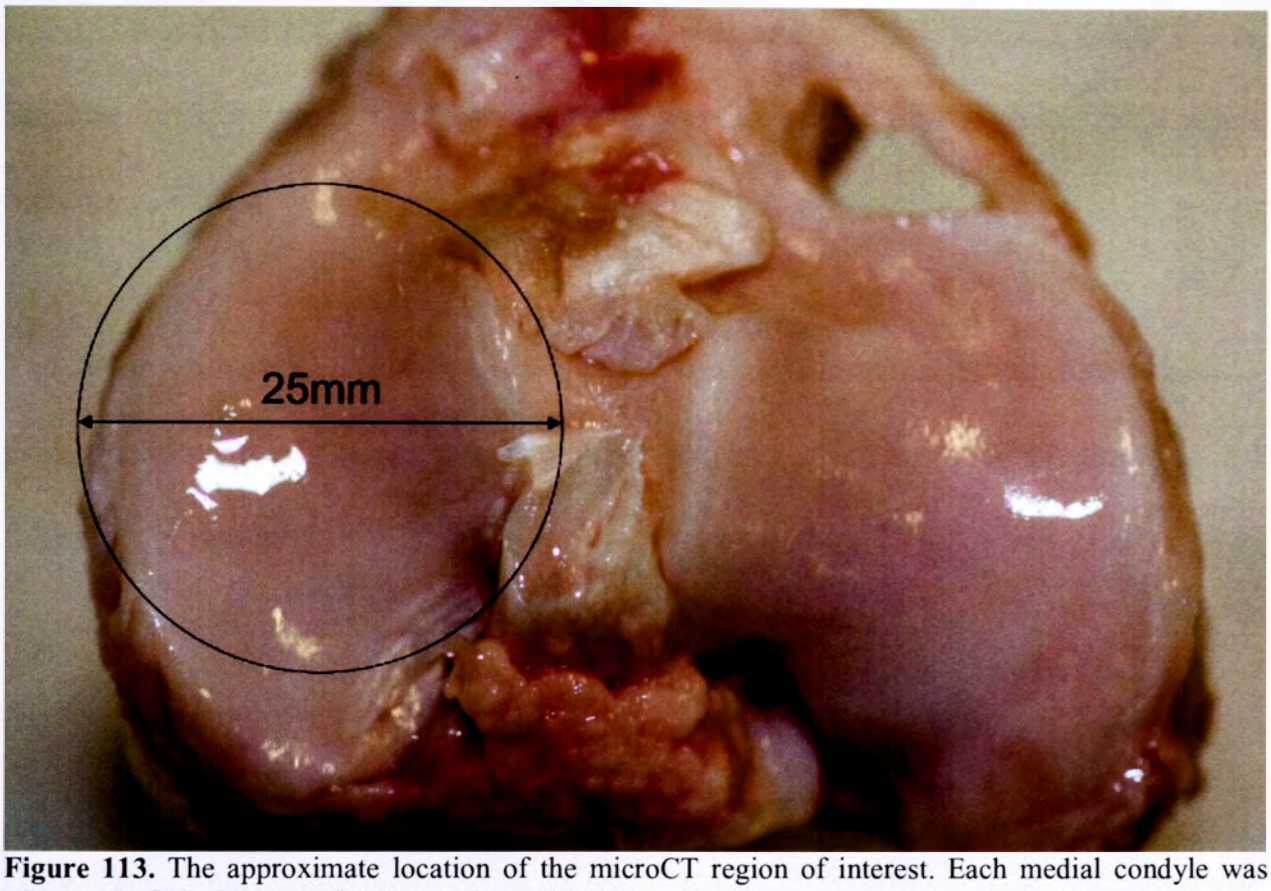


**Figure 113.** The approximate location of the microCT region of interest. Each medial condyle was trimmed to fit inside a specimen container with 25mm diameter.

## *6.3 Scan protocol*

Medial tibial condyle specimens were loaded into the specimen containers and covered with physiological buffered saline solution. The specimen must fit tightly within the specimen container so that there is no relative motion between the stage and the specimen as the stage rotates. When a tight fit was not achieved first go, a small piece of radiotransparent material was wedged between the specimen and the wall of the container. The specimen containers were then glued to the specimen stage

using double-sided carbon tape for the same purpose of avoiding relative motion as the stage rotates.

Specimens were scanned at the maximum energy (80kV and 100μA) with a 1mm Aluminium filter, as is standard for the typical bone specimen. The Skyscan device scanned from 0 to 180 degrees at increments of 0.9 degrees and magnification of 14x. Shadow images were recorded from the average of 2 exposures at each angle increment, with each exposure having duration of 5712ms.

The shadow images were reconstructed into cross sectional slices using the software package NRecon (Skyscan, Belgium). The reconstruction was carried out with the following parameters:

- Threshold from 0.0025 to 0.025
- Pre-smoothing radius = 2 pixels
- Ring artefact reduction = 12
- Beam hardening = 0
- Step size = 2

The output from NRecon is a series of bitmap files that show cross sectional images of the specimen. These bitmaps have pixel size of 19μm and can be analysed in either two or three dimensions using another software package, CTAn (Skyscan, Belgium). The first step in the analysis is to recut the images in the desired orientation, such that the image produced shows a layer of subchondral bone on top of the cancellous bone. This view is a slice in the coronal plane. First, the orientation of the cut is determined and then the number of cuts and the spacing between the cuts is selected (Figure 114).

In the current protocol, the orientation of the cut is made from the medial to lateral and 10 slices were made at a separation of 20 pixels. As such, the specimens are analysed along the entire length of the condyle (medial to lateral), and extending 3.8mm in the anterior/posterior direction. This is approximately equal to the maximum thickness of a specimen that will fit inside a regular histological cassette. In terms of the subsequent histological analysis on these specimens, the region analysed in microCT is approximately equal to block number 2 (Figure 115).

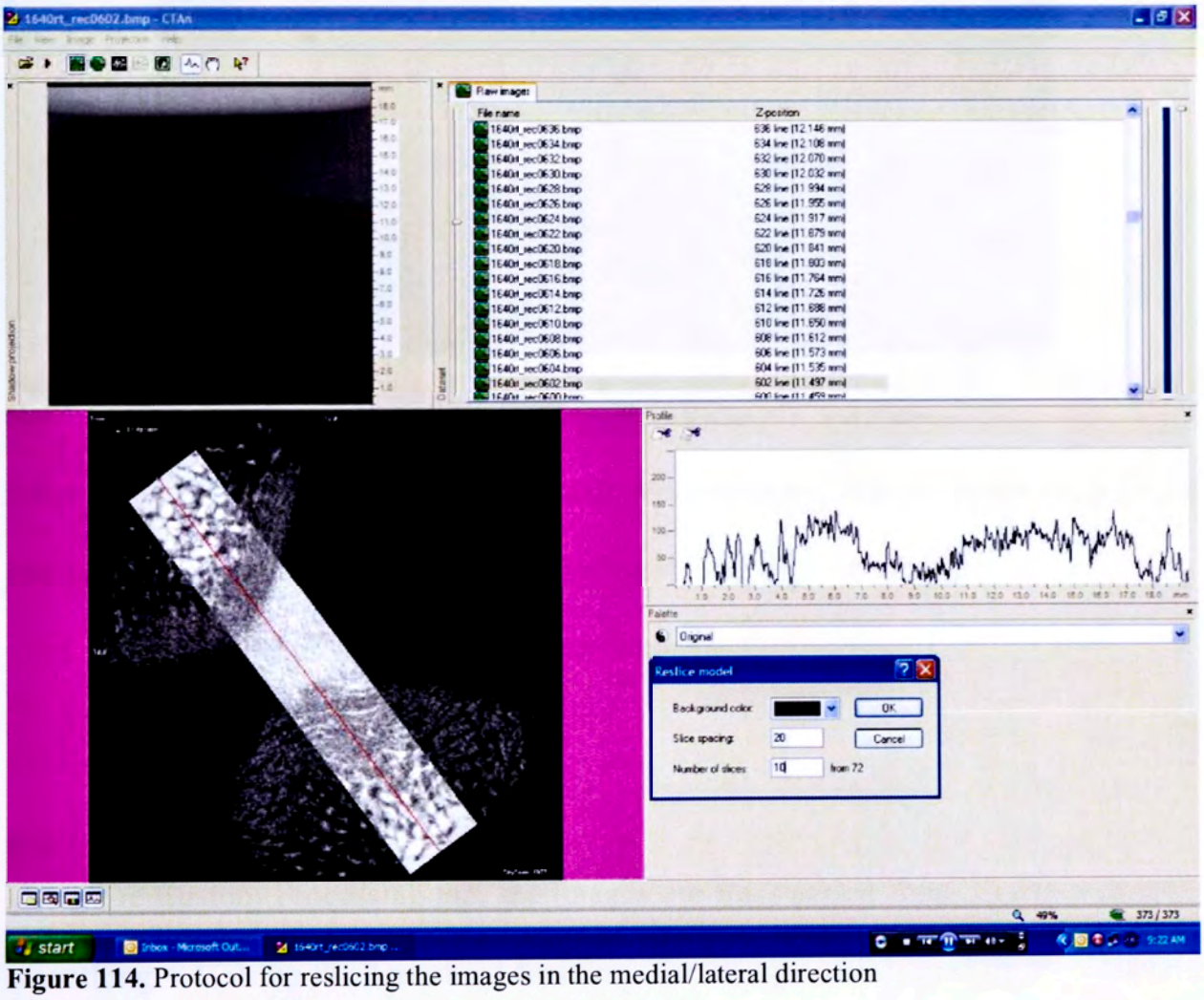


**Figure 114.** Protocol for reslicing the images in the medial/lateral direction

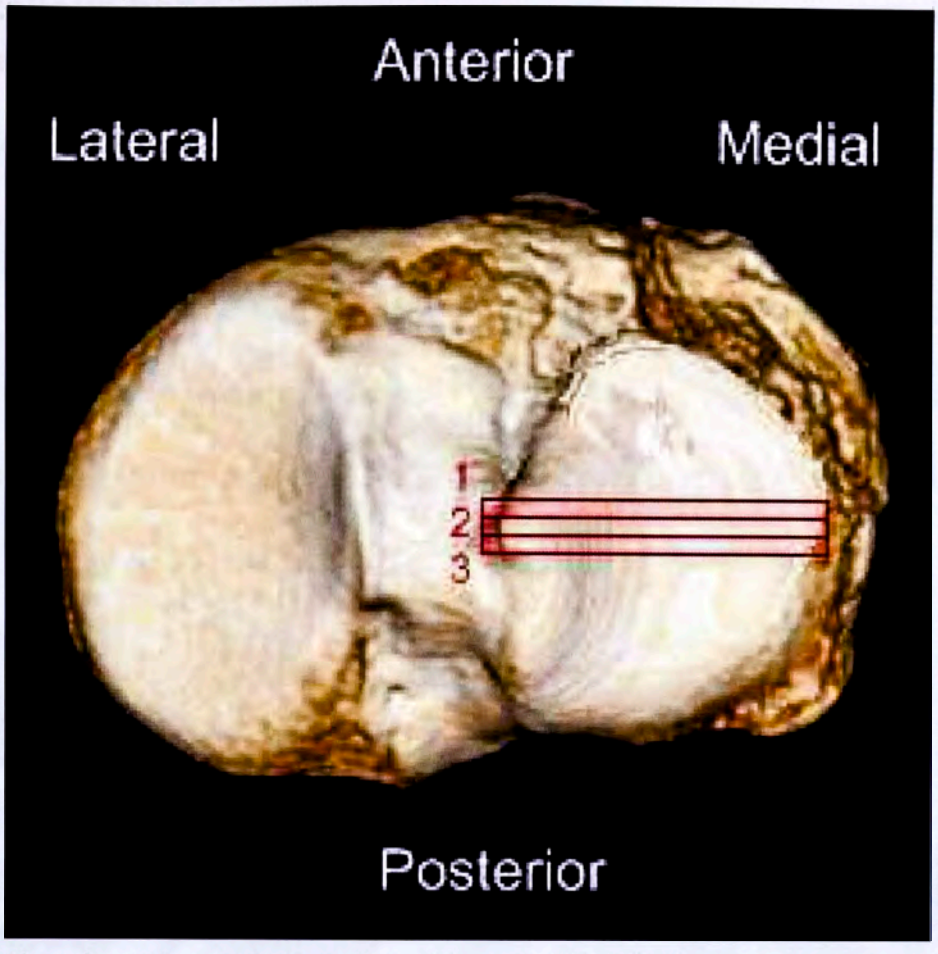


**Figure 115.** The microCT analysis is performed in approximately the same location as the histology block number 2. Histology is subsequently performed on all microCT specimens.

After reslicing the images, the new bitmap files are saved and the analysis in CTAn continues. Two different measurements are conducted on these images:

1. quantitiative properties of the cancellous bone
2. subchondral bone plate thickness

## 6.4 Image processing

Using the Custom Processing tab, the images are thresholded from 30-255 with pre-smoothing = 1, using the Threshold function. The images are cleaned up by removing black and white speckles with area less than 100 pixels (1.9mm$^2$), using the Despeckle function. Essentially, this method will remove pores or islands of bone that are less than 1.9mm$^2$, or approximately 1.5mm in diameter. The pores within the subchondral bone will therefore be excluded from the image, which is the desired result.

## 6.5 Cancellous bone

In CTAn, a rectangular region of interest (ROI) is drawn, 8mm wide by 4mm tall, in the cancellous bone between the subchondral bone and the growth plate (Figure 116). The software is then commanded to calculate the structural properties of the cancellous bone within the ROI on each of the 10 images in the image set. As such, the results from each specimen are calculated from the average of 10 slices. The parameters calculated from microCT in this study are Percentage Bone Volume, Bone Surface to Volume Ratio, Trabecular Thickness and Trabecular Separation.


**Figure 116.** Cancellous bone structural properties are calculated from the average of 10 two dimensional images using an 8x4mm ROI between the growth plate and subchondral bone.

Percentage Bone Volume (Bone Volume/Tissue Volume, %): the proportion of the volume of interest (VOI) that is occupied by solid bone. In the binary image, this is the percentage of solid black.

Bone Specific Surface (Bone Surface/Bone Volume, %): the ratio of the total bone surface area to the bone volume within the VOI. In the 2D image, this is the ratio of the perimeter to the area of the trabeculae.

Trabecular Thickness (mm): Using the parallel plate model, this is an estimation of the thickness of the trabeculae from 2D images using the formula Tb.Th = 2/(BS/BV)

Trabecular Separation: Using the parallel plate model, the trabecular separation is estimated from 2D images using the formula Tb.Sp= (1/Tb.N)-Tb.Th where Tb.N is the number of trabeculae.

## 6.6 Subchondral bone plate thickness

The same binary bitmap files produced in the custom image processing stage are used to measure the thickness of the subchondral bone plate. The first step is to overlay a vertical grid with line spacing of 50 pixels. The proximal boundary of the subchondral bone plate is clearly defined by the thresholding process, although the distal boundary is not well defined on immediate inspection. A repeatable, semi-automated process was devised to define the distal boundary for the purpose of reducing subjectivity and operator bias. This process results in a "line of best fit" that joins one void space to the shallowest adjacent void space within a horizontal distance of 100 pixels (Figure 117).

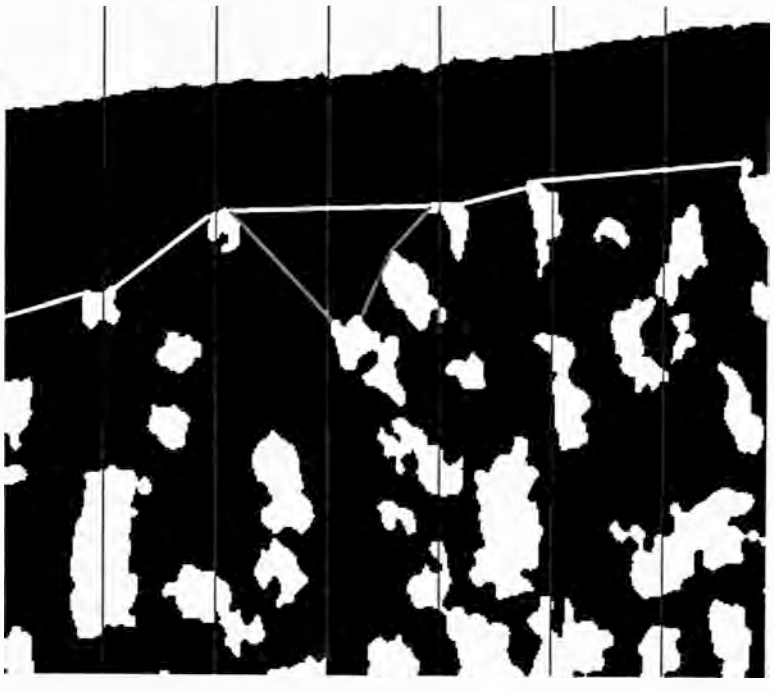

**Figure 117.** An illustrative example of defining the distal boundary of the subchondral bone plate. The white line is the correctly defined line, with straight lines joining one point to the highest void space within horizontal distance of100 pixels. The green line indicates an alternative method, which would be incorrect using the semi-automated procedure described in this protocol. The red lines are the overlying grid lines with 50 pixels separation. This method was devised to reduce the level of subjectivity in the measurement of the subchondral bone plate thickness.

The protocol for defining the thickness of the subchondral bone plate is as follows:

1. Overlay a 50pixel vertical grid onto each binary image
2. Starting from the most medial cancellous void space, draw a white line between that void space and the shallowest void space within a 100 pixel radius
3. From the end of that white line, draw another white line to the shallowest void space within a 100 pixel radius
4. Continue until the white line reaches the lateral edge of the image
5. Import images into Imagej
6. At each intersection of the gridlines with the surface of the subchondral bone, measure the distance perpendicular to the surface projected down to the white line (Figure 118).

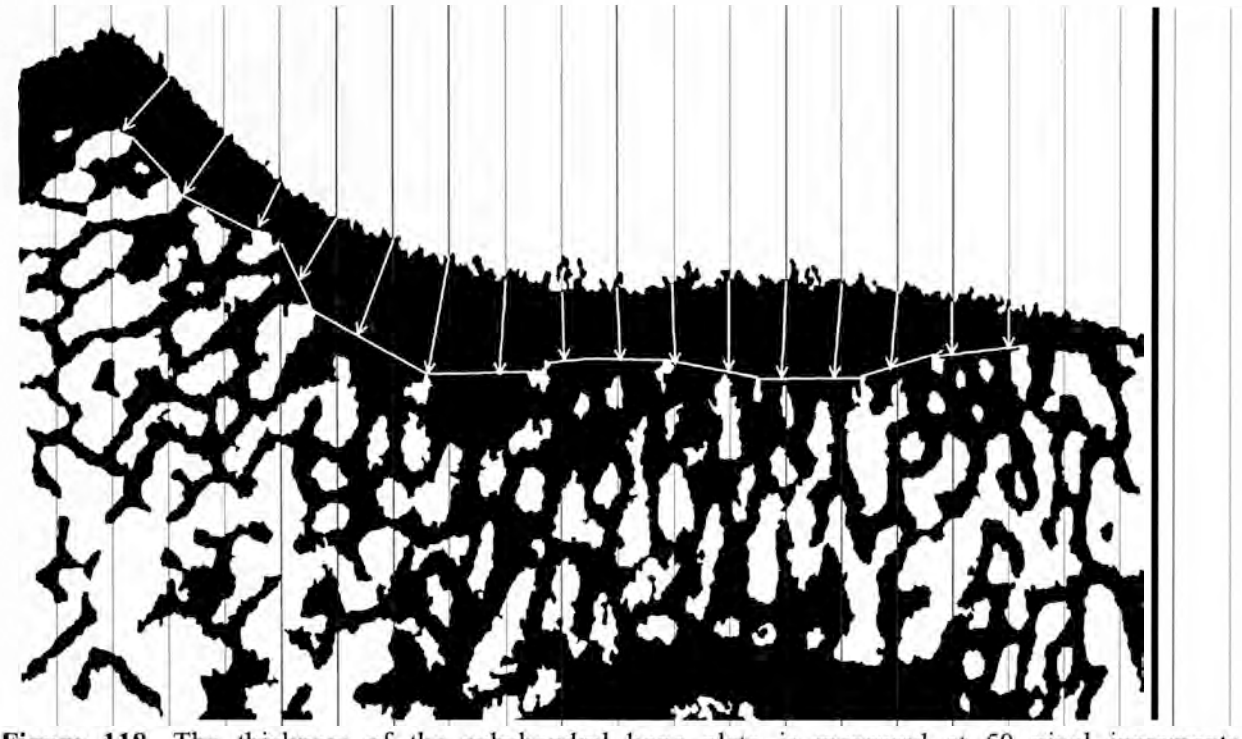

**Figure 118.** The thickness of the subchondral bone plate is measured at 50 pixel increments perpendicular to the bone surface.

This method for measuring the thickness of the subchondral bone plate is well defined and semi-automated by the establishment of clear rules in defining the distal penetration of the bone plate. Hence, subjectivity in the results is reduced, although a completely automated process such as a script written in Matlab would be the only way to completely remove the subjectivity. For the purposes of this study, however, the semi-automated approach is adequate. It should be noted that these results are not directly comparable to other studies that have used microCT or histology to measure the subchondral bone plate thickness, due to the fact that the distal boundary of the subchondral bone is defined differently, if at all, in those studies. However, this method does provide satisfactory data for comparison within this study and others that choose to use this method.

# 7. Tibio-femoral contact pressure in the sheep: the influence of osteochondral defects and metallic resurfacing implants in a discrete gait model

## *7.1 Introduction*

Tibio-femoral contact pressure is dependent on both the force applied across the joint and the pressure footprint, or in other words, the area of tissue that contributes to load bearing. As such, a large pressure footprint will result in lower stress on the articular cartilage and presumably less likelihood of both traumatic damage and wear. This is important in the intact knee, but also in any attempt for repair or replacement. For example, in an effort to reduce wear, modern total hip replacements are currently being designed with larger femoral head components than in previous designs. The same principles apply when a defect is introduced into the knee. A defect results in stress concentration along the rim of the defect, which may result in collapse of the defect wall and exacerbate the pathological condition (Raimondi and Pietrabissa 2005).

Cartilage and bone are also tissues that respond to mechanical loading and either remodel or become damaged depending on the magnitude of said loads. Where an osteochondral defect exists in the femoral condyle, apart from damage to the femur, the modification to loading throughout the joint may adversely affect the tibial surface. From Chapters 4 and 5, we know that a femoral defect does cause damage to the tibial cartilage, so the change in loading may well be part of the cause. This may also be a cause of additional pain to the patient and thus, it is desirable to repair the defect somehow. The idea of repairing a cartilage defect with a metallic device is an interesting idea due to the disparity in elastic modulus between the metal and the

adjacent cartilage, which is likely to result in a stress concentration over the metallic surface.

The aim of this project was to investigate the distribution of pressure in the knee joint of normal adult sheep and to quantify the changes when an osteochondral defect is introduced to the medial femoral condyle. Furthermore, the influence of a metallic resurfacing device was investigated. The tibio-femoral contact force, pressure and area were measured over a range of flexion angles and loads typical in the walking gait of the sheep.

## *7.2 Methods*

This method has been adapted from the technique pioneered in our laboratory and now widely used for joint contact stresses under total knee prostheses in vitro (Figure 119). The only variations from this standard technique are the angles and forces, which in the current study are specific to the sheep knee, and the soft tissue attachments which aid in aligning the joint physiologically. Briefly, the knee is aligned in the jig, a K-Scan digital pressure sensor (Tekscan, Boston) is positioned in the joint space and the force and contact area are recorded at predefined flexion angles, with known compressive loads.

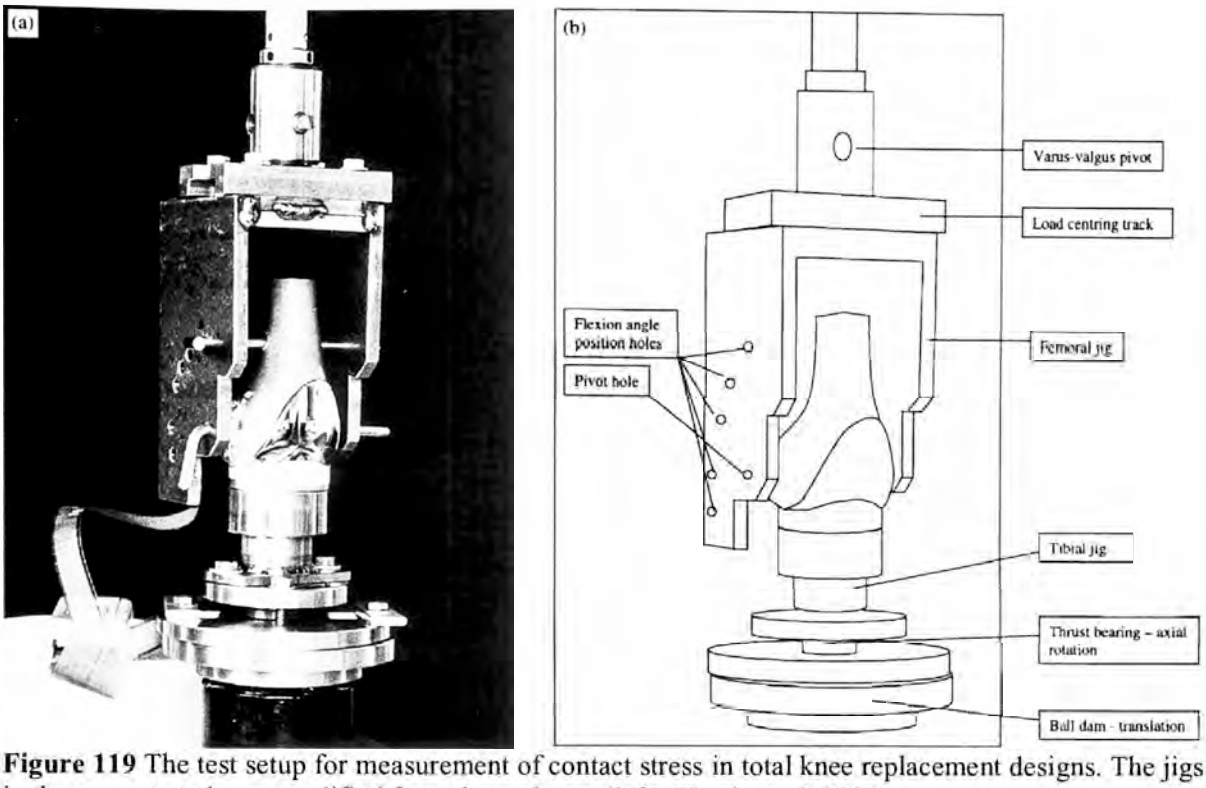


**Figure 119** The test setup for measurement of contact stress in total knee replacement designs. The jigs in the current study are modified from those shown (left) (Harris et al. 1999)

### 7.2.1 Study design

Four conditions were analysed in this study:

1. intact joint (n=3)
2. 6mm osteochondral defect in the medial femoral condyle (MFC) (n=3)
3. 9mm osteochondral defect in the MFC (n=1)
4. HemiCAP™ resurfacing over the 9mm defect (n=1)

The conditions were selected to represent the groups in the in vivo studies of this thesis (Chapters 3 and 5). All defects were created 6mm deep with a surgical punch (Arthrex, Naples, FL) and the resurfaced joint with the HemiCAP device represented a time zero condition. In other words, the implant was tested using the initial fixation, before any new bone was abutting the screw threads or the underside of the articulating component. Manual palpation and inspection of the implant confirmed that the implant was solidly fixed at the time of testing, and afterwards.

### 7.2.2 Design of Variable Flexion Jig

This experiment necessitated the design and fabrication of a jig that allowed the knee flexion angle to be varied according to the sheep gait cycle, which varies markedly from the human. Since the knee joint forces would be applied using a materials testing machine, the jig was also required to attach the femur and tibia to the actuator and load cell respectively. The basic design was based on the tibia being fixed vertically on the load cell with an X-Y table providing the ability to translate the tibia in the horizontal plane for initial alignment, but constraining all degrees of freedom during the test (Harris et al. 1999). Control of the flexion angle was therefore designed into the jig constraining the femur, which would be connected to the actuator. The actuator thus provides the compressive knee joint forces displacing the femur in an axial direction. Importantly the femoral jig allows for small corrections in the varus/valgus as the joint is loaded, ensuring loading follows the geometry of the joint. This is achieved by connecting the jig to the actuator with a pin in the anterior-posterior direction. The femur is constrained within the jig by two horizontal bars, a distal bar located at the centre of rotation of the femur and a proximal bar exactly 80mm from the distal bar. The distal bar inserts into the 6mm hole in the jig and through the distal hole in the femur. The proximal bar is a tie-rod, meaning it is threaded at each end, which is inserted into the slot arc of the jig. The slot makes an arc with radius of 80mm originating at the distal hole. The arc describes an angle ranging from 30 to 80 degrees from the vertical. Translating the proximal bar through the slot arc allows variation of the flexion angle, as shown in Figure 120. The flexion angle can be fixed with a pair of washer and nuts on each end of the bar, as shown in Figure 121.

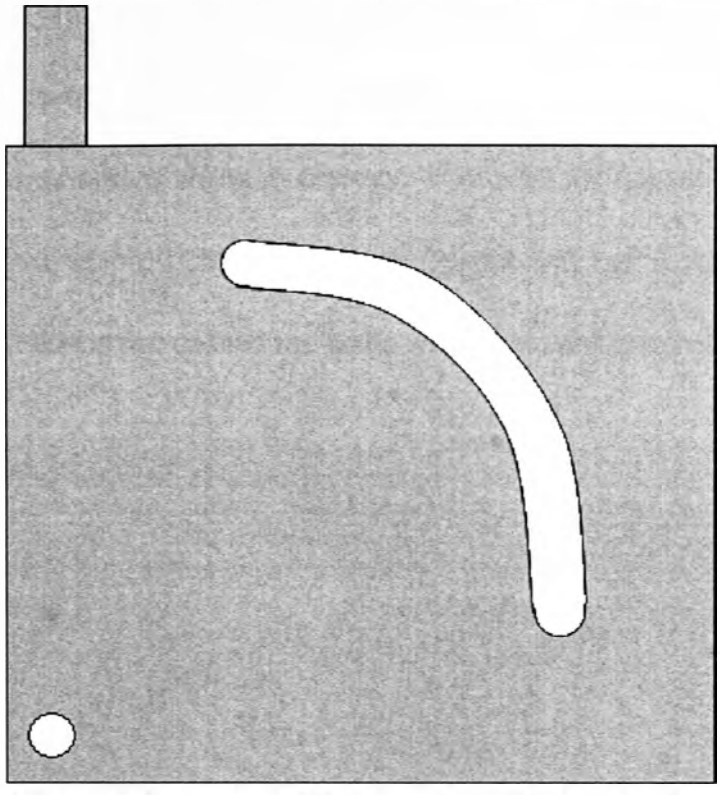

**Figure 120** Variable flexion angles are possible by translating the proximal bar through the slot arc. The slot arc is centred on the distal hole (pivot), which is located at the centre of rotation of the distal femur.

**Figure 121** A tie-rod is used to secure the proximal bar in the slot arc, providing control of the flexion angle of the knee. Nuts on either side of the slot arc provide compression to each sidewall, but not between the walls.

Originally a single nut and washer was used on each end of the rod, however, this applied a strong tensile load to the bar resulting in compression between the sidewalls that was sufficient to deform the flexion jig. Inward deformation of the sidewalls made control of the flexion angle difficult and inaccurate. To solve this problem, a second pair of nut and washer was added on the inside of the jig so that the clamping force was applied to each wall of the jig, but not between the walls.

The knee flexion jig thus consists of two sidewalls with a distal hole for a smooth bar and a slot arc for a tie-rod. A top plate is connected to the sidewalls with four bolts, so that the jig can be dismantled when necessary. The bolts are oriented vertically so that the compressive loading protocol of this experiment will not induce shear forces on the bolts, which would be the case if the bolts were oriented horizontally (Figure 122).

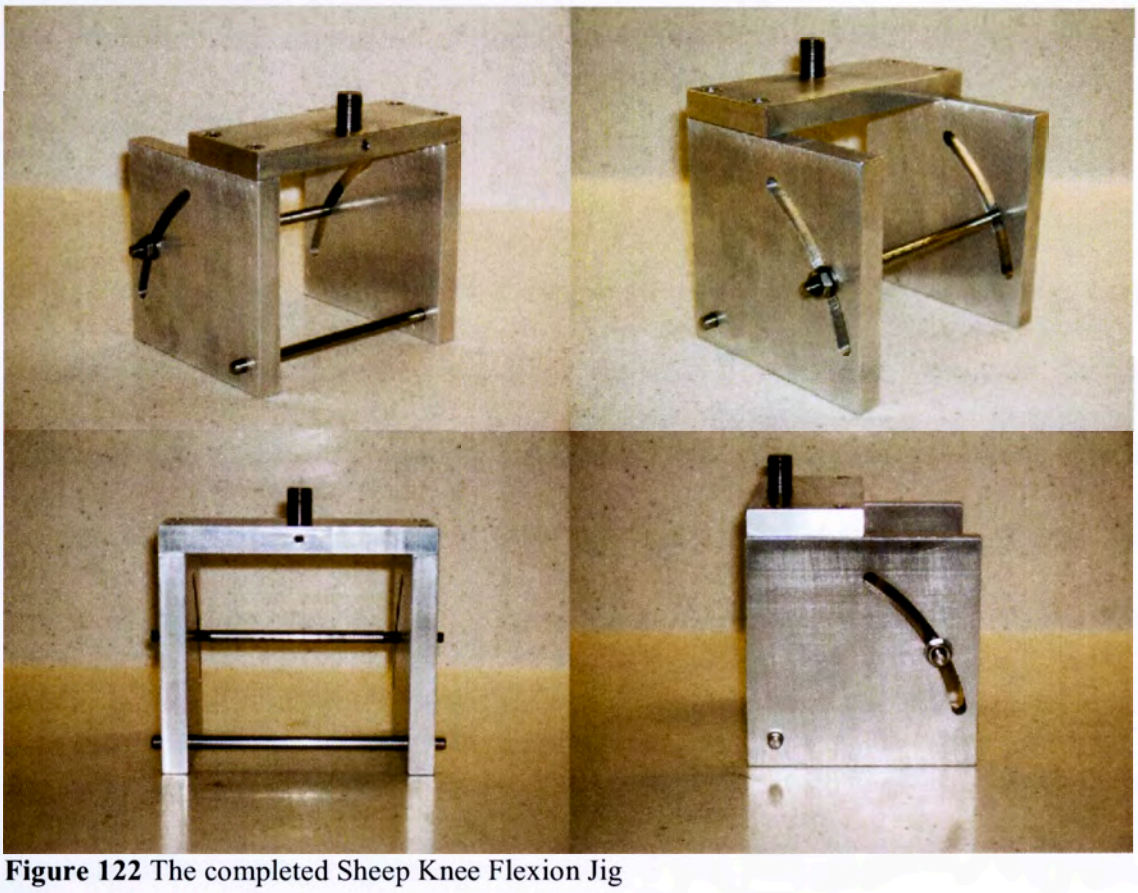

**Figure 122** The completed Sheep Knee Flexion Jig

The top part of the flexion jig is mounted to the actuator of the load unit with a male/female socket connector, secured with a cross-pin. This connection gives the system a small amount of freedom in varus/valgus rotation and allows the femur to "self locate" with the geometry of the tibia as a load is applied. In this manner, the position of the femur relative to the tibia is dictated by the geometry of the joint surfaces, as would be the case in the physiological scenario.

### 7.2.3 Preparation of the specimens

Hind limbs were harvested from recently deceased adult sheep for this study. The knees were carefully dissected, removing all musculature and the patella, taking care not to damage the supportive ligaments of the knee. The tibia was cut in the same plane as the tibial plateau to a length of approximately 100mm. The collateral ligaments, cruciate ligaments and meniscal insertions were left untouched to protect the physiological alignment of the knee whilst it was being prepared for the axial loading protocol of this experiment.

With ligaments attached, the tibia was fixed in a vice and the femur was rotated and translated by hand, bringing the knee through flexion and extension, to locate the approximate centre of rotation of the femur. This occurred approximately between the origins of the medial collateral ligament and lateral collateral ligament. When the centre of rotation was marked, a 2mm guide wire was drilled through the femur in a medio-lateral direction along the axis of rotation. The knee was then moved through the full range of flexion and extension to verify that the wire was approximately on the axis of rotation. A 7mm cannulated drill was then passed over the guide wire to ream out the distal hole. The femur was subsequently placed inside the flexion jig and a 6mm bar was inserted through the hole in the jig, passing through the hole in the femur and into the respective hole in the other side of the flexion jig. The femur was free to rotate about this bar and was also free to move in a medio-lateral direction.

Whilst located within the jig, a second 7mm hole was drilled in the proximal tibia, using the jog as a drill guide. The proximal hole was fitted with a tie rod and clamped in position with locking nuts. The flexion jig was then attached to the actuator of a servohydraulic materials testing machine (MTS Bionix, MTS, Eden Prarie, USA) to

allow for alignment of the tibia relative to the femur, and for the subsequent testing protocol (Figure 123).

The actuator was lowered, positioning the tibia into a cylindrical pot attached to an X-Y table atop the load cell of the MTS machine. The X-Y table allowed accurate positioning of the tibia relative to the femur, which was constrained within the flexion jig. Physiological alignment of the tibia was generally maintained by the intact ligaments around the knee, which at this stage had not been cut. Vertical fixation of the tibia was achieved with low melting point alloy (Wood's metal). This type of fixation was selected to reduce stress concentrations that might otherwise lead to failure of the tibia during the loading protocol, and to provide the most rigid fixation possible.

With the orientation and fixation of the knee complete, the collateral ligaments and cruciate ligaments were sharply dissected with a scalpel blade. The collateral ligaments were removed to allow the pressure sensors to be inserted into the knee joint and the cruciate ligaments were removed to allow proper positioning of the sensors once they were inside. The orthogonal alignment of the cruciate ligaments also had a propensity to rotate the femur with respect to the tibia as the ligaments naturally sought to straighten out. The attachments of the meniscus on the tibia were retained, but those on the femur were cut. In this way, the femur and the tibia were completely separated, although correct alignment of the knee was already certified by preparing the knee with these ligaments intact.

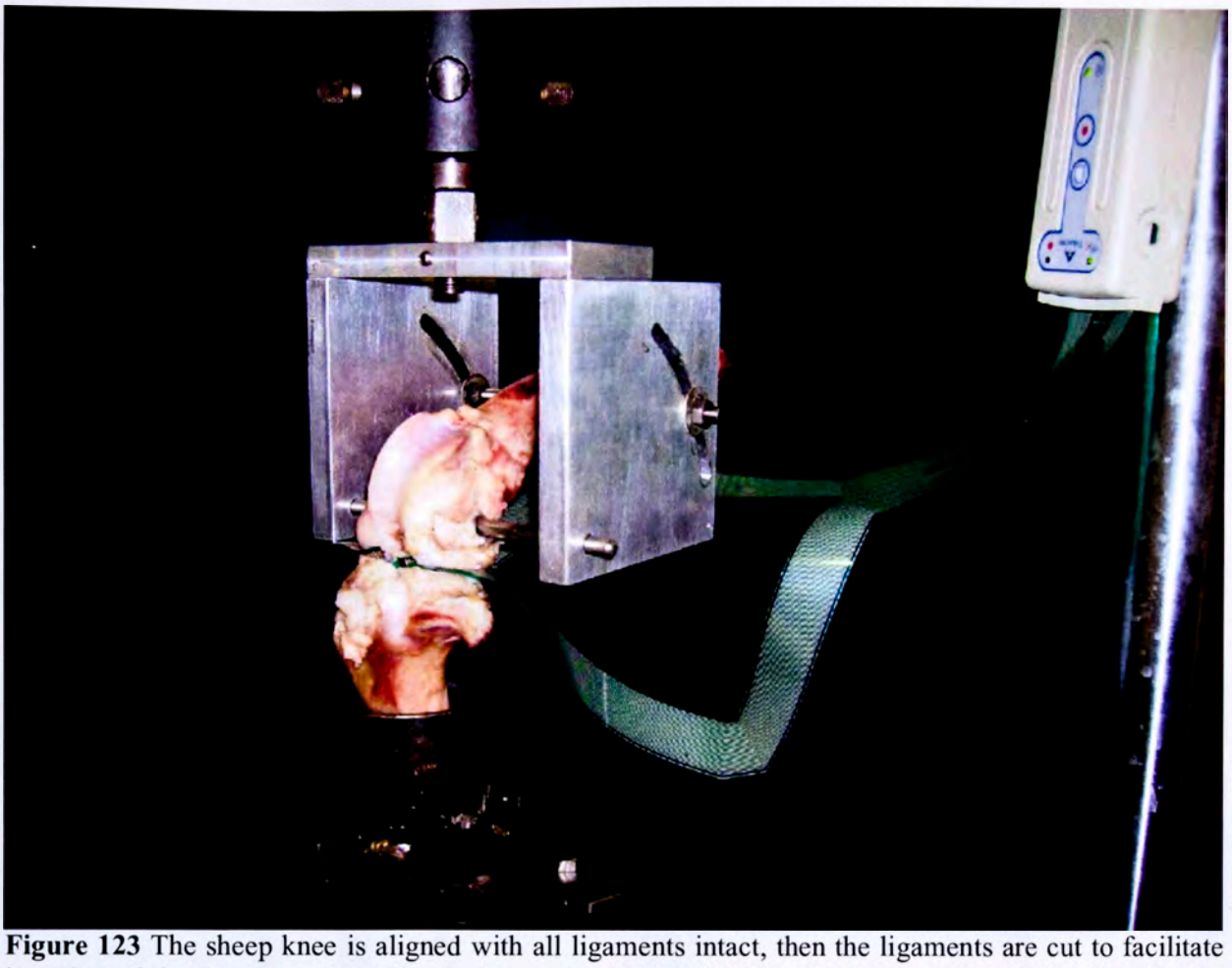

**Figure 123** The sheep knee is aligned with all ligaments intact, then the ligaments are cut to facilitate insertion of the K-scan sensor. The flexion angle is controlled by sliding the proximal bar through the slotted arc and fixing with nuts on either side of the wall.

Alignment of the tibia with respect to the femur was checked by inserting the pressure sensors and loading the knee in compression from 0N to approximately 500N. A feature of the TekScan software allows us to monitor the position of the centre of mass, which is very helpful in determination of correct alignment of the knee. The condition for satisfactory alignment was that the centre of mass should be situated midway between the two condyles at low loads (Harris et al. 1999).

### 7.2.4 Testing protocol

The testing protocol was designed based on the recent work of Taylor, et al who found that the average range of flexion of the sheep knee through normal gait is from 49 to 70 degrees (Figure 124). They also reported that the maximum knee joint force was approximately two times body weight. The average body weight of the sheep for

the purposes of the current study was calculated from the average of 24 adult sheep as 63kg, or 618N.

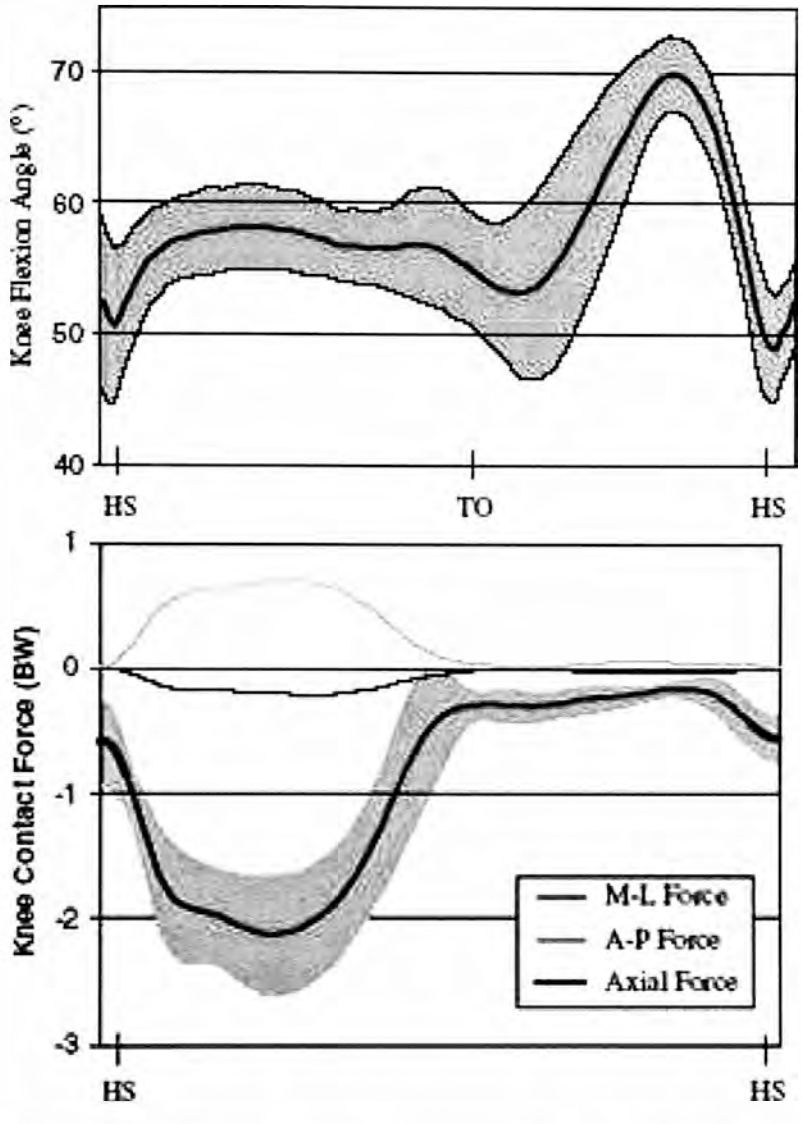


**Figure 124** Knee flexion angle and contact force in the normal gait of sheep (Taylor, Ehrig, Heller, Schell, Seeback, & Duda 2006)

A testing protocol was designed based on the sheep gait analysis and the perceived accuracy of the flexion jig built for this experiment. This jig was conservatively assumed to have inter-specimen reproducibility of plus/minus 5 degrees. Thus, over the range of 49 to 70 degrees, the test angles of 50, 60 and 70 degrees could be reproduced with a satisfactory level of certainty.

### 7.2.5 Justification of Simplified Testing Protocol

In the current study, it was not possible to recreate the complicated flexion-extension profile of the knee whilst also controlling the compressive load. Hence there was a need to convert the continuous gait analysis data set into some discrete regions which can describe the important regions of the full data set and be used to approximate the complexity of the continuous data. In this study, the sheep gait cycle has been modelled based on four discrete points that feature predominantly in the sheep gait cycle (Figures 125 and 126). Point 1 represents heel-strike, Point 2 represents the maximum contact force, Point 3 represents toe-off and Point 4 represents the maximum flexion angle. In the case of Point 2 and Point 3, the average flexion angles from the sheep gait analysis were approximately 55 degrees. However, in the current study these angles were rounded up to 60 degrees to fit with the decided test angles of 50, 60 and 70 degrees. Using an average sheep body weight of 618N, the sheep gait analysis was simplified with the following protocol:

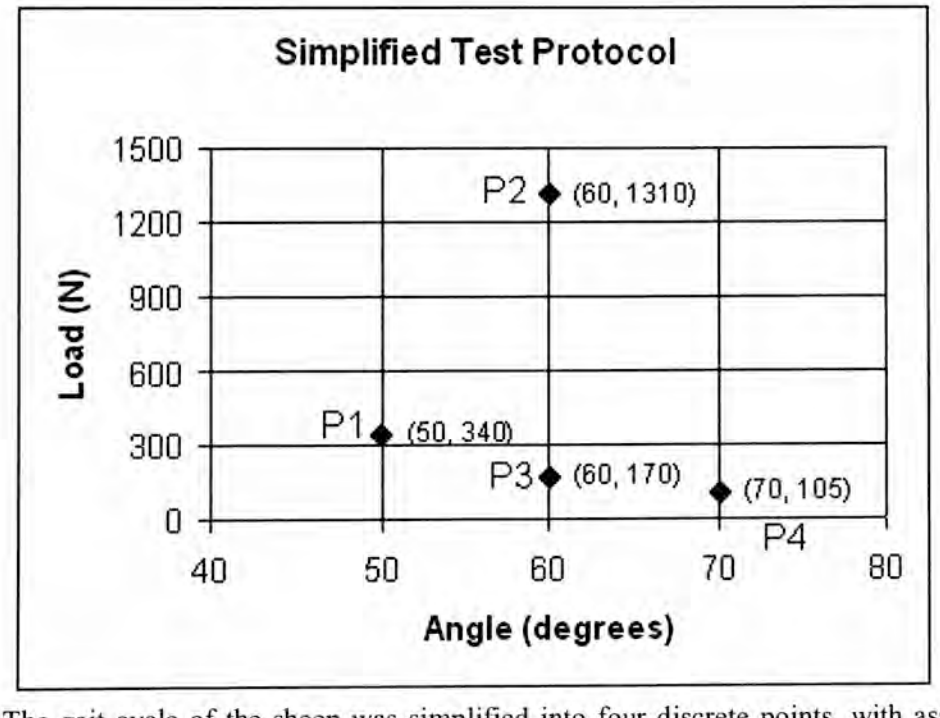


**Figure 125** The gait cycle of the sheep was simplified into four discrete points, with associated load and flexion angle as determined from Taylor, et al.

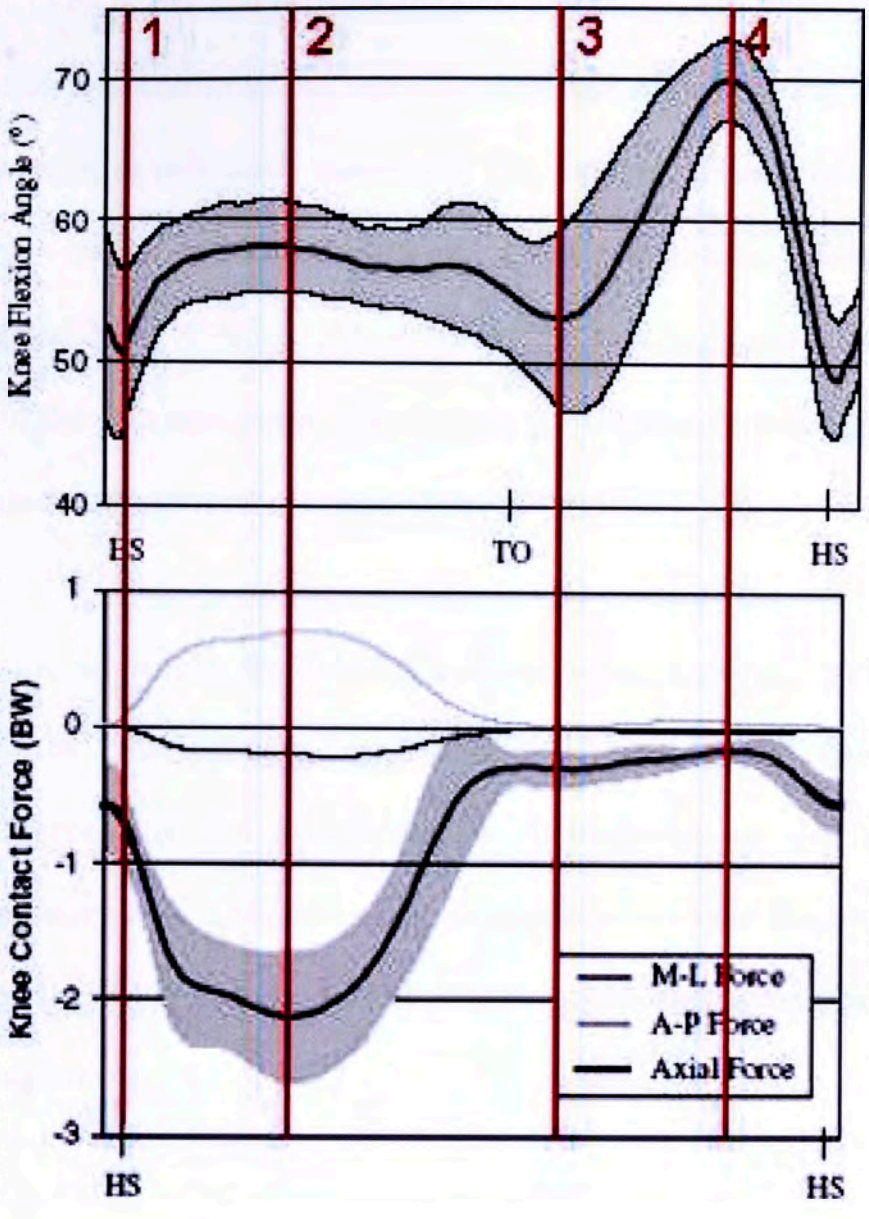


**Figure 126** Four discrete points were selected from the sheep gait to approximate the continuous data set: Point 1: 50 degrees of flexion and 340N (0.55xBW) of compressive load. This condition corresponds to heel strike (HS) in the sheep gait cycle.
Point 2: 60 degrees of flexion and 1310N (2.12xBW) of compressive load. This condition corresponds to the point of maximum knee contact force.
Point 3: 60 degrees of flexion and 170N (0.28xBW). This condition represents average values around the toe-off (TO) region of the sheep gait cycle.
Point 4: 70 degrees of flexion and 105N (0.17xBW). This condition corresponds to the point of highest flexion angle in the sheep knee, which is coincident with the point of minimum knee contact force.

### 7.2.6 Pressure footprint method

In preparation for testing, the tibia was potted and fixed to the load cell, the femur was secured within the flexion jig and attached to the actuator and the flexion angle was fixed at the relevant test angle. The supportive ligaments were sectioned to allow the

pressure sensors to be positioned between the tibia and femur, and above the menisci. Correct orientation was confirmed by approximately equal load sharing between the condyles at low loads, as previously mentioned. The Tekscan device was calibrated at each angle using a minimum load of 100N and a maximum load of 600N at 50deg, 1400N at 60deg and 200N at 70deg. Hence, the system was calibrated across the load range for each of the four test points. The Tekscan software calibrates linearly based on these two points, and converts raw force units to Newtons.

After calibration at one angle, the Tekscan software was commanded to begin data acquisition and the corresponding knee joint force was applied and held for approximately 5 seconds before being released. At this time, the data acquisition ceased and the pressure sensor file was saved for analysis. The knee flexion angle was then changed to the next test angle and the sensor re-calibrated before initiating the respective loading profile.

At each flexion angle, the Tekscan device recorded force and contact at each pixel of the K-Scan sensor. This data is then transformed into peak pressure, average pressure and contact area over the medial and lateral compartments.

## *7.3 Results*

A representative case of the pressure footprint in the medial condyle of each test condition at each load is shown graphically in Figures 127 to 130 below. The average joint stress, peak joint stress and contact area in the medial and lateral condyles are reported in Figures 131 to 133.

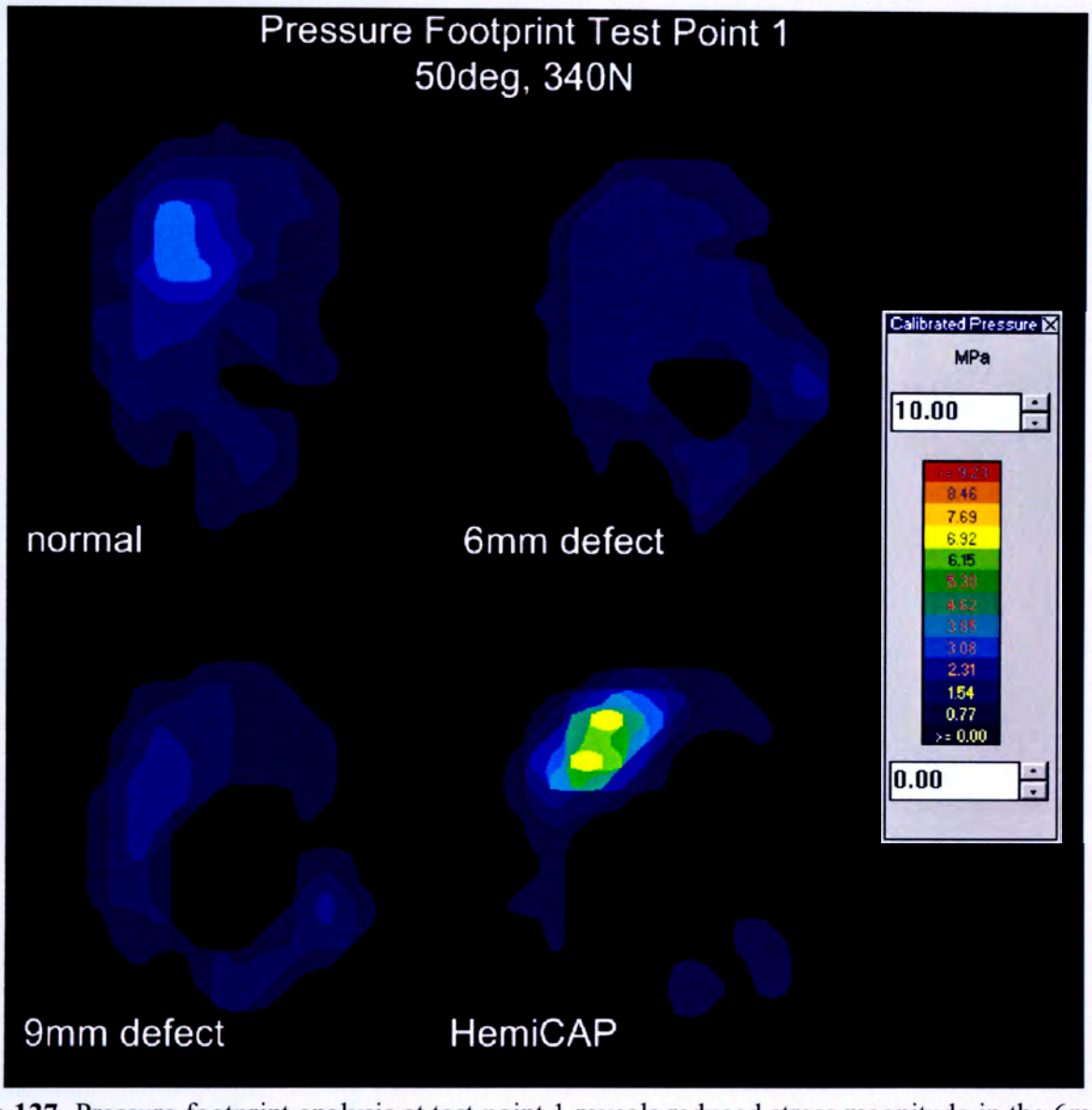


**Figure 127.** Pressure footprint analysis at test point 1 reveals reduced stress magnitude in the 6mm and 9mm defect groups when compared to the intact knee. In contrast, peak stress in the HemiCAP group was increased and a large area of the condyle was shielded from the applied load.

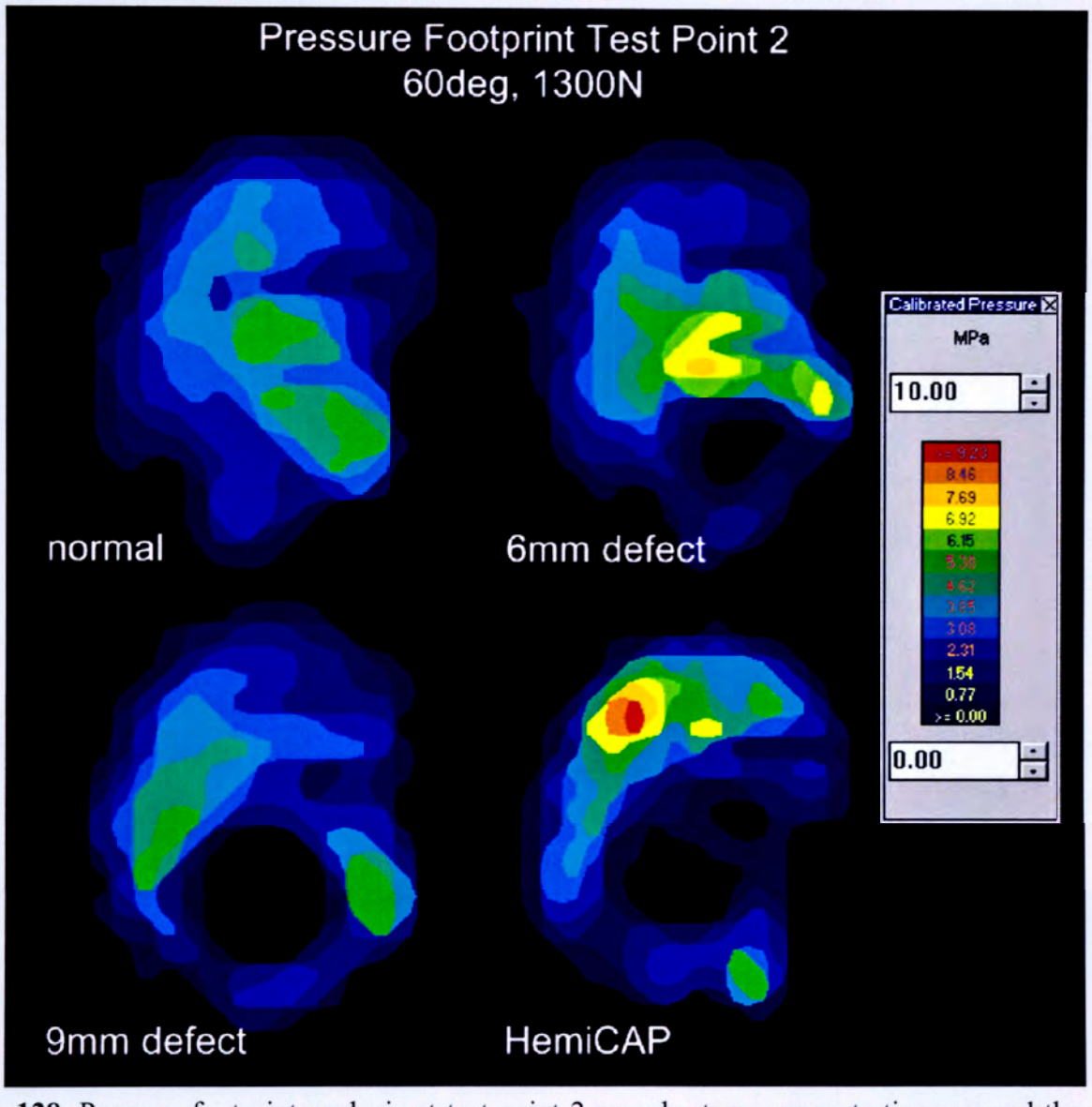


**Figure 128.** Pressure footprint analysis at test point 2 reveals stress concentrations around the rim of the defect, especially in the 6mm defect and HemiCAP groups. Both the 6mm defect and HemiCAP groups also had increased magnitude of peak stress when compared to the intact knee. The HemiCAP device shielded the adjacent cartilage from the applied load, but the point of contact between the device and the opposing tibial surface recorded peak stress above 8MPa.

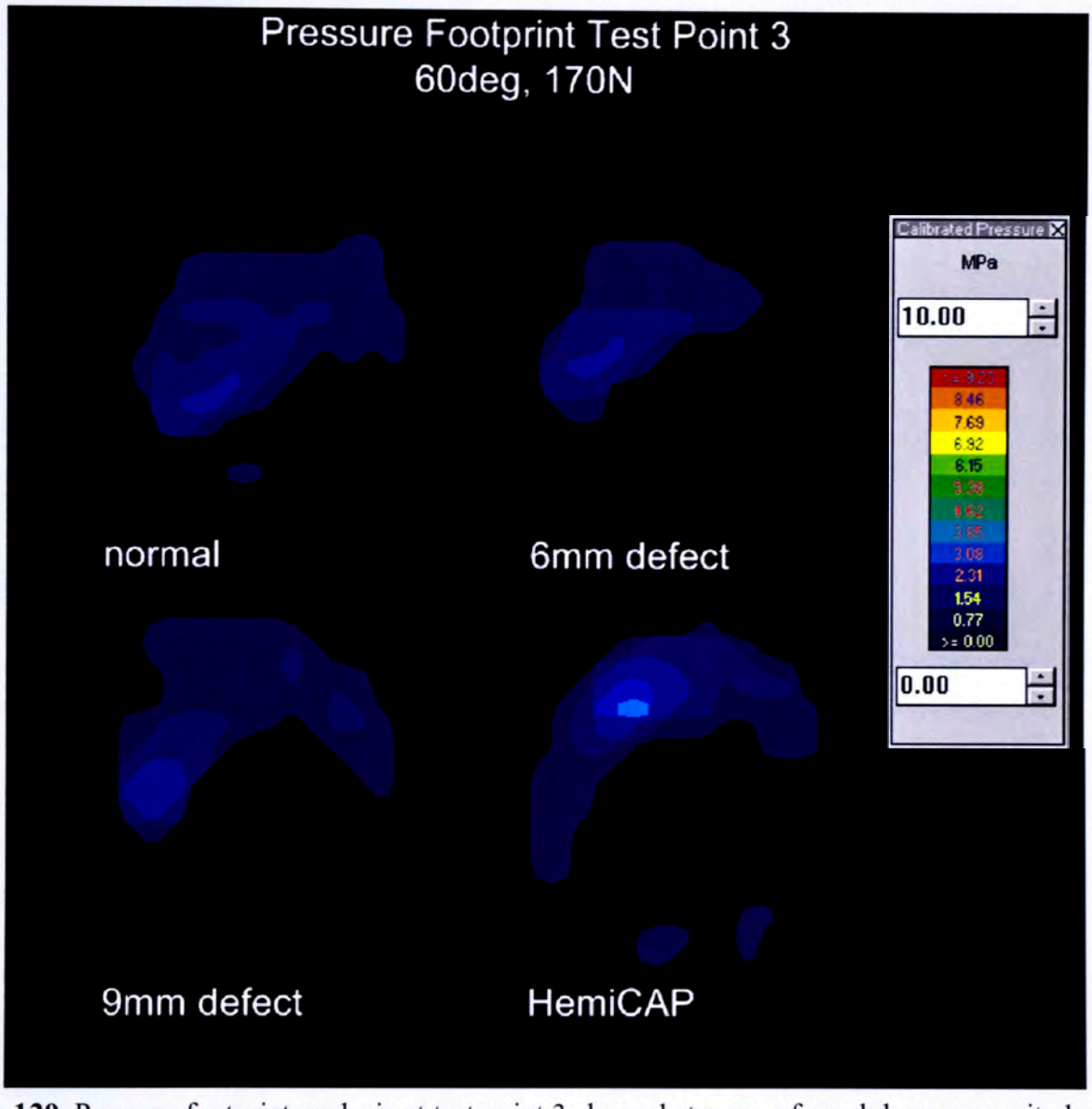


**Figure 129.** Pressure footprint analysis at test point 3 showed stresses of much lower magnitude due to the lower applied loads. The normal and 6mm defect had almost identical pressure footprints suggesting that at this angle and with such a low load, the defect was not in a load bearing location. Again, the HemiCAP group showed some point loading and stress shielding to the adjacent cartilage.

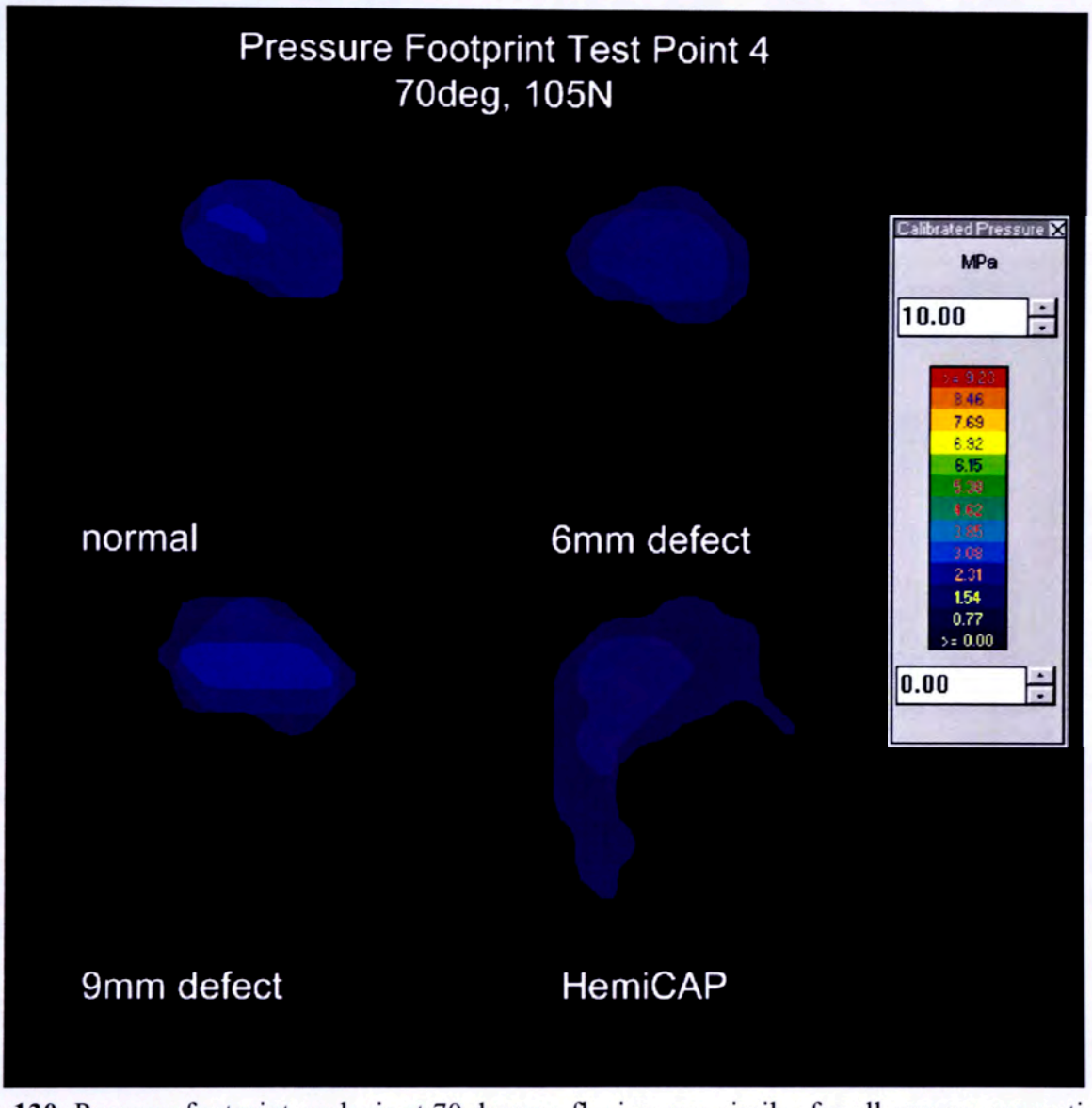


**Figure 130.** Pressure footprint analysis at 70 degrees flexion was similar for all groups, suggesting that the defect and implant were not in contact with the opposing surfaces at this angle.

## 7.3.1 Average Joint Stress

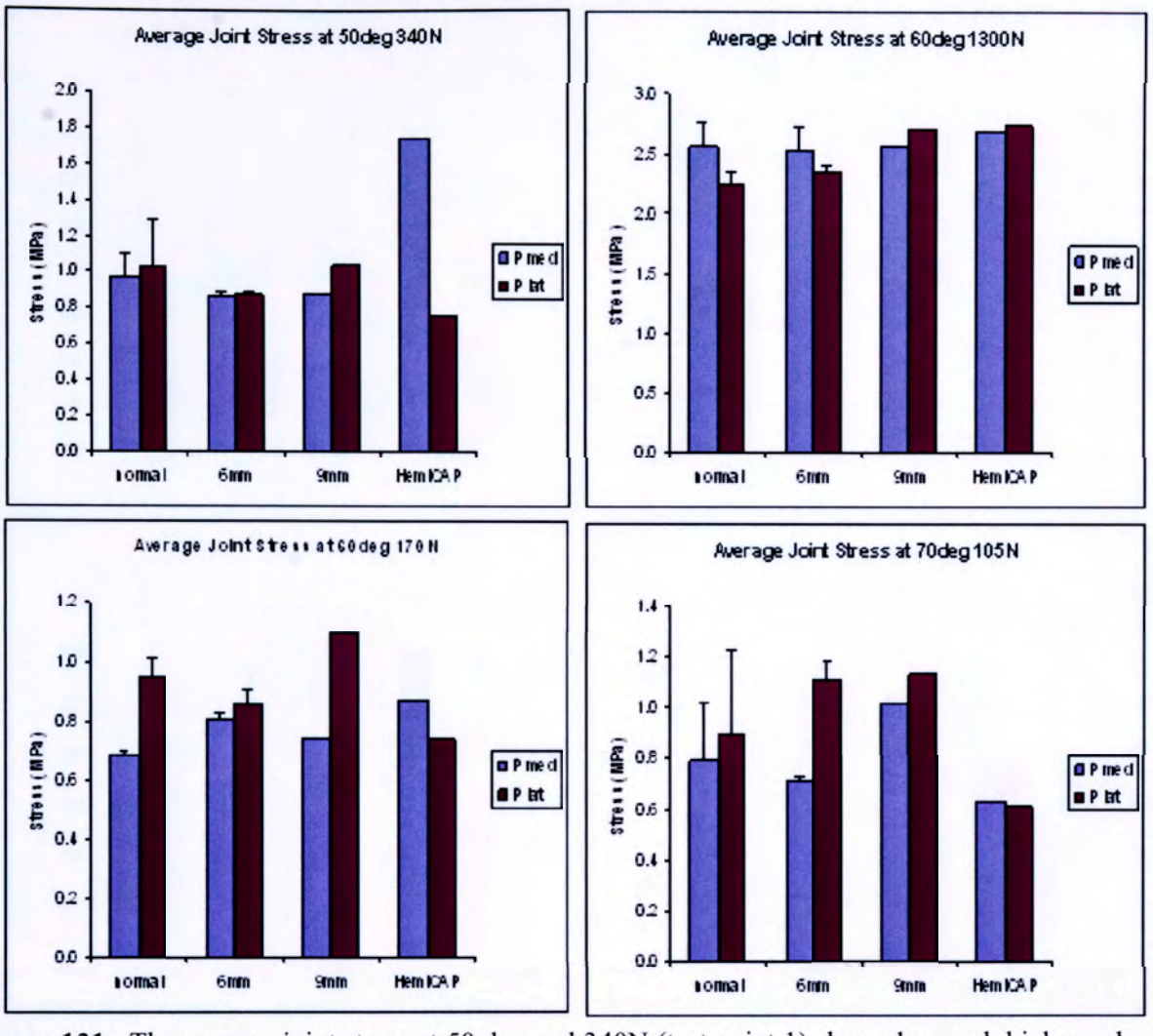


**Figure 131.** The average joint stress at 50 deg and 340N (test point 1) showed a much higher value in the medial condyle in the HemiCAP group when compared to all other groups. The lateral condyle in the HemiCAP group also appeared to have reduced average stress, indicating that the medial compartment was taking up most of the load through the joint. The average joint stress at 60 deg and 1300N (test point 2) was consistent in the medial condyle for all groups, but slightly elevated in the lateral condyle for the 9mm and HemiCAP groups. Test points 3 and 4 showed more variability in the average joint stress, due to the low applied loads and hence no clear pattern can be discerned.

## 7.3.2 Peak Joint Stress

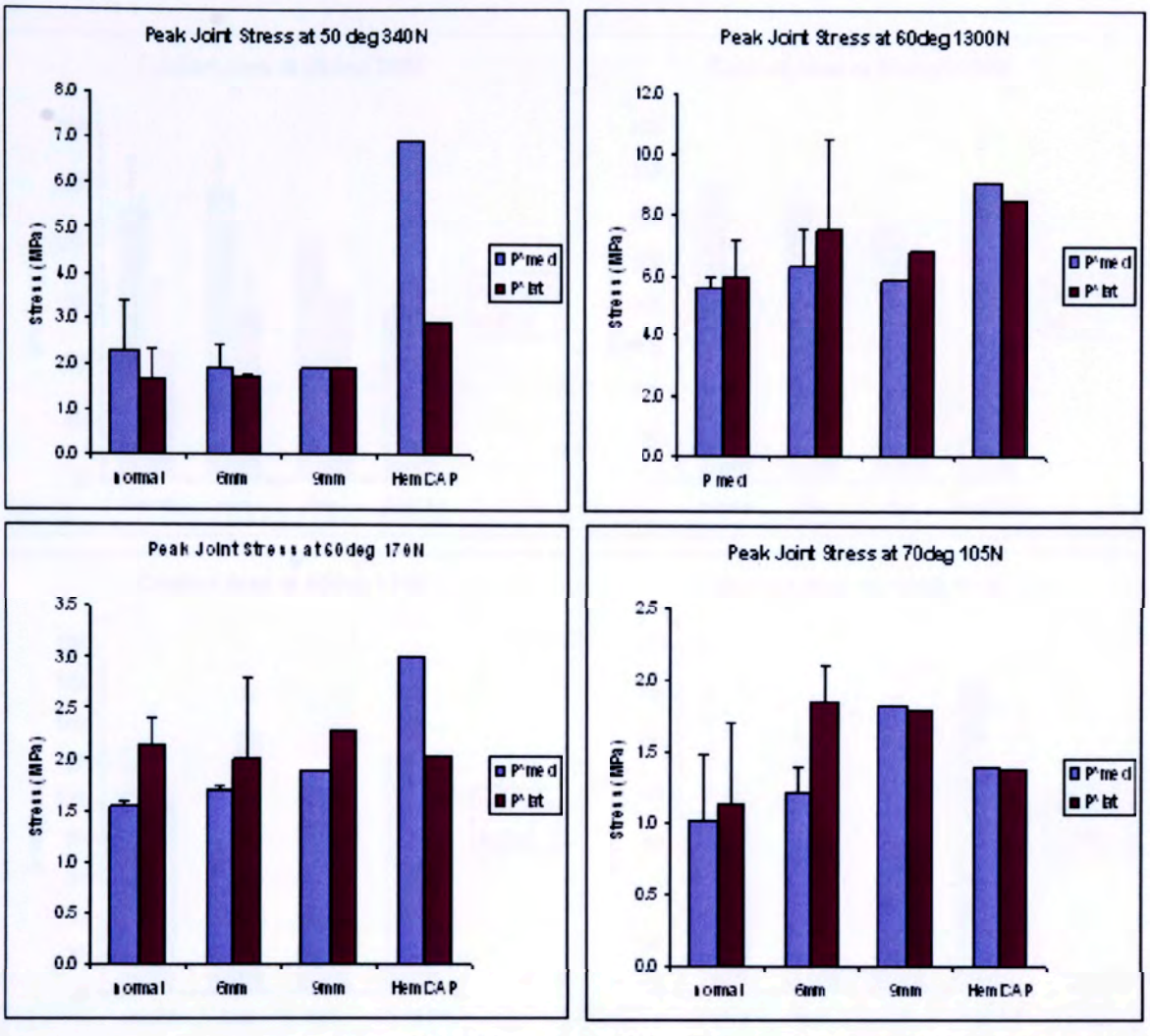


**Figure 132.** The peak joint stress at 50 deg and 340N (test point 1) showed similar values for the normal knee, the 6mm defect and the 9mm defect. However, the medial condyle of the HemiCAP specimen experienced peak stress approximately three times greater than the normal knee. The lateral condyle of the HemiCAP groups was also much increased. At 60 deg and 1300N (test point 2) the medial and lateral peak joint stresses appeared to be larger than the normal knee whilst the others were similar. At 60 deg and 170N (test point 3) the lateral peak stress was similar for all groups, however the medial peak stress increased from the normal state, to the 6mm defect, to the 9mm defect and then increased considerably in the HemiCAP group. Again, the low loads in test point 4 made it difficult to interpret the data.

## 7.3.3 Joint Contact Area

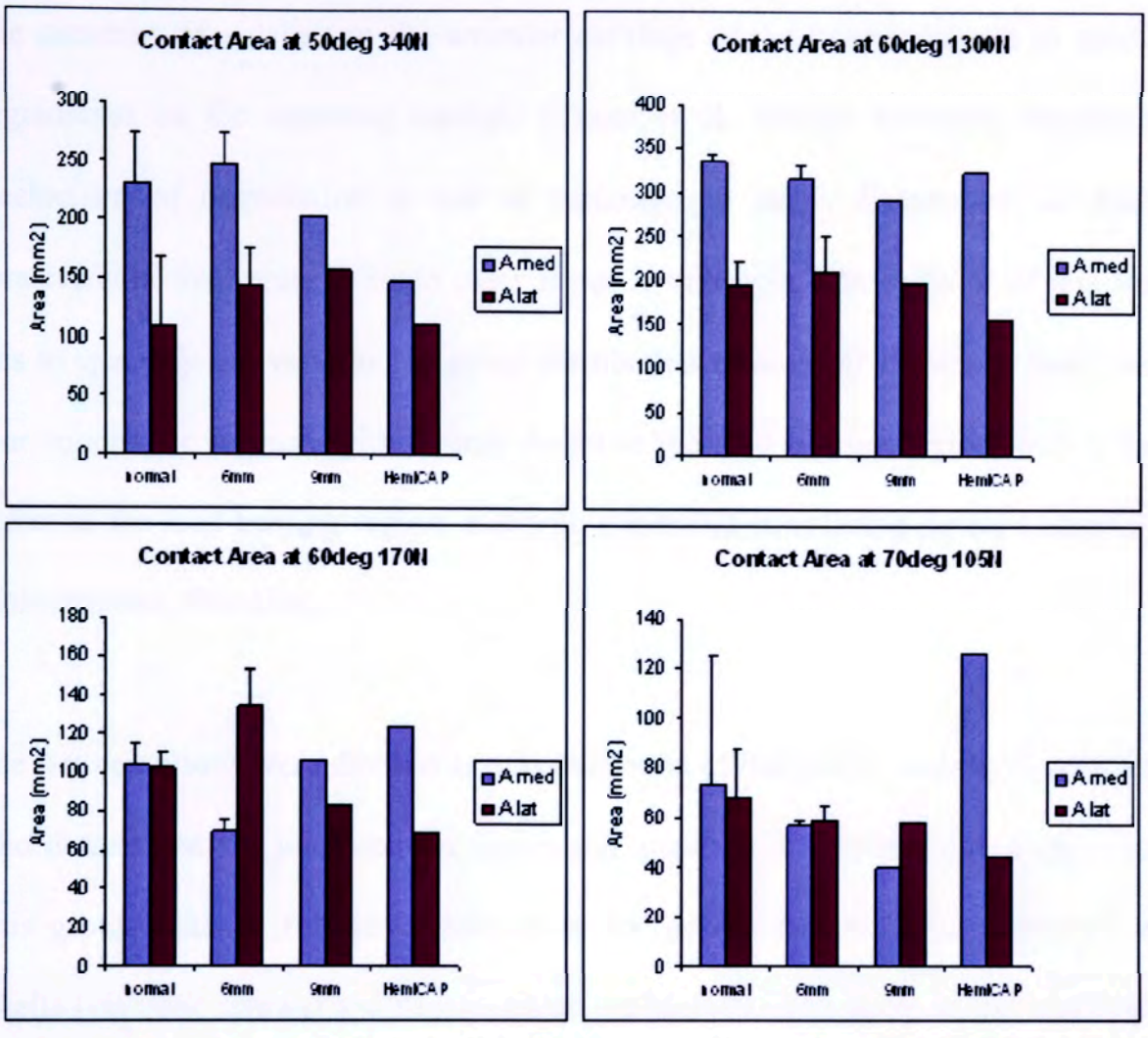


**Figure 133.** The contact area at 50 deg and 340N (test point 1) showed reduced values in the medial condyle for the 9mm defect and HemiCAP group when compared to the normal knee. At 60 deg and 1300N (test point 2), the medial contact area was reduced in the 9mm defect whilst the other groups were similar. At 60deg and 170N (test point 3) the medial contact area was reduced in the 6mm defect compared to the normal. Again, large variability was seen at 70 deg and 105N (test point 4), although the 9mm defect had reduced contact area and the HemiCAP group had increased contact area when compared to the normal knee.

## 7.4 Discussion

The presence of a defect in the articular cartilage of the knee is known to promote degradation on the opposing condyle (Vizesi et al. 2007a), however, whether the mechanism of degradation is due to variations in stress distribution, or due to abrasive/adhesive wear, or some other factor is unknown. The purpose of this study was to quantify the variation in stress distribution throughout the sheep knee under four conditions; normal, with a 6mm defect in the load bearing region, with a 9mm defect in the load bearing region, and with a metallic resurfacing device (HemiCAP, Arthrosurface, Franklin).

The test conditions were devised as a modification of the recent work by Taylor, et al who determined the joint contact forces and angles in the normal sheep gait cycle. This group attached reflective markers to the pelvis, femur, tibia, metatarsus and patella (via bone screws) and then recorded the biomechanics using an infrared optical system as the sheep walked over a force plate on a gangway. The paper reported the walking gait of the sheep and quantified both the angles and the contact forces in the knee during normal gait. As shown in Figure 124 above, the maximum joint force was approximately 2.12 times body weight at approximately 58 degrees of knee flexion. In comparison, the maximum joint force in the human knee during walking has been measured as 2.8 to 3.8 times body weight (Baltzopoulos 1995;Kellis 2001;Taylor et al. 2004;Zheng et al. 1998).

There has been little work published on the pressure footprint within the knee when a defect is present in the cartilage. Raimondi and Pietrabissa created idealised osteochondral cylinders from bovine knees and measured the contact area using static pressure films (Fuji, Japan) before and after the creation of a full thickness chondral

defect. As a final stage, the defect was then filled with fibrin glue, to represent the mechanical properties of currently available cellular constructs. The authors report that the introduction of a defect causes stress concentration around the rim of the defect, however, the peak pressure is lower than in the normal condition. This result was noted under some conditions in the current study, as well as in the literature (Brown et al. 1991). The paper by Raimondi and Pietrabissa is limited because of the static nature of the Fuji film, because non-anatomical, ideological specimens without menisci were used and because the loads applied to the specimen were relatively low. Nonetheless, it provides important fundamental information which has been built upon in the current study using anatomical specimens and varying the flexion angles and loads. Raimondi and Pietrabissa used low loads in their test because without the protective load distribution of the meniscus, their specimens were being destroyed in the test. Interestingly, I had the same problem in the current study when I attempted to add a meniscectomy group. When the meniscus was removed, the osteochondral defect could no longer bear the applied loads and the defect walls collapsed and destroyed the specimen.

Another recent study in which the pressure footprint was measured after full thickness chondral defects were introduced is provided by Guettler, et al. This group tested knees in three different states; intact, chondral defect, and chondral defect with meniscectomy. The aim of the study was to determine the change in load distribution as the knee was put into 3, 6 or 9 degrees of varus. Similarly to the current study, K-Scan sensors (Tekscan , Boston) were used, however, the knee was tested at only one flexion angle, namely 30 degrees (Guettler et al. 2007). Again, it was reported that the introduction of a defect created stress concentrations around the rim, although in this

study it was shown that the peak stress increased in response. Thus, it would appear that the peak stress in response to a cartilage defect may increase or decrease in comparison to the intact condition depending on the flexion angle, the location of the defect and the magnitude of the load.

In the current study, anatomical specimens were used which will inevitably introduce variability into the results because each sheep knee does not have identical dimensions and geometry. Other causes of variability include the location of the defect or implant, which is likewise difficult to reproduce exactly between specimens. However, the main aim of this study was to determine the effect on the tibial condyle of having a defect or an implant in the femoral condyle and in particular to determine at which part of the gait cycle the load distribution throughout the joint is most susceptible to change. Another significant limitation is the low sample size of n=3 for the intact knee and 6mm defect, and only a single specimen for the 9mm defect and HemiCAP group. Availability of the implant was the main reason that only a single specimen was completed with the HemiCAP, which was also the same specimen with the 9mm defect. Whilst larger numbers would have made statistical analysis possible, this study was borne from having a single HemiCAP device spare and the current data is sufficient for an initial exploration of the joint pressure footprint.

The biggest difference in the peak joint stress occurred in test point 1, which corresponds to heel strike. At this point, the peak joint stress in the HemiCAP group was three times that of the normal knee, primarily due to point loading on the metallic device. This is also supported by the observation that the contact area was also the lowest for the HemiCAP group at that same point. The HemiCAP device was

associated with increased peak stress when compared to the normal knee in three out of four test points, whilst with the 6mm and 9mm defects, the peak stress was dependent on the angle, the force and the geometry of the specimen. Thus, bearing in mind the contradictory results of the Raimondi and Guettler papers, it would appear that there is no simple answer to whether a defect increases or decreases the magnitude of stress throughout the joint.

# 8. Conclusions

This dissertation reports a significant body of work in the research of an animal model of osteochondral defect healing. The initial plan for this thesis was to characterise a 6mm defect in the medial femoral condyle of a sheep, and then to develop an implant to treat said defect. However, during the characterization of that model it became evident that the published literature has a distinct lack of information on the method of creating that defect. Thus it was deemed important to spend considerable effort on fully characterising the osteochondral defect model and in particular to determine if differences existed between creating the defect with a punch or with a powered drill. Anecdotal evidence suggests that the field generally agreed that a high speed drill was a less than favourable method and one publication existed that evaluated the cell viability within osteochondral grafts that were harvested with either a powered trephine or a punch, which concluded that the punch was a far superior method in that application (Evans, Miniaci, & Hurtig 2004). This result shows that articular cartilage is susceptible to cellular damage from high speed, aggressive cutting instrumentation which is likely a result of local heat generation, although this remains unproven.

As such, it was expected that a defect created with a punch would likely preserve the health of the adjacent cartilage more than if a powered drill was used. Indeed, especially in the early time-points, the health of the cartilage adjacent to a punched defect was histologically superior to the drilled defect and furthermore there was a lower incidence of fibrous tissue within the defect. Hence the punch technique provides researchers with greater control of their in vivo evaluation of a specific treatment, at least in the early stages. This is favourable where the spontaneous healing effect is to be minimised, since any repair tissue is more likely to be a result

of the treatment administered rather than of spontaneous healing. Such control would allow the researcher to isolate the active component of their implant, which may be a tissue engineered implant, cultured cells or any other biological component such as growth factors which are most active in the early stages. This would come to be valuable information for future studies, where we can now recommend that an evaluation of any biological implant should first begin with an osteochondral defect created with a punch rather than a drill.

Another very interesting outcome from this study with 6mm osteochondral defects was that the defects were not healed even by 52 weeks. Neither the chondral nor osseous regions were healed, even though from macroscopic inspection they appeared to have had moderate success with time. The osseous regions were completely empty at 4 weeks, partially filled and occasionally with some reconsititution of the subchondral bone at 26 weeks. These are the same findings of Jackson et al in a similar goat model. At 52 weeks, the cancellous bone appeared well healed in 75% of cases based on histology, but more detailed examination by way of microCT showed that none of the defects were completely healed and that significant resorption was evident below the original defect. These findings highlight the importance of filling an osteochondral defect with an implant of similar biomechanical properties such as an osteochondral graft or a synthetic mimic. Thus, future work on this model could use the observation of deep bony resorption, or the lack thereof, as another indicator for failure, or success of the implant being evaluated. In other words, if a device is implanted into an osteochondral defect, then success of that device would be dependent, in part, in preventing the original defect from becoming deeper in response to Wolff's Law, or from fluid pressure-induced osteolysis.

Macroscopic observation of the tibial surface in the 4 week group did not reveal any immediately obvious damage in response to the femoral defect, however, when the animals in the designated 26 and 52 week groups were culled, the opportunity to examine the tibiae by macroscopic inspection and histology was taken. Histology revealed that the creation of a defect in the medial femoral condyle caused noticeable damage to the tibial articular cartilage in the area that articulated and shared load with the defect on the femur. At 26 weeks, the grading on the Mankin scale was approximately 6 (out of a possible 14, where 0 represents healthy tissues), which was reduced to approximately 4 in the 52 week group. This suggests that the tibial cartilage does have some capacity for self-renewal or repair. Another observation from this study was an increased incidence of subchondral bone thickening at 26 weeks when compared to the 52 week group. This observation may well tie in with the observed improvement in cartilage appearance histologically at 52 weeks since subchondral bone remodeling is known to accompany osteoarthrisis and other degenerations of articular cartilage (Radin & Rose 1986b). The observation of bone remodeling on the tibia provided the impetus for microCT analysis of the tibia in subsequent studies.

With the knowledge that a 6mm defect was not technically a critical size defect, it was decided to use a defect 9mm in diameter in the next study. This defect was then treated with a metallic resurfacing device which was hypothesised to restore the joint congruency without damaging the tibial articular cartilage surface. The device (HemiCAP, Arthrosurface, Franklin, MA) had previously been evaluated in a goat model that was criticized for being too weak, since the device was implanted into a pristine knee (Jackson, Lalor, Aberman, & Simon 2001). Therefore, we created a new

model in which a defect is created in the femoral condyle and left untreated for 5 weeks to start the degenerative processes throughout the knee. After five weeks, the joint was reoperated to implant the device and then the animals were culled at designated time-points of 6 or 26 weeks in addition to the original 5 weeks.

The outcome of this study was that the metallic resurfacing device did not protect the tibial surface from damage caused by the introduction of the femoral defect, although it did not exacerbate it either. We already learned that empty defects on the femur cause damage to the tibia, but it was something of a surprise to find that the damage from a metallic implant was similar in magnitude. Whether that damage was caused by abrasion or from differences in the load distribution across the joint could not be determined from this study. Another potential cause could be alterations in the fluid flow throughout the tissues. However, considering the preliminary clinical results which suggest that the HemiCAP device relieves pain and restores joint mobility, the result that the device did not accelerate or exacerbate the damage compared to leaving the defect untreated, is then a positive result.

In hindsight, this model could be further improved by adding a second defect type in addition to the osteochondral defect. From the data presented herein, it is impossible to know what affect a full-thickness defect, rather than an osteochondral defect would have on the tibial cartilage. A model in which a defect is made only in the cartilage, but not penetrating the subchondral bone would be worthwhile for several reasons. Firstly, fixation of the device would be more secure and may have prevented the implant loosening that was seen in one case, and secondly, the lack of blood borne signalling factors may have either a positive or negative effect on the opposing

cartilage on the tibia. Therefore, it would be worthwhile to repeat this study with a full thickness chondral defect, keeping all other factors the same as the current study.

This dissertation also acknowledges the important role that the subchondral bone plays in the progression of osteoarthritis and the value of those changes in predicting variation in load distribution through a joint with degenerative or acute trauma to the tissues. MicroCT is an effective and sensitive tool for quantifying small changes in cancellous bone properties, although the manual method of analysis is rather subjective and may lead to bias in the results. Hence, a semi-automated process was developed to remove as much of this subjectivity as possible. This was especially important in the measurement of subchondral bone thickness where defining the boundary between the subchondral bone and the underlying cancellous bone is completely subjective without defining some conditions. Chapter 6 outlines the analysis methodology that was used in Chapter 5 to come to the conclusion that significant and measureable remodelling was occurring in the tibial cancellous bone in response to the femoral defect and/or metallic device. No differences were detected between treatment groups at any time-point, however, the animals at 11 weeks had significant changes when compared to the 5 week animals. Although by the final time-point at 31 weeks, these significant differences had resolved back to baseline. This observation indicates that the tissues on the tibial proximal surface are experiencing an altered loading state in response to the defect and the implant, and this altered loading condition requires that the cancellous bone remodels to adapt. We also know that the damage to the cartilage begins quickly, because it was observed after only 5 weeks, so in this model at least the bony remodelling occurs after the fact. The histological appearance of the cartilage on the tibia was worst at 11 weeks, which

was also when the cancellous bone showed significant differences from other time-points. Hence, there appears to be a correlation between bone remodelling and cartilage degeneration in this osteochondral defect model.

Since the bone remodelling is likely due to variation in the physiological joint loading, a logical direction to continue exploring and characterising the osteochondral defect model, both with and without the resurfacing device was to measure the pressure footprint through the joint. This experiment first required that the physiological loads and flexion angles through the joint be identified and replicated, which had recently been published by Taylor, at al. For the current study, the normal sheep gait was represented by four discrete points and dynamic pressure sensors were inserted between the femoral condyle and the tibia/meniscus with the knee attached to a materials testing machine in a custom made jig. The contact pressure and area were recorded with varying flexion angle and load, according to the four discrete points of the gait cycle. While the sample size was small in this study, it did show conclusively that the metallic device increased both peak and average joint stress, especially at heel strike and at the point of maximum joint load.

Based on this result, it would be expected that the empty defect and the HemiCAP-treated defects from the in vivo study of Chapter 6 would show statistical differences in the cancellous bone, subchondral bone thickness or in the health of the cartilage. The current model was not able to discern significant differences within any single time-point which suggests that the measured differences in pressure distribution in response to the metallic device may not be large enough to cause damage to the

opposing surface. It is possible that the variation in load may start to elicit changes and degradation with significant advancement of time, although it would be unlikely since the bony changes at 11 weeks had almost resolved to baseline by 31 weeks, and since the health of the cartilage was improved at 31 weeks in comparison to 11 weeks. Therefore, it would be recommended to run an animal model out to 5 years to truly understand the biological mechanisms and to definitively evaluate the benefit of the metallic resurfacing device.

Overall, this dissertation has provided a strong characterisation of two osteochondral defect models with an area of focus not only on the femoral defect, but additionally on the tibia and meniscus. Whenever an effort is made to treat a condition in one discrete location on the body, that effort must not be made at the expense of another. Therefore, when a device is implanted in the femoral condyle to treat a focal cartilage lesion, the scientist and the surgeon must also acknowledge the potential effects on the tibia and meniscus, since in the end, it is the health of the entire joint that must be protected for the patient to have satisfactory clinical outcomes.

Aamer, K. A., Sardinha, H., Bhatia, S. R., & Tew, G. N. 2004, "Rheological studies of PLLA-PEO-PLLA triblock copolymer hydrogels", *Biomaterials*, vol. 25, no. 6, pp. 1087-93.

Altman, R. D., Akermark, C., Beaulieu, A. D., & Schnitzer, T. 2004, "Efficacy and safety of a single intra-articular injection of non-animal stabilized hyaluronic acid (NASHA) in patients with osteoarthritis of the knee", *Osteoarthritis.Cartilage.*, vol. 12, no. 8, pp. 642-649.

Altman, R. D. & Moskowitz, R. 1998, "Intraarticular sodium hyaluronate (Hyalgan) in the treatment of patients with osteoarthritis of the knee: a randomized clinical trial. Hyalgan Study Group", *J.Rheumatol.*, vol. 25, no. 11, pp. 2203-2212.

Appleyard, R. C., Burkhardt, D., Ghosh, P., Read, R., Cake, M., Swain, M. V., & Murrell, G. A. 2003, "Topographical analysis of the structural, biochemical and dynamic biomechanical properties of cartilage in an ovine model of osteoarthritis", *Osteoarthritis and Cartilage*, vol. 11, no. 1, pp. 65-77.

Appleyard, R. C., Swain, M. V., Khanna, S., & Murrell, G. A. 2001, "The accuracy and reliability of a novel handheld dynamic indentation probe for analysing articular cartilage", *Phys Med Biol*, vol. 46, no. 2, pp. 541-550.

Ara, M., Watanabe, M., & Imai, Y. 2002, "Effect of blending calcium compounds on hydrolytic degradation of poly(DL-lactic acid-co-glycolic acid)", *Biomaterials*, vol. 23, no. 12, pp. 2479-83.

Armstrong, C. G. & Mow, V. C. 1982, "Variations in the intrinsic mechanical properties of human articular cartilage with age, degeneration, and water content", *J Bone Joint Surg Am*, vol. 64, no. 1, pp. 88-94.

Armstrong, S. J., Read, R., & Price, R. 1995, "Topographical variation within the articular carilage and subchondral bone of the normal ovine knee joint: a histological approach", *Osteoarthritis and Cartilage*, vol. 5, pp. 25-33.

Aspenberg, P. & Van, d., V 1998, "Fluid pressure may cause periprosthetic osteolysis. Particles are not the only thing", *Acta Orthop.Scand.*, vol. 69, no. 1, pp. 1-4.

ASTM. F 2451-05 Standard guide for in vivo assessment of implantable devices intended to repair or regenerate articular cartilage. 2005. Ref Type: Generic

Awad, H. A., Wickham, M. Q., Leddy, H. A., Gimble, J. M., & Guilak, F. 2004, "Chondrogenic differentiation of adipose-derived adult stem cells in agarose, alginate and gelatin scaffolds", *Biomaterials*, vol. 2004, no. 25, p. 16.

Baltzopoulos, V. 1995, "Muscular and tibiofemoral joint forces during isokinetic concentric knee extension", *Clin.Biomech.(Bristol., Avon.)*, vol. 10, no. 4, pp. 208-214.

Barrett, W. P. & Scott, R. D. 1987, "Revision of failed unicondylar unicompartmental knee arthroplasty", *J.Bone Joint Surg.Am.*, vol. 69, no. 9, pp. 1328-1335.

Bartlett, W., Skinner, J. A., Gooding, C. R., Carrington, R. W., Flanagan, A. M., Briggs, T. W., & Bentley, G. 2005, "Autologous chondrocyte implantation versus matrix-induced autologous chondrocyte implantation for osteochondral defects o fthe knee: a prospective, randomised study", *J Bone Joint Surg Br*, vol. 87, no. 5, pp. 640-5.

Bentley, G., Biant, L. C., Carrington, R. W., Akmal, M., Goldberg, A., Williams, A. M., Skinner, J. A., & Pringle, J. 2003, "A prospective, randomised comparison of autologous chondrocyte implantation versus mosaicplasty for osteochondral defects in the knee", *J Bone Joint Surg Am*, vol. 85, no. 2, pp. 223-30.

Braman, J. P., Bruckner, J. D., Clark, J. M., Norman, A. G., & Chansky, H. A. 2005, "Articular cartilage adjacent to experimental defects is subject to atypical strains", *Clin Orthop Relat Res* no. 430, pp. 202-7.

Breinan, H., Minas, T., Hsu, H., Nehrer, S., Sledge, C., & Spector, M. 1997, "Effect of cultured autologous chondrocytes on repair of chondral defects in a canine model", *J Bone Joint Surg Am.*, vol. 79, no. 10, pp. 1439-51.

Brittberg, M., Lindahl, A., Nilsson, A., Ohlsson, C., Isaksson, O., & Peterson, L. 1994, "Treatment of deep cartilage defects in the knee with autologous chondrocyte transplantation", *N Engl J Med*, vol. 331, no. 14, pp. 889-95.

Brittberg, M., Nilsson, A., Lindahl, A., Ohlsson, C., & Peterson, L. 1996, "Rabbit articular cartilage defects treated with autologous cultured chondrocytes", *Clin Orthop Relat Res*, vol. May, no. 326, pp. 270-83.

Broom, N. D. & Oloyede, A. 1998, "The importance of physicochemical swelling in cartilage illustrated with a model hydrogel system", *Biomaterials*, vol. 19, no. 13, pp. 1179-88.

Brown, T. D., Pope, D. F., Hale, J. E., Buckwalter, J. A., & Brand, R. A. 1991, "Effects of osteochondral defect size on cartilage contact stress", *J.Orthop.Res.*, vol. 9, no. 4, pp. 559-567.

Bryant, S. J. & Anseth, K. S. 2001, "The effects of scaffold thickness on tissue engineered cartilage in photocrosslinked poly(ethylene oxide) hydrogels", *Biomaterials*, vol. 22, no. 6, pp. 619-26.

Bryant, S. J., Anseth, K. S., Lee, D. A., & Bader, D. L. 2004, "Crosslinking density influences the morphology of chondrocytes photoencapsulated in PEG hydrogels during the application of compressive strain", *J Orthop Res*, vol. 22, no. 5, pp. 1143-9.

Buckwalter, J. A. 2002, "Articular cartilage injuries", *Clin Orthop Relat Res*, vol. 402, pp. 21-37.

Buckwalter, J. A., Kuettner, K. E., & Thonar, E. J. 1985, "Age-related changes in articular cartilage proteoglycans: electron microscopic studies", *J.Orthop.Res.*, vol. 3, no. 3, pp. 251-257.

Burks, R., Greis, P., Arnoczky, S., & Scher, C. 2006, "The use of a single osteochondral autograft plug in the treatment of a large osteochondral lesion in the femoral condyle: an experimental study in sheep", *Am J Sports Med.*, vol. 34, no. 2, pp. 247-55.

Cain, E. L. & Clancy, W. G. 2001, "Treatment algorithm for osteochondral injuries of the knee", *Clin.Sports Med.*, vol. 20, no. 2, pp. 321-342.

Cake, M. A., Read, R. A., Guillou, B., & Ghosh, P. 2000, "Modification of articular cartilage and subchondral bone pathology in an ovine meniscectomy model of osteoarthritis by avocado and soya unsaponifiables (ASU)", *Osteoarthritis.Cartilage.*, vol. 8, no. 6, pp. 404-411.

Carranza-Bencano, A., Perez-Tinao, M., Ballesteros-Vazquez, P., Armas-Padron, J. R., Hevia-Alonso, A., & Crespo, F. M. 1999, "Comparative study of the reconstruction of articular cartilage defects with free costal perichondrial grafts and free tibial periosteal grafts: An experimental study on rabbits", *Calcified Tissue Int*, vol. 65, pp. 402-7.

Caterson, E. J., Nesti, L. J., Li, W. J., Danielson, K. G., Albert, T. J., Vaccaro, A. R., & Tuan, R. S. 2001, "Three-dimensional cartilage formation by bone marrow-derived cells seeded in polylactide/alginate amalgam", *J Biomed Mater Res*, vol. 57, no. 3, pp. 394-403.

Chacon, G., Bower, D., Larsen, P., McGlumphy, E., & Beck, F. 2006, "Heat production by 3 implant drill systems after repeated drilling and sterilization", *J Oral Maxillofac Surg*, vol. 64, no. 2, pp. 265-9.

Chang, P. C., Pradhan, R. M., Mitra, A. K., Sim, C. S., & Tay, B. K. 1999, "The results of autogenous tibial periosteal transplants for full thickness cartilage defects in the knee joints of pigs", *Ann Acad Med Singapore*, vol. 28, no. 1, pp. 8-14.

Chen, G., Sato, T., Ushida, T., Ochiai, N., & Tateishi, T. 2004, "Tissue engineering of cartilage using a hybrid scaffold of synthetic polymer and collagen", *Tissue Eng*, vol. 10, no. 3-4, pp. 323-30.

Clar, C., Cummins, E., McIntyre, L., Thomas, S., Lamb, J., Bain, L., Jobanputra, P., & Waugh, N. 2005, "Clinical and cost-effectiveness of autologous chondrocyte implantation for cartilage defects in knee joints" systematic review and economic evaluation", *Health Technol Assess*, vol. 9, no. 47, pp. 1-82.

Cohen, S. B., Meirisch, C. M., Wilson, H. A., & Diduch, D. R. 2003, "The use of absorbable co-polymer pads with alginate and cells for articular cartilage repair in rabbits", *Biomaterials*, vol. 24, no. 15, pp. 2653-60.

Coutts, R. D., Healey, R. M., Ostrander, R., Sah, R. L., Goomer, R., & Amiel, D. 2001, "Matrices for cartilage repair", *Clin Orthop Relat Res* no. 391 Suppl, pp. 271-9.

Custers, R. J. H., Dhert, W. J. A., van Rijen, M. H. P., Verbout, A. J., Creemers, L. B., & Saris, D. B. F. 2007, "Articular damage caused by metal plugs in a rabbit model for treatment of localized cartilage defects", *Osteoarthritis and Cartilage.*

Dahlberg, L. & Kreicbergs, A. 1991, "Demineralized allogeneic bone matrix for cartilage repair", *J Orthop Res*, vol. 9, no. 1, pp. 11-9.

Dekel, S. & Weissman, S. L. 1978, "Joint changes after overuse and peak overloading of rabbit knees in vivo", *Acta Orthop Scand*, vol. 49, pp. 519-528.

Ding, C., Cicuttini, F., Scott, F., Glisson, M., & Jones, G. 2003, "Sex differences in knee cartilage volume in adults: role of body and bon esize, age and physical activity", *Rheumatology (Oxford)*, vol. 42, no. 11, pp. 1317-23.

Dorotka, R., Windberger, U., Macfelda, K., Bindreiter, U., Toma, C., & Nehrer, S. 2005, "Repair of articular cartilage defects treated by microfracture and a three-dimensional collagen matrix", *Biomaterials*, vol. 26, no. 17, pp. 3617-29.

Elisseeff, J., McIntosh, W., Fu, K., Blunk, B. T., & Langer, R. 2001, "Controlled-release of IGF-I and TGF-beta1 in a photopolymerizing hydrogel for cartilage tissue engineering", *J Orthop Res*, vol. 19, no. 6, pp. 1098-104.

Evans, P. J., Miniaci, A., & Hurtig, M. B. 2004, "Manual punch versus power harvesting of osteochondral grafts", *Arthroscopy*, vol. 20, no. 3, pp. 306-10.

Falez, F. & Sciarretta, F. V. 2005, "Treatment of osteochondral symptomatic defects of the knee with SaluCartilage", *J Bone Joint Surg Br*, vol. 87-B, p. S202.

Fisher, J. P., Jo, S., Mikos, A. G., & Reddi, A. H. 2004, "Thermoreversible hydrogel scaffolds for articular cartilage engineering", *J Biomed Mater Res A*, vol. 71, no. 2, pp. 268-74.

Frenkel, S. R., Bradica, G., Brekke, J. H., Goldman, S. M., Ieska, K., Issack, P., Bong, M. R., Tian, H., Gokhale, J., Coutts, R. D., & Kronengold, R. T. 2005, "Regeneration of articular cartilage - Evaluation of osteochondral defect repair in the rabbit using multiphasic implants", *Osteoarthritis Cartilage*, vol. 13, no. 9, pp. 798-807.

Frenkel, S. R. & Di Cesare, P. E. 1999, "Degradation and repair of articular cartilage", *Front in Biosci*, vol. 4D, pp. 671-685.

Furukawa, T., Eyre, D. R., Koide, S., & Gilmcher, M. J. 1980, "Biochemical studies on repair cartilage resurfacing. Experimental results in the rabbit knee", *J Bone Joint Surg Am*, vol. 62, pp. 79-89.

Gao, J., Knaack, D., Goldberg, V. M., & Caplan, A. I. 2004, "Osteochondral defect repair by demineralized cortical bone matrix", *Clin Orthop Relat Res* no. 427 Suppl, pp. 62-6.

Grande, D. A., Pitman, M. I., Peterson, L., Menche, D., & Klein, M. 1989, "The repair of experimentally produced defects in rabbit articular cartilage by autologous chondrocyte transplantation", *J Orthop Res*, vol. 7, no. 2, pp. 208-18.

Gratz, K. R., Wong, V. W., Chen, A. C., Fortier, L. A., Nixon, A. J., & Sah, R. L. 2006, "Biomechanical assessment of tissue retrieved after in vivo cartilage defect repair: tensile modulus of repair tissue and integration with host cartilage", *J Biomech*, vol. 39, no. 1, pp. 138-46.

Gray, H. 1918, *Anatomy of the Human Body* Bartleby.

Grigolo, B., Roseti, L., Fiorini, M., Fini, M., Giavaresi, G., Aldini, N. N., Giardino, R., & Facchini, A. 2001, "Transplantation of chondrocytes seeded on a hyaluronan derivative (hyaff-11) into cartilage defects in rabbits", *Biomaterials*, vol. 22, no. 17, pp. 2417-24.

Guettler, J., Glisson, R., Stubbs, A., Jurist, K., & Higgins, L. 2007, "The triad of varus malalignment, meniscectomy, and chondral damage: a biomechanical explanation for joint degeneration", *Orthopedics*, vol. 30, no. 7, pp. 558-566.

Guilak, F., Butler, D. L., & Goldstein, S. A. 2001, "Functional tissue engineering: the role of biomechanics in articular cartilage repair", *Clin Orthop Relat Res* no. 391 Suppl, pp. 295-305.

Guo, X., Wang, C., Zhang, Y., Xia, R., Hu, M., Duan, C., Zhao, Q., Dong, L., Lu, J., & Qing Song, Y. 2004, "Repair of large articular cartilage defects with implants of autologous mesenchymal stem cells seeded into beta-tricalcium phosphate in a sheep model", *Tissue Eng*, vol. 10, no. 11-12, pp. 1818-29.

Hall, B. K. & Newman, S. 1991, *Cartilage: Molecular Aspects* CRC Press, Boston.

Harman, B. D., Weeden, S. H., Lichota, D. K., & Brindley, G. W. 2006, "Osteochondral autograft transplantation in the porcine knee", *Amer J Sports Med*, vol. 34, no. 6, pp. 913-8.

Harrington, K. D. 1992, "Long-term results for the McKeever patellar resurfacing prosthesis used as a salvage procedure for severe chondromalacia patellae", *Clin.Orthop.Relat Res.* no. 279, pp. 201-213.

Harris, M. L., Morberg, P., Bruce, W. J. M., & Walsh, W. R. 1999, "An improved method for measuring tibiofemoral contact areas in total knee arthroplasty: a comparison of K-scan sensor and Fuji film", *J Biomech*, vol. 32, pp. 951-958.

Hayes, W. C., Keer, L. M., Herrmann, G., & Mockros, L. F. 1972, "A mathematical analysis for indentation tests of articular cartilage", *J Biomech*, vol. 5, no. 5, pp. 541-51.

Hodge, W. A. 1991, "Vitallium-mold arthroplasty of the knee. A case report with 30-year follow-up study", *J.Arthroplasty*, vol. 6, no. 3, pp. 195-197.

Hoffman, A. S. 2002, "Hydrogels for biomedical applications", *Adv Drug Deliv Rev*, vol. 54, no. 1, pp. 3-12.

Homminga, G. N., Bulstra, S. K., Bouwmeester, P. S., & van der Linden, T. J. 1990, "Perichondrial grafting for cartilage lesions of the knee", *J Bone Joint Surg Br*, vol. 72B, pp. 1003-7.

Horas, U., Pelinkovic, D., Herr, G., Ainger, T., & Schnettler, R. 2003, "Autologous chondrocyte implantation and osteochondral cylinder transplantation in cartilage repair of the knee joint. A prospective, comparative trial", *J Bone Joint Surg Am*, vol. 85, no. 2, pp. 185-92.

Hunter, W. 1743, "On the structure and diseases of articulating cartilages", *Philos.Trans.Roy.Soc.*, vol. 42(B), pp. 514-521.

Huntley, J., McBirnie, J., Simpson, A., & Hall, A. 2005, "Cutting-edge design to improve cell viability in osteochondral grafts", *Osteoarthritis Cartilage*, vol. 13, pp. 665-671.

Hunziker, E. B. 1999a, "Articular cartilage repair: are the intrinsic biological constraints undermining this process insuperable?", *Osteoarthritis Cartilage*, vol. 7, no. 1, pp. 15-28.

Hunziker, E. B. 1999b, "Biologic repair of articular cartilage. Defect models in experimental animals and matrix requirements", *Clin Orthop Relat Res* no. 367 Suppl, pp. 135-46.

Hunziker, E. B. 2001, "Growth-factor induced healing of partial-thickness defects in adult articular cartilage", *Osteoarthritis and Cartilage*, vol. 9, no. 1, pp. 22-32.

Hunziker, E. B. 2002, "Articular cartilage repair: basic science and clinical progress. A review of the current status and prospects", *Osteoarthritis Cartilage*, vol. 10, no. 6, pp. 432-63.

Hunziker, E. B., Driesand, I. M., & Morris, E. A. 2001, "Chondrogenesis in cartilage repair is induced by members of the transforming growth factor-beta superfamily", *Clin Orthop*, vol. 391, pp. 171-181.

Huskisson, E. C. & Donnelly, S. 1999, "Hyaluronic acid in the treatment of osteoarthritis of the knee", *Rheumatology.(Oxford)*, vol. 38, no. 7, pp. 602-607.

Insall, J. N. 1967, "Intra-articular surgery for degenerative arthritis of the knee. A report of the late K. H. Pridie", *J Bone Joint Surg Br*, vol. 49-B, pp. 211-28.

Insall, J. N. 1974, "The Pridie debridement operation for osteo-arthritis of the knee", *Clin Orthop*, vol. 101, pp. 61-7.

Jackson, D. W., Lalor, P. A., Aberman, H. M., & Simon, T. M. 2001, "Spontaneous repair of full-thickness defects of articular cartilage in a goat model. A preliminary study", *J Bone Joint Surg Am*, vol. 83-A, no. 1, pp. 53-64.

Johnstone, B., Hering, T. M., Caplan, A. I., & Goldberg, V. M. 1998, "In vitro chondrogenesis of bone marrow-derived mesenchymal progenitor cells", *Exp Cell Res*, vol. 238, no. 1, pp. 265-72.

Kangarlu, A. & Gahunia, H. K. 2006, "Magneitic resonance imaging characterization of osteochondral defect repair in a goat model at 8T", *Osteoarthritis and Cartilage*, vol. 14, no. 1, pp. 52-62.

Kellis, E. 2001, "Tibiofemoral joint forces during maximal isokinetic eccentric and concentric efforts of the knee flexors", *Clin.Biomech.(Bristol., Avon.)*, vol. 16, no. 3, pp. 229-236.

Kim, H. K. W., Moran, M. E., & Salter, R. B. 1991, "The potential for regeneration of articular cartilage in defects created by chondral shaving and subchondral abrasion- an experimental investigation in rabbits", *J Bone Joint Surg Am*, vol. 73, pp. 1301-15.

Kirker-Head, C. A., Van Sickle, D. C., Ek, S., & McCool, J. C. 2006, "Safety of, and biological and finctional response to, a novel metallic implant for the management of focal full-thickness cartilage defects: Preliminary assessment in an animal model out to 1 year", *J Orthop Res*, vol. 24, pp. 1095-1108.

Klompmaker, J., Jansen, H., Veth, R. P., Nielsen, H., & de Groot, J. H. 1992, "Porous polymer implants for repair of full-thickness defects of articular cartilage: an experimental study in rabbit and dog", *Biomaterials*, vol. 13, pp. 625-634.

Knutsen, G., Endebretsen, L., Ludvigsen, T. C., Drogset, J. O., Grontvedt, T., Solheim, E., Strand, T., Roberts, S., Isaksen, V., & Johansen, O. 2004, "Autologous chondrocyte implantation compared with microfracture in the knee. A randomized trial", *J Bone Joint Surg Am*, vol. 86, no. 3, pp. 455-64.

Kuroki, H., Nakagawa, Y., Mori, K., Kobayashi, M., Okamoto, Y., Yasura, K., Nishitani, K., & Nakamura, T. 2007, "Sequential changes in implanted cartilage after autologous osteochondral transplantation: postoperative acoustic properties up to 1 year in an in vivo rabbit model", *Arthroscopy*, vol. 23, no. 6, pp. 647-54.

Lange, J., Follak, N., Nowotny, T., & Merk, H. 2006, "[Results of SaluCartilage implantation for stage IV chondral defects in the knee joint area]", *Unfallchirurg*, vol. 109, no. 3, pp. 193-199.

Laprell, H. & Peterson, W. 2001, "Autologous osteochondral transplantation using the diamon bone-cutting system: 6-12 years' follow-up on 35 patients with osteochondral defects at the knee joint", *Arch Orthop Trauma Surg*, vol. 121, pp. 248-53.

Lee, C. S., Gleghorn, J. P., Won Choi, N., Cabodi, M., Stroock, A. D., & Bonassar, L. J. 2007, "Integration of layered chondrocyte seeded alginate hydrogel scaffolds", *Biomaterials*, vol. 28, no. 19, pp. 2987-93.

Livesley, P., Doherty, M., Needoff, M., & Moulton, A. 1991, "Arthroscopic lavage of osteoarthritic knees", *J Bone Joint Surg Br*, vol. 73-B, pp. 922-6.

Lu, L., Zhu, X., Valenzuela, R. G., Currier, B. L., & Yaszemski, M. J. 2001, "Biodegradable polymer scaffolds for cartilage tissue engineering", *Clin Orthop Relat Res* no. 391 Suppl, pp. 251-70.

Mackay, A. M., Beck, S. C., Murphy, J. M., Barry, F. P., Chichester, C. O., & Pittenger, M. F. 1998, "Chondrogenic differentiation of cultured human mesenchymal stem cells from marrow", *Tissue Eng*, vol. 4, no. 4, pp. 415-28.

Mandelbaum, B., Browne, J. E., Fu, F., Micheli, L. J., Moseley, J. B., Erggelet, C., & Anderson, A. F. 2007, "Treatment outcomes of autologous chondrocyte implantation for full-thickness articular cartilage defects of the trochlea", *Amer J Sports Med.*

Mankin, H. J. 1982, "The response of articular cartilage to mechanical injury", *J Bone Joint Surg Am*, vol. 64, no. 3, pp. 460-6.

Mankin, H. J., Mow, V. C., & Buckwalter, J. A. 2000, "Chapter 18: Articular cartilage repair and osteoarthritis," in *Orthopedic Basic Science.*

Mankin, H. J., Mow, V. C., Buckwalter, J. A., Iannotti, J. P., & Ratcliffe, A. 2000, "Chapter 17: Articular cartilage structure, composition, and, function," in *Orthopedic Basic Science*.

Marcacci, M., Berruto, M., Brocchetta, D., Delcogliano, A., Ghinelli, D., Gobbi, A., Kon, E., Pederzini, L., Rosa, D., Sacchetti, G. L., Stefani, G., & Zanasi, S. 2005, "Articular Cartilage Engineering with Hyalograft(R) C: 3-Year Clinical Results", *Clin Orthop Relat Res* no. 435, pp. 96-105.

Marcacci, M., Zaffagnini, S., Kon, E., Visani, A., Iacono, F., & Loreti, I. 2002, "Arthroscopic autologous chondrocyte transplantation: technical note", *Knee Surg Sports Traumatol Arthrosc*, vol. 10, no. 3, pp. 154-9.

Miller, B. S., Joseph, T. A., Barry, E. M., Rich, V. J., & Sterett, W. I. 2007, "Patient satisfaction after medial opening high tibial osteotomy and microfracture", *J Knee Surg*, vol. 20, no. 2, pp. 129-33.

Miniaci, A. & Martineau, P. A. 2007, "Technical aspects of osteochondral autograft transplantation", *Instr Course Lect*, vol. 56, pp. 447-55.

Mitchell, N. & Shepard, N. 1987, "Effect of patellar shaving in the rabbit", *J Orthop Res*, vol. 5, pp. 388-92.

Morisset, S., Frisbie, D. D., Robbins, P. D., Nixon, A. J., & McIlwraith, C. W. 2007, "IL-1ra/IGF-1 gene therapy modulates repair of microfractured chondral defects", *Clin Orthop Relat Res*.

Mow, V. C., Proctor, C. S., & Kelly, M. A. 1989, "Biomechancis of articular cartilage," in *Basic Biomechanics of the Musculoskeletal System*, M. Nordin & V. H. Frankel, eds., Lea & Febinger, Philadelphia.

Mow, V. C. & Ratcliffe, A. 1997, "Structure and function of articular cartilage and meniscus," in *Basic orthopedic biomechanics*, 2nd edn, V. C. Mow & W. C. Hayes, eds., Lippincott-Raven Publishers, Philadelphia.

Mow, V. C. & Wang, C. C. 1999, "Some bioengineering considerations for tissue engineering of articular cartilage", *Clin Orthop Relat Res* no. 367 Suppl, pp. 204-23.

Nehrer, S., Domayer, S., Dorotka, R., Schatz, K., Bindreiter, U., & Kotz, R. 2005, "Three-year clinical outcome after chondrocyte transplantation using a hyaluronan matrix for cartilage repair", *Eur J Radiol.*

Nigg, B. M. & Herzog, W. 1998, *Biomechanics of the musculo-skeletal system*, Second edn, John Wiley & Sons, West Sussex.

O'Driscoll, S. W. 1998, "The healing and regeneration of articular cartilage", *J Bone Joint Surg Am*, vol. 80, no. 12, pp. 1795-812.

O'Driscoll, S. W., Keeley, F. W., & Salter, R. B. 1986, "The chondrogenic potential of free autogenous periosteal grafts for biological resurfacing of major full-thickness defects in joint surfaces under the influence of continuous passive motion. An experimental investigation in the rabbit", *J Bone Joint Surg Am*, vol. 68, no. 7, pp. 1017-35.

Panula, H. E., Helminen, H. J., & Kiviranta, I. 1997, "Slowly progressive osteoarthritis after tibial valgus osteotomy in young beagle dogs", *Clin Orthop*, vol. 343, pp. 192-202.

Park, G. E., Pattison, M. A., Park, K., & Webster, T. J. 2005, "Accelerated chondrocyte functions on NaOH-treated PLGA scaffolds", *Biomaterials*, vol. 26, no. 16, pp. 3075-82.

Pearce, S. G., Hurtig, M. B., Clarnette, R., Kalra, M., Cowan, B., & Miniaci, A. 2001, "An investigation of 2 techniques for optimizing joint surface congruency using multiple cylindrical osteochondral autografts", *Arthroscopy*, vol. 17, no. 1, pp. 50-5.

Peretti, G., Randolph, M., Zaporojan, V., Bonassar, L., Xu, J., Fellers, J., & Yaremchuk, M. 2001, "A biochemical analysis of an engineered cell-scaffold implant for cartilage repair", *Ann Plast Surg.*, vol. 46, no. 5, pp. 533-7.

Petrella, R. J. & Petrella, M. 2006, "A prospective, randomized, double-blind, placebo controlled study to evaluate the efficacy of intraarticular hyaluronic acid for osteoarthritis of the knee", *J.Rheumatol.*, vol. 33, no. 5, pp. 951-956.

Poole, A. R., Kojima, T., Yasuda, T., Mwale, F., Kobayashi, M., & Laverty, S. 2001, "Composition and structure of articular cartilage: a template for tissue repair", *Clin Orthop Relat Res* no. 391 Suppl, pp. 26-33.

Radin, E. L. & Rose, R. M. 1986a, "Role of subchondral bone in the initiation and progression of cartilage damage", *Clin.Orthop.Relat Res.* no. 213, pp. 34-40.

Radin, E. L. & Rose, R. M. 1986b, "Role of subchondral bone in the initiation and progression of cartilage damage", *Clin.Orthop.Relat Res.* no. 213, pp. 34-40.

Rahfoth, B., Weisser, J., Sternkopf, F., Aiger, T., von der Mark, K., & Brauer, R. 1998, "Transplantation of allograft chondrocytes embedded in agarose gel into cartilage defects of rabbits", *Osteoarthritis and Cartilage*, vol. 6, no. 1, pp. 50-65.

Raimondi, M. T. & Pietrabissa, R. 2005, "Contact pressures at grafted cartilage lesions in the knee", *Knee Surg Sports Traumatol Arthrosc*, vol. 13, no. 6, pp. 444-50.

Sah, R. L. 2001, "Introduction to bioengineering," in *Advanced series in biomechanics*, Y. C. Fung, ed., World Scientific, Singapore.

Sakaguchi, Y., Sekiya, I., Yagishita, K., & Muneta, T. 2005, "Comparison of human stem cells derived from various mesenchymal tissues: superiority of synovium as a cell source", *Arthritis Rheum*, vol. 52, no. 8, pp. 2521-9.

Schindler, O. S. 2007, "Osteochondritis dissecans of the knee", *Current Orthopaedics*, vol. 21, pp. 47-58.

Schneider, U., Schlegel, U., Bauer, S., & Siebert, C. 2003, "Molecular markers in the evaluation of autologous chondrocyte implantation", *Arthroscopy*, vol. 19, no. 4, pp. 397-403.

Schreiber, R. E., Ilten-Kirby, B. M., Dunkelman, N. S., Symons, K. T., Rekettye, L. M., Willoughby, J., & Ratcliffe, A. 1999, "Repair of osteochondral defects with allogenic tissue engineered cartilage implants", *Clin Orthop Relat Res*, vol. 369, pp. 382-95.

Sellers, R. S., Zhang, R., Glasson, S., Kim, H. D., Peluso, D., D'Augusta, D. A., Beckwith, K., & Morris, E. A. 2000, "Repair of articular cartilage defects one year

after treatment with recombinant human morphogenetic protein-2", *J Bone Joint Surg Am*, vol. 82-A, no. 2, pp. 151-160.

Shapiro, F., Koide, S., & Glimcher, M. J. 1993, "Cell origin and differentiation in the repair of full-thickness defects of articular cartilage", *J Bone Joint Surg Am*, vol. 75, no. 4, pp. 532-53.

Shelbourne, K. D., Jari, S., & Gray, T. 2003, "Outcome of untreated traumatic articular cartilage defects of the knee", *J Bone Joint Surg Am*, vol. 85, pp. 8-16.

Sherwood, J. K., Riley, S. L., Palazzolo, R., Brown, S. C., Monkhouse, D. C., Coates, M., Griffith, L. G., Landeen, L. K., & Ratcliffe, A. 2002, "A three-dimensional osteochondral composite scaffold for articular cartilage repair", *Biomaterials*, vol. 23, no. 24, pp. 4739-51.

Siguier, T., Siguier, M., Judet, T., Charnley, G., & Brumpt, B. 2001, "Partial resurfacing arthroplasty of the femoral head in avascular necrosis. Methods, indications, and results", *Clin.Orthop.Relat Res.* no. 386, pp. 85-92.

Steadman, J., Rodkey, W., Briggs, K., & Rodrigo, J. 1999, "The microfracture technique in the management of complete defects in the knee joint", *Orthopedics*, vol. 1999, no. 28.

Sun, D. D., Guo, X. E., Likhitpanichkul, M., Lai, W. M., & Mow, V. C. 2004, "The influence of the fixed negative charges on mechanical and electrical behaviors of articular cartilage under unconfined compression", *J Biomech Eng*, vol. 126, no. 1, pp. 6-16.

Szerb, I., Hangody, L., Duska, Z., & Kaposi, N. P. 2005, "Mosaicplasty: Long term follow up", *Bull Hosp Jt Dis*, vol. 63, no. 1-2, pp. 54-62.

Taylor, W. R., Ehrig, R. M., Heller, M. O., Schell, H., Seeback, P., & Duda, G. N. 2006, "Tibio-femoral joint forces in sheep", *J Biomech*, vol. 39, no. 5, pp. 791-8.

Taylor, W. R., Heller, M. O., Bergmann, G., & Duda, G. N. 2004, "Tibio-femoral loading during human gait and stair climbing", *J.Orthop.Res.*, vol. 22, no. 3, pp. 625-632.

Tibesku, C. O., Szuwart, T., Kleffner, T. O., Schlegel, P. M., Jahn, U. R., Van Aken, H., & Fuchs, S. 2004, "Hyaline cartilage degenerates after autologous osteochondral transplantation", *J Orthop Res*, vol. 22, no. 6, pp. 1210-4.

Uematsu, K., Hattori, K., Ishimoto, Y., Yamauchi, J., Habata, T., Takakura, Y., Ohgushi, H., Fukuchi, T., & Sato, M. 2005, "Cartilage regeneration using mesenchymal stem cells and a three-dimensional poly-lactic-glycolic acid (PLGA) scaffold", *Biomaterials*, vol. 26, no. 20, pp. 4273-9.

Ushio, K., Oka, M., Hyon, S. H., Hayami, T., Yura, S., Matsumura, K., Toguchida, J., & Nakamura, T. 2004, "Attachment of artificial cartilage to underlying bone", *J Biomed Mater Res B Appl Biomater*, vol. 68, no. 1, pp. 59-68.

van den Berg, W., van der Kraan, P., Scharstuhl, A., & van Beuningen, H. 2001, "Growth factors and cartilage repair", *Clin Orthop Relat Res*, vol. Oct, no. 391 Suppl, pp. 244-50.

Van, d., V, Aspenberg, P., Marti, R. K., Tigchelaar, W., & Van Noorden, C. J. 1998, "Fluid pressure causes bone resorption in a rabbit model of prosthetic loosening", *Clin.Orthop.Relat Res.* no. 350, pp. 201-208.

Vince, K. G. & Cyran, L. T. 2004, "Unicompartmental knee arthroplasty: new indications, more complications?", *J.Arthroplasty*, vol. 19, no. 4 Suppl 1, pp. 9-16.

Vizesi, F., Oliver, R., Gothelf, T., Smitham, P., Yu, Y., & Walsh, W. R. "Untreated osteochondral defects degrade the opposing tibial articular cartilage surface", in *Orthopaedic Research Society.*

Vizesi, F., Oliver, R., Smitham, P., Gothelf, T., Yu, Y., & Walsh, W. R. 2007b, "Influence of surgical preparation on the in vivo response of osteochondral defects", *J Eng Medicine.*

Wakitani, S., Goto, T., Pineda, S. J., Young, R. G., Mansour, J. M., Caplan, A. I., & Goldberg, V. M. 1994, "Mesenchymal cell based repair of large, full-thickness defects of articular cartilage", *J Bone Joint Surg Am*, vol. 76, no. 4, pp. 579-592.

Wakitani, S., Kimura, T., Hirooka, A., Ochi, T., Yoneda, M., Yasui, N., Owaki, H., & Ono, K. 1989, "Repair of rabbit articular surfaces with allograft chondrocytes embedded in collagen gel", *J Bone Joint Surg Br*, vol. 71, no. 1, pp. 74-80.

Walsh, W. R. & Christiansen, D. L. 1995, "Demineralized bone matrix as a template for mineral-organic composites", *Biomaterials*, vol. 16, pp. 1363-71.

Wight, T. N. & Heinegard, D. K. 1991, "Cell Biology of the Extracellular Matrix," in *Proteoglycans: Structure and Function*, Hay, ed., Plenum Press, New York.

Willers, C., Wood, D. J., & Zheng, M. H. 2003, "A current review on the biology and treatment of articular cartilage defects (part I and II)", *J Muskoskel Res*, vol. 7, no. 3&4, pp. 157-181.

Yasunaga, T., Kimura, M., & Kikuchi, S. 2001, "Histologic changes of the meniscus and cartilage tissue after meniscal suture", *Clin Orthop Relat Res* no. 387, pp. 232-40.

Yoneno, K., Ohno, S., Tanimoto, K., Honda, K., Tanaka, N., Doi, T., Kawata, T., Tanaka, E., Kapila, S., & Tanne, K. 2005, "Multidifferentiation potential of mesenchymal stem cells in three-dimensional collagen gel cultures", *J Biomed Mater Res A*, vol. 75, no. 3, pp. 733-41.

Zarnett, R. & Salter, R. B. 1989, "Periosteal nonchondrogenesis for biologically resurfacing joints: its cellular origin", *Can J Surg*, vol. 32, pp. 171-4.

Zheng, M. H., Willers, C., Kirilak, L., Yates, P., Xu, J., Wood, D. J., & Shimmin, A. 2007, "Matrix-induced autologous chondrocyte implantation (MACI): Biological and histological assessment", *Tissue Eng*, vol. 13, no. 4, pp. 737-746.

Zheng, N., Fleisig, G. S., Escamilla, R. F., & Barrentine, S. W. 1998, "An analytical model of the knee for estimation of internal forces during exercise", *J.Biomech.*, vol. 31, no. 10, pp. 963-967.

# Appendix: HemiCAP surgical technique

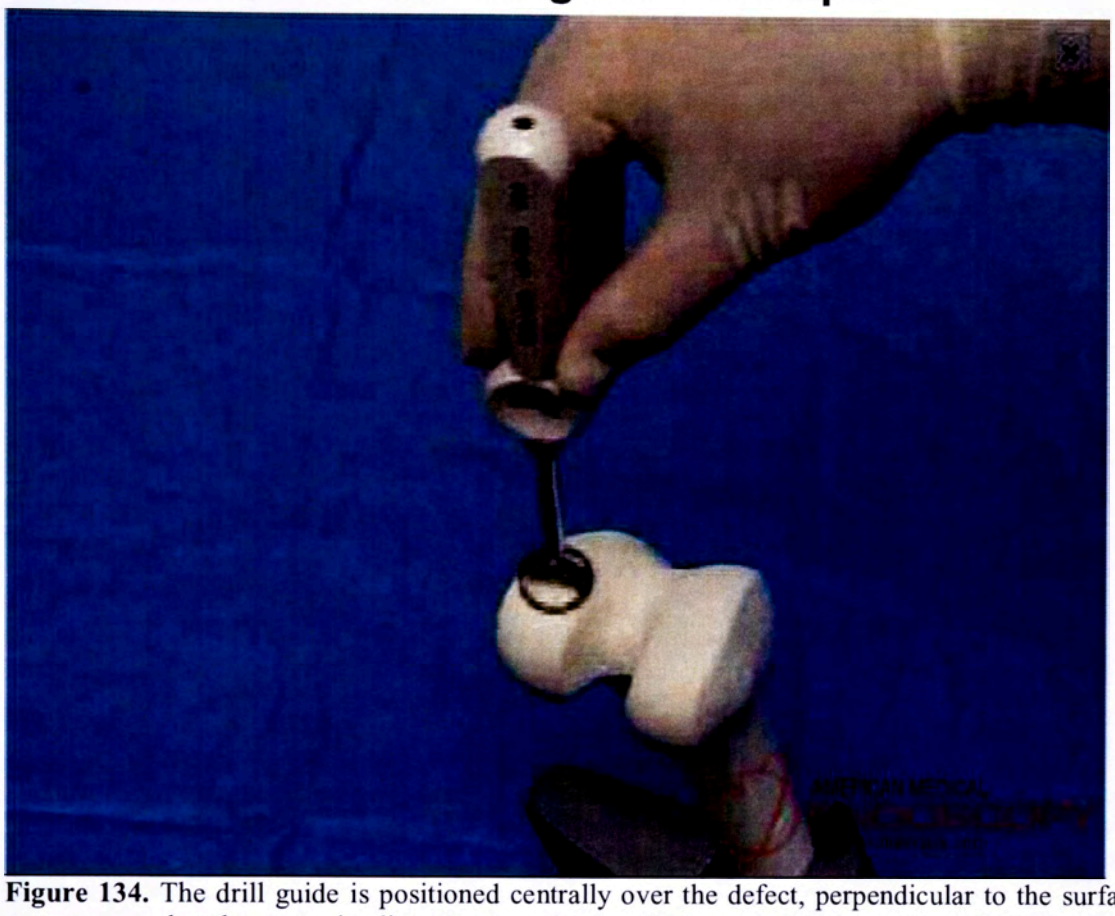

**Figure 134.** The drill guide is positioned centrally over the defect, perpendicular to the surface. This step ensures that the screw is aligned appropriately and that the defect will be completely covered by the articulating component. A screw that is malpositioned may result in the articulating component being implanted proud, recessed or at an angle such that one side is proud and the other is recessed.

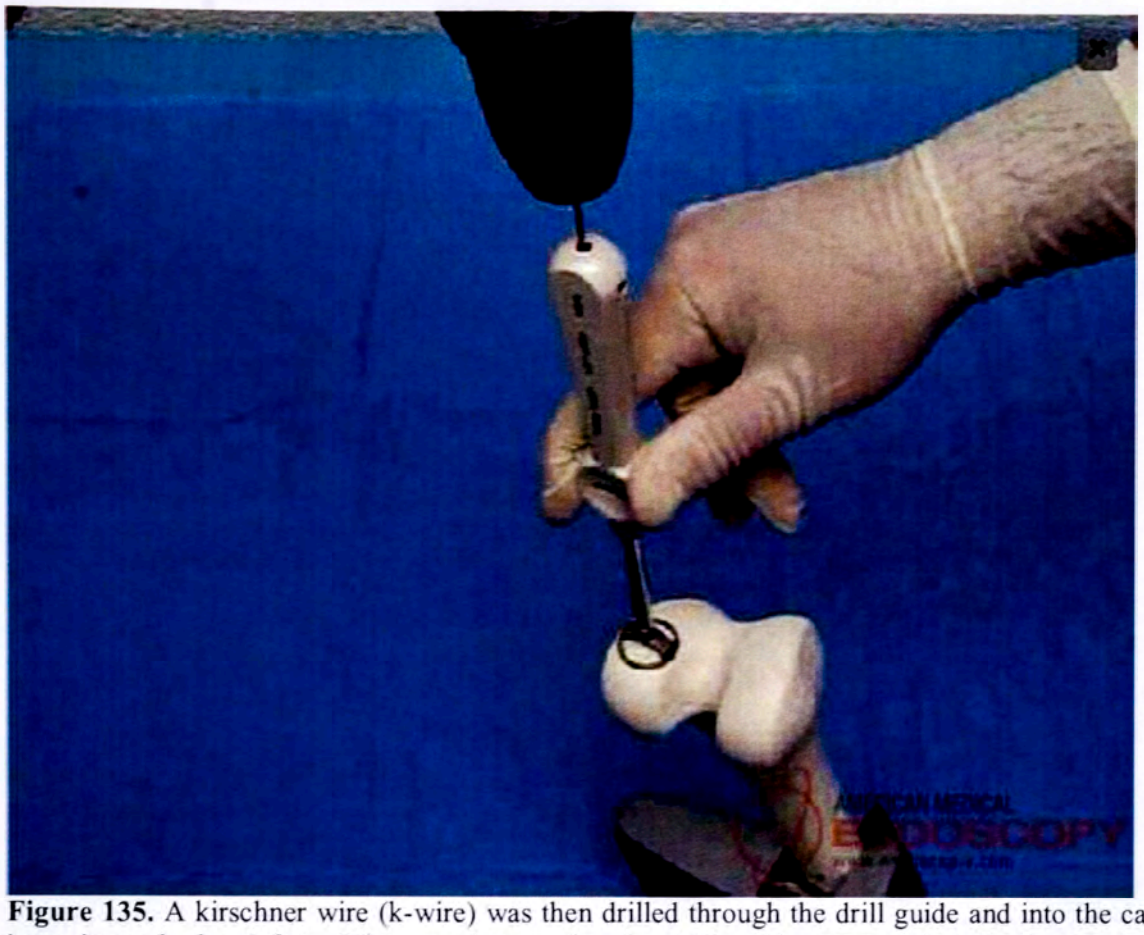

**Figure 135.** A kirschner wire (k-wire) was then drilled through the drill guide and into the cancellous bone beneath the defect. When used properly, the drill guide ensures that the k-wire is inserted perpendicular to the cartilage surface. The orientation of the device is controlled by the orientation of the k-wire, so this first step is vitally important for a successful resurfacing procedure.

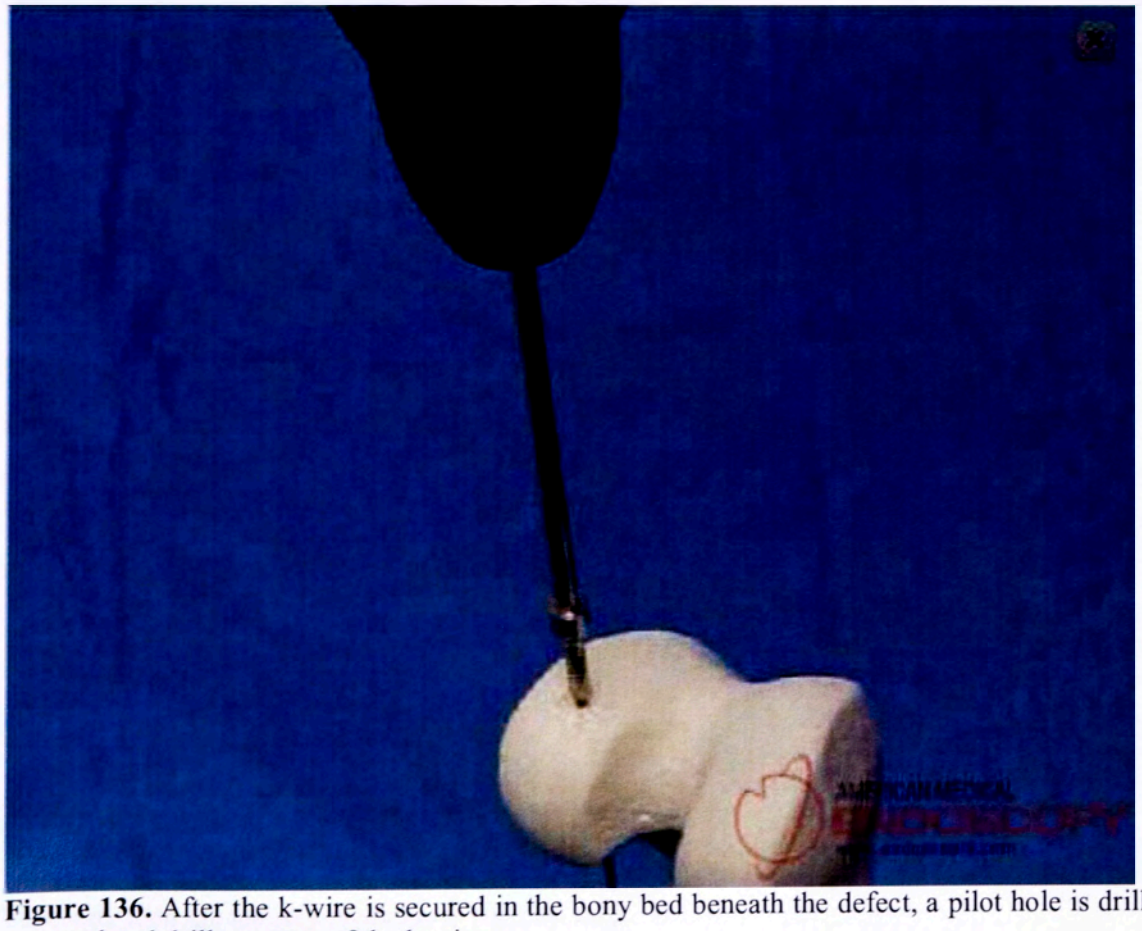

**Figure 136.** After the k-wire is secured in the bony bed beneath the defect, a pilot hole is drilled using a cannulated drill over top of the k-wire.

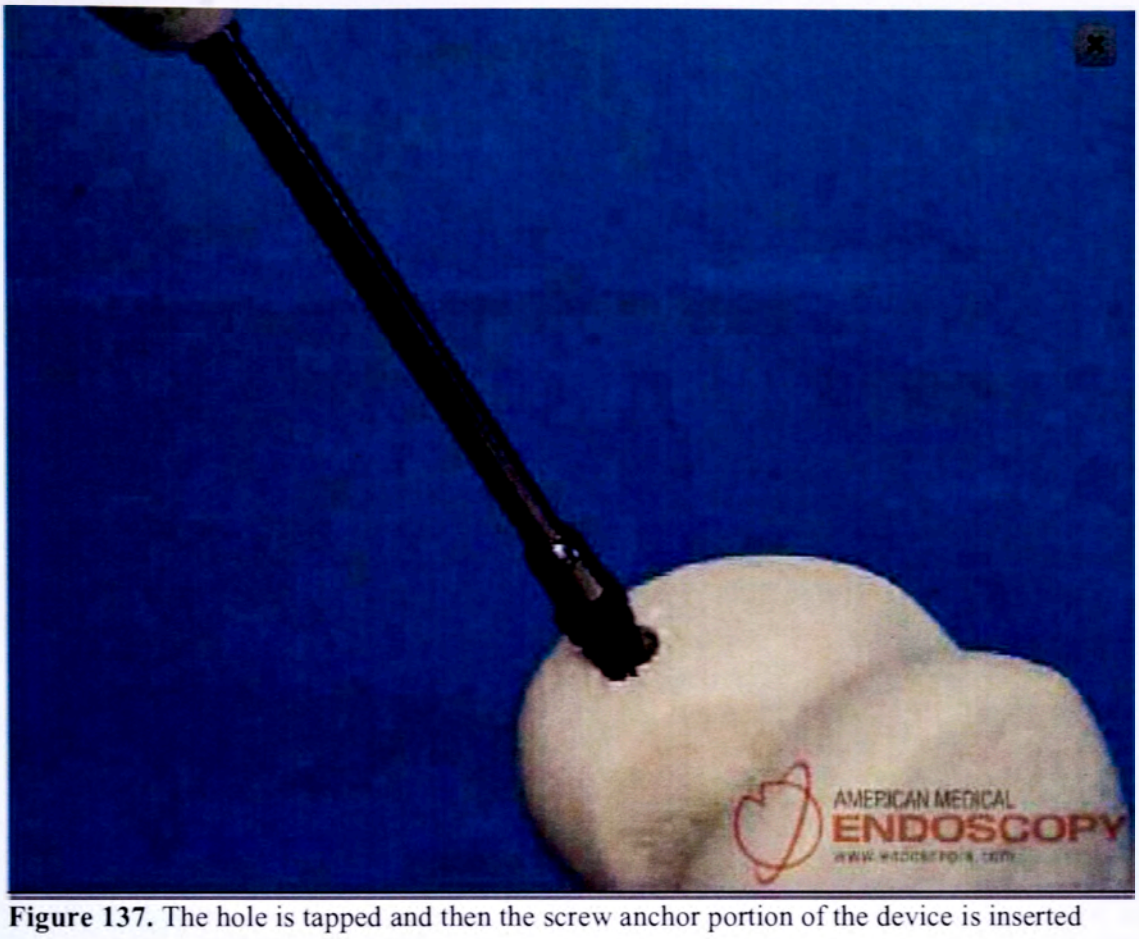


**Figure 137.** The hole is tapped and then the screw anchor portion of the device is inserted

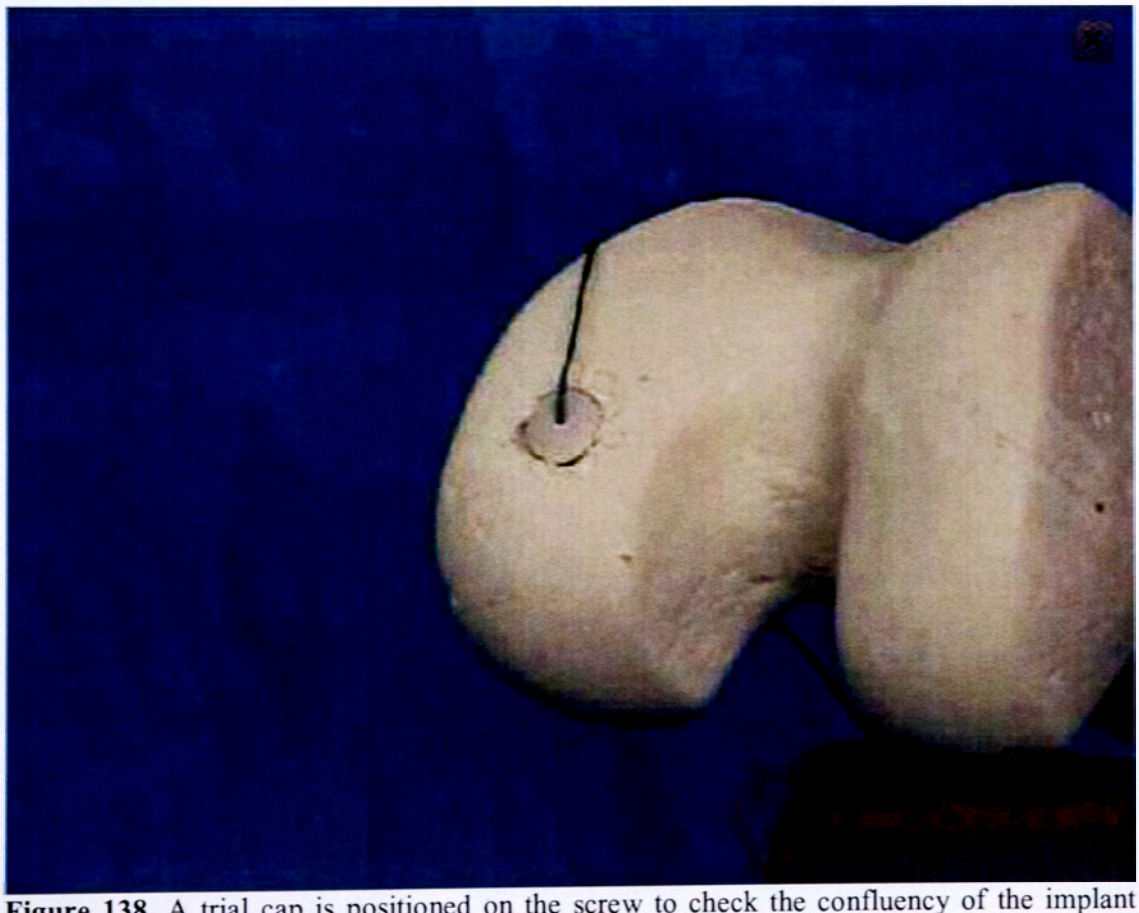

**Figure 138.** A trial cap is positioned on the screw to check the confluency of the implant with the adjacent cartilage surface. The string provides a convenient method of checking the height of the implant, and also a means to remove the trial cap. If the trial cap is flush with the surface of the cartilage, then the surgery proceeds to the next step.

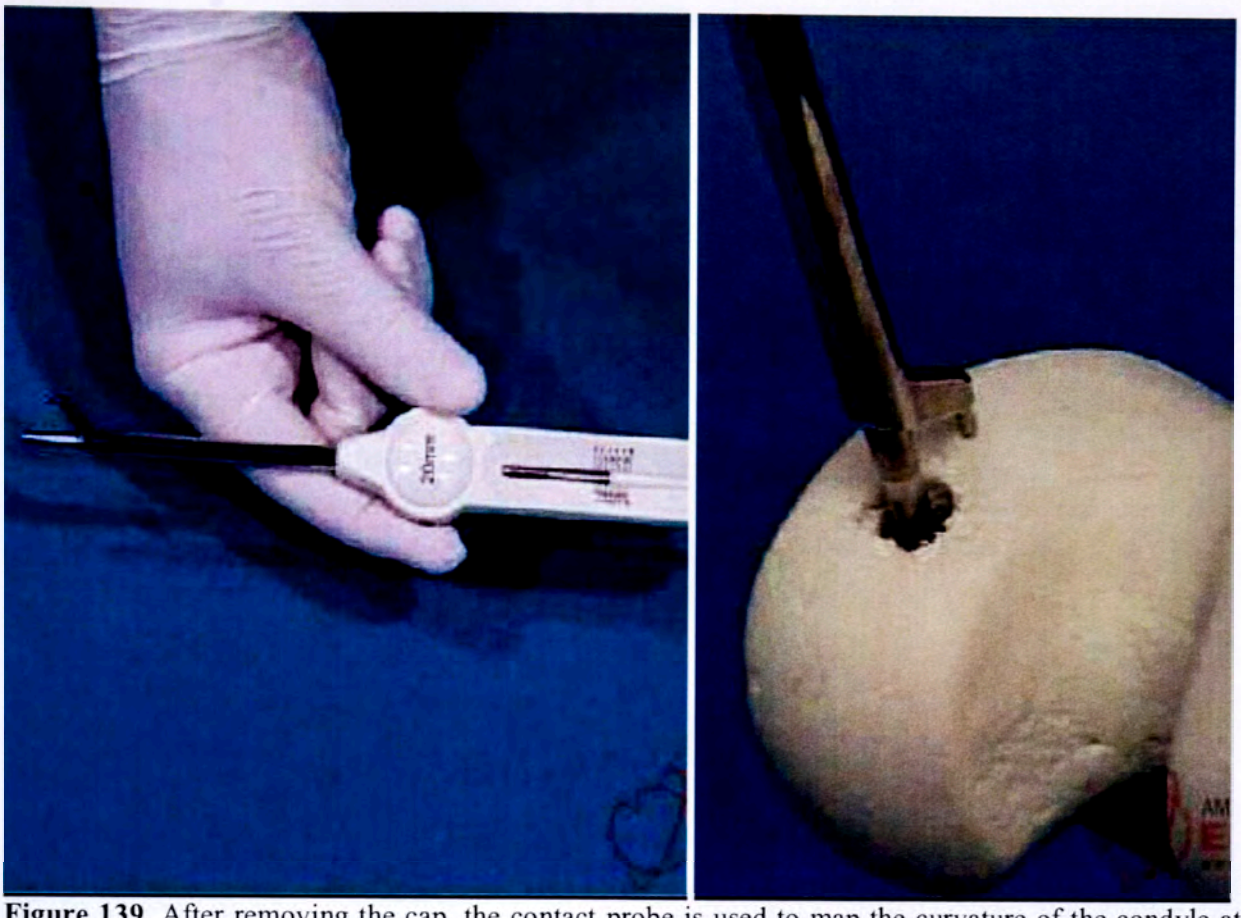

**Figure 139.** After removing the cap, the contact probe is used to map the curvature of the condyle at the superior, medial, inferior and lateral aspects of the device. These measurements determine the size of the articulating component to be used.

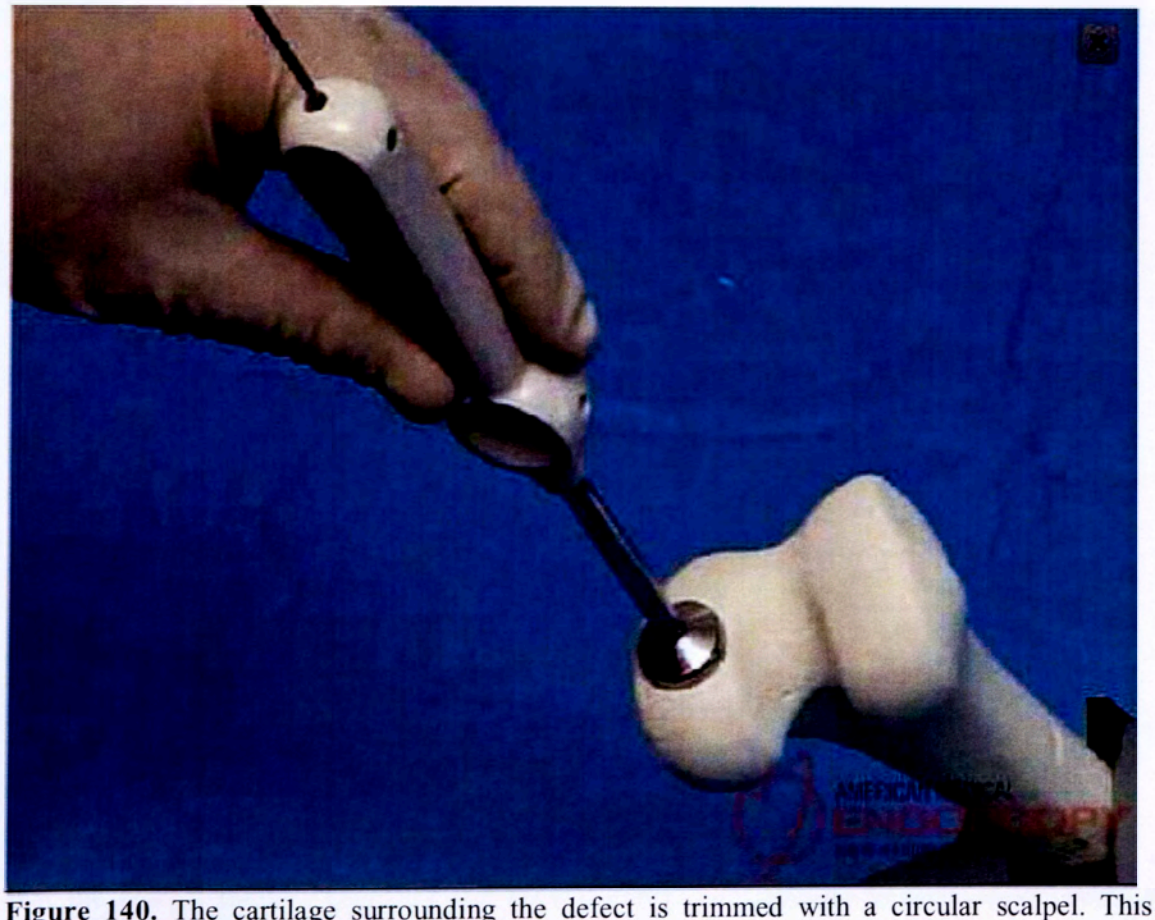

**Figure 140.** The cartilage surrounding the defect is trimmed with a circular scalpel. This step is important to ensure that the articulating component sits flush against the bone underneath.

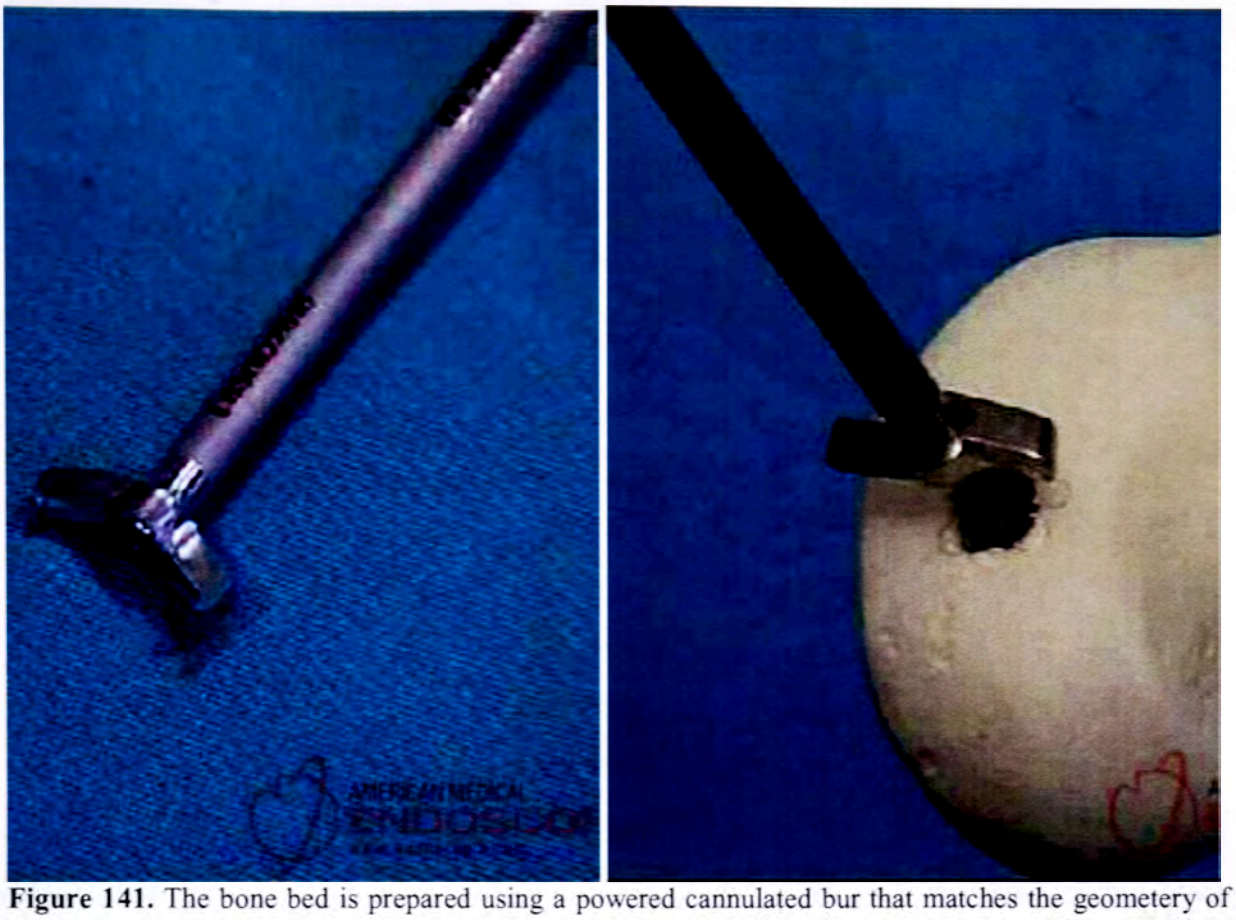

**Figure 141.** The bone bed is prepared using a powered cannulated bur that matches the geometery of the underside of the articulating component. As a result, the articulating component is fully seated into the bone bed.

**Figure 142.** A second trial cap is inserted to verify the preparation of the bone bed and also to check that the correct implant geometry has been selected. The articulating component should never be implanted proud of the surrounding cartilage.

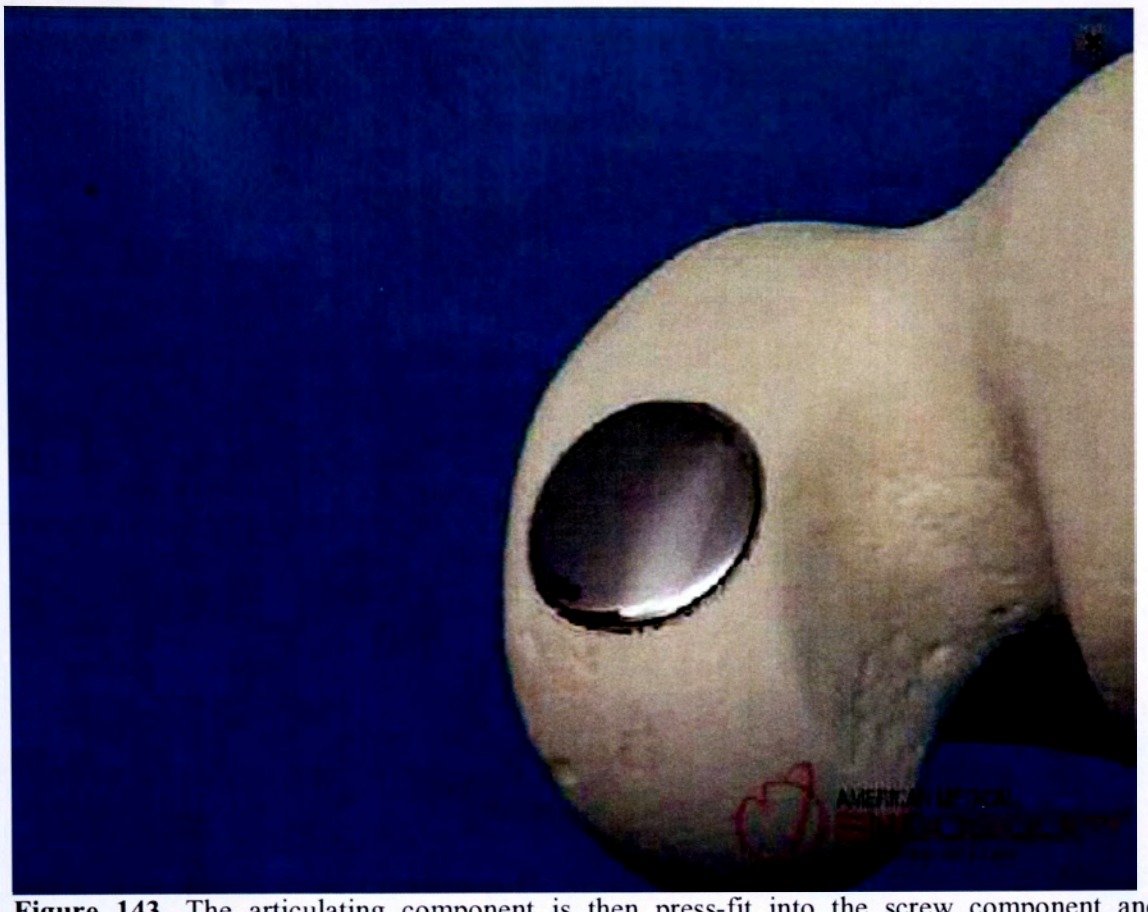

**Figure 143.** The articulating component is then press-fit into the screw component and gently hammered to engage the morse taper lock. The procedure is now complete and the joint is routinely closed in layers.

FIND LIB